The Dissertation Committee for Muhammad Ashraf Muhammad certifies that this is the approved version of the following dissertation:

Interception Capacity of Curb Opening Inlets

Committee:

Ben R. Hodges, Supervisor

Michael E. Barrett

Paola Passalacqua

Polina Sela

Joel P. L. Johnson

Interception Capacity of Curb Opening Inlets

by

Muhammad Ashraf Muhammad

DISSERTATION

Presented to the Faculty of the Graduate School of

The University of Texas at Austin

in Partial Fulfillment

of the Requirements

for the Degree of

DOCTOR OF PHILOSOPHY

THE UNIVERSITY OF TEXAS AT AUSTIN

December 2018

Dedicated to my mentor and intellectual friend: The philosopher, the artist, and the man.. *Friedrich Nietzsche*.

Acknowledgments

I would like to thank my supervisor, Dr. Ben Hodges, for all the guidance he provided. Whether I needed technical advice, help with administrative matters, or an intellectual conversation; he was always there to over-deliver. I would like to also thank my dissertation committee members. Dr. Michael Barrett provided valuable insights, practical advice, and ideas that helped the progress of research and ensured I stay on track. I would have missed many opportunities have Dr. Barrett not been there to point them out to me. I would like to thank Dr. Paola Passalacqua for being a great professor and friend. Her Stochastic Hydrology class was instrumental in both my M.S. thesis and my Dissertation. I must say that it has been a true joy conversing with Dr. Lina Sela; her wit, humor, and academic rigor made each encounter, quite literally, a memorable experience. Finally, I am thankful to Dr. Joel Johnson for his advice on practical experimental aspects and providing support whenever needed.

I am grateful to have shared a memorable discussion or interaction with almost every single faculty member of the Environmental and Water Resources Engineering department at UT-Austin. I am especially thankful for the fruitful technical discussions with Dr. Spyros Kinnas. I truly enjoyed the conversations I had with Saul Nuccitelli, Chief Hydraulics Engineer at TxDOT, and appreciate his efforts to support and publicize the findings of this study. I am grateful for all the support and advice I received from my peers in graduate school: Julien Botto, Jonthan Gingrich, Erin Berns, Luke Snell, Milena Daskalova, Olivia Beck, Kyle Wright, Jonathan Lala, Julie Faure, Ying Shi, Michael Wade, Jonathan Lasco, and Kyle Michelson. I would like to especially thank Dr. Hodges research group for all their

help in the lab and for being great friends: Zhi Li, Dongyu Feng, Cheng Wei Yu, Yongsik Kim, and Eddie Tiernan. This study would not have been possible without the great work of Frank Schalla in setting up the modeling facility. I am thankful for his patience and valuable instructions on operating and adjusting the lab. Frank also significantly participated in the model runs for the depressed inlets of 15 and 5 ft length as part of fulfilling his M.S. thesis at the University of Texas. I can not thank enough Mohamed Bennis and Michael Link for being the best companions one could ever ask for. I am thankful for my brothers and sister for their continuous care and support. Finally, I am truly grateful to my parents, Dr. Ashraf Ismail and Dr. Fatma Sallam, for all their support and guidance without which I would not be where I am today.

The work presented in this study was supported by the Texas Department of Transportation, Research and Technology Implementation Office in coordination with the Center for Transportation Research at the University of Texas at Austin. Additional support was provided under Cooperative Agreement No. 83595001 awarded by the U.S. Environmental Protection Agency to The University of Texas at Austin. It has not been formally reviewed by EPA. The views expressed in this document are solely those of the authors and do not necessarily reflect those of the Agency.

Interception Capacity of Curb Opening Inlets

Publication No. _____

Muhammad Ashraf Muhammad, Ph.D.
The University of Texas at Austin, 2018

Supervisor: Ben R. Hodges

Curb inlets are sized and placed along a road to maintain a safe spread of water from the curb to reduce the chances of vehicle hydroplaning and flood hazards at assets near the roadway. The accepted curb inlet design standard is the Hydraulic Engineering Circular No.22 (HEC-22), which contains the FHWA's guidelines and recommended design procedures. However, the source and assumptions in the design equations are not well-documented in the HEC-22 report. This dissertation uses full-scale physical model and experimental data reported in the literature to evaluate the HEC-22 design approach and prepare updated guidance for the sizing of curb inlets. The studies presented herein provide key insights into the hydraulics of curb inlet flow. The first study provides a detailed derivation and discussion of the assumptions in HEC-22 equations for depressed and undepressed inlets, at 100% interception and bypass flow conditions. The derivation shows that the 100% interception equations from HEC-22 deviate from their supposed theoretical basis through significant rounding up of numerical coefficients in the equations and by introducing a parameter to model depressed inlets without providing any justification. The inconsistencies in the 100% interception equations led HEC-22 to

deviate from theory once more by introducing a bias in the partial interception equation in an attempt to compensate for the bias in the 100% equations. The second study shows that HEC-22 significantly underestimates the 100% interception of undepressed inlets. Experimental data reported in the literature was used to provide a new design equation that reduced the relative error by a factor of 2 compared to HEC-22. The data was used as well to propose a modification to the partial interception equation and to show that Froude scaling in physical models of undepressed inlets only provides accurate results at smooth roadway surface with minimal effects of friction. In the third study, a full-scale model is modified and operated to assess the assumptions in HEC-22 equations for depressed inlets, such as the inaccurate assumption of a linear water profile along the inlet length. Data from this study was then combined with data from five other studies to provide a correction factor for the 100% interception as computed by HEC-22, and the correction factor reduced the RMSE by a factor of 3.75. A new approach was proposed as well for partial interception condition that has the advantage of providing better predictions and being structured in a way that facilitate checking and updating it using experimental data. The Fourth study modifies the depressed inlet model to test a 10 ft model of an inlet with a channel extension. The inlet was found to be robust towards flow restriction when installed on-grade. However, the capacity of the inlet extension when submerged regresses into only 23% of the expected capacity. Experimental data from this study and data reported in the literature was provided in the Appendix to facilitate future research on curb inlets hydraulics. Finally, an analysis is provided for the interception of recessed inlets in the Appendix as well. All these studies have important implications in the safe and economical design of urban stormwater drainage.

Table of Contents

List of Tables

List of Figures

Chapter 1

Introduction

1.1 Motivation

The flow of stormwater on streets is not merely an aesthetic nuisance; wet pavements can be hazardous as they cause vehicle hydroplaning. In the US, there is an estimated 1.5 million vehicle accidents annually associated with wet asphalt (Pisano et al., 2008). If stormwater is allowed to accumulate on streets, flow might inundate the curb and cause damage to nearby houses and assets. Also, stormwater is one of the main causes of pavement deterioration. The US Federal Highway Administration (FHWA) estimates that the required annual investment for roadways maintenance in the US amounts to 4.5 Billion US$ (FHWA and FTA, 2017). Consequently, major investments are directed into the construction of expensive and extensive underground sewer networks to safely direct stormwater to natural streams or treatment plants. However, if the curb inlet structures cannot meet the desired inflow requirements then the expensive underground system will not achieve its design goals. This dissertation examines fundamental failings of the existing design guidance for curb inlets that causes inlets to be undersized for a range of flow conditions.

Several types of storm drain inlets are constructed to collect and convey stormwater into the sewers, including the common curb-opening inlet. Such inlets are vertical openings in the curb that are covered by a top slab (Figure 1.1). Curb-opening inlets are commonly used instead of horizontal gratings as the inlets

are less susceptible to clogging by debris, pose minor interference to traffic operation, and are safe for pedestrians and cyclists (TxDOT, 2016).

Figure 1.1: 15-ft curb-opening inlet.

Curb inlets are sized and spaced along a road to maintain a safe spread of water from the curb to reduce the chances of vehicle hydroplaning. Consequently, the hydraulic design of curb inlets is mainly concerned with determining the interception capacity of the inlet, which is the maximum gutter flow that can be captured by the inlet under certain road configurations. Inlet interception can be increased by increasing the inlet length, roadway cross slope, and/or roadway roughness, all of which help direct flow into the inlet. Conversely, the inlet interception is decreased by increasing the roadway longitudinal slope (Jens, 1979), which tends to make water flow past the inlet. Experiments have also shown that depressing the gutter section at an inlet also increases interception (Johns Hopkins University, 1956). Hence, inlets on gutters with a simple cross-slope are known as *undepressed inlets*, and inlets on a

depressed gutter section are known as *depressed inlets*. Another method of increasing the design inlet interception is by allowing a small portion of the flow in the gutter to bypass the inlet. Because of nonlinearity in the inlet equations, allowing a small bypass flow ($< 5\%$) typically increases the inlet interception greater than the bypassed amount, thus leading to a more cost-effective configuration for a series of inlets (Karaki and Haynie, 1961). This dissertation examines both undepressed and depressed inlets with a focus on the full capture and low bypass conditions that are often used as design criteria.

The majority of equations in the literature for sizing curb inlets are based on empirical data fit to experiments. Experiments were conducted for specific depression geometry and inlet length(s), and for one or more roadway slope combinations. Regression analysis is then carried out to relate the intercepted flow into the inlet to the flow depth or spread. Examples of these studies are McEnroe et al. (1999), Kranc et al. (1998), and Yong (1965). Equations based solely on fits to empirical data should be applied only to inlets matching the tested configuration for road slope, inlet length, and the range of flow conditions. Unlike most design equations, the approach presented in the Hydraulic Engineering Circular No. 22 (Brown et al., 2009 —herein HEC-22) is applicable to most inlet and roadway configurations. The equations in HEC-22 are recommended by the Federal Highway Administration (FHWA); therefore these equations are widely used in engineering practice (Hammonds and Holley, 1995) and within commercial stormwater design models. For example, the *StormCAD V8 XM* user manual states that HEC-22 1996 edition is used for inlet computations and *Innovyze InfoSWMM* allows users to specifically select HEC-22 inlets as well as other approaches. Because the HEC-22 equations are used for a wide variety of curb inlet configurations, their foundations

and range of limitations should be known to roadway designers. Unfortunately, the sources and assumptions of the HEC-22 equations are not well documented in that report or elsewhere in the literature.

Also, recent experiments show that these equations have significant error in predicting full-capture and low bypass design conditions (Schalla, 2016; Schalla et al., 2017), which calls for revisiting their fundamental basis. Since the 2009 edition of HEC-22, only a few studies provided updates/modifications to the HEC-22 equations (Guo et al., 2012; Comport and Thornton, 2012). These studies were limited to a specific gutter configuration and roadway roughness, and most experiments were conducted over a wide range of bypass flow conditions with most of the experiments being focused at high-bypass flow. Although these studies provided satisfactory results within the tested conditions, their applicability is uncertain over the wide range of full interception, low-bypass flow, and different inlet/gutter geometries used by roadway designers. Finally, most curb inlets experiments were conducted on scaled models based on Froude number similarity (Li et al., 1951; Uyumaz, 1992; Hammonds and Holley, 1995). This experimental scaling requires the assumption that Reynolds number effects are invariant over a wide range of scales. However, several studies have showed discrepancies between full-scale prototypes and scaled model results, especially for shallow gutter flow (Grubert, 1988; Zwamborn, 1966; Argue and Pezzaniti, 1996). This dissertation uses full-scale testing to evaluate the performance of depressed inlets. Also, experimental data from scaled models reported by other studies are scaled back to model dimensions (actual tested dimensions) before being included in the current analysis.

The simple geometry of undepressed inlets facilitated studying them using theoretical approaches. These approaches range from simple models (Li et al., 1951;

Izzard, 1950) to highly complex ones (Wasley, 1960). All these models use some simplifying assumptions that are then tested and calibrated against experimental data. Due to the difficulties associated with setting up and modifying experimental models, each study only tested model assumptions against a limited set of parameters (e.g., roadway roughness, slope configurations, and flow conditions). It can be argued that the more uniform flow conditions in the vicinity of undepressed inlets enhances the applicability of scaled models in the study of undepressed inlets, in contrast to the questions that have been previously raised for scale modeling of depressed inlets (Grubert, 1988). Analyzing the hydraulics of undepressed inlets and the available experimental data-sets might shed the light on cases where the use of scaled models is applicable for undepressed inlets. In this dissertation, analysis of experimental data from various studies provides guidance on the applicability of scaled models to undepressed inlets.

In the case of depressed inlets, several studies apply modifications to the theoretical analyses of undepressed inlets to extend their approach to depressed inlets (Li et al., 1951; Izzard, 1950; Zwamborn, 1966). However, Wasley (1960) noted that extending the analysis to depressed inlets might introduce further complications if an oblique hydraulic jump forms at the outer edge of the gutter. Such disturbance in the water profile was experimentally observed by Bauer and Woo (1964) during full-scale experiments. The complex hydraulics at depressed inlets makes an analytical analysis quite cumbersome, especially for providing an approach convenient for use in design by practitioners (Hammonds and Holley, 1995). This dissertation uses a statistical approach that utilizes the available experimental data in the literature for a wide range of inlet, gutter, roadway, and flow conditions to provide updated design equations.

Finally, the standard hydraulic calculations for the design of on-grade curb inlets assume free-fall overflow from the lip of the inlet into the sewer system, and submerged inlets in a sag configuration are based on orifice flow controlled by the inlet opening. However, some designs of long curb inlets divide the inlet into a main bay with side extension chambers. Unlike a conventional inlet, flow intercepted through an extension does not fall directly into the main bay. Instead the extension provides a horizontal channel directing the intercepted flow into the main basin. For a compact design the cross-section of the extension channel might be smaller than the cross-section of the curb inlet itself. This reduction in cross-section can cause the intercepted flow to be significantly less than the design flow predicted by equations for conventional inlets. This dissertation uses full-scale experimental modeling to investigate the potential flow restriction in inlets with channel-extensions. Table 1.1 summarizes the recommendations from this dissertation and the section where they are discussed.

1.2 Research Objectives

The motivations (discussed above) that directly lead to the objectives of this research can be briefly summarized. Firstly, curb inlet studies have largely focused on performance characteristics of specific inlets using Froude-scaled physical models in experiments dominated by high-bypass flow conditions. These prior studies cannot address concerns regarding the adequacy of scaled models, especially with shallow gutter flow and at or near full capture. Secondly, the generalized design equations proposed by HEC-22 have been shown to fail under certain design conditions. Finally, inlets with channel extensions are widely used, but the potential effects of flow constrictions in these extensions have not been analyzed.

Table 1.1: Summary of recommendations and conclusions form this dissertation.

Design Condition \ Curb Inlet Type		Undepressed Inlets	Locally Depressed Standard Inlet	Locally Depressed PCO Inlet	Inlet with Continuously Depressed Gutter	Recessed Depressed Inlet
On-grade	100% Interception	(Section 3.3) HEC-22 generally underestimates interception. Use Equation 3.16	(Section 4.6) Compute interception using Equation 4.5, 4.6	(Sections 4.6 and 5.5) Compute interception using Equations 4.5, 4.6 or Equation 5.4	(Section 4.5) HEC-22 underpredicts interception of short inlets (<5 ft) and overpredicts long inlets (>10 ft)	(Appendix C) 25% reduction in interception compared to locally depressed standard inlet under some conditions.
	Partial Interception	(Section 3.3) HEC-22 provides a reasonable estimate. Use Equations 3.17, 3.18, and 3.19	(Section 4.7) Compute efficiency using Equation 4.8	(Sections 4.7 and 5.4) Compute efficiency using Equation 4.8. Expected reduction in capture at high bypass (>> 0.5 cfs)		
	Flat S_x and Steep S_L	(Section 3.4) Degradation in inlet performance			(Section 3.4) Potential degradation in Inlet performance	
	Flush Slab Supports	(Section 5.3) 50% reduction in interception is highly unlikely	(Section 5.3) 6" wide supports have no effect on interception. Supports should be included in inlet opening length			
Sag		Interception is expected to follow HEC-22		Section (5.5) Significant reduction in capacity. Recommend using a standard inlet. Compute extension capacity by Equation 5.2	Interception is expected to follow HEC-22	
Froude Number Scaled Models		(Section 3.6) Applicable for smooth surfaces or considerably large flow depth	(Section 3.6) Further work is required to confirm their validity in the case of smooth roadway. Inaccurate modeling at rough roadway surface.			

This dissertation addresses the above mentioned concerns by pursuing the following objectives:

1. Provide a detailed derivation of the inlet interception-capacity equations for undepressed and depressed inlets in HEC-22, illustrating the explicit and implicit assumptions in the design equations (§2).

2. Propose a more accurate approach for computing the interception capacity of undepressed inlets based on investigating the inlet hydraulics and the applicability of Froude number scaling to experimental models (§3).

3. Experimentally investigate the assumptions in HEC-22 equations for depressed inlets, and propose a modification that addresses potential inaccuracies in the equations (§4).

4. Quantify the effect of potential flow restrictions on the interception capacity of inlets with channel extensions (§5).

5. Provide a comprehensive collection of available experimental data-sets for curb inlet studies in the literature (Appendix A).

1.3 Outline

This Dissertation is organized as follows:

- **Chapter 2:** Presents a detailed derivation and discussion of assumptions of HEC-22 design equations.

- **Chapter 3:** Discusses hydraulics of undepressed inlets, updated design equations, and applicability of Froude number scaling to undepressed inlets.

- **Chapter 4:** Contains experimental assessment of assumptions in HEC-22 equations for depressed inlets and a proposed correction factor for HEC-22.
- **Chapter 5:** Contains experimental assessment of the effects of potential flow restriction on the interception capacity of curb inlets with channel extensions.
- **Chapter 6:** Provides a summary of conclusions and design recommendations form this study.
- Finally, the appendices provide measured experimental data from this study and data reported in the literature.

Chapter 2

Derivation of HEC-22 Equations

2.1 Overview

[1] On-grade curb inlets are installed along the hard curb edge of a roadway to totally or partially capture the upstream gutter flow of a design storm. The typical design goal is to limit the maximum spread of water from the curb across the roadway for vehicular safety. The Hydraulic Engineering Circular No. 22 (Brown et al., 2009 —herein HEC-22) contains the design guidelines and equations recommended by the U.S. Federal Highway Administration (FHWA), which have also been included in many state and local hydraulic design manuals. A variety of HEC-22 equations are also found in commercial stormwater design software (e.g., SewerGems®, XPSWMM). Recent full-scale experiments at the University of Texas (Schalla et al., 2017) showed that the HEC-22 equations for depressed, on-grade curb inlets will overestimate the 100% interception capacity for long inlets of 3.05 and 4.57 m (10 and 15 ft). Interestingly, the equations underestimate the capacity for short inlets of 1.52 m (5 ft). Addressing the limitations of these equations is hampered by the lack of a derivation and/or citations supporting the equations and their coefficients, both in HEC-22 and the broader literature. Indeed, even the FHWA has been unable to document the equation sources (Krolak, 2018).

[1]This chapter is adapted from a manuscript that is under review at the *Journal of Hydraulic Research* under the title "Derivation of the HEC-22 design equations for on-grade curb inlets." This dissertation author is the lead author of the manuscript and co-authors are the co-supervisors of this study: B.R. Hodges and M.E. Barrett.

The present work remedies this problem by providing detailed derivations for the HEC-22 equations for conveyance in a compound gutter and capture by on-grade curb inlets. Note that design equations inlets installed in a sag are based on the hydraulics of weir or orifice flow, which are not considered herein.

First, we provide a general derivation of gutter conveyance. The following two sections are derivations of equations for full interception by on-grade undepressed and depressed inlets, respectively. Finally, an analyses of the HEC-22 approach and theory for partial interception (bypass flow) is provided.

2.2 Derivation of Gutter Conveyance

There are two common cross-slope sections used in roadways, as shown in Figure 2.1.

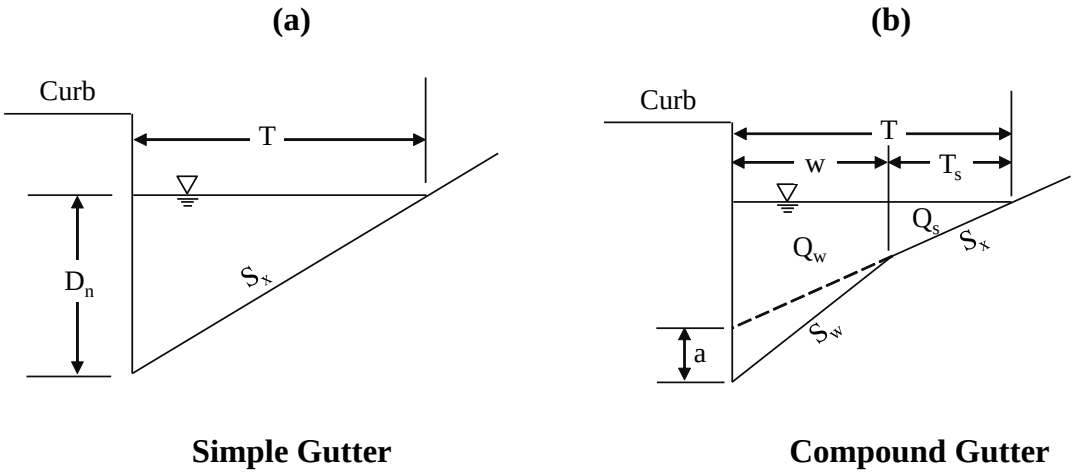

Figure 2.1: Roadway sections: (a) uniform section, (b) composite section.

A uniform gutter (Figure 2.1-a) consists of a single cross-slope along the entire width of the road, where T is the water spread across the roadway and S_x is the uniform cross slope. In contrast, a depressed gutter is created with a compound

section (Figure 2.1-b) where the edge of the gutter at the curb inlet is depressed beyond the normal gutter cross slope by a few centimeters. Depressing the gutter section is a common practice to reduce the spread for a given gutter flow. From geometry the depressed gutter cross-slope, S_w, is

$$S_w = S_x + \frac{a}{w} \tag{2.1}$$

where w is the depressed gutter width and a is the depression height.

Conveyance for a uniform gutter cross-section can be modeled using Manning's equation (more formally the Gaukler-Manning-Strickler equation) for triangular channel. However, Izzard and Hicks (1947) argued that the hydraulic radius of Manning's equation applied to the overall cross-section was inappropriate for gutter flow due to the shallow depths. They proposed a cross-section integrated approach to address this issue. What has become known as "Izzard's equation" is developed by applying Manning's equation in a local sense; by considering the velocity of a strip of flow of width dx and depth D, and at a distance x away from the curb (Figure 2.2). The result is

$$v(x) = \frac{k}{n} D^{2/3} {S_L}^{1/2} \tag{2.2}$$

where v is the along-gutter velocity in the differential strip, n is Manning's roughness coefficient (unitless), and dimensional consistency for standard SI or US Customary units requires $k = 1.0$ m$^{1/3}$ s^{-1} or 1.49 ft$^{1/3}$ s^{-1}, and S_L is the longitudinal slope of the roadway. Since geometry provides $D = (T - x)S_x$ we obtain

$$v(x) = \frac{k}{n} [(T - x)S_x]^{2/3} {S_L}^{1/2} \tag{2.3}$$

To obtain a flowrate from $v(x)$, we note the differential strip (dx) in Figure 2.2 has a differential area (dA) across the gutter section given by:

$$dA = (T - x)S_x \, dx \tag{2.4}$$

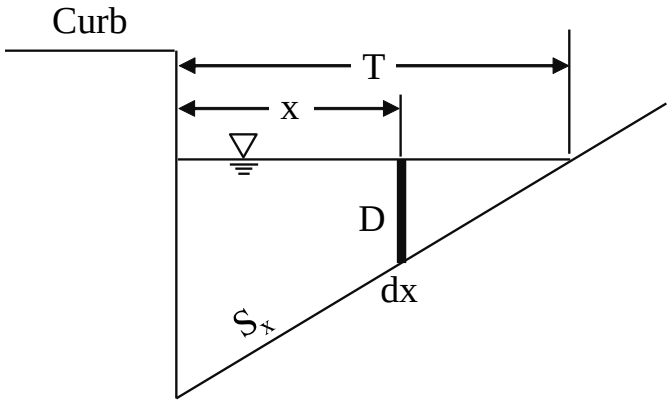

Figure 2.2: Schematic of uniform gutter section for derivation of Izzard's equation.

The flowrate in the differential strip is $dQ = v\,dA$, so using Eqs. (2.3) and (2.4) provides

$$dQ = \frac{k}{n}[(T-x)S_x]^{5/3} {S_L}^{1/2} dx \tag{2.5}$$

The total flow in the gutter is $Q_g = \int dQ$, or

$$Q_g = \frac{k}{n} {S_L}^{1/2} S_x^{5/3} \int_0^T (T-x)^{5/3} dx \tag{2.6}$$

which evaluates as

$$Q_g = \frac{3k}{8n} {S_L}^{1/2} S_x^{5/3} T^{8/3} \tag{2.7}$$

To remove T from the Q equation, we note that the water depth at the curb is typically taken as the normal flow depth, denoted as D_n. For a uniform gutter this is

$$D_n = S_x T \tag{2.8}$$

so that we have

$$Q_g = \frac{3k}{8n} \frac{{S_L}^{1/2}}{S_x} D_n^{8/3} \tag{2.9}$$

For hydraulic practice, it is convenient to lump coefficients together by defining

$$k_u \equiv \frac{3k}{8} \tag{2.10}$$

which has a value of 0.375 $m^{1/3}$ s^{-1} or 0.559 $ft^{1/3}$ s^{-1} for a dimensionally-consistent equation, where the former is exact and the latter is rounded to three digits. Note that the k_u for US customary units is often rounded to two significant digits as 0.56, which is oddly inconsistent with maintaining three digits in $k = 1.49$ $ft^{1/3}$ s^{-1} for Manning's equation. Using the above, Equation (2.9) becomes the standard form of Izzard's equation:

$$Q_g = \frac{k_u}{n\, S_x} {S_L}^{1/2} {D_n}^{8/3} \tag{2.11}$$

For conveyance in a compound gutter (Figure 2.1-b), conceptually, the flow is separated into flow through the quadrilateral area above the depressed section (Q_w) and flow in the triangular section over the roadway (Q_s). HEC-22 develops a design approach for depressed gutters based on the fraction of the total flow carried in the depressed section, defined as

$$E_o \equiv \frac{Q_w}{Q_g} \tag{2.12}$$

Without derivation, citation, or justification, HEC-22 provides a design relationship for E_o as

$$E_o = \left\{ 1 + \frac{S_w S_x^{-1}}{\left[1 + \frac{S_w S_x^{-1}}{(T w^{-1}) - 1}\right]^{2.67} - 1} \right\}^{-1} \tag{2.13}$$

Although the source of Equation (2.13) is not documented in HEC-22, it is straightforward (albeit with substantial algebra) to show that it results from application of the Izzard and Hicks (1947) approach of integrating Manning's equation over differential cross-sections for the compound gutter, similar to what we

show above for a simple gutter. Because the derivation is not available elsewhere in the literature, it is presented here as Appendix B.

As a further complication, HEC-22 applies Equation (2.13) only to inlets with continuously depressed gutters and provides a modified expression for inlets with a locally-depressed gutter; i.e., where a uniform gutter section transitions into a depressed section at the inlet. HEC-22 assumes that the transition length is short enough that it does not direct significant flow from the roadway (S_x) into the depression (S_w), therefore the portion of the flow in the depressed section is determined from the flow in the uniform gutter section upstream of the transition. For this uniform section $S_w = S_x$, so it follows that Equation (2.13) is reduced to:

$$E_o = 1 - \left[1 - \frac{w}{T}\right]^{2.67} \tag{2.14}$$

This HEC-22 assumption is arguably a conservative design approach as it underestimates the water in the depressed gutter that is readily available for capture. E_0 plays a role in the computation of an "equivalent" cross slope of a depressed inlet, which is presented in §2.4.

2.3 Undepressed Inlets

The HEC-22 design equation for the length of undepressed inlet (L_T) for 100% capture of gutter flow Q_g is

$$L_T = k_i \, Q_g^{0.42} S_L^{0.3} \left(\frac{1}{n S_x}\right)^{0.6} \tag{2.15}$$

where the coefficient is given as k_i= 0.817 $s^{0.42}$ $m^{-0.26}$ or 0.6 $s^{0.42}$ $ft^{-0.26}$ for a dimensionally-consistent equation. The above is based on Izzard (1950), which used the following approximations and assumptions:

1. inlet inflow is modeled as weir flow with critical depth across the inlet lip,

2. water depth is assumed to decrease linearly along the inlet length (Figure 2.3-a),

3. energy head at the upstream end of the inlet is equal to the depth of the approach flow, which presumes the kinetic energy of the gutter flow is negligible (Figure 2.3-b), and

4. transverse velocity component in the approach flow is negligible.

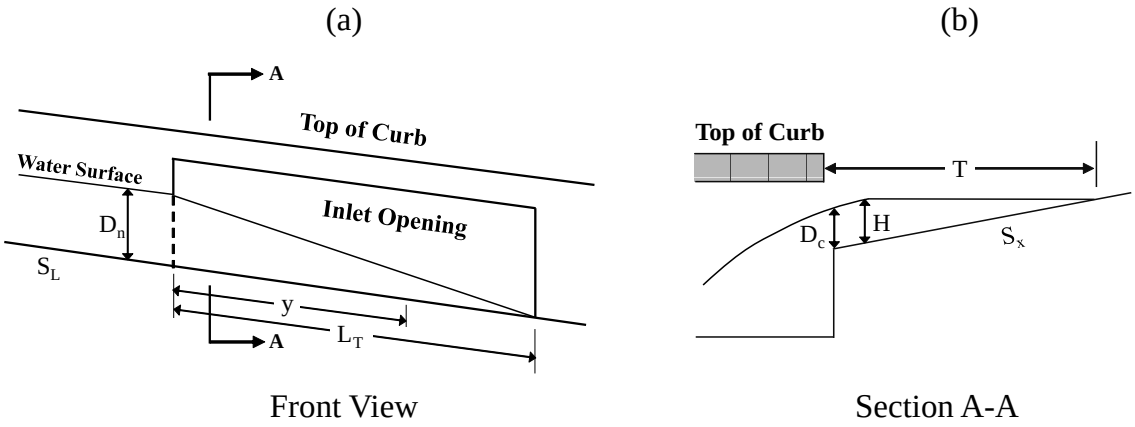

Figure 2.3: a) along-grade assumed linear profile, b) cross-section of inlet modeled as weir flow

The first assumption of Izzard's approach requires the velocity into the inlet (u_i), at any point y along the inlet, to be critical (Fr = 1), which implies

$$u_i(y) = \sqrt{gD_c(y)} \tag{2.16}$$

where $D_c(y)$ is the local critical depth. The flowrate per unit length along the inlet is $u_i D_c$, or

$$dQ = g^{1/2} \left[D_c(y)\right]^{3/2} \, dy \tag{2.17}$$

Note that if we define H as the specific energy head (or simply the head) directed into the curb inlet, i.e., $H = D + u_i^2(2g)^{-1}$, then with Equation (2.16) we obtain:

$$D_c(y) = \frac{2}{3}H(y) \tag{2.18}$$

The above presumes that $u_i(y) > v(y)$, where $v(y)$ is the characteristic along-gutter velocity at location y, which is implicit in assumption 3, above. Using Equation (2.18) in Equation (2.17) then provides the differential flow consistent with assumptions 1 and 3 as

$$dQ = g^{1/2}\left(\frac{2}{3}H(y)\right)^{3/2} dy \tag{2.19}$$

Assumption 2 of Izzard's approach requires the water depth to vary linearly along the inlet from the upstream gutter value, i.e., from D_n at $y = 0$ to zero at $y = L_T$. Neglecting the kinetic energy head, $u^2(2g)^{-1}$, at the upstream gutter (assumption 3) and along the gutter (assumption 4) implies

$$H(y) = D_n\left(1 - \frac{y}{L_T}\right) \tag{2.20}$$

It follows that

$$dQ = g^{1/2}\left[\frac{2}{3}D_n\left(1 - \frac{y}{L_T}\right)\right]^{3/2} dy \tag{2.21}$$

The total intercepted flow is then

$$Q_i = g^{1/2}\left(\frac{2}{3}D_n\right)^{3/2}\int_0^{L_T}\left(1 - \frac{y}{L_T}\right)^{3/2} dy \tag{2.22}$$

It can be shown that the integral evaluates to $2L_T/5$ so that

$$Q_i = g^{1/2}\,\frac{2}{5}\left(\frac{2}{3}\right)^{3/2} D_n^{3/2} L_T \tag{2.23}$$

To remove D_n from the flow equation, we note that Equation (2.9) provides the normal depth in the gutter at the upstream cross-section as

$$D_n = \left(\frac{8nQ_gS_x}{3kS_L^{1/2}}\right)^{3/8} \tag{2.24}$$

Furthermore, for 100% interception we require $Q_i = Q_g$ so we can substitute Equation (2.24) into (2.23) as

$$Q_g = g^{1/2}\frac{2}{5}\left(\frac{2}{3}\right)^{3/2}\left(\frac{8nQ_gS_x}{3kS_L^{1/2}}\right)^{9/16} L_T \tag{2.25}$$

which is solved for L_T as

$$L_T = \frac{1}{g^{1/2}}\frac{5\left(3^{3/2}\right)\left(3^{9/16}\right)k^{9/16}}{2\left(2^{3/2}\right)\left(8^{9/16}\right)}\left(\frac{S_L^{1/2}}{nS_x}\right)^{9/16} Q_g^{7/16} \tag{2.26}$$

which is the formal analytical form that is consistent with the approximate forms found in HEC-22.

The above can be written with a multiplicative coefficient to four significant digits as

$$L_T \approx 2.645\frac{k^{9/16}}{g^{1/2}}\left(\frac{S_L^{1/2}}{nS_x}\right)^{9/16} Q_g^{7/16} \tag{2.27}$$

It follows that to get a form similar to HEC-22, as presented in Equation (2.15), we can define

$$k_i \equiv \begin{cases} 2.645\left(\frac{1^{9/16}}{\sqrt{9.807}}\right) & = 0.8447\frac{\mathrm{s}^{7/16}}{\mathrm{m}^{5/16}} \quad \text{SI} \\ 2.645\left(\frac{1.49^{9/16}}{\sqrt{32.17}}\right) & = 0.5837\frac{\mathrm{s}^{7/16}}{\mathrm{ft}^{5/16}} \quad \text{US Customary} \end{cases} \tag{2.28}$$

so that Equation (2.27) becomes

$$L_T = k_i Q_g^{7/16} S_L^{9/32}\left(\frac{1}{nS_x}\right)^{9/16} \tag{2.29}$$

Table 2.1 shows the coefficients and powers in the HEC-22 equations and the formally-derived equations. It appears that the HEC-22 approach is based on this derivation, but with significant rounding of coefficients and powers. It seems likely that this rounding was useful for the preparation of nomographs and the use of slide rules, but does not seem justified for present computational work. Note that because

Equation (2.29) includes power for a dimensional term (Q_g), this implies any change of the power (e.g., rounding or empirical fitting) will change the units of k_i and hence should change the value of k_i. This issue does not appear to have been considered in HEC-22 or elsewhere.

term	derived	HEC-22
k_i (SI)	~ 0.8447	0.817
k_i (US)	~ 0.5837	0.6
Q power	0.4375	0.42
S_L power	0.28125	0.3
nS_x power	0.5625	0.6

Table 2.1: Comparison of derived coefficients and power values versus HEC-22. The $\sim$ indicates values rounded to four significant digits, all other values are exact.

2.4 Depressed Inlets

Based on the same assumptions used for undepressed inlets, Izzard (1950) proposed the following equation for the capacity of depressed inlets:

$$Q_i = g^{1/2} \frac{2}{5} \left(\frac{2}{3}\right)^{3/2} (D_n + a)^{3/2} L_T \tag{2.30}$$

where a is the depression height illustrated in Figure 2.1(b). However, instead of using Izzard's approach, HEC-22 extends the non-depressed inlet equation for use with depressed curb inlets by defining an equivalent cross slope, S_e, to replace S_x in Equation (2.15):

$$S_e = S_x + S_w{}' \, E_o \tag{2.31}$$

where $S_w{}'$ is the added cross slope of the depressed gutter section, i.e., a slope relative to a line along the cross slope of the pavement, given by $S_w{}' = aw^{-1}$. Noting that geometry provides $S'_w = S_w - S_x$ and $0 \leq E_0 \leq 1$, it follows that

$$S_e = S_x(1 - E_o) + S_w \, E_o \tag{2.32}$$

which indicates the HEC-22 definition of S_e is simply a linear weighting of the compound gutter slopes based on the portion of the flow in the gutter depression versus that on the roadway. The resulting value of S_e replaces the uniform cross-slope S_x in Equation (2.15), so the HEC-22 depressed inlet equation is

$$L_T = k_i \, Q_g^{0.42} S_L^{0.3} \left(\frac{1}{n S_e} \right)^{0.6} \tag{2.33}$$

However, as shown in Equation (2.24), the S_x that appears in Equation (2.15) for undepressed inlets occurs because the normal depth at the upstream cross-section is used to represent the available head at the beginning of the inlet. Thus, there is an inconsistency in using S_e derived from a linear weighting and the original justification for the use of S_x. It seems likely that the HEC-22 approach using S_e is an approximation that allows better fitting to experimental data, as discussed in the following section.

2.5 Partial Interception

Allowing some gutter flow to bypass an inlet (i.e., less than full capture) is a recognized approach for cost-effective roadway design (Kranc et al. 1998; MacCallan and Hotchkiss 1996). Let $Q_g = Q_i + Q_b$ where Q_b is the bypass and Q_i is the intercepted flow over curb inlet length L_c, then it can be shown that the integral in Equation (2.22) evaluated over $\{0, L_c\}$ is

$$\frac{2}{5} L_T \left(1 - \left[1 - \frac{L_c}{L_T} \right]^{\alpha} \right) \tag{2.34}$$

where $\alpha = 5/2$ is required in the formal derivation. Similar to Equation (2.23) for full interception over L_T, we obtain the partial interception over L_c as

$$Q_i = g^{1/2} \, \frac{2}{5} \left(\frac{2}{3} \right)^{3/2} D_n^{3/2} L_T \left(1 - \left[1 - \frac{L_c}{L_T} \right]^{\alpha} \right) \tag{2.35}$$

The partial interception flowrate Q_i appears in HEC-22 with the inlet "efficiency" (E), defined as

$$E = \frac{Q_i}{Q_g} \tag{2.36}$$

Using Equation (2.23) for Q_g (full capture) and (2.35) for Q_i, the efficiency is formally derived as

$$E = 1 - \left(1 - \frac{L_c}{L_T}\right)^{\alpha} \tag{2.37}$$

Indeed, HEC-22 uses the above form for E, but with $\alpha = 1.8$ rather than the $\alpha = 2.5$ that is required by the derivation. Unfortunately, HEC-22 is silent on the precise reason for modifying the efficiency exponent. Unspecified experimental work at Colorado State University and the study of Bauer and Woo (1964) were cited as sources for their design procedures for curb inlets, with the latter relying on experiments of Karaki and Haynie (1961). Neither of the cited sources directly supports the use of $\alpha = 1.8$. However, we can make a reasonable case that the reduced exponent in the HEC-22 approach is related to the use of the equivalent slope (S_e) in Equation (2.33) for depressed inlets.

As noted in the previous section, use of S_e is inconsistent with the derivation of L_T for the undepressed inlet, which uses the normal depth at the upstream cross-section to represent upstream head. We hypothesize that matching experimental data while using the inconsistent L_T equation necessitated a smaller exponent of the efficiency equation. To test this hypothesis, we used the experimental data by Karaki and Haynie (1961) to compute L_T following HEC-22 with Equation (2.33). The computed L_T values were used to compute the inlet efficiency from Equation (2.37) while varying the exponent over $0.25 < \alpha < 2.75$. Our hypothesis is supported if the exponent $\alpha \sim 1.8$ provides the best match with the experimentally-observed efficiency,

which can be illustrated by computing the RMSE and R^2 for observed compared to computed efficiencies, as shown in Figure 2.4. The RMSE is a minimum between $1.5 < \alpha < 2$, and the R^2 does not significantly increase for $\alpha > 1.75$. Thus $\alpha = 1.8$ is a reasonable fit to the experiments and is clearly better than the derived value of $\alpha = 2.5$. The implication of fitting α to experimental data with a significantly different exponent is that it brings into question the L_T values in Equation (2.33). It seems likely that the mismatch is caused by a combination of rounding the equation's exponents and the inconsistent use of the equivalent cross-slope, S_e.

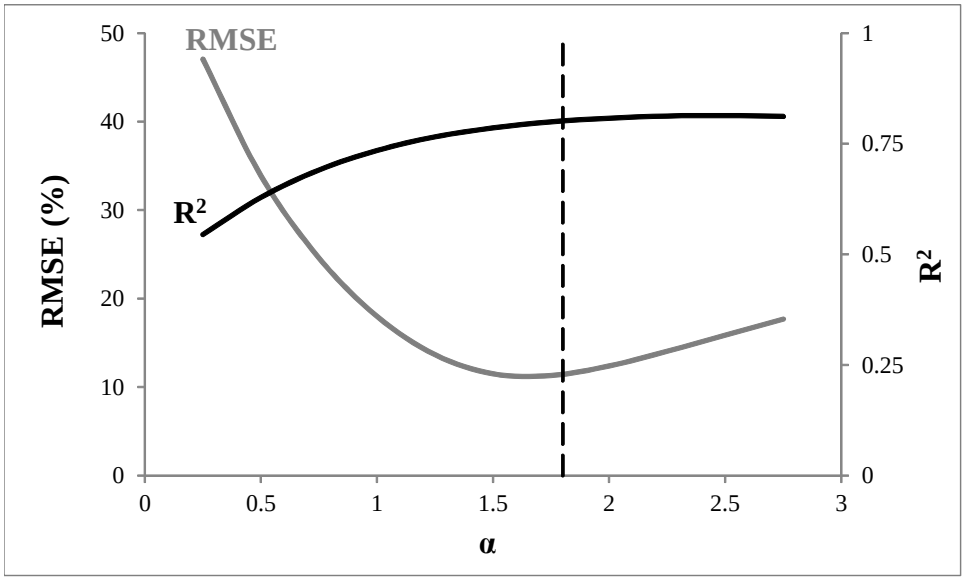

Figure 2.4: The RMSE and R^2 for comparing observed inlet efficiencies (Karaki and Haynie, 1961) and efficiencies computed by varying the exponent α of Equation (2.37).

2.6 Conclusions

Widely-used urban storm drainage guidelines are found in the U.S. Federal Highway Administration Circular No. 22 (HEC-22). Unfortunately, the accuracy of their curb inlet equations has been questioned in recent work (Schalla et al., 2017), and the report itself does not cite sources or explicitly derive the equations in

question. Herein, the missing theory and derivations for the on-grade HEC-22 curb inlet equations are developed. We have identified inconsistencies in the HEC-22 approach (as applied to depressed inlets) and departures of HEC-22 from theory derived using the approach of Izzard (1950). A notable conclusion is that the equations in HEC-22 equations have exponents that have been rounded, likely for simplicity in slide-rule computations. Furthermore, there is a significant discrepancy between the exponent in the inlet efficiency (E) equation derived from theory and the equation recommend in HEC-22. This discrepancy is a concern as it cannot be accounted for by simple rounding, and thus indicates a likely problem in the transition from theory to empirical fitting of the equations. It seems likely that this discrepancy results from an empirical fit that is compensating for inconsistencies in the HEC-22 approach to defining an equivalent cross slope (S_e) for a compound gutter.

Chapter 3

Hydraulics of Undepressed Inlets On-grade

3.1 Introduction

Sizing of curb inlets involves many structural, economical, and aesthetic considerations. From a hydraulic stand point, the design of curb inlets is mainly concerned with the interception capacity, which is the gutter flowrate captured by the installed inlet length given the upstream gutter and roadway conditions. Directing greater flow towards the inlet leads to an increase in the interception capacity, which can be achieved by increasing the roadway cross-slope and the roadway roughness. Conversely, increasing the roadway longitudinal slope directs more flow past the inlet (Jens, 1979). Another method of increasing the interception capacity is by depressing the edge of the gutter at the side of the curb by a few inches (Karaki and Haynie, 1961), hence inlets on a continuous cross-slope are known as undepressed inlets and inlets on a depressed gutter (compound section) are depressed inlets. However, a large depression can be unsafe to traffic and cyclists operations. Design manuals usually limit the depression height for fast-traveled roads, and some stipulate that depressed inlets are to be recessed into the curb. Recessing the inlets can be problematic if the sidewalk is not wide enough or if inlet would interfere with other utilities (TxDOT, 2016). Therefore, although depressed inlets have greater interception capacity compared to undepressed ones, several practical considerations make undepressed curb inlets a viable design option. Curb inlets are installed either 1) on-grade, where flow approaches the inlet from

one direction, 2) or in a sag, where the inlet is at a low point so the flow approaches the inlet from both directions. The current study is only concerned with the hydraulics of inlets on-grade.

Despite the utility of undepressed inlets, they were addressed by far fewer studies compared to depressed inlets. To illustrate this point: Among the 27 studies reviewed in preparation for the current study only two studies exclusively investigated undepressed inlets (Wasley, 1960; Spaliviero et al., 2000), five studies analyzed both undepressed and depressed inlets (Izzard, 1950; Hammonds and Holley, 1995; Li et al., 1951; Karaki and Haynie, 1961; Zwamborn, 1966), and the remaining studies dealt only with depressed inlets. Another concern that calls for further investigation of undepressed inlets is the significant discrepancies between the different proposed equations for undepressed inlets reported in the literature. Zwamborn (1966) observed significant difference in the inlet interception capacity at a given flow depth as given by equations from Li et al. (1951), Izzard (1950), and the proposed equation by Zwamborn. The current study provides a synthesis and evaluation of the available undepressed inlets equations. Based on this evaluation, updates to the design equations are proposed to provide more accurate predictions.

Setting up and modifying an experimental model is a laborious task associated with many challenges, which typically limits the range of tested conditions that are practical in a given laboratory (e.g., roadway roughness, slopes, flowrates). Where space and/or funds are limited, researchers resort to scaled physical models that are easier to manipulate and modify. Although the applicability of Froude-scaled models for depressed inlets is questionable (Grubert, 1988), for undepressed inlets the flow is more uniform over the cross-section, which can be argued to better support model scaling. The analysis of the hydraulics of undepressed inlets in this study provides

guidance about cases where scaled models are appropriate for undepressed inlets. Finally, unlike depressed inlets, a detailed theoretical model was proposed by Wasley (1960) for modeling flow in the vicinity of undepressed inlets. By investigating this model, and its shortcomings, the current study provides useful theoretical insights that future research may apply to other problems and applications.

The objectives of this study are to: 1) Evaluate the reported interception capacity equations for undepressed inlets and propose the updates to the equations where necessary, 2) Identify limitations in theoretical models of flow into undepressed inlets, and 3) Define cases where scaled models are applicable to undepressed inlets. First, we provide a review the available studies in the literature that investigated undepressed inlets and identify their underlying assumptions. The following section includes the discussion of proposed updates to undepressed inlet equations using experimental data from various studies. Section 3.4 provides a discussion of inlet-configurations that are disadvantageous for curb inlet effectiveness. The theoretical model provided by Wasley (1960) is analyzed in Section 3.5 and potential sources of discrepancies are identified. Finally, an analysis is provided for the application of scaled models to the study of undepressed inlets.

3.2 Review of Existing Inlet Capacity Equations

Overview

The equations presented in the literature for the interception capacity of undepressed inlets take the following form:

$$Q_i = b\, L_T\, d_n^e \tag{3.1}$$

where Q_i is the intercepted flow by the inlet at 100% interception condition (cfs), L_T is the inlet length required to capture 100% of the incoming gutter flow (ft), d_n is

the normal depth of gutter flow (ft), b is a constant whose dimensions depend on the exponent of d_n, and c is another constant (unitless). The normal depth d_n is related to the gutter flow Q_g using Manning's equation for gutter flow (Izzard and Hicks, 1947):

$$Q_g = \frac{0.56}{n\, S_x} {S_L}^{1/2} {d_n}^{8/3} \tag{3.2}$$

where Q_g is in cfs, S_L is the roadway longitudinal slope, S_x is the roadway cross-slope, n is Manning's roughness coefficient, and 0.56 has dimensions $\mathrm{ft}^{1/3}\mathrm{s}^{-1/2}$. Note that for 100% interception condition: $Q_g = Q_i$.

Izzard and HEC-22 equations

Izzard (1950) proposed the following equation for the interception capacity of undepressed inlets:

$$Q_i = 1.23\, L_T\, d_n^{3/2} \tag{3.3}$$

Izzard obtained the constant 1.23 $\mathrm{ft}^{1/2}$ s^{-1} based on theoretical considerations, however, Izzard modified the constant to be 0.7 based on experimental data. Hammonds and Holley (1995) showed that 1.23 is a significantly more accurate fit to their experiments. Equation (3.3) was adopted by HEC-22 with some modifications: HEC-22 used Manning's equation (Equation (3.2)) to eliminate d_n from Equation (3.3) and rounded the numerical coefficients in the final equation, as discussed in §2.3. Accordingly, the equation proposed by HEC-22 solves for L_T as:

$$L_T = 0.6\, Q_g^{0.42}\, S_L^{0.3} \left(\frac{1}{n S_x}\right)^{0.6} \tag{3.4}$$

Equation (3.4) can be converted back to the form presented in Equation (3.1)

(using Manning's Equation) to yield:

$$Q_i \approx 1.11\, L_T\, d_n^{1.57} \tag{3.5}$$

where 1.11 is in $\text{ft}^{0.43}\ \text{s}^{-1}$. Note that Equation (3.5) for HEC-22 does not converge with Equation (3.3) by Izzard due to the approximation of numerical coefficients by HEC-22. It is important to emphasize that HEC-22 uses a constant value for $b \approx 1.11$ and that the road slopes and roughness only appeared in Equation (3.4) due to using Manning's equation to eliminate d_n. In Equation (3.4), S_x has the same exponent as n and both have twice the exponent of S_L, as given by Manning's equation, which shows that HEC-22 accounts for the effects of roughness and road slopes implicitly in the term d_n.

The analysis by Izzard (followed by HEC-22) was based on some theoretical assumptions: The flow into the inlet was treated as flow over a broad crested weir, and integrated the flow along the inlet length to get the total intercept flow. As he lacked experimental observations of the water surface profile, Izzard assumed that the depth could be treated as linearly decreasing along the inlet length. Unfortunately, this assumption is inconsistent with later experiments of Wasley (1960) and Zwamborn (1966), who observed a sharp drop in the water depth a short distance from the upstream edge of the inlet. This sharp drop is followed by a semi-linear profile until the end of the inlet length. Comparison between the surface profile observed by Zwamborn (1966) and that assumed by Izzard (1950) is shown in Figure 3.1. Because the flow over a weir is proportional to the depth over the crest, treatment of the inlet flow as weir flow with a linear water profile that overestimates the depth will necessarily overestimate flow into the inlet.

Izzard also assumed that the transverse velocity component in the approach flow is negligible, i.e., the flow is driven into the inlet only by the flow depth and ignores the

contribution of the velocity head associated with the transverse velocity component. This assumption underestimates the flow into the inlet; the literature on flow into side weirs shows that the flow is not completely parallel to the side weir for both supercritical and subcritical flows (Bagheri and Heidarpour, 2011; Hager, 1987).

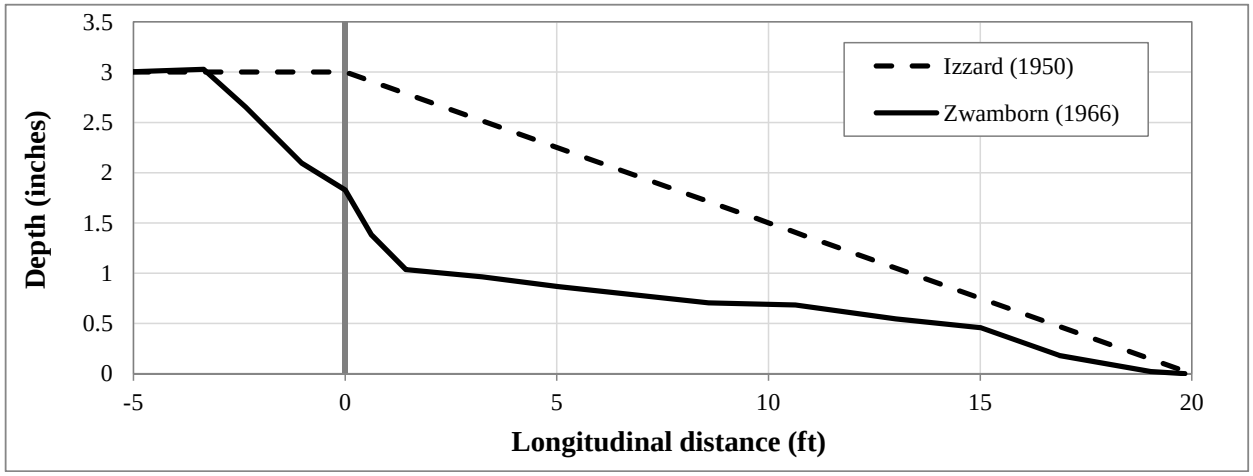

Figure 3.1: Assumed profile along undepressed inlets by Izzard (1950) vs observed profile by Zwamborn (1966) for S_L=0.625%, S_x=2.5%, and Q_g= 3 cfs, the inlet starts at station zero.

Zwamborn and the nonlinear water surface profile

Based on full-scale measurements, Zwamborn (1966) proposed the following equation to relate the depth d_o at the inlet (after the sharp drop) to the normal flow depth d_n to include effects of the nonlinear water surface profile:

$$d_o = 0.53\, d_n^{0.83} \tag{3.6}$$

where d_o and d_n are in ft. Zwamborn (1966) treated the flow into the inlet as weir flow and assumed a linear profile as well. However, the linear profile started at d_o instead of d_n, and the final proposed equation was:

$$Q_i = 0.8\, L_T\, d_n^{1.25} \tag{3.7}$$

where 0.8 is in $ft^{0.75}$ s^{-1}.

Li's free fall approach

Unlike Izzard and Zwamborn, Li et al. (1951) did not focus on the flow at the edge of the inlet but rather on the outer edge of the flow spread (farthest away from the curb). Li et al. (1951) assumed that the fall of flow from the edge of the spread (perpendicular to the curb) into the inlet is similar to a free-fall. By assuming a uniform velocity distribution and ignoring the resistance from friction, the inlet length could be found as the longitudinal distance covered by the flow until the outer edge of the flow *falls* into the inlet. The final proposed equation is (in the form of Equation (3.1)):

$$Q_i = K\, L_T\, d_n^{3/2} \tag{3.8}$$

where K is in $ft^{1/2}$ s^{-1}. Li et al. (1951) used 1/3 scaled experiments to determine the value of the parameter K, which varied only with S_x and was found to be 1.305 for S_x 8.33%, and 1.134 for S_x 4.167% and 2.083%. Li et al. (1951) assumed that the flow spread begins to decreases immediately at the cross-section at the upstream end of the inlet. However, observations in full-scale experiments by Wasley showed that the outer edge of the flow spread remains constant for a given distance downstream the beginning of the inlet before the spread begins to decrease towards the curb (Figure 3.2). The assumption of a premature decrease in flow spread is likely to overestimate the flow directed into the inlet, which will be evaluated using experimental data in the following section.

Wasley's dam failure approach

Wasley (1960) applied a complex theoretical approach to describe the velocity field in the vicinity of the inlet. The flow was simulated as the superposition of two elements 1) the instantaneous failure of a dam with a triangular reservoir and 2) an incoming velocity distribution (upstream the inlet). In Wasley's analysis, once the flow reaches the beginning of the inlet opening, a negative surge moves in the transverse direction towards the end of the flow spread. This negative surge is analogous to the surge that would be created in a reservoir in front of a dam that has just failed. However, the surge in the case of the inlet flow moves diagonally across the transverse section due to the effect of the incoming velocity distribution of the flow (highest velocity at the deepest section near the wall and velocity decreases towards the end of the spread, in contrast to a still triangular reservoir), as shown in Figure 3.2.

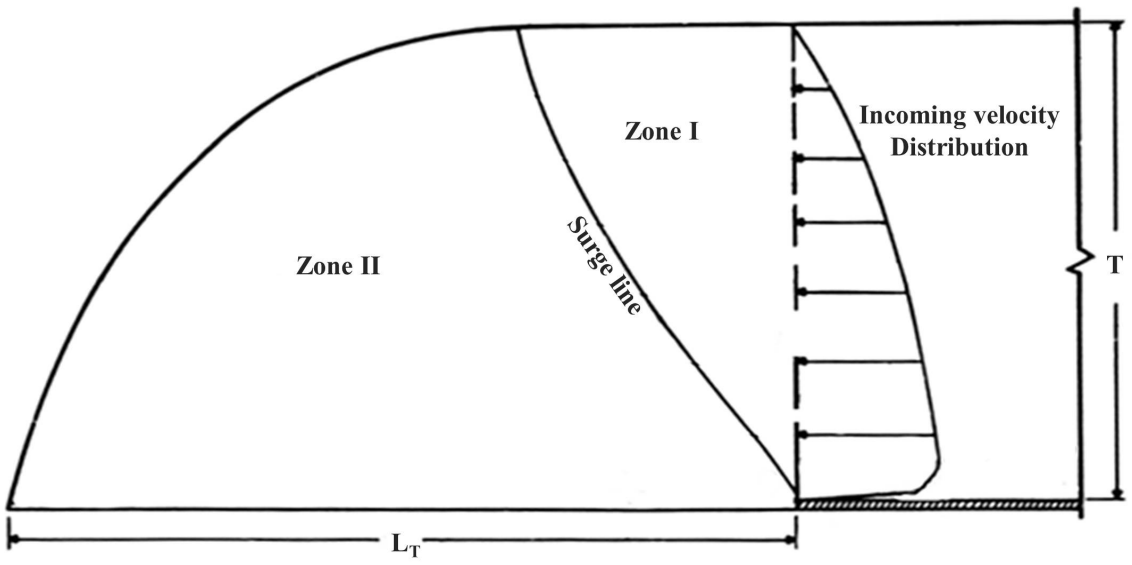

Figure 3.2: Plan view of two zones characterizing flow into undepressed inlets (modified after Wasley (1960)).

Wasley reported that this diagonal surge line could be observed visually during

experiments, and this line delineates Zone I of the flow that was not affected by the existence of inlet, i.e., where the incoming flow depth and velocity distribution were still similar to conditions upstream of the inlet. Zone II begins once the surge reaches the end of the spread, and at this zone Wasley assumed that the flow will fall into the inlet under gravity (alone) due to the existence of the slope S_x, which is similar to the assumed behavior by Li et al. (1951). Wasley (1960) did not provide a direct capacity relationship, and this approach was not widely used in design due to its complexity, especially at solving for an inner stream-line for a condition when the inlet intercepts less than 100% of the flow (Brandson, 1971). However a simple formula for the inlet length required for 100% interception can be derived using the following equations:

$$L_T = \frac{C_o T}{g}\left(1 + \frac{1}{\sqrt{2}}\right) \tag{3.9}$$

where T is the spread of the normal flow (ft), and C_o is computed as:

$$C_o = \sqrt{\frac{8\,g\,S_L}{f}} \tag{3.10}$$

where f is Darcy's friction coefficient. Substituting Equation (3.10) into (3.9) and eliminating T using the continuity equation ($Q = AV$) yields:

$$Q_i = 1.17\,L_T\,d_n^{1.5} \tag{3.11}$$

where 1.17 is in $\mathrm{ft}^{1/2}\ \mathrm{s}^{-1}$. The above is based solely on the theoretical derivation without empirical fitting to experiment, and showed good agreement with Wasley's experimental results except for flat cross-slopes (S_x) where shallow flows occurred. Wasley (1960) suggested that the discrepancy between the theoretical equation and the experimental results were due to ignoring the effects of friction and surface tension, which gain importance at shallow flow depths.

Spaliviero's empirical analyses

Spaliviero et al. (2000) conducted full-scale experiments, however only short inlets were tested (of lengths 1.64 and 0.82 ft) where the flow varied from 0.38 to 0.002 cfs, and only three tests were conducted for 100% interception. No equation for 100% interception was provided, only an equation for partial interception condition was provided by fitting of experimental data as follows:

$$E = 1 - 0.361 \frac{Q_g}{d_n^{1.5} L_c} \tag{3.12}$$

where E is ratio of intercepted flow to total gutter flow, and L_c is the installed inlet length (ft). This equation implies that 100% is achieved under the condition:

$$2.77 >> \frac{Q_g}{d_n^{1.5} L_c} \tag{3.13}$$

However, this method can not be used for design at 100% interception condition as no exact estimate is provided for the intercepted flow.

Hammonds and Holley empirical fitting

Finally, Hammonds and Holley (1995) conducted experiments on 3/4 scaled model for undepressed and depressed inlets. The model dimensions of the tested inlets were 3.75 and 11.25 ft. The final equation was obtained by fitting the intercepted flow per unit inlet length to the normal flow depth, which can be expressed in the form of Equation (3.1) as:

$$Q_i = 0.643 \; d_n \; L_T - 0.0248 \, L_T \tag{3.14}$$

where 0.643 is in ft s^{-1} and 0.0248 is in ft^2 s^{-1}. The above equation was based solely on empirical fitting of experimental data.

Summary

The constants b and c from different studies are summarized in Table 3.1.

Table 3.1: Constants b and c for undepressed capacity equations presented as Equation (3.1). The $\sim$ indicates that these values are approximate due to rounding up of coefficients by HEC-22.

Study	**b (units)**	**c**
HEC-22	$\sim$1.11 ($ft^{0.43}$ s^{-1})	$\sim$1.57
Izzard (1950)	1.23 ($ft^{1/2}$ s^{-1})	1.5
Zwamborn (1966)	0.8 ($ft^{0.75}$ s^{-1})	1.25
Li et al. (1951)	[1]1.134–1.305($ft^{1/2}$ s^{-1})	1.5
Wasley (1960)	1.17 ($ft^{1/2}$ s^{-1})	1.5
[2]Hammonds and Holley (1995)	0.643 (ft s^{-1})	1

[1] Varies with S_x, see text.
[2] The term $-0.0248L_T$ is added to the equation.

3.3 Updates to Inlet Equations

The literature is reviewed for experimental data that can be used to evaluate and update the coefficients of the inlet equations. Data was collected from five studies for undepressed inlets: Li et al. (1951), Wasley (1960), Spaliviero et al. (2000), Hammonds and Holley (1995), and Karaki and Haynie (1961). Unfortunately, the work of Zwamborn (1966), which considered effects of nonlinear water surface profiles, only provided graphs and partial results without the detailed experimental data needed for inclusion in the following analyses. Only two data points can be reliably obtained from one of the graphs in Zwamborn's study. Both Li et al. (1951) and Hammonds and Holley (1995) reported experiments and analyses based on Froude-scaled models so that smaller geometry and flowrates in the laboratory could be used to represent larger inlets and flowrates in the real world. Their results were mostly reported in terms of the larger inlets and flowrates

that were their study objectives. Herein, the results from these studies have been *unscaled*, i.e., their data has been returned to the original physical experiment dimensions by inverting the scale parameters. Using the physical model dimensions avoids potential errors that can be caused by scaling. The data from these five studies provided a total of 118 observations for 100% interception and 127 for less than 100% ($Q_g > Q_i$). Inlets with flat cross-slopes ($S_x < 3$) represents 30% of the dataset, and 30% of the inlets had flat longitudinal slopes ($S_L < 1\%$) where the flow conditions may follow the subcritical flow regime. Table 3.2 shows the ranges of parameters in the final dataset.

Table 3.2: Ranges of parameters in the final dataset of undepressed inlets.

	S_L (%)	S_x (%)	Q_g (cfs)	L_T (ft)	n
Max	6	8.33	6.48	35	0.017
Median	1	6	0.132	3.75	0.01
Min	0.2	1.042	0.002	0.82	0.01

The Pearson R and Kendall's τ correlation coefficients are computed between the intercepted flow Q_i and each of S_L, S_x, n, and d_n using the collected dataset, as summarized in Table 3.3. Both d_n and S_x should strong correlation with Q_i: Correlation coefficients are > 0.9 and > 0.48 for d_n and S_x, respectively. The correlation between S_x and Q_i is consistent with the findings of Li et al. (1951) where the coefficient b varied with S_x. As for S_L, only a weak correlation is observed as both correlation coefficients are of opposite signs and of value close to zero. In the case of n, a τ value of 0.16 suggests a possible influence of roughness on interception, which can be observed in the existing dataset through the variation of the coefficient of d_n with the roadway roughness. Li et al. (1951), Wasley (1960), and Spaliviero et al. (2000) conducted experiments on a smooth roadway (n=0.01),

while Hammonds and Holley (1995) used a rough roadway (n=0.017). The best fit for only the experiments with a smooth surface results in a exponent for d_n that is roughly 1.5, however, the exponent for the rough roadway is roughly 1 (Figure 3.3).

Table 3.3: Correlation between 100% interception flow and several parameters.

Coefficient	Parameter			
	d_n	S_L	S_x	n
$\boldsymbol{\tau}$	0.91	0.03	0.48	0.16
$\boldsymbol{R}$	0.99	-0.14	0.49	0.02

Non-linear regression analysis is conducted on the final dataset to evaluate various coefficients for the 100% interception equation, which takes the following form:

$$Q_i = b\, S_x^{a_1}\, n^{a_2}\, S_L^{a_3}\, d_n^c\, L_T \tag{3.15}$$

where a_1, a_2, and a_3 are dimensionless exponents.

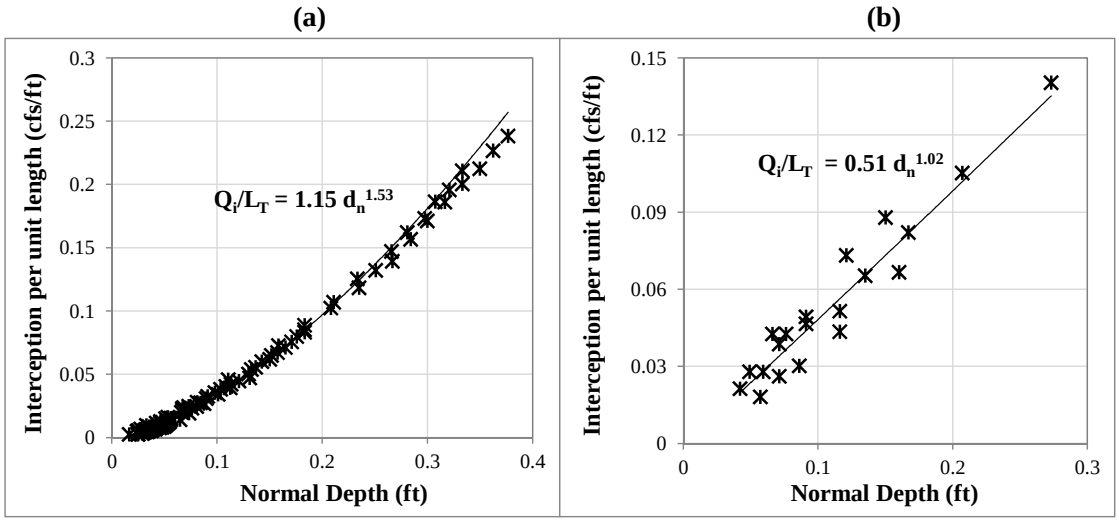

Figure 3.3: Fitting of experimental data: a) Smooth roadway, b) rough roadway.

If the target of the analysis is to minimize the RMSE, observations for high Q_i can overshadow low Q_i. Accordingly, the Mean Absolute Percentage Error (MAPE) is set

to a minimum in the analysis. The results of the regression analysis are summarized in Table 3.4.

Table 3.4: Summary of evaluated alternatives for updating the 100% interception equation.

#	b (units)	c	a_1	a_2	a_3	R^2	MAPE (%)	RMSE (cfs)
1	1.237 ($ft^{0.414}/s$)	1.586	0	0	0	0.995	16.43	0.073
2	1.65 ($ft^{0.59}/s$)	1.41	0.21	0	0	0.992	11.48	0.095
3	11.95 ($ft^{0.61}/s$)	1.39	0.23	0.43	0	0.994	9.74	0.08
4	13.89 ($ft^{0.62}/s$)	1.38	0.245	0.48	-0.016	0.992	9.68	0.094

Although Alternative#1 shows high R^2 and low RMSE, it systematically overestimates the interception of inlets with flat cross-slopes ($S_x < 3$), which is the reason for the high MAPE. Introducing S_x in Alternative#2 improves the MAPE, and further improvement is attained by using n as well, as shown in Alternative#3. Introducing S_L into the analysis does not result in a significant improvement in the MAPE, and conversely leads to a decrease in R^2 and an increase in RMSE. Consequently, Alternative#3 is chosen as the proposed update, and the updated 100% interception capacity equation is then:

$$Q_i = 11.95\, S_x^{0.23}\, n^{0.43}\, d_n^{1.39}\, L_T \tag{3.16}$$

Experimental data can be compared to the existing equations and the best-fit equation (above), providing the RMSE and the MAPE shown in Table 3.5. Among the existing equations, HEC-22 and Wasley (1960) provide the best predictions in terms of the RMSE and MAPE. Izzard (1950) and Li et al. (1951) provide low MAPE yet high RMSE. Conversely, Zwamborn (1966) and Hammonds and Holley (1995) provide low RMSE but high MAPE, note that the negative term in the empirical fit of Hammonds and Holley (1995) Equation (3.14) computes results in negative

interception values for inlets with small interception. Ultimately, the proposed best-fit equation of the present work results in the RMSE and MAPE among the evaluated equations, roughly halving the MAPE of the second best equation (HEC-22).

Table 3.5: RMSE and R^2 from comparing experimental data to undepressed inlets design equations.

	MAPE (%)	**RMSE (cfs)**
HEC-22	18.05	0.102
Izzard (1950)	23.36	0.165
Li et al. (1951)	21.49	0.204
Hammonds and Holley (1995)	53.12	0.109
Zwamborn (1966)	43.52	0.104
Wasley (1960)	19.87	0.107
Proposed	9.74	0.08

The performance of HEC-22 equations for 100% interception is evaluated more closely and compared to the proposed equation, as shown in Figures 3.4 and 3.5. Generally, Figures 3.4-a and 3.5-a show that HEC-22 underestimates the inlet capacity, and the underestimation exceeds 25% for many observations. Conversely, Equation (3.17) provided good match with the data; as can be observed by the limited scatter of observations in the graph Figures 3.4-b and 3.5-b. Consequently, we recommend using Equation (3.17) for computing the 100% interception capacity of undepressed inlets.

The depth of flow is not readily known by designers, usually the roadway slopes, roughness, and gutter flow are known and are used to compute the spread or depth of flow using Manning's equation. To facilitate the application of Equation (3.17), Manning's equation (for gutter flow) was used to replace the depth in terms of known roadway parameters. The final form of Equation (3.17) is similar to Equation (3.4)

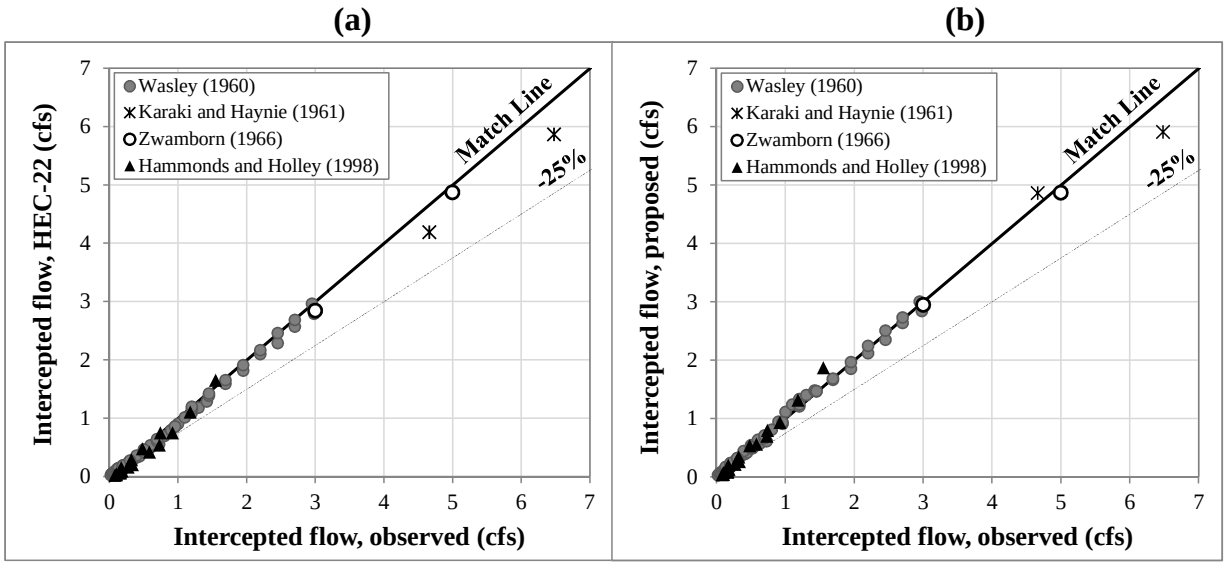

Figure 3.4: Observed vs computed 100% intercepted flow for high gutter flows: a) HEC-22, b) Equation (3.16).

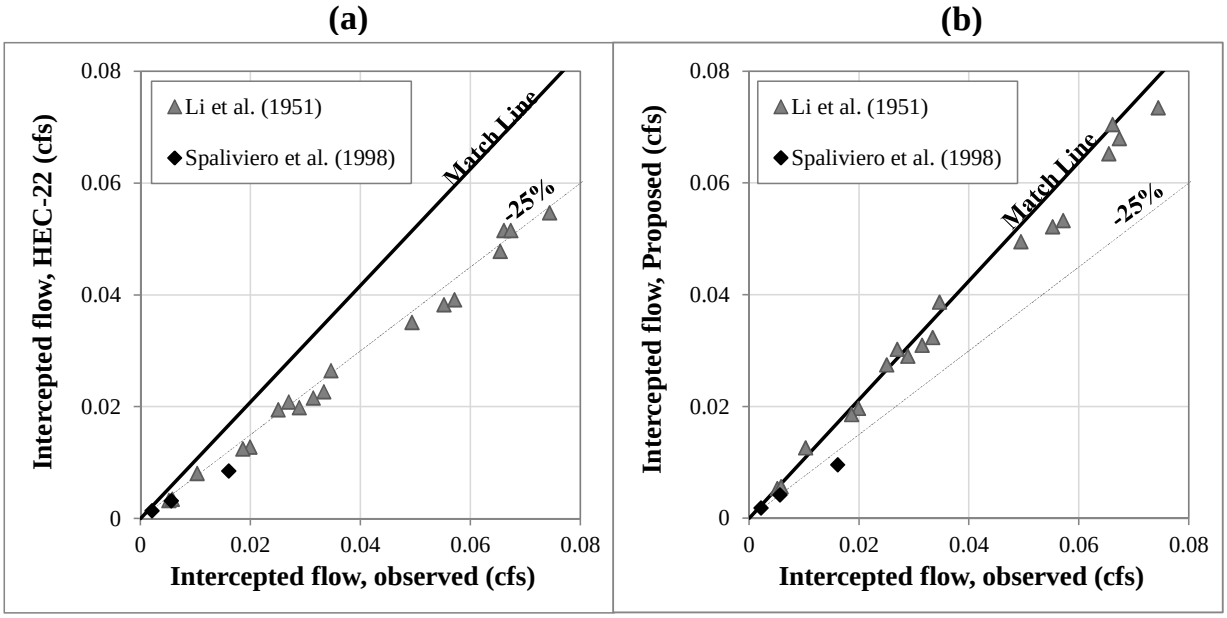

Figure 3.5: Observed vs computed 100% intercepted flow for low gutter flows: a) HEC-22, b) Equation (3.16).

provided by HEC-22 (but with different numerical coefficients):

$$L_T = 0.062\, Q_g^{0.47}\, S_L^{0.26}\, n^{-0.95}\, S_x^{-0.75} \tag{3.17}$$

where L_T is in ft, Q is ft^3 s^{-1}, n is taken as non-dimensional, and the dimensions of the coefficient provide consistency between right and left sides of the equation.

Inlets operate at partial interception condition when the incoming gutter flow is higher than the 100% interception capacity of the inlet, and also allowing a small portion of flow to bypass the inlet is a common cost-effective approach in roadway drainage design TxDOT (2016). HEC-22 defines the inlet efficiency (E) as the ratio between intercepted flow and incoming gutter flos (i.e., Q_i/Q_g). The efficiency equation is reported in several studies as:

$$E = 1 - \left[1 - \frac{L_c}{L_T}\right]^{\alpha} \tag{3.18}$$

where L_c is the installed inlet length (ft), L_T is the required length to intercept 100% of the gutter flow (ft), and α is a constant. HEC-22 uses 1.8 as the value of α, Zwamborn (1966) uses 1.5, and Izzard (1950) uses 2.5. Relatively few experiments can be used to verify Equation (3.18) as typically L_c is fixed and L_T is simply presumed. A notable exception is the study by Karaki and Haynie (1961) where the gutter flow was fixed and the inlet length was changed in increments until the entire gutter flow was captured. Figure 3.6 shows the comparison between observed and computed efficiency by HEC-22 (α=1.8) where E is computed both with the HEC-22 value for L_T (from Equation (3.4)) and the experimentally-observed value for L_T. In general, computing E using the HEC-22 values for L_T provides better agreement than the actual measured L_T. Using the observed L_T (which should be more accurate) results in a bias towards underestimating L_T, thus indicating that the HEC-22 computation for L_T has a bias that is compensating for bias in the L_T equation. It follows that

any approach that provides accurate values of L_T (e.g., Equation (3.17)) if coupled with the HEC-22 Equation for E will lead to an uncompensated bias of E for bypass flow.

Figure 3.7 shows that E computed using the observed L_T provides good match with observed E if α=1.35 is used (rather than 1.8). However, α might not be a constant and the value 1.35 might be for the specific configuration tested by Karaki and Haynie (1961). Regression analysis is applied to Equations (3.17) and (3.18) to determine the value of α that computes E best matching with observations. The best match was obtained when α was computed as a function of the cross-slope. Including the roughness coefficient and the longitudinal slope did not significantly improve the predictions. Accordingly, the final expression for computing α:

$$\alpha = \frac{0.42}{S_x^{0.42}} \tag{3.19}$$

Applying Equation (3.19) to the experiments of Karaki and Haynie (1961) yields α=1.37, which is quite similar to the value 1.35 obtained from experimental results.

The overall accuracy of the best-fit approach proposed in this study, Equation (3.17), can be tested against available experimental data for bypass flow conditions. The L_T is computed from Equation (3.17) then E is computed using Equation (3.18) with α computed from Equation (3.19). The E computed from the proposed best-fit approach and from HEC-22 are compared to observed E in Figure 3.8. Most values for the computed E by both approaches are within the $\pm$25% bounds. However, generally HEC-22 underestimates the interception by the inlet, with severe underestimation beyond 25% in some cases.

Comparing the computed vs. observed E for both approaches shows that the R^2

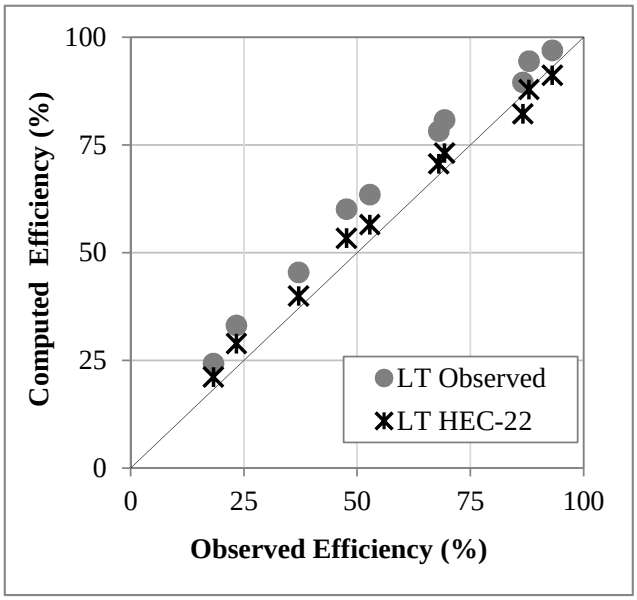

Figure 3.6: Computed inlet efficiency based on HEC-22 values for L_T and observed values L_T, as compared to observed efficiency of Karaki and Haynie (1961).

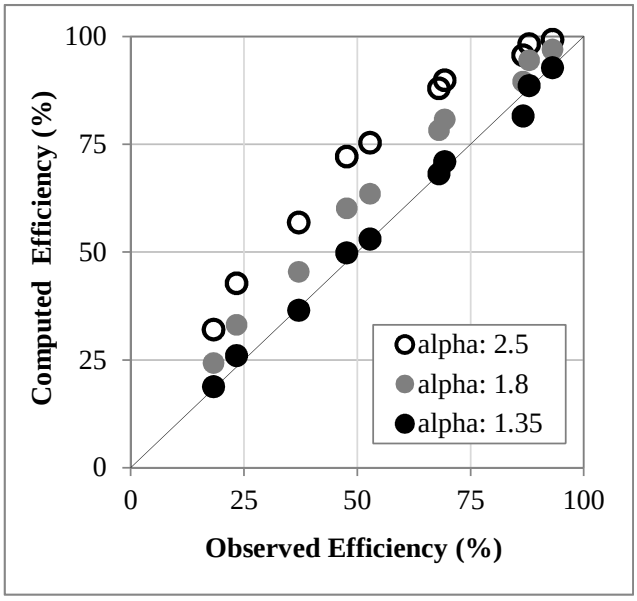

Figure 3.7: Computed inlet efficiency based on Equation (B.6) using observed L_T and α= 1.8 and 1.35, as compared to observed efficiency of Karaki and Haynie (1961).

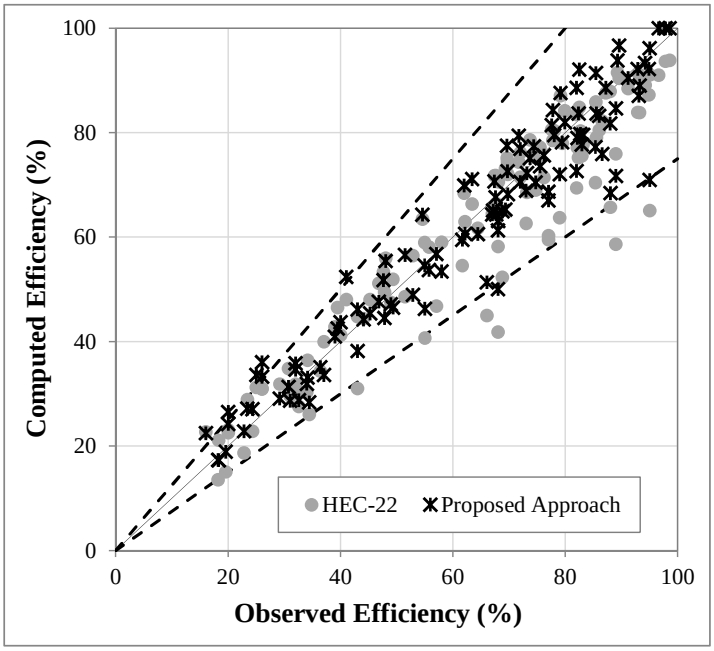

Figure 3.8: Computed efficiency using the proposed approach and using HEC-22, as compared to observed efficiency from several studies.

is 0.93 and 0.886, and the RMSE is 6.2% and 8.2% for the new best-fit approach and HEC-22, respectively. Generally, HEC-22 provides a reasonable estimate for E for partial interception, however, HEC-22 significantly underestimates the 100% interception capacity (as shown earlier in Figures 3.4-a and 3.5-a). Therefore, the new approach overcomes the HEC-22 limitations at 100% interception and also provides a better estimate of E compared to HEC-22 for partial interception condition.

3.4 Deficiency of Curb Inlets on a Combination of Steep Grade and Flat Cross Slope

Wasley (1960) conducted full-scale experiments for undepressed inlets at 100% interception. However, the 100% interception condition could not be achieved for slope configuration of S_L=5% and S_x =1.042%; as flow tended to simply go past the

inlet. All design equations (discussed in §3.2) significantly overestimated the inlet efficiency in this configuration, including HEC-22 (which was shown earlier to significantly underestimate the efficiency in other configurations). In support of Wasley's remark, the discrepancy between computed and observed efficiency decreased as the gutter flow increase (thus flow depth increases as well.), as shown in Figure 3.9. The ratio between E computed from HEC-22 and observed dropped from 2 (100% overestimation) at Q_g=0.0064 cfs to 1.25 at Q_g=0.09 cfs (25% overestimation). This phenomenon was observed in experiments for depressed inlets as well. During full-scale experiments conducted by Schalla (2016) for depressed inlets at 4% S_L and 2% S_x configuration, flow tended to go past the inlet along the outer edge of the gutter. The 100% interception condition for this configuration was barely achievable at steep longitudinal slopes. A similar tendency can be found in the work of Hammonds and Holley (1995), in the tests with S_L of 7% and 8% and S_x of 2.08%, the 100% interception could not be attained and the reported inflow was zero. Also, during tests for $S_L > 3\%$ and $S_x = 2.08\%$, the observed flow spread was on average twice the expected normal flow spread; which indicates that the flow is moving in the longitudinal direction over a wider section instead of accumulating towards the curb.

It is useful to note that the older FHWA design criteria in Jens (1979) recommended that undepressed inlets not be used for $S_L > 3\%$, which indicates there is likely some evidence that undepressed inlet behavior is compromised at steep slopes. However, experiments by Hammonds and Holley (1995) and Li et al. (1951) show that a curb inlet on a steep grade can still be effective on grades of 4% and 6% as long as a steep cross slope (>3%) was used as well. We speculate that the degradation in inlet performance is related to the flow depth, boundary layer

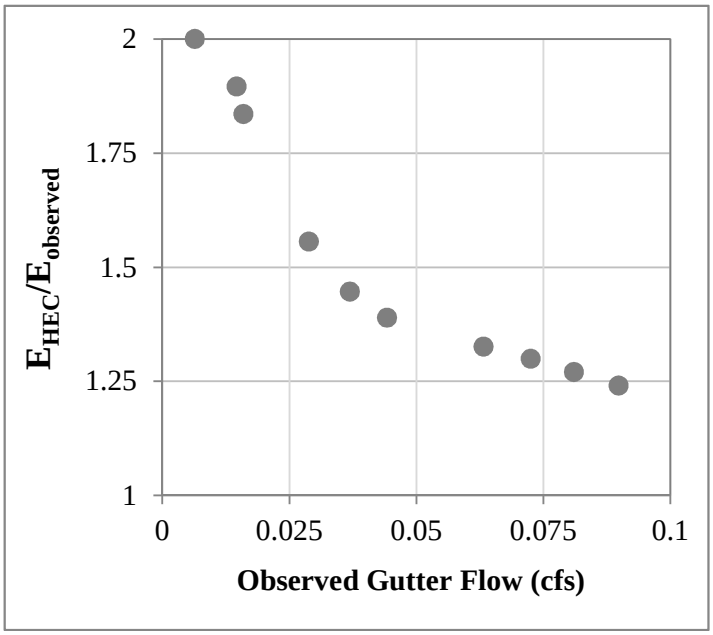

Figure 3.9: Ratio between HEC-22 computed and observed E for a range of gutter flow at S_L=5% and S_x =1.042% by Wasley (1960).

evolution, and/or the ratio between the flow depth and the roughness height of the roadway. In-depth analysis of these possibilities could be an interesting topic for future research. Nevertheless, despite the present lack of specificity in the existing research, it is clear that inlets (depressed and undepressed) on steep grades and flat cross-slopes are expected to have significantly lower interception compared to that computed from design equations. A different type of inlet (e.g., grate or combination inlet) may prove more effective at this slope-configuration.

3.5 Analysis of Wasley's Approach

The proposed best-fit approach in the current study (Equation (3.16) and α=1.4) shows good match with experimental data for 100% interception and bypass flow conditions. Beyond this new empirical fitting, a new analysis of the theoretical

model proposed by Wasley (1960) provides additional insight into the hydraulics of curb inlets flow. Wasley provided extensive experimental data for undepressed inlets, including the water surface profiles along the edge of the inlet for at least two runs at each slope configuration. Instead of delving into the details of Wasley's complex theoretical model, this data is used below with a weir-flow model for the inlet, similar to that used by Izzard (1950) and Zwamborn (1966).

Wasley provided experimental data for the water depth along the length of the inlet. We use the water profile data for the maximum and minimum discharge of each slope configuration but we exclude the data for $S_L = 5\%$ and $S_x = 1.042\%$ as they significantly departed from the norm (as discussed in §3.4). We nondimensionalize the water surface profile by dividing the depth at each increment of inlet length by the normal depth, and dividing each increment length by the total inlet length. The data converge neatly and the aggregated dimensionless water profile is presented in Figure 3.10.

Generally for the tested configurations, the water depth dropped sharply right after the beginning of the inlet followed by a mild decrease in depth until 80% of the inlet length, where the depth dropped sharply towards the end of the inlet. This water profile is similar to those observed by Zwamborn (1966), as shown earlier in Figure 3.1. For the present work, we fit the water profile using three straight lines to facilitate the integration over the inlet length. In this analysis, critical depth is assumed at the edge of the inlet. However, contrary to Izzard's (1950) assumption that the flow velocity *does not* contribute to flow into the inlet, herein the we will consider a velocity component towards the inlet (perpendicular to the main flow direction).The discharge per unit length of the inlet can be computed by the critical

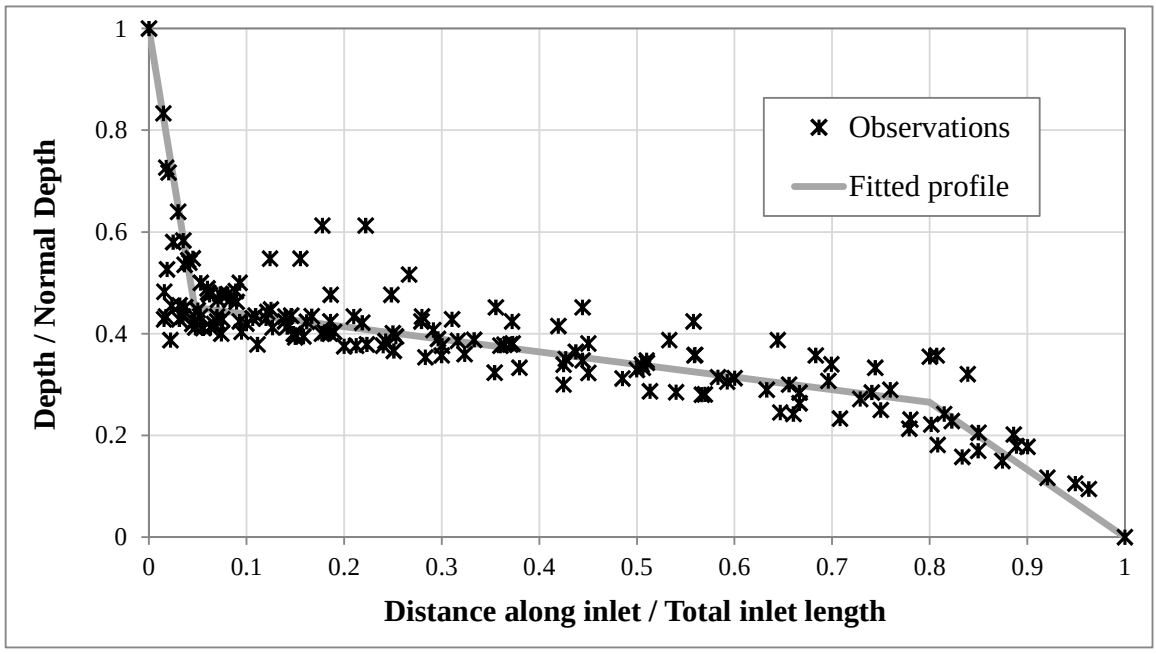

Figure 3.10: Aggregated dimensionless water surface profile at undepressed inlets, from experiments by Wasley (1960).

flow equation:

$$q = \sqrt{g\, d_c^3} \tag{3.20}$$

where q is the discharge per unit inlet length (cfs/ft) and d_c is the critical depth (ft), which is assumed to be equal to the depth d_i at any point along edge of the inlet. The inflow ΔQ_i along a segment ΔL of the inlet can be given by:

$$\Delta Q_i = g^{1/2}\, d_i^{3/2}\, \Delta L \tag{3.21}$$

Equation (3.21) can be nondimensionalized by diving both sides of the equation by $g^{1/2} d_n L_T$. The dimensionless discharge equation is then integrated over the three water profile segments, shown in Figure 3.10. The dimensional form of the equation is obtained again by multiplying both sides by $g^{1/2} d_n L_T$. The final equation is:

$$Q_i = 1.16\, L_T\, d_n^{1.5} \tag{3.22}$$

Equation (3.22) is strikingly similar to the design equation proposed by Wasley (Equation (3.11)), thus they will be treated as essentially the same for the rest of this analysis. Equation (3.22) provides accurate predictions for interception of inlets at steep S_x, however, the equation overestimates interception at flat S_x configurations. In the derivation of Equation (3.22), flow into the inlet is assumed to be perpendicular to the main flow direction, which is more likely to be the case for steep S_x. When the flow is perpendicular to the main flow direction, $\sin\theta = 1$ (Figure 3.11), and at the other extreme, $\sin\theta = 0$. For the case of sine(θ)=1, Equation (3.22) is simply multiplied by one. The case of $\sin\theta = 0$ resembles the flow over a broad crested weir with negligible velocity head. The flow per unit width in such case is given by Chaudhry (2007):

$$q = \left(\frac{2}{3}\right)^{3/2} \sqrt{g\, d_c^3} \tag{3.23}$$

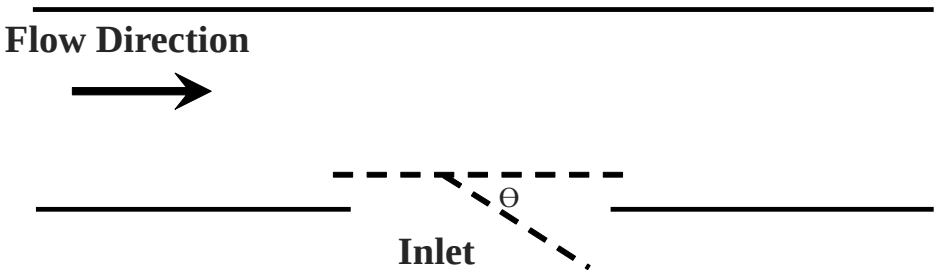

Figure 3.11: Schematic diagram for the angle of the inlet inflow with the main flow direction (θ).

Dividing Equation (3.20) by Equation (3.23) yields:

$$\frac{q_{90}}{q_0} = \frac{1}{0.544} \tag{3.24}$$

Any flow angle other than zero or 90 would introduce a factor to the calculations ranging from 1 (90 degrees) to 0.544 (zero degrees). To investigate whether the overestimation in inlet length by Equation (3.22) is due to ignoring the flow angle, a correction factor F_c is defined as:

$$F_c = \frac{Q_i}{1.16\, d_n^{3/2}\, L_T} \tag{3.25}$$

If the overestimation in Equation (3.22) was due to ignoring the flow angle, then the factor F_c should range from 0.544 to 1. The histogram of the values of F_c is shown in Figure 3.12. Almost all the values of F_c fall between 0.55 and 1 (with exception of two mild outliers with values 1.03 and 1.08). Guidance in determining an expression for θ may be sought in the literature for flow over side-weir such as Hager (1987). Experiments by Bagheri and Heidarpour (2011) showed that the angle of flow over the side-weir varies along the weir length, however obtaining a representative average value might suffice for design purposes.

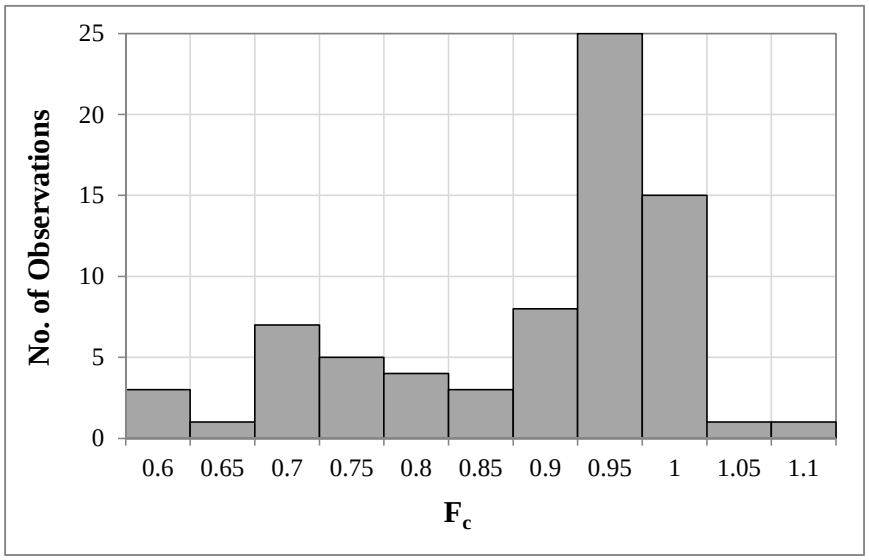

Figure 3.12: Aggregated dimensionless water surface profile at undepressed inlets, from experiments by Wasley (1960).

3.6 On the Use of Scaled Models

As discussed in Section 3.1, most of the experimental inlet studies reported in the literature were conducted on scaled models, which have been widely accepted in the past but have recently been critically questioned. Russo and Gómez (2013) provided a discussion of the Comport and Thornton (2012) inlet experiments with a question as to whether the use of a 1:3 scale model is appropriate for such flows. Similarly, Grubert (1988) performed full-scale and 1:2 scaled experiments for depressed inlets and argued that Froude Number scaling can accurately model inlet flow only after applying a correction factor to the scaling ratio. Argue and Pezzaniti (1996) compared results from full-scale and 1:2.5 scaled models, and concluded that the scaled model significantly underestimates the inlet's capacity. Zwamborn (1966) conducted full-scale and 1:6 scaled experiments for both depressed and undepressed models, these experiments showed that scaled models underestimates the inlet interception capacity, especially at shallow flow. Zwamborn observed that the discrepancy between full-scale and scaled models was larger in the case of depressed inlets, and that this discrepancy in the case of undepressed inlets becomes trivial as the flow depth increases. These studies suggest that the effects of Reynolds number (e.g., on the boundary layer) are significant in depressed inlets and for shallow flows in undepressed inlets, therefore scaled models might not be appropriate for the study of curb inlets for a wide range of conditions. Conversely, Johns Hopkins University (1956) reported that their 1:2 scaled experiments matched field tests within 2% difference (Note that Li et al. (1951) performed their experiments as part of this study). Also, Spaliviero et al. (2000) performed tests on 1.64 and 0.82 ft undepressed inlets, and concluded that the inflow into 0.82 ft inlet when scaled up to match a 1.64 ft inlet is equivalent to the flow intercepted by the tested 1.64 ft

inlet. These conflicting results call for further investigation of this issue.

Experimental data for undepressed inlets from Wasley (1960), Li et al. (1951), Spaliviero et al. (2000), and Hammonds and Holley (1995) can be examined in search for inlet lengths within the same study that can be related with a scaling ratio. For example, Hammonds and Holley (1995) tested 3.75 ft inlets for various slope configurations, then they tested 11.25 ft inlets for the same slope configurations. Consequently, the 3.75 ft inlets are treated as a 1:3 model of the 11.25 ft inlets. Flow into short inlets is scaled up using the following relation:

$$Q_p = \frac{Q_m}{L_r^{5/2}} \tag{3.26}$$

where Q_m is the flow at the model in cfs (short inlet), Q_p is the flow at the prototype in cfs (long inlet), and L_r is the geometric scale ratio (e.g., 1:3 or 1:2). We can apply this same procedure to data from the other three studies where a sufficient number of observations were available at 1:2 scale. The capacity of the full-scale (long inlets) is compared to the scaled (short inlets) in Figure 3.13. There is no observable difference between scaled and full-scale inlets in the cases of data from Wasley (1960), Li et al. (1951), and Spaliviero et al. (2000). Conversely, there is a significant discrepancy in the case of using data from Hammonds and Holley (1995). A possible explanation for this outcome is that the first three studies used smooth roadway surfaces (n=0.01), while Hammonds and Holley used a very rough surface (n=0.017). In the case of the smooth surface, friction plays less of a role compared to gravity, unlike the case of a rough surface.

This proposition can be elaborated further by examining the form of the undepressed inlet capacity equation. Figure 3.3 (presented earlier in §3.3) shows that the exponent of the normal depth in the capacity equation varies with the

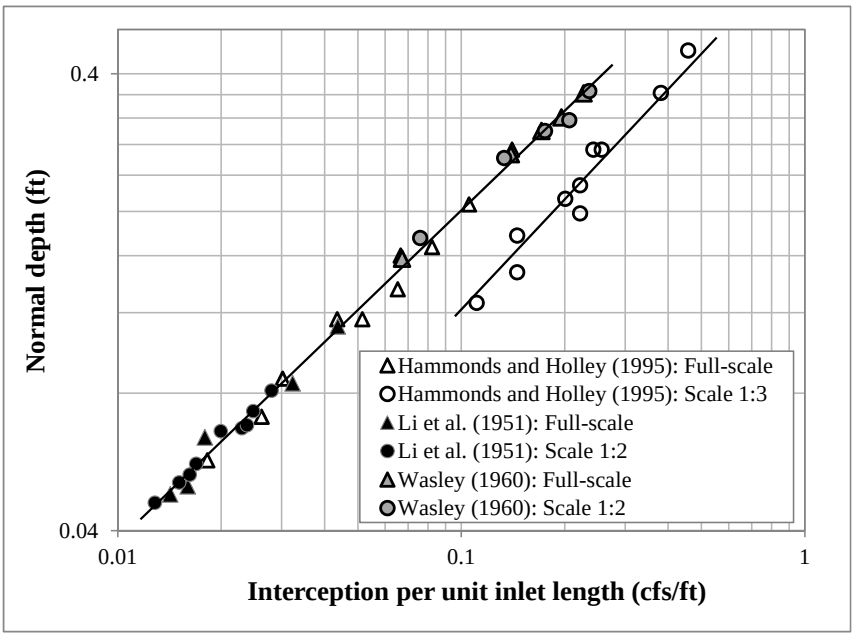

Figure 3.13: Comparison between full-scale and scaled interception of undepressed inlets.

roadway roughness: The exponent is equal to 1.5 for smooth roadway and 1 for rough roadway. A dimensionally consistent relationship can be readily developed as a function of new coefficients b_1, b_2, b_3 and b_4. For the case of a smooth roadway, the capacity equation is rewritten as:

$$Q_i = b_1 \, L_T \, d_n^{3/2} \tag{3.27}$$

where $b_1 = b_2 \sqrt{g}$. From dimensional homogeneity, b_2 is a dimensionless constant (it is not affected by scaling). By applying scaling to Equation (3.27), Q_p is obtained as:

$$\begin{aligned} Q_p =& b_2 \sqrt{g} \left(\frac{d_n}{L_r}\right)^{3/2} \left(\frac{L_T}{L_r}\right) \\ Q_p =& b_2 \sqrt{g} \, (d_n)^{3/2} \, L_T \, L_r^{-5/2} \end{aligned} \tag{3.28}$$

which is the same result from the Equation (2.20) for Froude Number scaling. In the case of the rough surface:

$$Q_i = b_3 \, L_T \, d_n \tag{3.29}$$

where $b_3 = b_4 \sqrt{g}$. From dimensional homogeneity, b_4 has the dimensions of $L^{1/2}$, i.e., length scaling will be applied to the parameter b_4. The additional scaling of a parameter of less-studied nature might be the source of discrepancy in case of the rough surface models. This analysis helps to explain the findings of Johns Hopkins University (1956) and Spaliviero et al. (2000) regarding the validity of scaled modeling as they used a smooth surface for their model (n=0.01). Conversely, Zwamborn (1966) and Argue and Pezzaniti (1996) used a rough surface (n=0.014), which is shown here not to follow Froude scaling.

Applying a similar analysis to depressed inlets is more challenging as the dimensions of the depressed gutter should be taken into consideration while scaling the inlet length, therefore fewer observations are available to conduct this analysis. Karaki and Haynie (1961) conducted full-scale experiments for depressed inlets on a smooth roadway (n=0.0093). Two of the tested configurations included a gutter with width 2 ft and depression 2 inch, and width 1 ft and depression 1 inches. These two configurations are used herein as a full-scale and 1:2 scaled models. Schalla (2016) conducted full-scaled experiments on 5-ft and 15-ft depressed inlets on a roadway with roughness n=0.0166, and Hammonds and Holley (1995) tested depressed inlets of lengths 3.75-ft and 11.25-ft with roadway roughness n=0.017 (less than 2.5% difference from the roughness tested by Schalla et al.). The depressed gutter tested by Hammonds and Holley (1995) can approximately scale into 3/4 model for Schalla's gutter, which fulfills the scaling for the inlet length as well (e.g., 11.25/15 = 3/4). Figure 3.14 shows the difference between the observed and scaled interception for experiments at the same longitudinal and cross slopes. For the case of the smooth roadway (Karaki and Haynie (1961)), the difference between scaled and full-scale interception was 2.46% on average. However, the

scaled experiments (Hammonds and Holley (1995)) for the rough roadway overestimated interception by 50% on average compared to full-scale (Schalla (2016)). These results are in agreement with the analysis in Figure 3.13. However, only few observations are available for the case of a depressed inlet on a smooth roadway, therefore further experiments should be provided before confidence be obtained in the validity of scaled models for depressed inlets on smooth roadways.

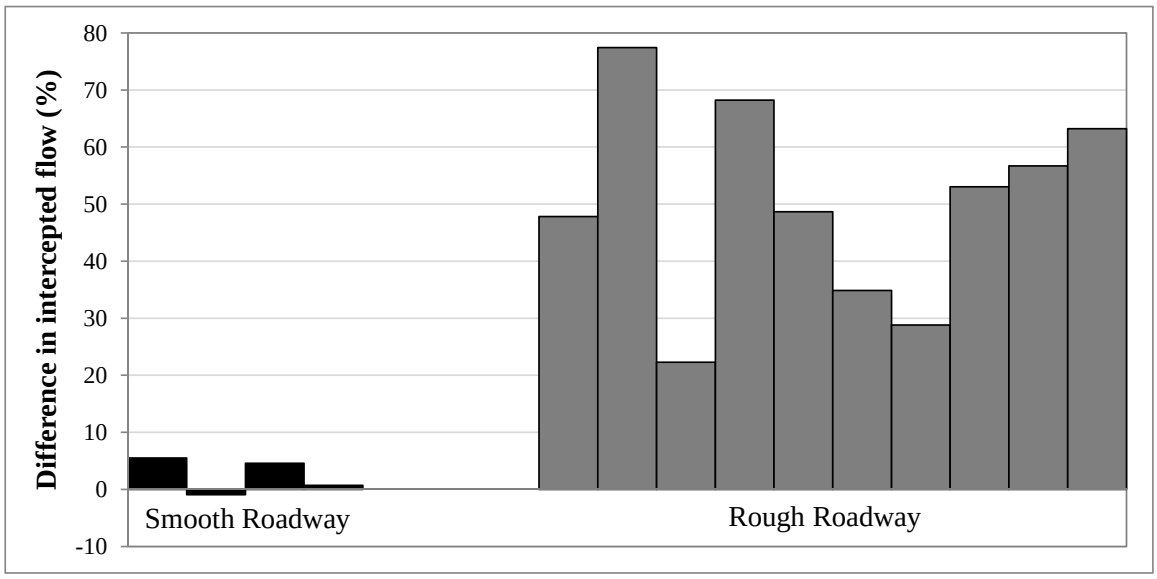

Figure 3.14: Comparison between full-scale and scaled interception of depressed inlets.

In conclusion, this analysis suggests that scaled models are appropriate for modeling undepressed inlets on smooth roadways but is questionable for the higher surface roughness that is typical of real-world roadways. Note that further investigation is required to validate this analysis for depressed inlets on smooth roadways due to the current lack of experimental data.

3.7 Conclusions

Undepressed curb inlets are installed where a gutter depression is unsafe and where grates are not desirable due to either clogging or safety concerns. Several design equations for undepressed inlets are reported in the literature, but the most commonly used are the HEC-22 equations recommended by the FHWA. In the present study, the HEC-22 equations and other design approaches were evaluated with a new analysis that combines experimental data from several prior studies.

In the present analysis, HEC-22 equations is shown to generally underestimate the inlet capacity at 100% interception. Similarly, the HEC-22 equations for partial interception overestimate the inlet efficiency when observed values of inlet length are used in the efficiency computation; however, their equations provide accurate efficiency predictions when the erroneous HEC-22 100% capture inlet lengths are used. Thus, the HEC-22 approach for partial interception is consistent with observations *only when the full HEC-22 approach is used.* This observation indicates that the efficiency equation proposed by HEC-22 has an offsetting bias that compensates for the bias in the HEC-22 100% interception equation. Regression analysis was applied to literature data and data collected in this research to develop coefficients for Equation (3.1) that are consistent across all the available data for 100% interception. The new coefficients reduce the percentage error by a factor of 2 compared to HEC-22 computations. A different exponent was proposed for the efficiency equation, and the overall new approach provided better match with the data at bypass condition compared to HEC-22.

Several prior studies showed that the effectiveness of both depressed and undepressed inlets deteriorates when a flat cross-slope is used with a steep longitudinal slope. These results were confirmed, albeit in a limited fashion, by the

few experiments conducted herein on steep slopes. Wasley (1960) conducted extensive theoretical and experimental investigations for the performance of undepressed inlets that included flat cross-slopes, which were re-analyzed herein. Wasley's model was inaccurate for inlets on a flat cross-slope. The new analysis of the experimental data from all available sources inspired a new, alternative derivation of Wasley's design equation, which suggests that inaccuracies in Wasley's predictions are due to ignoring the angle of flow into the inlet. However, we do not as yet have enough data in the literature to develop robust design equations for steep longitudinal slopes across a range of cross slopes. Until further work is conducted, designers should be aware that curb inlets will not perform according to any design equations in such configurations.

Finally, we presented an analysis that provides a potential explanation for the apparent conflict in the reviewed literature regarding the applicability of scaled models to the study of curb inlets. In each experimental dataset, short inlets are scaled to correspond to long inlets and the observed vs. scaled discharge are compared. Froude number scaling is shown to be applicable for undepressed inlets on a smooth surface, but does not accurately model inlets on a rough surface. Primarily results provide evidence supporting the validity of scaled models for depressed inlets on a smooth roadway. Further investigation is required to confirm the findings in the case of depressed inlets due to the current lack of experimental data.

Chapter 4

Interception Capacity of Depressed Curb Inlets On-grade

4.1 Introduction

The hydraulic design of curb inlets is mainly concerned with the interception capacity of the inlet, which is the amount of flow a given inlet length can capture at certain approach flow, gutter, and roadway conditions. Clearly, a desired gutter capacity can (in theory) be reached by extending the inlet length, but there are limitations in the design of manholes and curb structures that limit the maximum inlet opening. An accepted way to increase the inlet capacity for a fixed inlet length is by allowing a small amount of flow to bypass the inlet at design flow conditions. Due to the non-linearity in the interception equations, a small bypass (reduction in inlet efficiency) is recognized as having a disproportionate effect on the actual inlet capture. For example, Fiuzat et al. (2000) noted that a 5% bypass as a design condition allows inlets that are 25% shorter. Another common practice to increase interception is by depressing the gutter edge for a few inches below the road cross-slope (Jens, 1979). For example, full-scale experiments by Karaki and Haynie (1961) showed that depressing the inlet by two inches decreased the required inlet length for 100% interception by 25%-42%. Inlets on a uniform road cross-slope are called undepressed inlets, and inlets on a depressed gutter are known as depressed inlets.

The hydraulics in and around curb inlets has yet to be elucidated in a consistent theoretical framework that covers the range of flow behaviors caused by gutter

depressions and the structural supports that may interrupt the smooth flow down an inlet's length, so we continue to rely on empirical fitting for design equations. Arguably, the closest we have to an internally-consistent theory is that of Wasley (1960), where a rigorous mathematical analysis was applied to describe the velocity field in the vicinity of the curb inlet. However, Wasley's approach was (i) applied to simple inlet geometry, without gutter depression or intervening structure, (ii) only analyzed for 100% interception, and (iii) did not account for friction effects, which led to inaccurate predictions under some flow conditions. Excluding Wasley's relatively unused theoretical approach, curb inlets equations reported in the literature fall into two groups. First, equations that are a best fit of empirical data such as the work of MacCallan and Hotchkiss (1996), Fiuzat et al. (2000), and Conner (1946). Second, equations based on theory with empirically-calibrated coefficients for equations derived from simplified hydraulics theory, such as the work of Izzard (1950), Li et al. (1951), and Uyumaz (1992). In general, the purely empirical equations should be applied only to inlets matching the range of tested conditions (gutter and inlet geometry, flow conditions, and roadway configurations), whereas equations that are theoretically-derived and empirically-fitted can be (arguably) more widely applied. However, as a practical matter the line between the two approaches is somewhat blurred by the fact that the theoretically-derived equations *do not* include effects of either gutter depressions or intervening structures. The claim to supremacy and extensibility for existing hydraulic theory is somewhat suspect as the fundamental form of the theoretical equations are not necessarily supported by the observed physics. For example, Schalla (2016) examined the effect of slab structural supports on inlet interception and found that the net effect was indiscernible, despite the fact that the observed flow structure was not at all represented by the assumptions underpinning Izzard (1950) and

subsequent theoretically-based equations. Furthermore, evidence reported in Schalla et al. (2017) and Zwamborn (1966) indicate the fundamental approximation in Izzard (1950) of the free surface as a linearly-decreasing along an inlet is simply wrong for 100% interception. Thus, the approach of using a theoretically-derived equations with empirical fitting of coefficients can be seen as a desirable goal, but not yet achieved in practice. Instead, we can think of the existing approach, as encapsulated in HEC-22, as empirical fitting that is guided by theory, which is the approach taken herein.

A further caveat to empirical fitting in the existing curb inlet literature (whether theory-based or not) is that a majority of studies used scaled physical models, but discrepancies have been noted between predictions based on scaled vs. full-scale models (Zwamborn, 1966; Argue and Pezzaniti, 1996; Grubert, 1988). Among the 26 experimental studied reviewed in this dissertation,roughly 25% used full-scale models. Finally, empirically-based equations used in design to achieve 95% to 100% inlet efficiency might be questionable due to a bias towards high-bypass flow in the fitting analysis. A majority of studies are dominated by experiments at low efficiency (high bypass) conditions (e.g. Spaliviero et al., 2000; Bowman, 1988; Comport and Thornton, 2012), but the highly-nonlinear free surface at full capture (e.g. Schalla, 2016) is likely dissimilar to the free surface at high bypass (although empirical evidence does not yet exist). It follows that different coefficients will likely be developed if the empirical fit is only over the desirable low-bypass design conditions rather than a wide range of conditions.

The guidelines and design equations presented in the Hydraulic Engineering Circular No. 22 (Brown et al., 2009 —herein HEC-22) are recommended by the U.S. Federal Highway Administration (FHWA) and are widely used by U.S. states,

counties, and cities. Furthermore, the HEC-22 equations are implemented within many commercial stormwater design software, such as Bentley's StormCAD and Innovyze's InfoSWMM. Unfortunately, several recent studies have questioned the validity of HEC-22 inlet capacity predictions. For example, HEC-22 predictions did not provide a satisfactory match with experiments by Guo et al. (2012) and Comport and Thornton (2012). Each study used their own data to update the numerical coefficients in the HEC-22 equations. Similarly, recent experimental work by the author's research team (Schalla et al., 2017) showed inaccuracies in the predictions of HEC-22 for 5-ft and 15-ft inlets. The present study attempts to mitigate the problems in the HEC-22 design equations through a comprehensive reanalysis of all the full-scale experimental data in the literature. Maintaining the fundamental form of the HEC-22 equations makes this approach "theoretically-guided," but empirically-fitted based only on conditions that are relevant to design (i.e. 95% to 100% capture).

The objectives of this study are to assess the predictions of HEC-22 equations for depressed curb inlets on-grade, analyze the assumptions in HEC-22, and provide updated design guidance. In Section 4.2, we provide the background and assumptions for the HEC-22 equations. Section 4.3 provides the description of the modeling facility and the experiments. Sections 4.4 and 4.5 present the experimental results and discussion, respectively. A new approach for determining computing the interception capacity of inlets at the 100% interception condition is provided in Section 4.6. The approach for full capacity is extended to bypass flow conditions in Section 4.7. A practical recipe for an updated design procedure based on the modified HEC-22 equations is provided in Section 4.8. The conclusions in Section 4.9 provide a summary of the results and their potential impact on design.

4.2 Assumptions in HEC-22 Design Equations

HEC-22 presents the length of undepressed inlet (L_T) for 100% capture of gutter flow Q_g as:

$$L_T = 0.6\, Q_g^{0.42} S_L^{0.3} \left(\frac{1}{nS_x}\right)^{0.6} \tag{4.1}$$

where L_T is in ft, Q_g is the incoming gutter flow (cfs), S_L is the roadway longitudinal slope, S_x is the roadway cross-slope, n is Manning's roughness coefficient. Although HEC-22 does not mention the equation's source, Chapter 2 above shows that the equation is based on the work of Izzard (1950), which assumes the flow depth will decrease linearly along the inlet length. Depressed inlets are represented as a compound section where the gutter slope is steeper than the road slope to concentrate the flow near the curb, as previously illustrated in Figure 2.1. The depressed gutter cross-slope (S_w) is related to the road cross-slope (S_x) by:

$$S_w = S_x + \frac{a}{w} \tag{4.2}$$

where a is the depression height (ft), and w is the width of the depressed gutter (ft). HEC-22 extends Equation (4.1) to depressed inlets by replacing S_x with an equivalent slope S_e, which provides:

$$L_T = 0.6\, Q_g^{0.42} S_L^{0.3} \left(\frac{1}{nS_e}\right)^{0.6} \tag{4.3}$$

where the expression given by HEC-22 for S_e is:

$$S_e = S_x(1 - E_o) + S_w E_o \tag{4.4}$$

where E_o is the ratio between flow in the depressed section to the total gutter flow. The details of this substitution are handled in Section above with Equation . For the present purposes, we note that the substitution is not entirely based on flow

physics, but represents an assumption based on a convenient form for geometry. That is, Equation (4.4) can be interpreted as the effect of each slope in the compound gutter (S_w and S_x) is weighted based on two assumptions: first, that the flow has a uniform, flat free-surface across the gutter (as in Figure 2.1 and second, that the fraction of the flow in each segment (E_o) as computed by the Manning's equation with a uniform flat free surface leads to an effective slope, S_e that is adequate for design purposes. Introducing S_e and E_o deviates from the work of Izzard (1950) and has not been justified in either HEC-22 or any of the literature reviewed herein. Furthermore, for inlets with a locally-depressed gutter (depression only near the inlet), HEC-22 computes E_o as a function of the geometry of the uniform gutter upstream the depression, i.e., assuming the local depression does not direct the flow into the depressed section. Note that even if HEC-22 accurately computes E_o, the idea that a single equivalent slope can account for the effects of the compound gutter section is unproven and should be viewed with skepticism.

To summarize, there are three main assumptions used by HEC-22: 1) Linearly decreasing water profile along the inlet length, 2) simplification of flow conditions immediately upstream of the inlet, and 3) introducing S_e to account for the effects of the compound gutter at depressed inlets. Experiments and analyses below are used to assess these assumptions.

4.3 Methods

4.3.1 Physical Model

This study used an existing model at the University of Texas at Austin, which was used earlier for several other stormwater related studies (Holley et al., 1992; Hammonds and Holley, 1995; Qian et al., 2013). The model consists of a 64-ft long

by 10.5-ft wide roadway with adjustable longitudinal and cross-sectional slopes. The model was modified by Schalla (2016) to accommodate a full-scale model of a locally-depressed curb inlet, where a 16-inch wide gutter at the inlet was depressed by three inches from the road cross-slope. The modifications included: 15 ft curb inlet consisting of three 5-ft modular units, 10 ft upstream and downstream depression transition sections, a headbox for controlling flow onto the model, V-notch weirs and approach channels for flow measurement. The model's road surface is sealed with layers of fiberglass and resin. The surface is textured with a mean diameter particle size of 1.3 mm (Hammonds and Holley, 1995). Recent roughness calculations performed by Qian et al. (2013) show an average Manning's roughness coefficient of 0.0166. The roughness coefficient value was later confirmed by Schalla (2016) as well. Figure shows an overall view of the Model. The current study uses and modifies the inlet model used by Schalla (2016).

Figure 4.1: Overall view of the physical model.

The inlet is tested at the model's original roughness (n=0.016 as reported by Qian et al. (2013)) and a modified smoother surface (n=0.012). The modified roughness is achieved by coating the model surface with four layers of epoxy. The surface of the roadway is roughened before the application of each new epoxy layer to ensure mechanical bonding between the old and new layers. The flow spread is measured under various slopes and flow conditions and substituted into Manning's equation to determine the roughness coefficient coefficient n.

4.3.2 Experiments

Schalla (2016) tested 5 and 15 ft inlets at the original model roughness (n=0.0166). In the current study, the 10-ft inlet was tested under various flow conditions and various slope configurations. A summary of the overall tested conditions (from both studies) is provided in Table 4.1. To determine the 100% interception flow, the gutter flow was gradually increased until barely an observable trickle of water is flowing past the inlet. The inlet is tested several bypass flows, and the maximum bypass flow was 0.5 as set by TxDOT (2016). The intercepted and bypass flowrate are measured, and the flow spread and depth are measured along multiple sections as well. Since HEC-22 assumes that the local depression does not direct flow towards the inlet, the flow spread at the uniform gutter and immediately upstream the inlet are measured for comparison.

Following the same experimental procedures of tests at original model roughness, a total of 39 tests were conducted for the 10 ft inlet configuration at the modified roughness (n=0.012). To evaluate the HEC-22 assumptions regarding the water profile along the inlet and the follow conditions upstream the inlet, a point gage is used to measure the water profile along the inlet length and at the

Table 4.1: Tested configurations for analysis of interception of depressed curb inlets.

Property	Tested
Longitudinal slope (%)	0.1, 0.5, 1.0, 2.0, 4.0
Cross slope (%)	2.0, 4.0, 6.0
Inlet length (ft)	15, 10, 5
Roadway Manning's coeff.	0.0166, 0.012
Flow Rate Conditions	100% interception, bypass (0.1, 0.3, 0.5 cfs)

cross-section immediately upstream the inlet for various slope combinations. Surface disturbances and the shallow depth of the gutter flow introduced uncertainties in the depth measurements, which were quantified to be on average ±0.125 inches.

4.4 Results

4.4.1 Inlet Interception Capacity

Figure 4.2 shows the comparison between the intercepted flow at the original and the modified roughness for the 10-ft inlet. Overall, the inlet interception decreased at the modified (smoother) roughness. The decrease in interception is 6% on average, and reaches 29% for 0.1% longitudinal slope and 4% cross slope configuration. There is a general decrease in the ponded width at the modified roughness as well. The decrease in ponded width is 9% on average, and reaches 22% at the 0.1% longitudinal slope and 4% cross slope configuration.

Hydraulic Toolbox software program (FHWA, 2018) is used to compute HEC-22 results at similar road geometry configurations and roughness as the physical model data. Comparisons of the physical model and HEC-22 design equations are shown in Figure 4.3. For 15-ft inlet, HEC-22 over-predicts intercepted flowrates by an average factor of 1.62 when compared to the physical model. The Root Mean Squared Difference (RMSD) between the physical model and HEC-22 is 2.4 cfs. Similarly

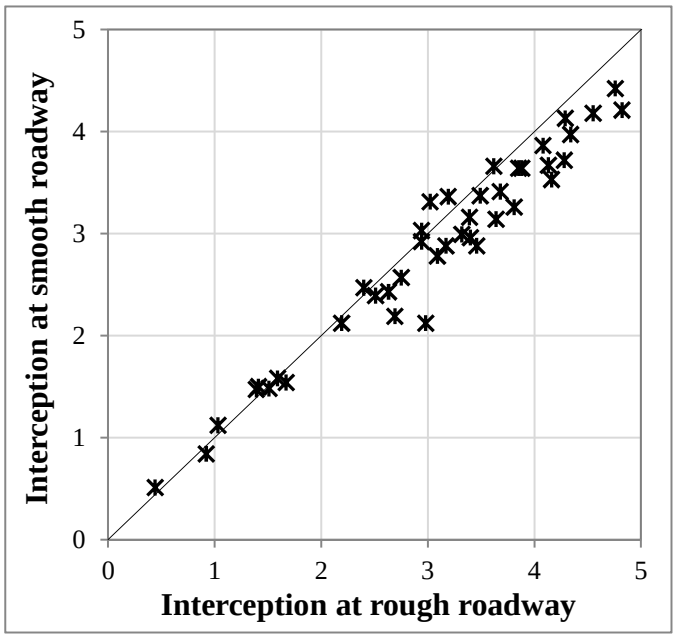

Figure 4.2: Comparison between the intercepted flow by 10-ft inlet at rough and smooth roadway surface.

with the 10 ft inlet, HEC-22 over-predicts, but the difference between HEC-22 and the physical model decreased compared to the case of the 15 ft inlet. If tests with longitudinal slope of 0.1% are excluded for the 10 ft inlet (which could not be modeled in the 15 ft due to model limitations), then the RMSD in the case of the 10 ft inlet is 1.2 cfs (compared to 2.4 cfs in the case of the 15 ft inlet). For 5 ft inlet, the two HEC-22 points that deviate significantly from the match line are for extremely flat longitudinal slopes (S_L) of 0.1%, otherwise HEC-22 underestimates the inlet's capacity. Without considering S_L=0.1% data, the RMSD is 0.47 cfs; when considering S_L =0.1% data the RMSD is 0.6 cfs. Overall, HEC-22 overestimates interception of 15 and 10 ft inlets and underestimates interception of 5 ft inlets.

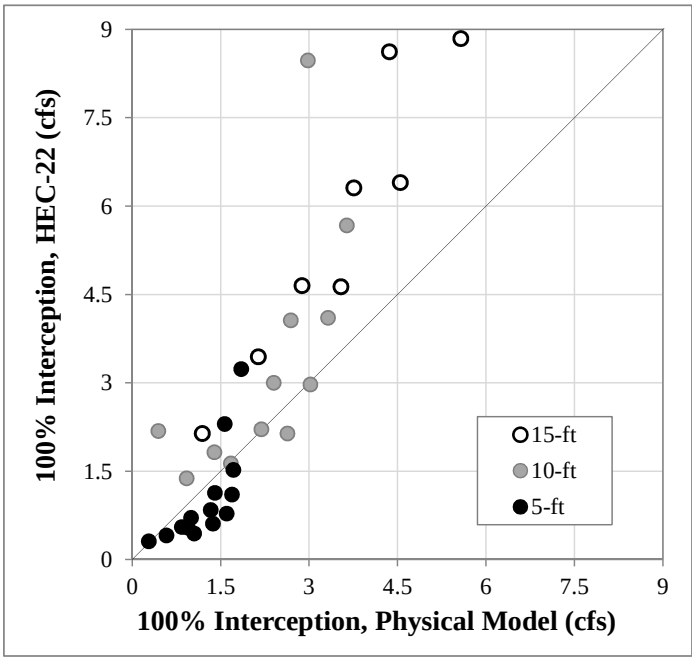

Figure 4.3: Comparison between 100% interception computed by HEC-22 and observed at physical model.

4.4.2 Observations on HEC-22 Assumptions

Figure 4.4 shows the observed water surface profile for two tests for 15 ft depressed inlet, and the dashed line in the figure represents the assumed linear water profile by Izzard (1950) (and adopted by HEC-22). The observed water surface profile is significantly lower than the assumed linear profile.

The spread of flow at the uniform gutter and immediately upstream the inlet (for the same test run) are compared in Figure 4.5. The spread at the uniform section is invariably larger than the spread at the depresseed inlet. Along the transition from to the depressed gutter, a break in the water surface is observed along the direction of the flow spread (perpendicular to the inlet), as shown in Figure 4.6. The reduction in the spread along the transition length and the variation in water surface profile in the direction of the spread show that the flow is *spilling* into the depressed section.

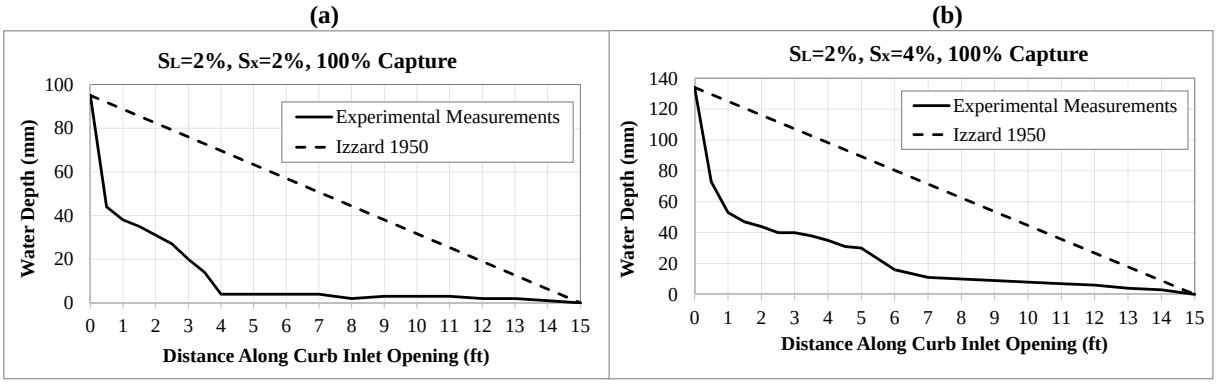

Figure 4.4: Along-inlet water surface profile (measured from the depressed inlet's opening) at 100% interception for 15 ft inlet with (a) SL=2%; Sx=2%, (b) SL=2%; Sx=4%.

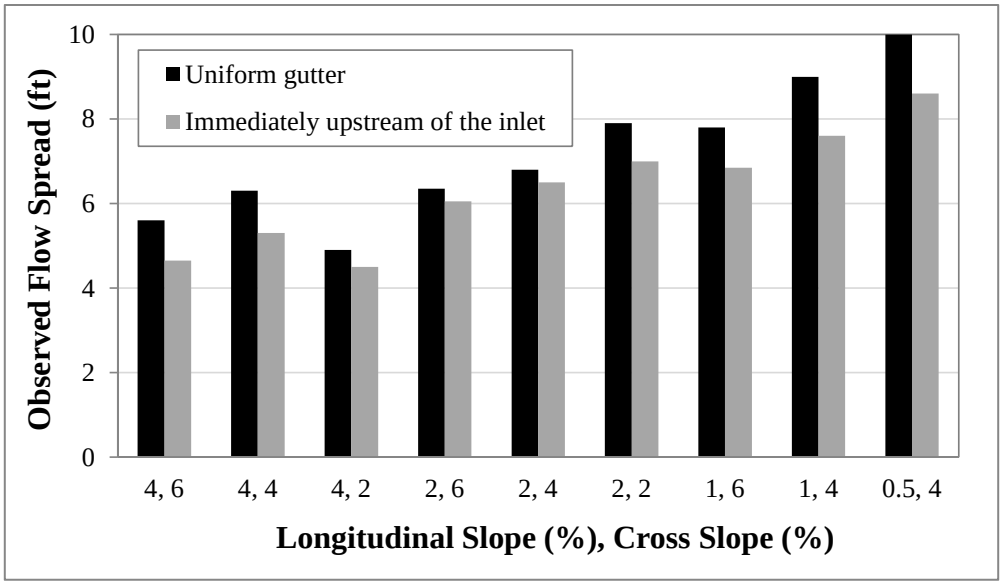

Figure 4.5: Observed flow spread at the uniform gutter and the observed spread immediately upstream the depressed inlet.

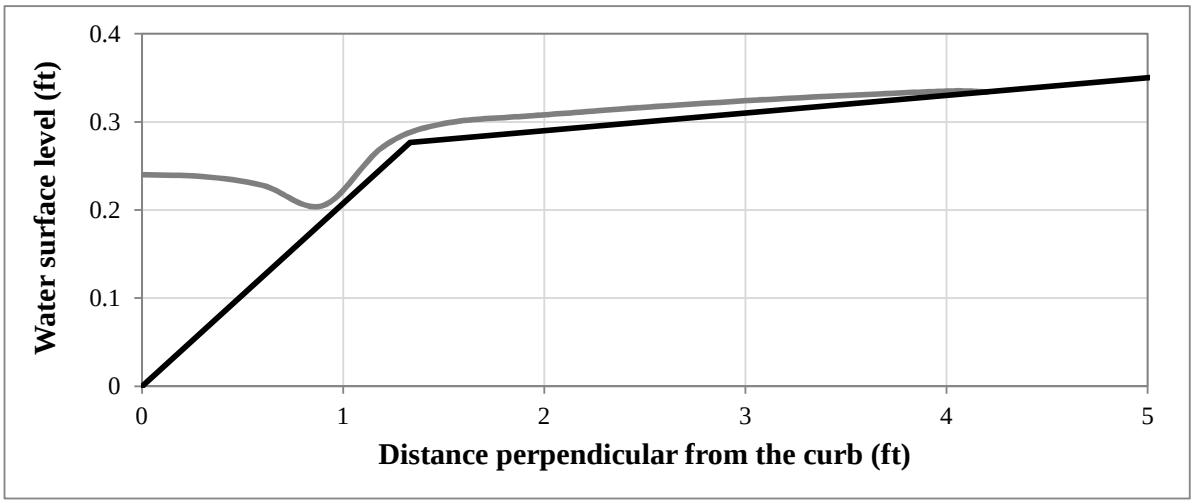

Figure 4.6: Cross-section of observed water surface elevation immediately upstream a 10 ft depressed inlet at SL=4% and Sx=2%. (Not to scale)

4.5 Discussion

As for the effect of changing the roadway roughness, changing the roughness results in a limited decrease in interception (Figure 4.2). The decrease in ponded width in the case of a smooth roadway (compared to the rough surface) helps in explaining why the effect of roughness is less pronounced in decreasing the intercepted flow than anticipated. Lower ponded width means more flow is concentrated in the gutter near the curb, i.e., a smoother roadway may well hamper the fall of flow into the inlet from the outer edge of the ponded width, yet a smoother surface may increase the capacity of the depressed gutter section thus directing more flow into the inlet. The off-setting effects of these two factors may dampen down the overall effect of changing the roughness. Karaki and Haynie (1961) presented the results of their full-scale experiments in non-dimensional plots where the dimensionless inlet length was obtained by diving the actual inlet length by the product of the normal flow spread and the Froude number of the flow. The change in inlet efficiencies (ratio of intercepted to total gutter flow) between inlets with the same road slopes and

dimensionless inlet length but with different roughness is presented in Table 4.2. The comparison shows that changing the roughness does not result in significant changes in the inlet performance, similar to observations in the current study.

Table 4.2: Change in inlet efficiency due to change in road roughness, data from Karaki and Haynie (1961).

S_L%	S_x%	n rough	n smooth	n Change	Efficiency Change
1	6	0.0157	0.0108	-31%	2.5%
4	6	0.011	0.015	-27%	0.6%
4	1.5	0.0131	0.0096	27%	-2.7%
4	1.5	0.016	0.009	44%	-5.1%

Regarding the assumed linear water profile by HEC-22, Figure 4.4 shows that the bulk of the flow approaching the inlet is captured in the first few feet of the inlet, and only a thin layer of flow is observed along the rest of the inlet length. Figure 4.7 shows the non-dimensional plot of water surface profile for inlets of different lengths. As the inlet length decreases the discrepancy between the observed profile and the linear profile decreases, which might account for why the overestimation error in HEC-22 equations decreases as the inlet length decreases (overestimation error for 15-ft inlet is double that of the 10-ft inlet in this study). The observed break in the surface profile is consistent with the analysis provided by Izzard (1977) proposing that the inlet will have high capture until its length exceeds a certain length scale L_2 and the rest of the inlet length (beyond L_2) performs significantly poorly. The conclusion that, every thing remaining the same, error in HEC-22 moves from underestimation to overestimation as the inlet length increases is illustrated by comparing HEC-22 predictions to experimental data from Clemson University (Bowman, 1988; Soares, 1991). These experiments were conducted on inlets with both a local depression and a continuously depressed gutter, and inlets of lengths 2, 4, 6, and 8 ft were tested.

The comparison between the observed inlet efficiency (intercepted flow/total gutter flow) and HEC-22 computed efficiencies (Figure 4.8) shows that underestimation error occurs for 2 and 4 ft inlets, while over-prediction occurs for 6 ft and 8 ft inlets, which is consistent with observations at the current study.

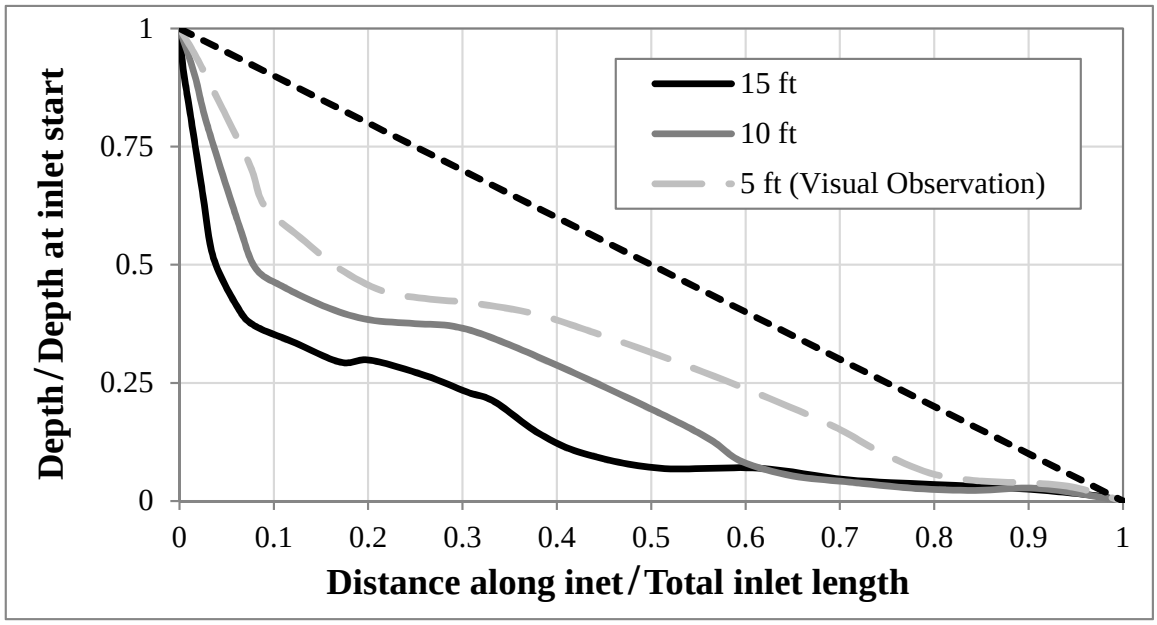

Figure 4.7: Non-dimensional water surface profile along inlet length for SL=2% and Sx=4%.

Regarding the HEC-22 assumed flow conditions upstream the inlet, the spread of flow at the uniform gutter is shown to be larger than the spread immediately upstream the inlet (in §4.4.2); indicating that the flow is spilling into the depressed section along the transition length. The hydraulics of the spill of flow into the depressed section (shown in Figure 4.6) is too complex to be captured by HEC-22, and this spill indicates that the transition length affects the distribution of flow approaching the inlet and inlet performance. Over-simplified flow conditions upstream of depressed inlets were also used by Li et al. (1951) as they assumed a horizontal water surface immediately upstream the inlet, contrary to observations from the current study.

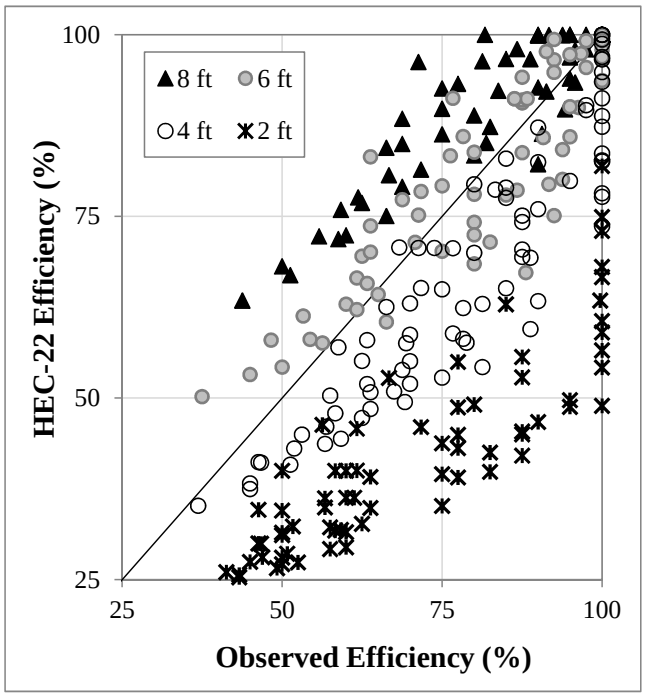

Figure 4.8: Comparison between computed HEC-22 and observed inlet efficiencies from Bowman (1988) and Soares (1991).

Computing the ratio E_o at the inlet is not straight-forward due to the complex hydraulics; hence experiments were conducted herein where the value of E_o was known. In these experiments, flow was adjusted until the spread immediately upstream the inlet was exactly equal to the width of the depressed gutter, which is the maximum gutter flow for which $E_o = 1$ (i.e., all the gutter flow is concentrated in the depressed section). The E_o computed according to HEC-22 is compared to the observed E_o at the inlet ($E_o = 1$), as shown in Figure 4.9. E_o computed by HEC-22 is less than the observed E_o at the inlet for all tested configurations. That is to say, the HEC-22 approach for estimating E_o is conservative (an underestimation), which might be one of the factors leading to underestimation by HEC-22 for 100% interception at $L = 5$ ft experiments in the current study.

To test the validity of using the equivalent slope S_e by HEC-22, the observed

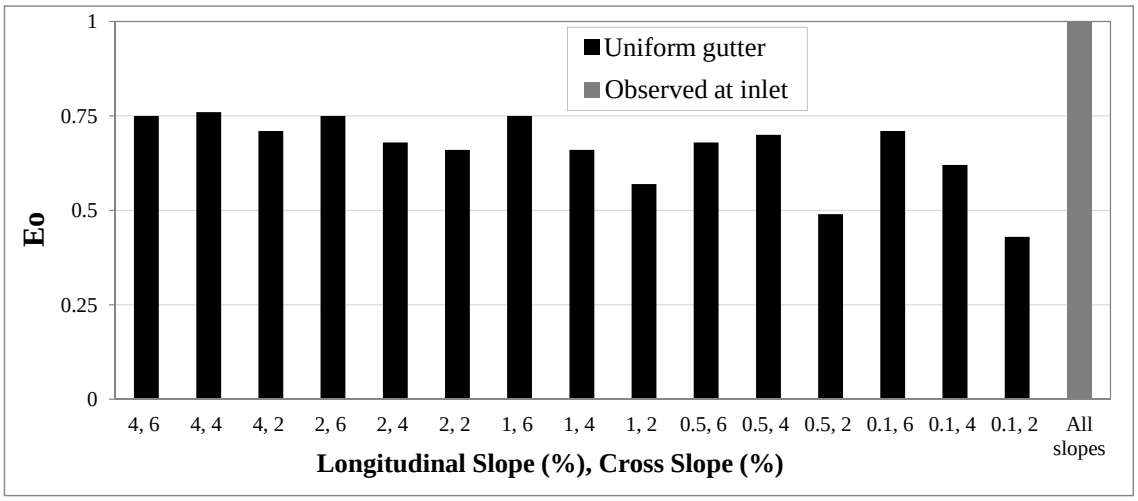

Figure 4.9: Observed vs HEC-22 computed E_o for experiments with spread at inlet equal to depressed gutter width.

flowrates are used to solve the HEC-22 interception equation (Equation (4.3)) in terms of S_e. In other words, for a given inlet length and observed inlet interception, the value of S_e leading to accurate interception predictions is determined. Then the computed *accurate* values of S_e are used to compute E_o. The histogram of E_o computed through this approach is shown in Figure 4.10. Some values of E_o are zero or negative, and others are more than unity, all of which are physically implausible. This analysis suggests that one slope value (S_e) does not accurately represent the composite gutter section, at least not for all configurations.

4.6 Correction Factor for HEC-22 at 100% Interception

The discussion in §4.5 shows several potential sources of error in the assumptions of HEC-22. The discussion also suggests that the hydraulics upstream the inlet is more complex than represented by HEC-22 and have not been previously captured in a simple manner suitable for a design manual. Accordingly, the purpose of this section is to propose a new design approach that is accessible to practitioners and

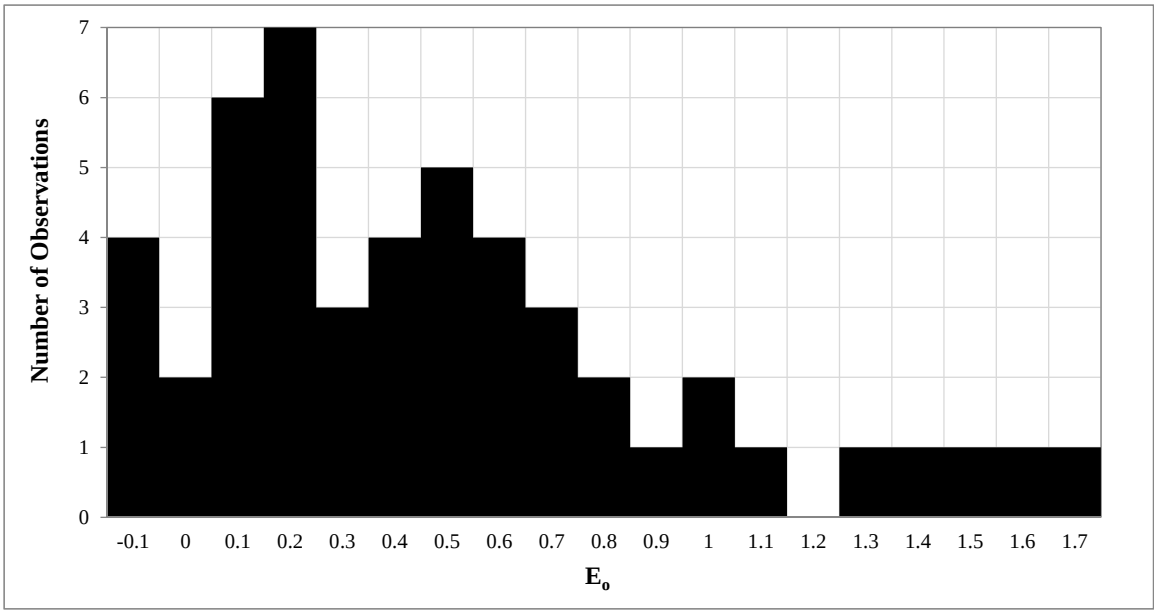

Figure 4.10: Histogram of E_o values based on S_e computed from observed interception.

provides good estimates for a wide variety of design conditions.

The literature is reviewed for reported experimental results and data is collected from five studies for locally depressed inlets: Li et al. (1951), Karaki and Haynie (1961), Hammonds and Holley (1995), MacCallan and Hotchkiss (1996), Kranc et al. (1998). No experimental data is found for the 100% interception of inlets with a continuously depressed gutter, so the analysis in this section is limited to locally depressed inlets. Kranc et al. (1998), Li et al. (1951) and Hammonds and Holley (1995) reported experiments and analyses based on scaled models, i.e., using Froude-number scaling so that smaller geometry and flowrates in the laboratory could be used to represent larger inlets and flowrates in the real world. Their results were mostly reported in terms of the larger inlets and flowrates that were their study objectives. Herein, the results from these studies are *unscaled*, i.e., their data is returned to the original physical experiment dimensions by inverting the scale parameters. Analyses

using the physical model dimensions avoids errors that can be caused by scaling (as discussed in §4.5). The data from these five studies are combined with the results from the current study, providing a total of 117 observations for 100% interception at locally depressed inlets. Table 4.3 shows the ranges of parameters in the final dataset.

Table 4.3: Parameter ranges in the final dataset.

Parameter	**Min**	**Median**	**Max**
Inlet Length, L_i (ft)	1	6	30
Intercepted flowrate, Q_i (cfs)	0.021	1.03	5.57
% Longitudinal Slope, S_L	0.1	2	6
% Cross-sectional Slope, S_x	1.5	4	8.333
Manning roughness coefficient, n	0.01	0.012	0.017
Depression height, a (ft)	0.0833	0.246	0.4167
Depression width, w (ft)	0.75	1.124	3.25
Upstream Transition Length, L_{Tr} (ft)	1.15	3.75	10

A Correction Factor (CF) that corrects a HEC-22 computed flowrate to the expected flowrate (based on the full range of experiments) can be defined as:

$$C_F = \frac{Q_{expected}}{Q_{HEC}} \tag{4.5}$$

Where Q_{HEC} is the intercepted flow by the inlet for 100% interception condition as computed by HEC-22, and $Q_{expected}$ is the expected 100% interception of the inlet. In the case of experimental data, $Q_{expected}$ is equal to the observed inlet interception. Correlation analysis is carried out between different parameters and CF, and the four most significant parameters are: a/d_n (depression height/normal flow depth), w/T (depression width/normal flow spread), $S_L + S_{Tr}$ (the longitudinal slope of the roadway plus the transition slope), and S_w (the depressed gutter slope), where d_n and T are computed using Q_{HEC}. These parameters compensate for the missing factors affecting interception and for inaccurate assumptions in HEC-22. The effects of the upstream transition section on interception were disregarded in HEC-22 due

to over-simplification of flow condition upstream the inlet. Therefore, the parameters S_w and $S_L + S_{Tr}$ are used to represent the effects of the transition geometry (total longitudinal slope and the cross-slope of the depressed gutter). Also, a/d_n is a dimensionless parameters that captures the effect of the local depression (misrepresented in HEC-22). Finally, the HEC-22 approach for locally depressed inlets computes E_o as a function of only w/T, so this parameters is included in the correction factor to compensate for the errors in computing E_o by HEC-22. A MATLAB script is written to perform multiple nonlinear regression analysis, and the chosen equation from the regression analysis is:

$$CF = 2.8 \left(\frac{a}{d}\right)^{0.24} \left(\frac{w}{T}\right)^{0.8} (S_L + S_{Tr})^{-0.13} S_w^{0.22} \tag{4.6}$$

where S_{Tr} is the transition slope computed as a/L_{Tr}. Figure 4.11-a shows the comparison between the observed intercepted flow at 100% interception and the computed flow using HEC-22, and Figure 4.11-b shows the same comparison after applying the correction factor CF. HEC-22 significantly overestimates many observations from the present study, Hammonds and Holley (1995), and Karaki and Haynie (1961). Interestingly, HEC-22 significantly underestimates observations by MacCallan and Hotchkiss (1996) and Li et al. (1951). The correction factor significantly improves the R^2 across all the experiments (from 0.72 to 0.91) and the RMSE decreased from 1.46 cfs to 0.39 cfs. Thus, applying the correction factor reduces the RMSE by a factor of 3.75; significantly improving HEC-22 predictions.

Finally, we observed a deficiency in curb inlets on a combination of steep grade and flat cross slope. During experiments for inlets at 4% S_L and 2% S_x configuration, flow tended to go past the inlet along the outer edge of the depressed gutter. The 100% interception condition for this configuration is barely achievable for both rough and smooth roadway surfaces. This deficiency was discussed in more detail at §3.4. When

computing the intercepted flow from experiments with this slopes-configuration, HEC-22 both with and without *CF* correction drastically overestimate the inlet capacity beyond 0.5 cfs, with an average error of 160% and 255% respectively. Consequently, we propose a preliminary breakpoint where if $S_L/S_x \leq 2$ then HEC-22 and the correction are expected to fail, and a different type of inlet would be recommended (combination or a grate inlet).

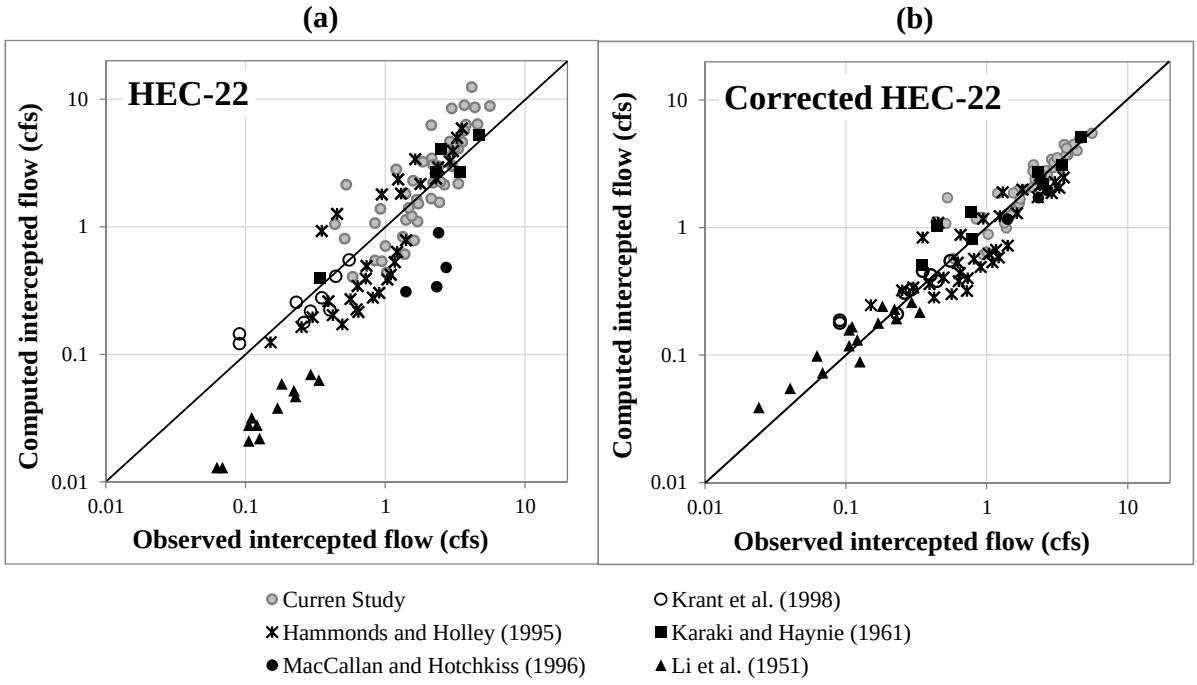

Figure 4.11: Measured intercepted flowrates for 100% interception and computed by: a) HEC-22, b) HEC-22 after applying correction factor *CF*.

4.7 Bypass Flow Condition

Bypass flow occurs when the flow in the gutter exceeds the 100% interception capacity of the inlet. The present work did not include experiments with significant bypass flow, however, data from prior studies are combined with current experiments to develop an approach for computing bypass efficiency E (the ratio of captured flow,

Q_i, to gutter flow, Q_g) that is consistent with the *CF* approach for 100% interception. A revised approach for bypass efficiency is needed because (as illustrated below) the empirical approach in HEC-22 for computing L_T and E have offsetting biases.

HEC-22 proposes the following equation for computing inlet efficiency:

$$E = 1 - \left(1 - \frac{L_c}{L_T}\right)^{1.8} \tag{4.7}$$

where E is the inlet efficiency, L_c is the installed curb inlet length, and L_T is the required length to intercept 100% of the gutter flow as computed by Equation (4.3). Relatively few experiments can be used to verify the HEC-22 efficiency equation as typically L_c is fixed and L_T is simply presumed. A notable exception is the study by Karaki and Haynie (1961) where the gutter flow was fixed and the inlet length was changed in increments until the entire gutter flow was captured. Figure 4.12 shows the comparison between observed and computed efficiency by HEC-22 where E is computed both with the HEC-22 value for L_T (from Equation 4.2) and the experimentally-observed value for L_T. In general, computing E using the HEC-22 values for L_T provides better agreement than the actual measured L_T. Using the observed L_T (which should be more accurate) results in a bias towards underestimating E, thus indicating that the HEC-22 computation for E has a bias that is compensating for bias in the L_T equation. It follows that using the *CF* approach to computing the 100% interception will lead to an uncompensated bias in the estimation of E for bypass flows when coupled with Equation (4.7).

Data in Hammonds and Holley (1995) show that the spread of the approach flow tends to increase linearly with the increase of the intercepted flow into the inlet. A non-dimensional plot of the same data can be obtained for a given inlet length by dividing the spread of each gutter flow with the spread corresponding to the 100%

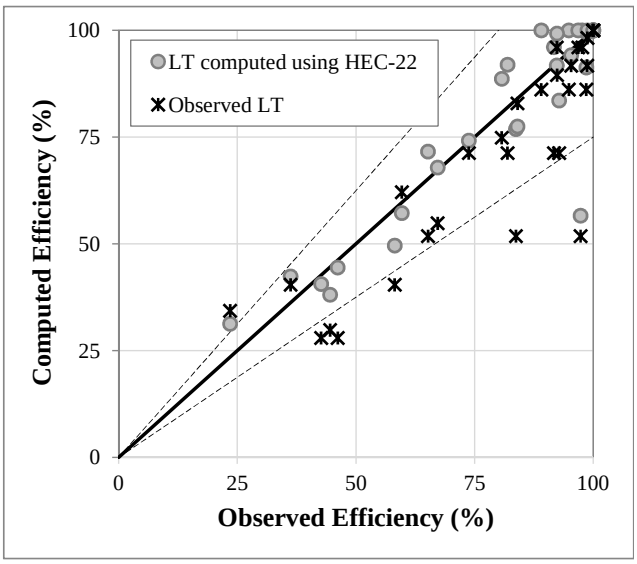

Figure 4.12: Computed inlet efficiency based on HEC-22 values for L_T and observed values L_T, as compared to observed efficiency of Bauer and Woo (1964)

interception flow (T_{100}), and dividing the flow into the inlet (at each gutter flow) by the intercepted flow corresponding to 100% interception condition ($Q_{i,100}$). The same linear trend is observed in other studies. The slope of the linear relationship in the non-dimensional plots varies from 1.3 to 3.2, with an average value of 2.25. For a specific linear relationship (slope m), the intercepted flow (Q_i) for any gutter flow can be computed by:

$$Q_i = Q_{i,100}\left[1 - m\left(1 - \frac{T}{T_{100}}\right)\right] \tag{4.8}$$

By relating the intercepted flow to the properties of the gutter flowing rather the length L_T, an expression is developed that can be verified and revised by vast experimental datasets reported in the literature. A multiple nonlinear regression analysis is performed on data from the six studies to derive an expression for the linear slope (m). The final expression is:

$$m = \left(\frac{L_{Tr}}{d_{n,100}}\right)^{0.22} \tag{4.9}$$

where L_{Tr} is the length of the upstream transition (ft), and $d_{n,100}$ is the normal flow depth associated with $Q_{i,100}$ (ft). A total of 303 observations were available (excluding the 100% efficiency observations), and the observations cover a wide range of efficiencies (as low as 30% interception) and roughly 65% of observations are concentrated at high efficiencies ($E > 80\%$). In Figure 4.13 the observed inlet efficiencies are compared to both the HEC-22 approach (Equation (4.7)) and efficiencies computed using Equation (4.8). Figure 4.13-a shows a significant scatter using the HEC-22 approach, with erroneous 100% interception for a significant number of experiments. Figure 4.13-b shows that all efficiencies computed by Equation (4.8) were within the 25% deviation region. The R^2 of observations computed by HEC-22 and Equation (4.8) is 0.38 and 0.87, respectively, and the RMSE is 17.7% and 5.6%, respectively. The new technique is an improvement over the HEC-22 method for computing bypass efficiency based on the reduction of RMSE by a factor of three, the significant increase in R^2, and the narrow scatter of data.

The analysis for Equation (4.8) in Figure 4.13-b is based on experimentally-observed $Q_{i,100}$ reported in the cited studies. To further extend the utility of this approach, Figure 4.14 compares the efficiency based on $Q_{i,100}$ using HEC-22, e.g., as in Figure 4.13-a, against the efficiency computed using the *CF* approach coupled with Equation (4.8). The *CF* approach significantly reduces the scatter as almost all data lie between the 25% deviation lines. The RMSE before correction is 17.7%, and is reduced after correction to 7.1% (a reduction by a factor of 2.5).

Note that application of the proposed approach involves computing m by Equation (4.9), which requires knowledge of the transition length for the depressed

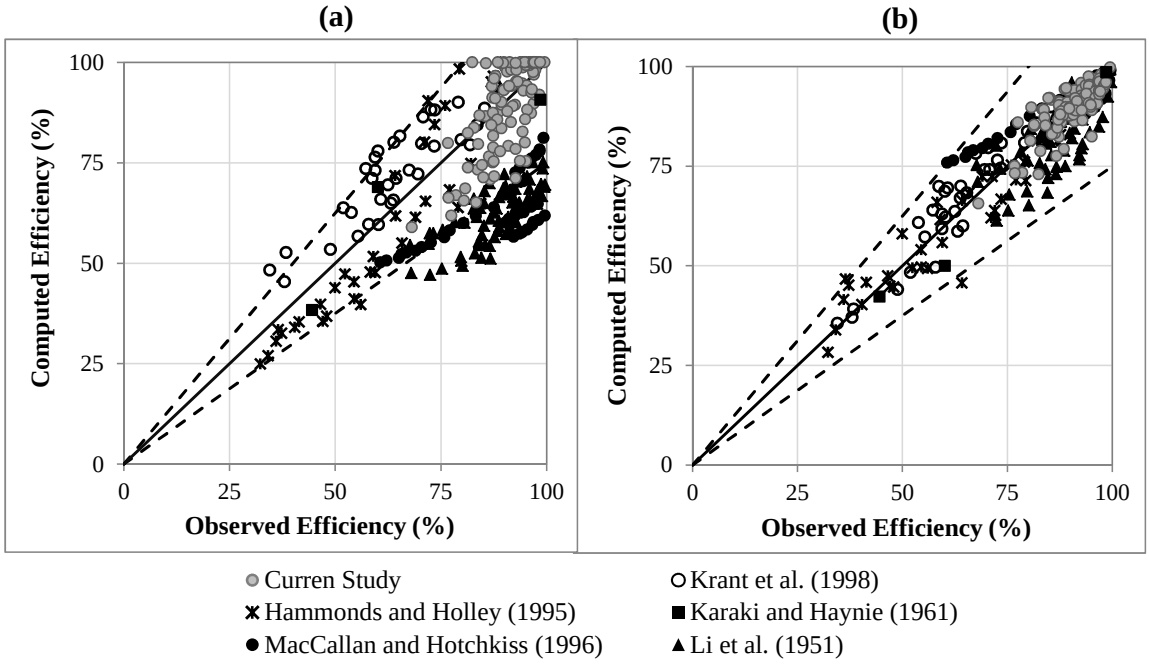

Figure 4.13: Comparison between observed inlet efficiency from different studies and the computed efficiency using: a) HEC-22, b) Proposed approach.

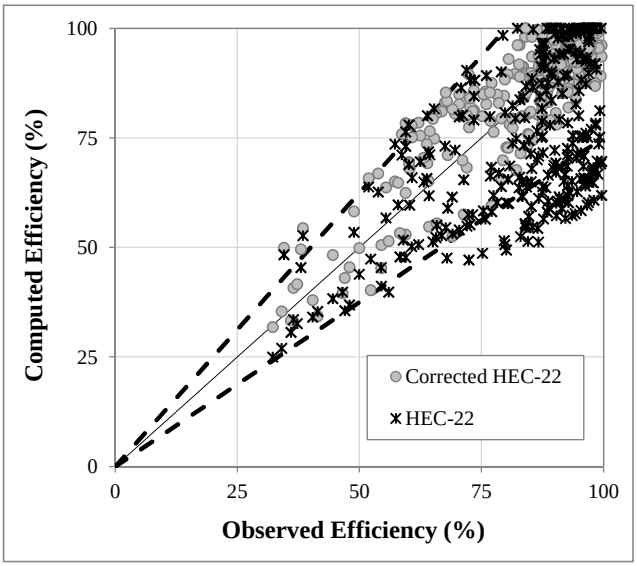

Figure 4.14: Efficiencies computed using HEC-22 with and without *CF* correction.

inlet. In cases where the transition length is not available or the computed value of m seems doubtful (e.g., $m < 1$ or $m > 4$), then $m = 2.25$ based on averages over the six prior studies can be used. Using the average m (2.25) slightly reduces the R^2 from 0.87 to 0.83, and the RMSE increases from 5.6% to 6.4%. Experimental data by Hahn (1972) was obtained after the current analysis was finalized, which can be used to verify the use of m=2.25 and generally the approach proposed in Equation (4.8), as shown in Figure 4.15. Overall, HEC-22 overestimates the inlets efficiency for this dataset, and using Equation (4.8) reduces the RMSE from 15.8% (as given by HEC-22) to 5.8%, which further shows that using m=2.25 provides satisfactory predictions for inlet efficiencies given accurate values for $Q_{i,100}$.

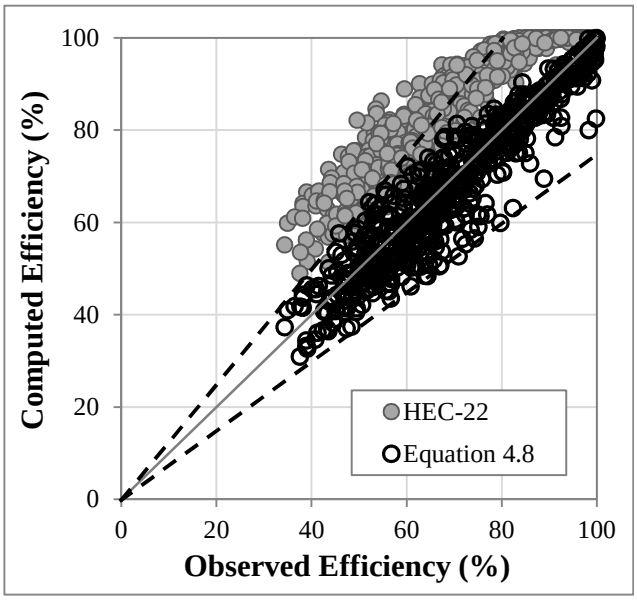

Figure 4.15: Efficiencies computed using HEC-22 and Equation (4.8) with m=2.25 for experiments by Hahn (1972).

4.8 Updated Design Procedure for Depressed Inlets On-grade

The new design procedure for 100% interception condition can be summarized in the following steps:

Given input: L_i, S_x, S_L, S_{Tr}, n, w, a

1. Compute the flowrate for 100% interception condition (Q_{HEC}) per instructions in HEC-22 (e.g., using FHWA Hydraulic Toolbox)

2. Using the computed Q_{HEC} , compute T (spread of normal flow) using Manning's formula for gutter flow:

$$T = \left(\frac{Q_{HEC}\, n}{0.56\sqrt{S_L}}\right)^{3/8} S_x^{-5/8} \tag{4.10}$$

3. Compute $d_n = TS_x$

4. Compute a/d_n and w/T, then apply Equation (4.6)

5. Compute $Q_{expected} = CF\, Q_{HEC}$

If flow in the gutter (Q_g) is given and the required is to determine the inlet length for 100% interception, then an iterative procedure is given in the following steps:

(A) Assume L_i, recommended to start with a small length (e.g., 1 ft)

(B) Perform steps 1-5, above for computing $Q_{expected}$

(C) Compute difference between given Q_g and computed $Q_{expected}$ as $(Q_g - Q_{expected})$

(D) If $Q_g > Q_{expected}$ (difference is positive), assume larger L_i and repeat steps A-C, if $Q_g < Q_{expected}$ then assume a smaller L_i and repeat steps A-C till the difference becomes insignificant.

The design procedure for inlets at bypass condition can be summarized in the following steps:

Given input: $L_i, S_x, S_L, n, w, a, L_{Tr}$, and Q_g

1. Compute the flowrate for 100% interception $Q_{expected}$
2. If $Q_{expected} \geq Q_g$, then inlet is operating at 100% efficiency. If $Q_{expected} < Q_g$, then $Q_{expected} = Q_{i,100}$
3. Compute T_{100} from Equation (4.10) using $Q_{i,100}$
4. Compute $d_{n,100} = T_{100} S_x$
5. Compute m from Equation (4.9) (using $d_{n,100}$) or use $m = 2.25$
6. Compute T from Equation (4.10) using Q_g
7. Compute Q_i from Equation (4.8)
8. $E = Q_i/Q_g$

It is strongly recommended that the HEC-22 efficiency (i.e., using Equation (4.7)) should *not* be combined with the CF approach for bypass flow computations. Combining the two different approaches lacks rigor in the derivation and introduces the bias in E as illustrated in Figure 4.12 when the observed L_T is applied.

4.9 Conclusions

A full-scale model of a depressed inlet is used to assess the inlet's interception capacity and the assumptions in the HEC-22 design equations. Changing the roughness of the model surface does not result in a significant change in the

interception capacity of the 10 ft inlet, possibly due to the increase in the capacity of the depressed gutter associated with a smoother surface. Experiments show that HEC-22 provides inaccurate predictions of the 100% interception flowrates, specifically overestimation for the 10 and 15 ft inlets and underestimation for 5 ft inlets. Experiments are carried out to test the assumptions employed by HEC-22. The experimentally observed water profile along the inlet does not conform with the linear water profile assumed by HEC-22. The assumed profile by HEC-22 is expected to be the main reason for overestimation errors. Measurements of spread and depth immediately upstream the inlet show that HEC-22 over-simplifies the flow conditions and disregards the effects of the upstream transition section on the flow approaching the inlet.

A statistical approach is developed to revise HEC-22 and propose a technique suitable for application by designers and practitioners. Experimental data from this study and from five other studies are used to derive a correction factor for the 100% interception flowrate computed by HEC-22. Applying the correction factor to HEC-22 produced satisfactory results, reducing the RMSE by a factor of 3.75. A linear relationship is observed between the spread of gutter flow and the flow intercepted by the inlet. This relationship is used to develop a new formula for evaluating the efficiency of inlets at bypass flow condition. The main advantage of this formula is its compatibility with the typical experimental procedures in curb inlets studies; therefore the formula can be tested against a large pool of data from the literature (303 observations) compared to the HEC-22 formula (27 observations). The new formula for bypass flow shows good agreement with the experimental results, reducing the RMSE from HEC-22 by a factor of three. Finally, a detailed step-by-step description is provided for the updated design procedure.

Chapter 5

Interception Capacity of Curb Inlets with Channel Extensions

5.1 Introduction

Conventional curb inlets consist of an opening in the curb that leads to an underground basin that spans the entire inlet length. The standard hydraulic calculations for the design of on-grade curb inlets assume free-fall overflow from the lip of the inlet into the sewer system, and submerged inlets in a sag configuration are based on orifice flow controlled by the inlet opening (TxDOT, 2016). Some designs of curb inlets restrict the length of the basin to only a portion of the total inlet length (i.e., main bay), and the rest of the inlet length is added as a channel (extension) attached on one or both sides of the main bay, as shown in Figure 5.1. Saving on excavation, concrete, and installation costs is the main motivation behind this inlet design. Curb inlets with channel extensions are commonly used around the United States, e.g., South Carolina inlet Type-5, 7, 17, 18; TxDOT Type-C; Arkansas rectangular drop inlet; and Oregon attachment to CG-1 and CG-2 inlets.

Unlike a conventional inlet, flow intercepted through an extension does not fall directly into the main bay; instead the extension provides a horizontal channel directing the intercepted flow. For a compact design, the cross-section of the extension channel is typically smaller than the cross-section of the curb inlet itself. For example, the Texas Department of Transportation (TxDOT) PCO inlet consists of a 5 ft main bay and one or two 4.5 ft extension chambers. The cross-section of

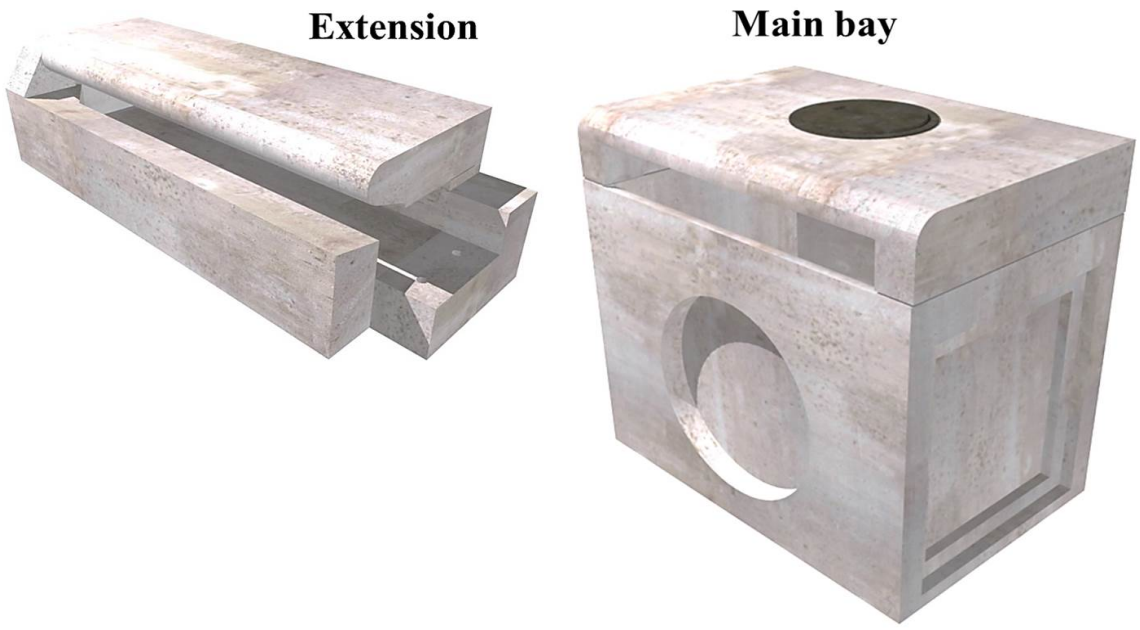

Figure 5.1: Illustration of the main bay and extension of a curb inlet (OldCastle, 2018).

the extension is 5" high and 12" wide, which is 20% of the area of the opening of the inlet (as shown in Figure 5.2 with the connection area highlighted). Accordingly, flow intercepted by the 4.5 ft extension passes through a much smaller section compared to the inlet opening of the extension. This reduction in cross-section can cause the intercepted flow to be significantly lower than the design flow predicted by equations for conventional inlets.

There is a concern that inlet extensions might have the potential to induce flow restrictions affecting the interception capacity. Considering inlets installed on-grade: 1) the flow restriction at the connection of the upstream extension to the main chamber with a low tail-water could limit the inflow into the main chamber and thus degrade the interception capacity, and 2) a high tail-water condition that submerged the connection between the extension and the main chamber could cause further degradation in capacity. As for inlets in a sag, when the flow depth in the

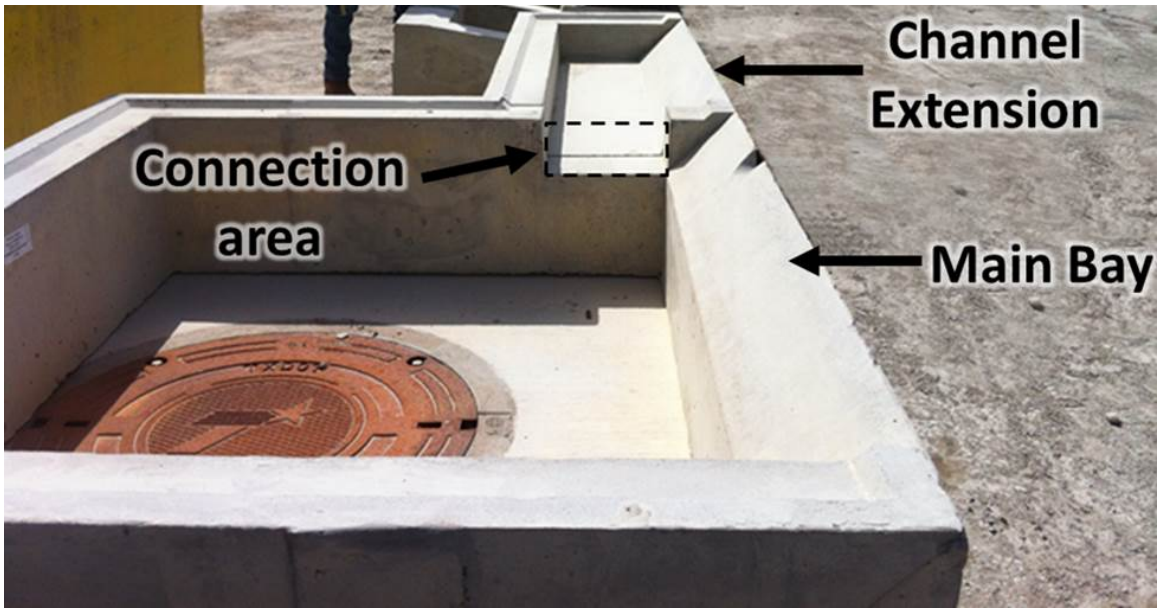

Figure 5.2: Upper inlet basin of TxDOT PCO 10-ft inlet. Manhole and concrete floor are of separate component on which the upper inlet is stacked (photograph courtesy of TxDOT).

gutter exceeds the height of the inlet opening, a conventional curb-inlet is expected to operate as an orifice with the inlet-opening acting as the effective opening area of the orifice. However, the reduction of the flow section at the extension might shift the controlling orifice area from the inlet opening to the relatively smaller area of the throat connecting the extension to the main bay. A decrease in the orifice area is likely to alter the expected inlet-operation and reduce the interception capacity. The current study uses a full-scale model of inlet with a channel extension on-grade and in a sag to evaluate these potential flow restrictions.

Hammonds and Holley (1995) studied the backwater effects in TxDOT inlets type C and D. For both inlets, the back wall of the inlet box was only 6 inches away from the inlet lip, which led to concerns that the captured fall would strike the back wall and back out into the street. Hammonds and Holley (1995) observed the flow conditions for an on-grade configuration and dismissed the occurrence of backwater

effects. They argued that the flow was supercritical, therefore any disturbance at the inlet box could not be transmitted upstream without drowning the supercritical flow and shifting it to subcritical. Flow striking the back wall of the inlet created a small roller (up to 4 inches in size), which eventually fell back into the inlet. This roller increased by increasing the gutter flow, but never became large enough to splash out of the inlet for the tested flow conditions. This observation suggests that curb inlets on-grade are somewhat resilient to box restriction. However, the concerns regarding the performance of extensions on-grade under different tail-water conditions and in a sag configuration are yet to be addressed. Hammonds and Holley (1995) noted that none of the literature they reviewed addressed backwater effects in inlets. Typically, curb inlets are modeled by simply removing the curb, and captured flow falls freely into a basin/channel to be measured afterwards. That is to say, the internal geometry of the inlet were not considered in previous studies (e.g., Karaki and Haynie (1961); Wasley (1960); Spaliviero et al. (2000)).

Finally, flush structural slab-supports are used in the design of many long inlets (length $>$ 5-ft), including the TxDOT PCO inlet which uses 6-inch flush supports for the top slab when extensions are used on the right, left, or both sides of the main inlet (Figure 5.3). HEC-22 states that these supports can "reduce the effectiveness of openings downstream of the support by as much as 50%". Schalla (2016) performed an extensive literature review and found no evidence supporting this statement by HEC-22. Moreover, Schalla conducted full-scale experiments for 15-ft inlet with and without slab supports, which showed no difference in intercepted flow between the two cases. The current study provides further experiments to confirm these findings.

The objective of this study is to quantify the effects of potential flow restrictions on the interception of curb inlets with channel extensions for on-grade and in a sag

Figure 5.3: 15-ft PCO inlet with two slab supports highlighted.

configurations, and to provide design guidance for TxDOT PCO inlets and flush slab supports. Section 5.2 provides a description of the physical modeling facility and the details of the conducted experiments. Section 5.3 and 5.4 present the experimental results and discussion, respectively. An updated design procedure for TxDOT PCO inlets on-grade and in a sag is detailed in Section 5.5. Section 5.6 presents summary of the conclusions and recommendations for design from this study.

5.2 Methods

5.2.1 Physical Model

This study uses and modifies a physical modeling facility at the University of Texas at Austin that was used for various earlier stormwater drainage studies (Holley et al., 1992; Hammonds and Holley, 1995; Schalla, 2016; Schalla et al., 2017). The model consists of a 64 ft long roadway with adjustable longitudinal and cross-sectional slopes. The roadway is 10.5 ft wide with wooden curbs at the sides along the roadway length. Water is supplied to the model from an outdoors reservoir using two pumps with a maximum combined capacity of 7 cfs. Water conveyed by the pumps enters the model through a headbox consisting of 5 pipes each with a ball valve, which allow

for controlling the distribution of the flow along the headbox width. Hollow concrete block are placed just downstream the headbox to further regulate the incoming flow. A full-scale model of a 10-ft standard curb inlet is installed on one side of the roadway at an on-grade configuration. Flow entering the inlet falls freely into channels leading to V-notch measurement weirs (Figure 5.4). Any flow past the inlet falls into a basin leading to a V-notch weir for measuring bypass flow. The inlet is installed with a 3 inches local depression and 16 inches wide depressed gutter. Depression transition sections, 10-ft each, are placed upstream and downstream of the inlet. The gutter edge at the curb changes from undepressed to fully depressed gutter gradually along the transition length. The roadway has a smooth surface and the calibrated Manning's n roughness coefficient is 0.012. Detailed description of the model set-up and instrumentation is reported by Schalla (2016).

To test the PCO inlet, the first 5-ft portion of the inlet is converted into a box with inner dimensions 12" x 5" (dimensions of the upstream extension of the TxDOT PCO inlet shown in Figure 5.5). In this configuration, the downstream 5-ft section acts as the main bay of the PCO inlet (free-fall overflow along inlet edge), and the first 5-ft section acts as the channel extension of the PCO inlet.

The 15 ft PCO inlet is not modeled as it is expected to have a critical clogging problem when installed on-grade. Debris entering the upstream extension will move with the flow into the main bay, provided that the debris is not larger than the inner throat opening. However, recirculation is expected to occur at the corner of the downstream stream extension; debris will accumulate over time and block a significant portion of the downstream extension. Accordingly, designers are advised not to use the 15 ft PCO inlet on-grade, and the current study limits the on-grade experiments to the 10-ft PCO inlet with an upstream extension.

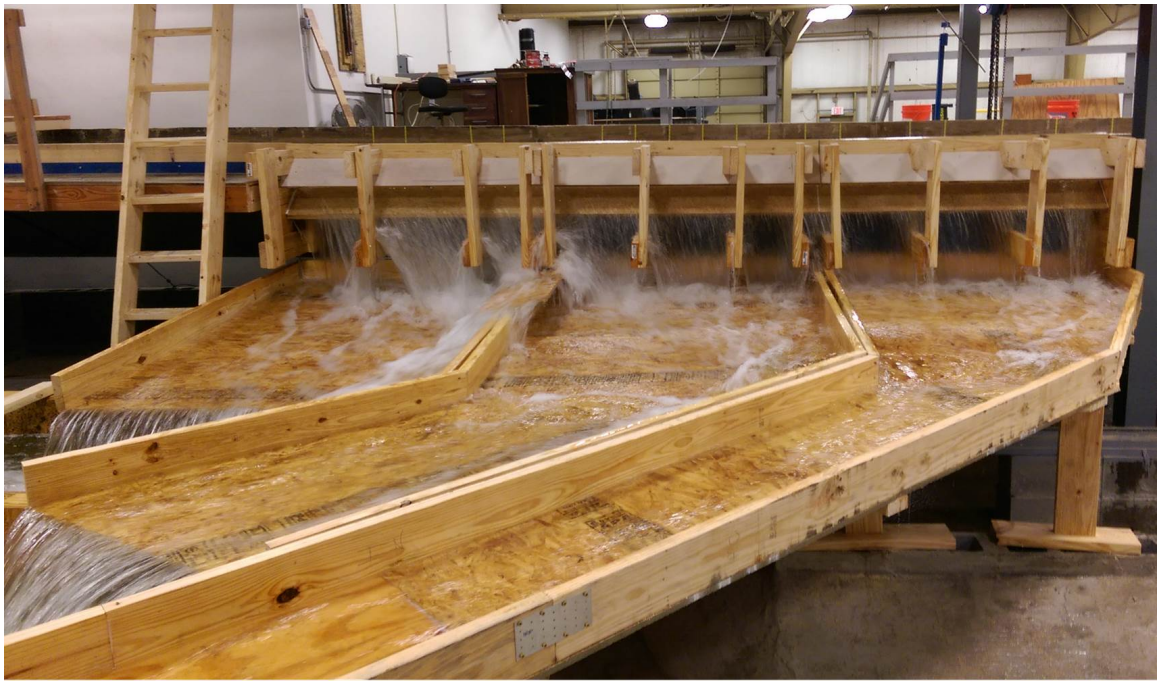

Figure 5.4: Rear view of the model of the standard inlet on-grade showing free-fall overflow into the inlet.

Figure 5.5: Opening connecting the two 5-ft sections in the model.

Considering a PCO inlet in a sag, the main bay of the inlet (middle 5-ft section) is designed as a conventional inlet and hence is expected to follow standard design equations for an inlet in a sag. Consequently, only the upstream extension is tested in this study. Modeling the extension alone instead of the entire 10-ft inlet avoids experiments at very high discharges, which are difficult within the experimental facility. To model a fully-submerged inlet condition, a wall is constructed across the roadway completely blocking off the flow to the downstream of the inlet and causing ponding of water at the inlet. This procedure provides a sufficiently high depth of water the inlet, as shown in Figure 5.6. The use of a wall to simulate the flow conditions for an inlet in a sag was applied in the experimental work of Sill et al. (1986), White and Pezzaniti (2002), and Kranc et al. (1998).

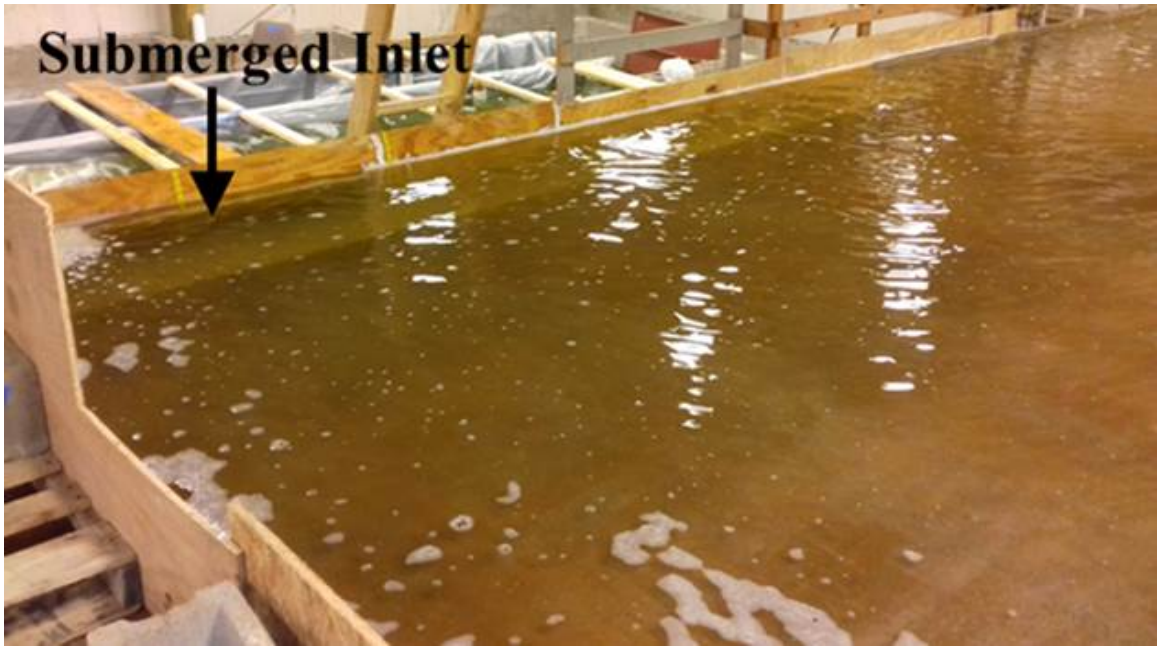

Figure 5.6: Fully-submerged inlet, looking upstream.

5.2.2 Experiments

The 10-ft standard inlet is tested with and without a slab support under five different combinations of longitudinal slopes and cross-slopes configurations, for 100% and bypass flow conditions. Another set of tests are carried out to investigate whether the PCO on-grade would have interception capacity similar to a standard inlet. A total of 27 tests are carried out for varied slope combinations and flow conditions as summarized in Table 5.1. The incoming flowrate in the gutter ranges from 0.46 cfs to 4.87 cfs.

TxDOT sets the maximum allowable tail-water (water level inside the inlet) at the upper lip of the inlet, which does not affect the inlet hydraulics. However, the design of the PCO inlet may cause its interception capacity to be affected by a rise in the tail water. When the tail water rises to the upper lip of the inlet, the upstream extension will be completely flooded. With a flooded extension, the capacity of the upper inlet may be controlled by the throat connecting the extension to the main chamber.

Table 5.1: Tested configurations for PCO inlet on-grade.

Property	**Tested**
Longitudinal slope (%)	0.1, 0.5, 1.0, 2.0, 4.0
Cross slope (%)	2.0, 4.0, 6.0
Flow Rate Conditions	100% interception, 0.3 and 0.5 cfs bypass

The effect of the tail-water on the inlet's interception capacity is investigated by running a series of tests at two water levels: The upper and lower lips of the inlet (levels A and B, respectively, as shown in Figure 5.7). To raise the tail water to the required level (level A or B), a box is constructed just below the lower lip of the inlet, and the height is of the side of the box facing the inlet is adjusted to the tested

level. The purpose of the box is to force water to accumulate to the desired level before it can flow over the edge of the box. Figure 5.8 shows the full box at level A setup, and the water level can be observed at the upper lip of the inlet. Three slope combinations were tested for each of levels A and B (10 tests in total).

Figure 5.7: The two tested tail water levels, looking from inside the inlet.

The goal of testing the extension in a sag is to investigate the change in the interception capacity as a function of the flow depth at the inlet. A total of 86 tests are carried out for the same slope combinations mentioned in Table 5.1, and 22 of these tests are carried out at fully-submerged inlet conditions. The incoming gutter flow ranges from 0.19 cfs to 2 cfs, and the depth at the beginning of the inlet varies from 1.8 inches to 11 inches.

5.3 Results

Experiments for 10 ft inlet, and 15 ft by Schalla (2016), show no measurable difference in interception capacity due to the presence of the slab supports, as shown in Figure 5.9. A standing wave is observed at the support reaching up to 2 feet both

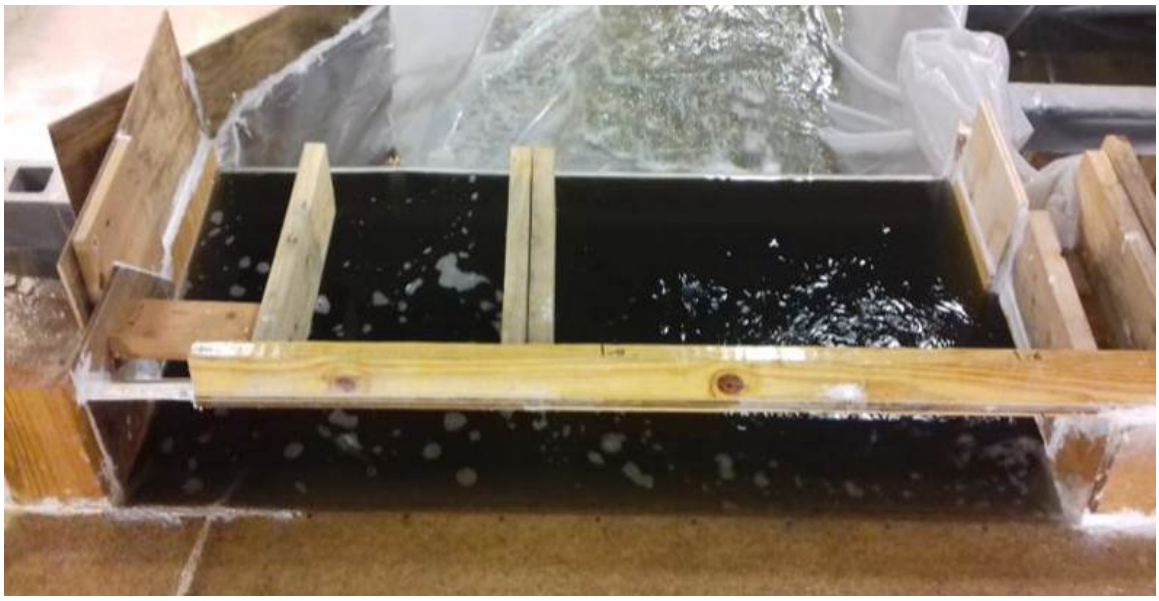

Figure 5.8: Full box at level A setup.

upstream and downstream of the slab supports. However, these local effects do not affect the ponded width or the interception capacity of the inlet; flow obstructed by the supports is simply diverted into the inlet upstream and/or downstream of the support.

The intercepted flowrates at the PCO inlet tests are compared to the flowrates from standard inlet tests (where the upstream section provides free-fall into its own chamber). The results (Figure 5.10) indicate no significant observable difference between the intercepted flowrates over the tested flow range. The average difference between the intercepted flowrates is 2.4%, which is below the uncertainty in flow measurement at the model, as reported by Schalla (2016).

As for tail-water condition tests, intercepted flowrates at these tests (box full till level A or B) are plotted against intercepted flowrates at low tail water condition (Figure 5.11). No observable difference is detected between the intercepted flowrates at low tail water conditions and at both levels A and B. Even when the upstream

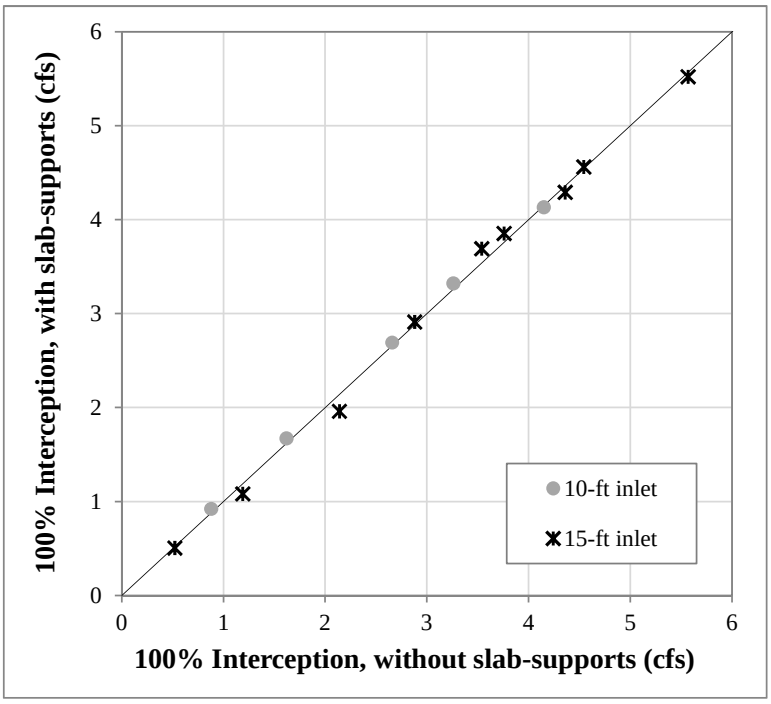

Figure 5.9: Comparison between 100% interception with and without slab supports for 10 and 15 ft inlets.

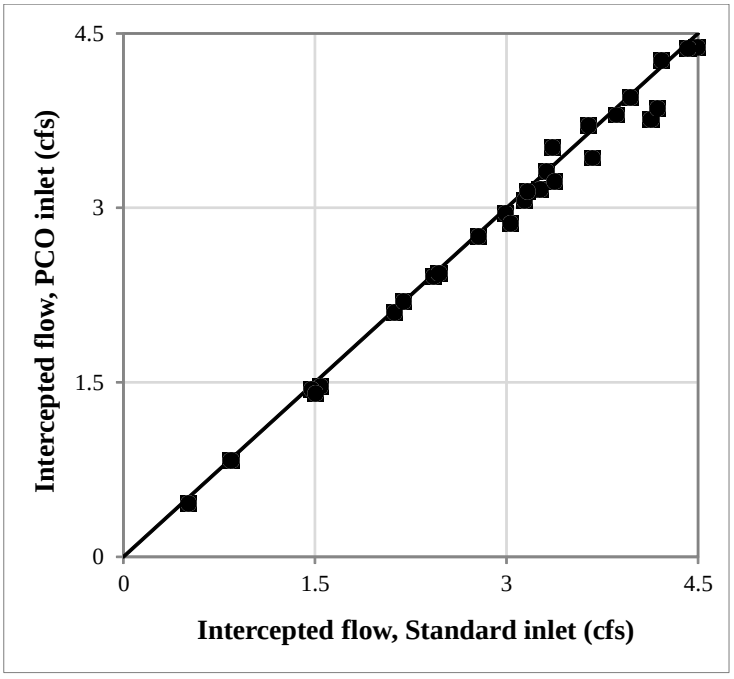

Figure 5.10: Comparison between interception of PCO and standard inlets on-grade.

extension is completely flooded, the excess inflow into the upstream extension is diverted into the main bay of the inlet so the total interception remained the same.

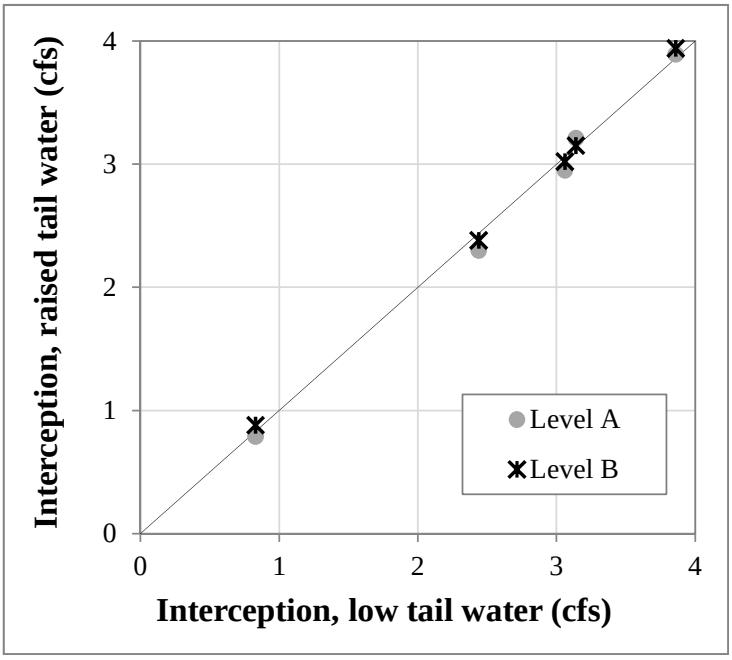

Figure 5.11: Comparison between interception low and raised tail water conditions.

The measured intercepted flowrates for the extension at a sag are plotted against the flow depth at the inlet (Figure 5.12). An initial exponential increase in the inlet capacity is observed as the depth increased. At a depth of about 4.5 inches, the exponential rate went through a milder transition before turning into a slow linear behavior as the water depth approaches the clear height of the inlet opening (6").

5.4 Discussion

Figure 5.9 shows that there is no difference between intercepted flow with and without slab supports. In other words, to compute the effective inlet opening the presence of the slab supports should be ignored and the length of the inlet be

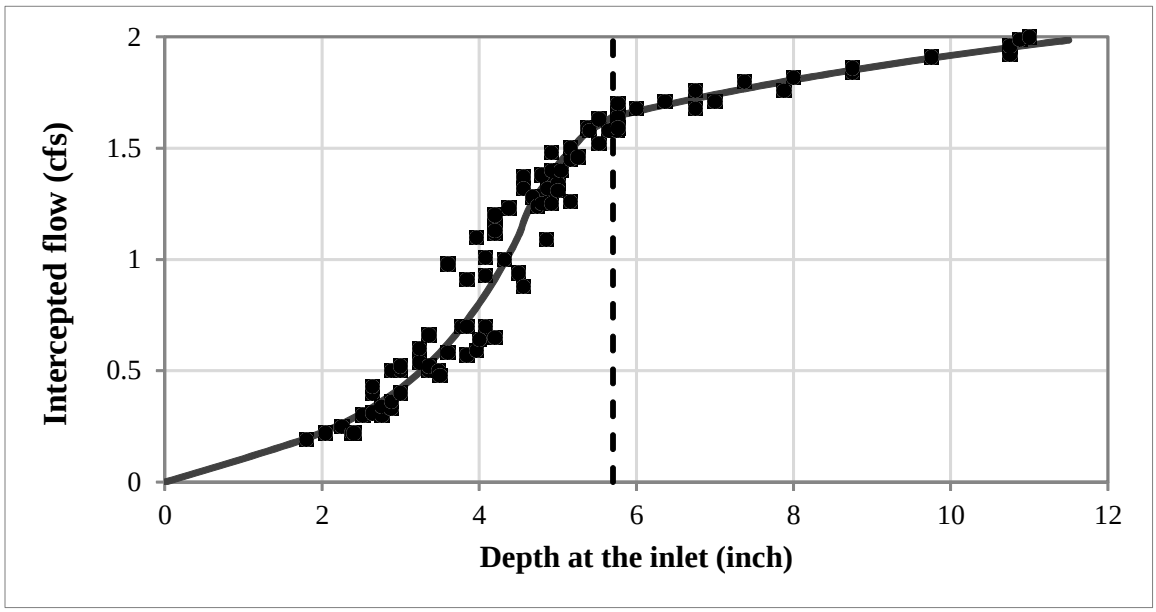

Figure 5.12: Intercepted flowrate at the extension of a PCO inlet (in a sag) as a function of the depth at the inlet.

considered as the distance from the upstream to the downstream ends of the curb opening (i.e., including the length nominally blocked by the slab support as long as such blockage is sufficiently similar to the 6-inch length of the tested slab supports). These results indicate that the HEC-22 statement about slab supports reducing inlet capacity is incorrect. However, this should not be taken as proof that slab supports are irrelevant for practical installation. We have not tested the effects of debris clogging, but can speculate on some of the likely effects. The presence of slab supports arguably makes clogging more likely as large debris (e.g., tree branches) can get caught on slab supports and collect additional debris. As for inlets with channel extensions, the effect of such clogging would depend on whether 1 bay, 2 bays, or an entire 3-bay system is clogged. Note that the PCO inlet extensions will likely have increased clogging due to the reduced area at the throat between the extension and the main basin.

The comparison in Figure 5.10 suggests that, from a hydraulic standpoint, the PCO inlet is equivalent to a standard inlet on-grade. This conclusion is consistent with the findings of Hammonds and Holley (1995) regarding the absence of backwater effects at constricted inlets on-grade. However, our observation of experiments shows that despite the results of Figure 5.10, the upstream section does become saturated at high flowrates; however the excess inflow is simply diverted to the downstream inlet section, which typically has much smaller interception. We conclude from this analysis that, compared to the standard inlet results, there is no observable decrease in the overall PCO inlet interception capacity for an incoming gutter flow up to 4.87 cfs. Furthermore, there is no indication that any decrease in the inlet capacity will occur for higher gutter flows as long as the operation is at conventional design conditions of 100% capture or low bypass. The hydraulics of 100% capture for the PCO inlet are different than a standard inlet, but the end result is the same for the tested conditions. However, we speculate that for high bypass conditions (>> 0.5 cfs bypass), the PCO inlet will have degraded capture compared to a standard inlet. This result should occur because an upstream extension of a PCO inlet will reach full submergence with smaller capture compared to a conventional inlet. Once a PCO extension reaches full submergence it seems likely that its overall performance will rapidly degrade compared to a conventional on-grade inlet. It can be expected that high bypass conditions for a PCO inlet will have both degraded capture and extended ponding width across the roadway. Note that recent full-scale experimental work established that interception by an on-grade standard 10-ft inlet is significantly less than predicted by HEC-22 equations under some slope configurations (Schalla et al., 2017). Thus, the PCO interception is not degraded relative to a standard inlet, but both configurations do not achieve the theoretical design capacity.

As for PCO inlet in a sag, the sharp drop in the inlet performance observed at the mild linear section of Figure 5.12 indicates a shift in the flow regime through the inlet, suggesting that the flow through the inlet is being controlled by the extension inner-throat rather than the extension's inlet opening. An orifice-flow equation is fitted to the observed intercepted flow at the linear section of Figure 5.12. The orifice equation is given by HEC-22 in the form of:

$$Q_i = C_o A_g \sqrt{2gd_o} \tag{5.1}$$

where Q_i is the intercepted flowrate (cfs), C_o is the orifice coefficient, A_g is the clear area of the orifice (ft^2), and d_o is the effective head on the center of the orifice opening (ft). On the fitting Equation (5.1) to measurements, the area of the extension throat is considered to be the orifice area and the obtained orifice coefficient is 0.55. The final form of the orifice equation for interception of a submerged PCO extension is:

$$Q_i = 1.84\sqrt{d_i - 0.292} \tag{5.2}$$

where d_i is the depth at the inlet (ft). HEC-22 uses an orifice coefficient equal to 0.67, and considers the inlet opening to be the control section of the orifice-flow, i.e., A_g is equal to the inlet opening area. Substituting the dimensions of the PCO extension (under the assumption that A_g is equal to the inlet opening) in Equation (5.1) yields:

$$Q_i = 12.1\sqrt{d_i - 0.181} \tag{5.3}$$

Equation (5.3), obtained from HEC-22, is based on orifice area equal to the inlet opening, while Equation (5.2) uses the extension throat as the orifice area. The area of the throat is 0.4167 ft^2 while the area of the extension is 2.25 ft^2; the area of the outlet is 18.5% of that of the inlet opening. Consequently, the interception capacity based on HEC-22 is expected to be greater than that of the PCO design by a factor of four or five. The comparison between the computed intercepted flowrates from Equations (5.3) and (5.2) is plotted in Figure 5.13. At small depths, the ratio of Q_model to Q_{HEC-22} is 0.26, but decreased to 0.19 for depths of 12 inches. The average ratio is 0.23, which is in agreement with the factor of four or five deduced from the analysis of the ratio between the control areas in the two equations.

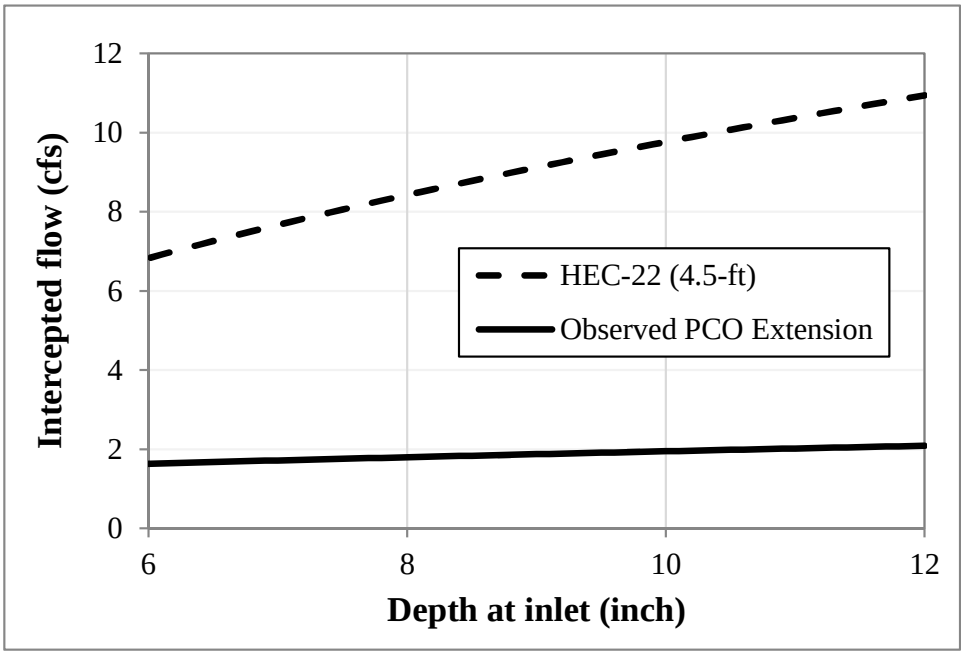

Figure 5.13: Intercepted flowrates at the PCO extension as a function of water depth at the inlet based on HEC-22 and Experimental results.

Figure 5.14 shows the ratio between the inlet interception based on physical model results and based on HEC-22 against the depth at the inlet for the case of

one extension, 10 ft and 15 ft PCO inlets. For 10-ft PCO, the ratio of Q_{model} to Q_{HEC-22} is 0.6 for small depths, and decreases to 0.56 for depths of 12 inches, with an average ratio of 0.58. For 15-ft PCO, the ratio of Q_{model} to Q_{HEC-22} is 0.49 and decreases to 0.44 for depths of 12 inches, with an average ratio of 0.47. The extension alone has a capacity of less than 25% of the HEC-22 estimate. The 15-ft PCO inlet is designed with two extensions, each of which is operating at a significantly lower capacity than the main bay and take up 2/3 of the nominal curb inlet area. In contrast, the 10-ft inlet has only one extension that takes of 1/2 of the nominal flow area. Consequently, the capacity of the 15-ft relative to the HEC-22 capacity (Q_{model}/Q_{HEC-22}) is lower than that of the 10 ft inlet. The 15-ft inlet represents a more critical case than the 10 ft inlet; the 15 ft inlet is operating at less than half the expected capacity.

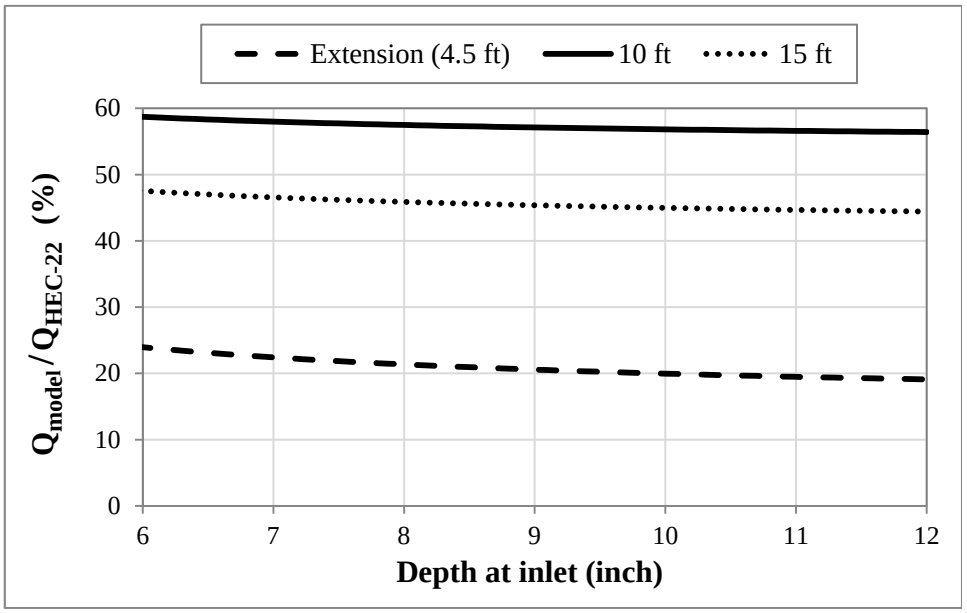

Figure 5.14: Intercepted flowrates at the PCO extension as a function of water depth at the inlet based on HEC-22 and experimental results.

5.5 Design Procedure of PCO Inlets

The discussion in §5.4 shows that a 10-ft PCO inlet on-grade is equivalent to a conventional inlet, from the stand point of inlet interception capacity (for 100% interception or up to 0.5 cfs bypass conditions). However, the HEC-22 equations for standard inlets on-grade was shown to make inaccurate predictions (Schalla et al., 2017). This analysis aims at deriving a new equation for computing the 100% interception capacity of PCO inlets. Regression analysis is applied to experimental results at 100% interception condition for PCO inlet without restrictions at the extension. Summary of the range of data used in this analysis is provided in Table 5.2.

Table 5.2: Range of experimental data used in developing the design equation for PCO inlet on-grade.

Property	**Lower Limit**	**Upper Limit**
Inlet Length, ft	5	10
Roughness coefficient n	0.012	0.016
Cross slope, %	2	6
Longitudinal Slope. %	0.1	4

The developed relationship between the intercepted flow (Qi) at 100% interception condition and the roadway configuration is:

$$Q_i = 8.4\ L_i\ n^{1/3}\ {S_x}^{7/8}\ {S_L}^{-1/8} \tag{5.4}$$

where Q_i is in cfs, L_i is the inlet length in ft, n is Manning's roughness coefficient, S_x is the roadway cross-slope, and S_L is the roadway longitudinal slope. Figure 5.15 shows the comparison between observed and computed 100% interception flowrate using Equation (5.4). The predicted flowrates are in good

agreement with the observed flow. The R^2 for this relationship is 0.93 and the RMSE is 0.25 cfs. Two considerations regarding using Equation (5.4): First, designers are advised not to use this equation beyond the tested conditions summarized in Table 5.2. Second, this equation applies only for the gutter geometry of the PCO inlet (gutter width 16 inches and local depression of 3 inches).

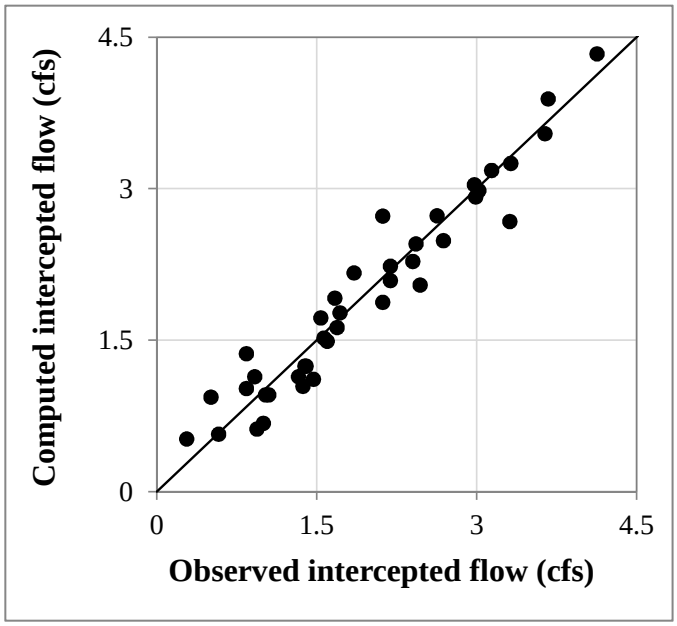

Figure 5.15: Observed and computed intercepted flow using Equation (5.4).

In practice, the PCO inlet in a sag is either installed as a main bay and one extension (10-ft total inlet length) or a main bay and two extensions (15-ft total inlet length). The main bay is designed as a standard inlet; so the interception capacity of this portion of the inlet can be determined following HEC-22. To determine the total capacity of the inlet, the following steps are to be followed:

1. The capacity of the main bay is computed by Equation (5.3),

2. if the total inlet length is 10 ft, then the capacity computed at step (1) is added to the capacity of one extension as computed by Equation (5.2),

3. if the total inlet length is 15 ft, then the capacity computed at step (1) is added to the capacity of two extensions by multiplying the capacity computed from Equation (5.2) by two.

5.6 Summary and Conclusions

Experiments on 10 ft inlets supported the findings of Schalla (2016) that there is no measurable difference in interception capacity due to the presence of the slab supports. During the tests, a standing wave is observed at the support reaching up to 2 feet both upstream and downstream of the slab supports. However, these local effects do not affect the interception capacity of the inlet; flow obstructed by the supports is simply diverted into the inlet upstream and/or downstream. During capacity calculations, the width of the slab supports should be included in the effective inlet length. This analysis did not test and thus does not invalidate the practical concerns regarding the use of slab supports such as increased risk of inlet clogging.

A series of tests is conducted to investigate the effect of the constricted upstream extension on the overall interception capacity of the PCO inlet on-grade. Results from these tests show no notable difference from interception capacity of a 10-ft inlet with a free-fall overflow along the entire inlet length. However, degraded inlet capture is expected at higher bypass flow conditions ($Q_bypass >> 0.5$ cfs). Another series of tests show that a tail water as high as the upper lip of the inlet (maximum allowable level by TxDOT) will not affect the inlet's interception capacity. Interestingly, the observed inlet capacities are very robust to the significant changes in the hydraulic configurations between the PCO and non-PCO inlets. Although the constriction of the upstream inlet did not cause further limitation of the inlet's interception capacity, the HEC-22 design equations cannot be directly applied to the PCO inlet under

all conditions. Regression analysis is applied to experimental data to provide an alternative design equation for the capacity of PCO inlets on-grade.

The capacity of the extension of the PCO inlet in a sag is investigated through a series of experiments. Results from these experiments showed that HEC-22 significantly overestimates the interception capacity of the extension. The design of the extension changes the orifice control-section from the inlet opening to the smaller opening of the inner throat. An equation is proposed for the capacity of the extension as a function of the depth at the inlet. This equation is used in combination with HEC-22 to determine the capacity of the 10 ft and 15 ft PCO inlets. This analysis shows that the capacity of the 10 ft and the 15-ft PCO inlet are about 58% and 47% of the capacities computed using HEC-22. The significant decrease in interception capacity of PCO inlets calls for careful consideration from designers upon deciding to install these inlets in a sag, particularly for a 15-ft inlet.

Chapter 6

Conclusions

6.1 Summary

The objective of this study is to provide insights into the hydrodynamics of curb inlets flow and to prepare updated design guidance for curb inlets. These objectives involved investigating the assumptions in HEC-22 equations, the hydraulics of undepressed inlets, the applicability of scaled models, the performance of conventional depressed inlets, and the potential flow restrictions in inlets with channel extensions. Extensive literature review for experimental data and a full-scale physical model of a depressed inlet mounted on a roadway with adjustable slopes were used to address these issues. A comparison between full-scale and scaled models of depressed and undepressed inlets in South Africa showed a significant mismatch between the two cases, especially at shallow water depth for depressed inlets. Therefore, the use of a full-scale model eliminated potential sources of error due to misrepresentation of Reynolds number effects in scaled models. Experimental data from this study and the literature were employed in assessing the design procedures in HEC-22 and proposing revisions to HEC-22. Conclusions and recommendations from this study are summarized in Table 6.1. Experimental data measured in this study, and data for depressed and undepressed inlets reported in the literature was provided in Appendix A. The performance of recessed inlets is discussed in Appendix C.

Table 6.1: Summary of recommendations and conclusions.

Design Condition \ Curb Inlet Type		Undepressed Inlets	Locally Depressed Standard Inlet	Locally Depressed PCO Inlet	Inlet with Continuously Depressed Gutter	Recessed Depressed Inlet
On-grade	100% Interception	(Section 3.3) HEC-22 generally underestimates interception. Use Equation 3.16	(Section 4.6) Compute interception using Equation 4.5, 4.6	(Sections 4.6 and 5.5) Compute interception using Equations 4.5, 4.6 or Equation 5.4	(Section 4.5) HEC-22 underpredicts interception of short inlets (<5 ft) and overpredicts long inlets (>10 ft)	(Appendix C) 25% reduction in interception compared to locally depressed standard inlet under some conditions.
	Partial Interception	(Section 3.3) HEC-22 provides a reasonable estimate. Use Equations 3.17, 3.18, and 3.19	(Section 4.7) Compute efficiency using Equation 4.8	(Sections 4.7 and 5.4) Compute efficiency using Equation 4.8. Expected reduction in capture at high bypass (>> 0.5 cfs)		
	Flat S_x and Steep S_L	(Section 3.4) Degradation in inlet performance			(Section 3.4) Potential degradation in Inlet performance	
	Flush Slab Supports	(Section 5.3) 50% reduction in interception is highly unlikely	(Section 5.3) 6" wide supports have no effect on interception. Supports should be included in inlet opening length			
Sag		Interception is expected to follow HEC-22		Section (5.5) Significant reduction in capacity. Recommend using a standard inlet. Compute extension capacity by Equation 5.2	Interception is expected to follow HEC-22	
Froude Number Scaled Models		(Section 3.6) Applicable for smooth surfaces or considerably large flow depth	(Section 3.6) Further work is required to confirm their validity in the case of smooth roadway. Inaccurate modeling at rough roadway surface.			

6.2 Derivation of HEC-22 Equations

HEC-22 equations are recommended by the FHWA and thus are widely used in storm drainage design. However, HEC-22 does not well-document the sources and assumptions in the equations. The need to investigate these assumptions was more pressing after recent experimental work (Schalla et al., 2017) questioned the accuracy of these equations. Therefore, a detailed derivation was provided for HEC-22 equations for undepressed and depressed inlets at 100% interception and bypass flow conditions. HEC-22 followed the analysis provided by Izzard (1950) for undepressed inlets, and rounded up the numerical coefficients in the final proposed equation. HEC-22 then departed from Izzard's analysis and extended the design equation to undepressed inlets by introducing the equivalent slope S_e. A major discrepancy was identified between the exponent in the inlet efficiency equation as derived from theory and as recommended by HEC-22. A likely explanation for the departure from theory is that HEC-22 is compensating for a bias in predictions that was introduced by the assumption of S_e.

6.3 Hydraulics of Undepressed Curb Inlets

An analysis was provided for the assumptions in HEC-22 design equations and other reported approaches for design of undepressed inlets, and the predictions of these equations were tested against experimental data. HEC-22 provided the poorest predictions for 100% interception, with underestimation exceeding 25% at various observations. A new equation for the 100% interception capacity of undepressed inlets was proposed that reduced the percentage error by a factor of 2 compared to HEC-22. The inlet efficiency equation proposed by HEC-22 compensates for the underprediction bias in HEC-22's 100% interception

computations. Consequently, this Equation should not be used with any approach that provides accurate estimate of L_T to avoid overestimation of the inlet efficiency. Given an accurate estimate of L_T, an expression is proposed to compute α as a function of the cross-slope. Using the computed α (from the proposed expression) in the efficiency equation provides better match with experimental data compared to HEC-22 at bypass condition. Experimental work on depressed and undepressed inlets show that the inlet performance will deteriorate at configurations with flat cross-slope and steep longitudinal slope. This observation is consistent with old design criteria by FHWA (Jens, 1979) that undepressed inlets should not be used for $S_L > 3$. However, experimental data from Hammonds and Holley (1995) and Li et al. (1951) should that undepressed inlets can still be effective at steep S_L if a steep S_x is used as well ($> 3\%$).

The most comprehensive theoretical study on the hydrodynamics of curb inlets was conducted by Wasley (1960), however, the model provided inaccurate predictions for inlets at flat cross-slope configurations. The current study used the experimental data by Wasley to provide an alternative derivation for Wasley's design equation, and the derivation suggested that the inaccuracy in Wasley's predictions was due to ignoring the angle of flow into the inlet. Finally, review of studies on the applicability of scaled models to the study on curb inlets showed conflicting findings. An analysis was presented herein that provided a potential explanation for the apparent conflict in the reviewed literature. Observations for short inlets from each study were scaled to correspond to long inlets and the observed vs. scaled discharge was compared. The inflow obtained from scaling relations matched well with the observed inflow for undepressed inlets on a smooth surface, whereas scaling provided inaccurate inflows for inlets on a rough surface.

This analysis suggests that Froude number scaling is appropriate for undepressed modeling inlets on smooth models, and preliminarily analysis shows that this applicability may extend to depressed inlets on smooth roadway, albeit with less confidence until confirmed with further research.

6.4 Interception Capacity of Depressed Curb Inlets on-grade

The 10 ft inlet was tested at original (Rough) and modified (smoother) model roughness. On comparing the tests for 10 ft inlets at different roadway roughness, only a minor decrease in inlet interception capacity was observed. The intercepted flowrates at 100% interception condition for the 5, 10, and 15 ft inlets (from this study and the work of Schalla (2016)) were compared to predictions by HEC-22. This comparison showed that HEC-22 overestimated the intercepted flow by the 10 and 15 ft inlets, and underestimated the capacity of 5 ft inlets. Potential sources of errors in the assumptions employed by HEC-22 include: 1) the invalid assumption of linear decrease in water surface profile along the length of the inlet, and 2) oversimplification of flow immediately upstream the inlet, and 3) using the equivalent slope Se to account for the combined effects of the two slopes (road cross slope and gutter slope) of the compound gutter section.

A comprehensive literature review produced a database for scaled and full-scale experiments on curb inlets from six different studies. Data from prior experiments was scaled to the present model dimensions to avoid potential errors from scaling comparisons. The final dataset was used to derive an expression for a correction factor to the 100% intercepted flow computed by HEC-22. The correction factor reduced the RMSE from HEC-22 by a factor of 3.75. A critical problem for designers is that the interception capacity of curb inlets rapidly degrades as the longitudinal

slope increases. This deficiency is compounded when a steep longitudinal slope is combined with a relatively flat cross slope, as witness by the tendency of flow to go past the inlet during experiments for such slope configurations.

During analysis of data for inlets at bypass condition (less than 100% efficiency), a linear relationship was observed between the intercepted flowrate (Q_i) and the spread of the gutter flow (T). The proposed formula by HEC-22 for bypass flow is based on the parameter L_T, the required inlet length for 100% capture of the approaching gutter flow. Experimental data for this parameter is scarce in the literature due to the practical difficulties of setting up experiments with variable inlet length. Proposing a formula based on Q_i and T allows for using vast experimental datasets reported in the literature. The new formula was tested against 303 observations from six different studies, and showed good agreement with these observations. The RMSE was reduced by a factor of three compared to the HEC-22 approach. Finally, step-by-step instructions were provided for computing the expected inlet interception at 100% interception and bypass conditions using the proposed approaches.

6.5 Interception Capacity of Curb Inlets with Channel Extensions

Full-scale experiments on 10 ft inlet with and without a slab support showed no observable difference in the intercepted flowrate in the two cases. These results are consistent with previous experiments by Schalla (2016) for 15 ft inlets with and without slab supports. Consequently, the statement by HEC-22 that flush slab supports decrease the effectiveness of the inlet by as much as 50% was shown to be incorrect. The effects of the slab support are local and do not interfere with the intercepted flow. Thus, the presence of short slab supports (6 inches wide) should

be ignored in hydraulic computations and the total inlet length should be computed from the inlet opening to the inlet end without any adjustment for slab supports. However, the HEC-22 statement that slab supports have a significant effect on inlet clogging is not contradicted by the present work and potential for clogging should be considered in any design.

The downstream extension of a 15 ft PCO inlet on-grade is expected to have clogging issues, so the use of the 15 ft PCO inlet on-grade is not recommended. In the current study, the first 5-ft section of the model was modified to mimic the dimensions of the upstream extension chamber of the PCO inlet. The model for 10 ft PCO inlet was tested on-grade and the isolated upstream extension was tested in a sag. Tests on-grade showed that the PCO inlet on-grade intercepts the same flowrate as a conventional inlet of the same length. Tests on high tail-water conditions showed that the on-grade PCO inlet is robust under these conditions as well.

To test the PCO extension in a sag, a wall was constructed along the width of the model to accumulate the flow at the inlet for testing a fully submerged inlet condition. The intercepted flow by the inlet was plotted against the depth at the inlet and this plot showed that once the inlet was submerged there was a sharp decline in the intercepted flow. An orifice-flow equation was fitted to the data for fully submerged inlet, which showed that the control section in this case shifted from the curb opening of the extension to the much smaller inner throat. This shift in the control section diminished the intercepted flow by the extension to 23% of the expected interception from a non-restricted inlet of the same length. Since the 10 and 15 ft PCO inlets use one and two extensions, respectively, it follows that the overall intercepted flow by 10 and 15 ft PCO inlets in a sag will be 58% and 47% of the expected interception of conventional inlets of the same length. Because of this poor

performance, designers are advised not to use a PCO inlet in a sag where the inlet is expected to be submerged. Finally, the PCO inlet on-grade was shown to have similar effectiveness to a conventional inlet. Accordingly, a design procedure was developed for obtaining the 100% interception flowrate of PCO inlets on-grade. Designers are advised not to apply this design procedure outside the tested conditions.

Appendices

Appendix A

Experimental Data for Curb Inlets

A.1 Overview

A pure analytical approach to the hydraulic design of curb inlets is generally deemed implausible due to the complexity of flow in the vicinity of curb inlets (Hammonds and Holley, 1995). Although computational models are possible, these require verification against experiments before confidence in their results can be gained. Also, design equations and charts are more accessible to practitioners compared to (commercial) numerical models, which contributes to the scarcity of the use of numerical models in the literature. Curb inlets installed on a uniform cross-slope are known as undepressed inlets, whereas inlets installed on a depressed gutter are known as depressed inlets. In turn, depressed inlets are classified into: 1) Inlets with a locally depressed gutter, where the uniform gutter section upstream the inlet transitions into a depressed section at the inlet then the depressed section transitions back into a uniform gutter downstream of the inlet, 2) inlets with a continuously depressed gutter, where the gutter upstream and downstream of the inlet is depressed along the entire curb length and an additional local depression is sometimes added at the inlet. Various experimental investigations are reported in the literature on the interception capacity of the different types of curb inlets. Many of these studies are decades old, some were even conducted more than half a century ago, and thus are not readily accessible to researchers (e.g., Conner (1946), Wasley (1960), and Karaki and Haynie (1961)). This study aims at providing a collection of

the available experimental data on curb inlets to facilitate future research efforts. Most of these studies were conducted on scaled models based on Froude number scaling. Several concerns were raised regarding the applicability of scaling for curb inlets flow, especially for depressed curb inlets (Grubert, 1988; Zwamborn, 1966; Argue and Pezzaniti, 1996). Accordingly, data reported herein will use the actual tested model dimensions and flows instead of the up-scaled prototype dimensions. TableA.1 contains the description and dimensions of the reported data. Data reported herein are for experiments conducted for inlets on-grade (as opposed to inlets in a sag or sump condition), unless otherwise specified.

Table A.1: Symbols and units of reported data.

Symbol	**Description**	**Units**
L	Inlet Length	ft
Q_i	Intercepted flowrate by the inlet	cfs
Q	Gutter flow upstream of the inlet	cfs
Q_b	Flow bypassing the inlet	cfs
E	Inlet Efficiency (Q_i/Q)	%
w	Depressed gutter width	ft
a	Local depression height	inch
a_g	Continuous gutter depression height	inch
S_L	Roadway Longitudinal Slope	%
S_x	Roadway Cross-Slope	%
T	Measured normal flow spread	ft
d	Measured normal depth	ft
T_0	Measured Spread at the beginning of the inlet	ft
d_0	Measured depth at the beginning of the inlet	ft
L_u	Length of upstream transition	ft
L_d	Length of downstream transition	ft
n	Manning's roughness coefficient	ft

A.2 Measurements from The University of Texas Study

In 2015, the Texas Department of Transportation (TxDOT) commissioned The University of Texas at Austin to study the interception capacity of the TxDOT PCO inlet. The study included the testing of standard locally depressed inlets on-grade, inlets with channel-extensions on-grade, and inlet-extension in a sag. The experiments were conducted for 100% Efficiency and low bypass conditions (Q_b maximum $\sim$ 0.5 cfs). The study also investigated the effect on flush slab supports on the interception capacity, however, no observeable difference was found between experiments with and without slab supports; therefore only experimental data with slab supports was reported. The reported normal spread (T) and depth (d) were measured 10-ft upstream of the inlet. The reported data includes measurements by Schalla (2016). The parameters used in this study:

Scale: Full-scale (1:1); L = 5, 10, 15 (specified in table caption); w = 1.333; a=3; a_g=0; L_u = 10; L_d = 10; n = 0.0166 and 0.012 (specified in table caption); Y is the distance along inlet length starting upstream (ft); X is distance from curb (ft); GL is ground level (ft); D is flow depth (ft); WL is water surface level (ft).

Table A.2: Interception capacity for L= 15 and n=0.0166.

S_L	S_x	Q	Q_i	Q_b	E	T	d	T_0
4	6	3.54	3.54	0	100	5.6	0.28	4.65
4	6	5.78	5.49	0.29	94.98	7	–	5.7
4	6	5.46	5.24	0.22	95.97	6.8	0.29	5.5
4	6	4.58	4.53	0.05	98.91	6.1	–	5.1
4	4	2.14	2.14	0	100	6.3	0.19	5.3
4	4	4.56	4.15	0.41	91.01	9.4	0.22	7.5
4	4	3.81	3.63	0.18	95.28	8.95	–	6.7
4	4	3.46	3.37	0.09	97.4	8.6	0.21	6.35
4	2	0.523	0.523	0	100	5.1	0.08	4.9
4	2	2.36	1.9	0.46	80.51	10.3	0.13	9.7
4	2	1.82	1.58	0.24	86.81	9.6	0.12	8.5
4	2	1.23	1.15	0.08	93.5	8.1	0.1	7.05
2	6	4.545	4.545	0	100	6.35	0.35	6.05
2	6	5.609	5.54	0.069	98.77	6.95	0.43	6.7
2	6	5.608	5.537	0.071	98.73	6.95	0.44	6.65
2	6	5.83	5.68	0.15	97.43	7.15	0.4	6.8
2	4	2.88	2.88	0	100	6.8	–	6.5
2	4	4.59	4.32	0.27	94.12	9	0.28	7.6
2	4	4.17	4.01	0.16	96.16	8.6	–	7.3
2	4	3.82	3.74	0.08	97.91	8.1	0.26	7.1
2	2	1.19	1.19	0	100	7.9	0.11	7
2	2	1.73	1.69	0.04	97.69	10	0.13	8.6
1	6	5.57	5.57	0	100	7.8	–	6.85
1	6	5.9	5.88	0.02	99.66	7.8	0.41	7.1
1	4	3.76	3.76	0	100	9	–	7.6
1	4	4.59	4.49	0.1	97.82	10	0.3	8.1
0.5	4	4.36	4.36	0	100	10	0.3	8.6

Table A.3: Interception capacity for L= 10 and n=0.0166.

S_L	S_x	Q	Q_i	Q_b	E	T	d	T_0
4	6	2.63	2.63	0	100	4.4	0.25	4.45
4	6	4.71	4.16	0.55	88.32	6.05	0.31	5.2
4	6	4.14	3.81	0.33	92.03	5.55	0.3	5.05
4	6	3.59	3.46	0.13	96.38	5.05	0.29	4.85
4	4	1.67	1.67	0	100	4.8	0.17	4.65
4	4	3.67	3.19	0.48	86.92	7.5	0.21	6.1
4	4	3.24	2.94	0.3	90.74	7	0.2	5.9
4	4	2.6	2.51	0.09	96.54	6.1	0.19	5.5
4	2	0.443	0.44	0.003	99.32	4.65	0.06	4.5
4	2	2.08	1.59	0.49	76.44	9.15	0.12	8.6
4	2	1.71	1.41	0.3	82.46	8.65	0.11	7.9
4	2	1.13	1.03	0.1	91.15	7.33	0.1	6.45
4	6	3.02	3.02	0	100	5.45	0.3	4.95
2	6	4.83	4.34	0.49	89.86	6.65	0.36	6.1
2	6	4.38	4.08	0.3	93.15	6.4	0.34	5.8
2	6	3.72	3.62	0.1	97.31	6	0.32	5.35
2	4	2.19	2.19	0	100	6.2	0.21	5.35
2	4	3.87	3.4	0.47	87.86	7.9	0.27	6.85
2	4	3.39	3.09	0.3	91.15	7.5	0.25	6.6
2	4	2.84	2.75	0.09	96.83	6.6	0.24	6.1
2	2	0.92	0.92	0	100	7.05	0.1	6.4
2	2	1.6	1.51	0.09	94.38	9.05	0.13	8.2
2	2	2.09	1.82	0.27	87.08	10.1	0.15	9.4
2	6	3.32	3.32	0	100	6.5	0.33	5.2
1	6	5.25	4.76	0.49	90.67	7.6	0.4	6.7
1	6	4.54	4.29	0.25	94.49	7.1	0.36	6.1
1	6	3.99	3.88	0.11	97.24	7	0.35	5.7
1	4	2.4	2.4	0	100	7.4	0.25	5.85
1	4	4.2	3.68	0.52	87.62	9.3	0.31	8
1	4	3.7	3.39	0.31	91.62	8.7	0.3	7.5
1	4	3.04	2.94	0.1	96.71	8.1	0.27	6.8
1	2	1.39	1.39	0	100	9.7	0.15	7.9
1	6	3.64	3.64	0	100	7.2	0.35	6
0.5	6	5.63	5.14	0.49	91.3	8.65	0.43	7.2
0.5	6	4.74	4.55	0.19	95.99	8.2	0.4	6.9
0.5	6	4.38	4.28	0.1	97.72	8	0.38	6.55
0.5	4	2.69	2.69	0	100	8.75	0.26	7

Table A.3 – continued from previous page

S_L	S_x	Q	Q_i	Q_b	E	T	d	T_0
0.5	4	4.29	3.85	0.44	89.74	10.2	0.33	8.65
0.5	4	3.72	3.49	0.23	93.82	9.9	0.31	8.1
0.5	4	3.27	3.17	0.1	96.94	9.4	0.29	7.7
0.5	6	4.13	4.13	0	100	9	0.46	7.15
0.1	6	5.69	5.41	0.28	95.08	9.6	0.49	8.3
0.1	6	4.92	4.82	0.1	97.97	9.6	0.49	7.75
0.1	4	2.98	2.98	0	100	9.3	0.29	8.1

Table A.4: Interception capacity for L= 5 and n=0.0166.

S_L	S_x	Q	Q_i	Q_b	E	T	d	T_0
4	6	0.84	0.84	0	100	3	0.14	1.2
4	6	2.52	1.98	0.54	78.57	4.7	0.24	4
4	6	2.18	1.89	0.29	86.7	4.35	0.23	3.75
4	6	1.84	1.75	0.09	95.11	3.9	0.21	3.4
4	4	1.05	1.05	0	100	4	–	3.6
4	4	1.02	1.02	0	100	4.1	0.13	3.8
4	4	2.31	1.79	0.52	77.49	6.25	0.18	5.1
4	4	2.04	1.7	0.34	83.33	5.9	0.17	4.9
4	4	1.64	1.52	0.12	92.68	5.3	0.16	4.6
4	2	0.28	0.28	0	100	3.7	–	2.95
4	2	1.63	1.11	0.52	68.1	8.3	0.1	8.2
4	2	1.25	0.96	0.29	76.8	7.6	0.1	7.3
4	2	0.88	0.76	0.12	86.36	6.4	0.09	6.15
2	6	1.6	1.6	0	100	4.4	–	2.8
2	6	2.76	2.31	0.45	83.7	4.95	0.28	4.5
2	6	2.56	2.24	0.32	87.5	4.9	0.27	4.3
2	6	2.16	2.05	0.11	94.91	4.7	0.25	3.65
2	4	1.37	1.37	0	100	5.2	0.16	4.35
2	4	2.44	1.97	0.47	80.74	6.5	0.23	5.85
2	4	2.21	1.88	0.33	85.07	6.25	0.22	5.75
2	4	1.91	1.79	0.12	93.72	5.95	0.2	5.2
2	2	0.58	0.58	0	100	6	0.08	5
2	2	1.69	1.36	0.33	80.47	9.5	0.13	8.5

Table A.4 – continued from previous page

S_L	S_x	Q	Q_i	Q_b	E	T	d	T_0
2	2	1.37	1.2	0.17	87.59	8.7	0.12	7.7
2	2	1.09	1.01	0.08	92.66	7.85	0.11	7.15
1	6	1.69	1.69	0	100	4.9	0.25	3.5
1	6	3.03	2.54	0.49	83.83	6.15	0.31	4.85
1	6	2.62	2.34	0.28	89.31	5.9	0.3	4.5
1	6	2.2	2.1	0.1	95.45	5.4	0.29	4.1
1	4	1.33	1.33	0	100	6.05	0.19	4.1
1	4	2.74	2.23	0.51	81.39	7.8	0.26	6.5
1	4	2.3	2.01	0.29	87.39	7.25	0.23	5.58
1	4	1.79	1.7	0.09	94.97	6.7	0.24	5
1	2	0.94	0.94	0	100	8.1	0.12	6.4
1	2	1.64	1.39	0.25	84.76	10.15	0.15	8.65
1	2	1.46	1.3	0.16	89.04	9.8	0.15	8.3
1	2	1.24	1.17	0.07	94.35	9.4	0.14	7.75
0.5	6	1.717	1.717	0	100	5.6	0.26	4
0.5	6	3.21	2.7	0.51	84.11	7.05	0.32	5.8
0.5	6	2.81	2.51	0.3	89.32	6.6	0.31	5.3
0.5	6	2.35	2.24	0.11	95.32	6.25	0.29	4.8
0.5	4	1.4	1.4	0	100	6.75	0.2	4.8
0.5	4	2.74	2.23	0.51	81.39	8.7	0.25	7.15
0.5	4	2.28	1.99	0.29	87.28	8.1	0.24	6.4
0.5	4	1.83	1.73	0.1	94.54	7.6	0.22	5.7
0.5	2	1	1	0	100	10	0.12	7.25
0.5	2	1.17	1.15	0.02	98.29	10.4	0.13	7.8
0.1	6	1.85	1.85	0	100	6.2	0.32	4.7
0.1	6	3.48	2.98	0.5	85.63	8.2	0.42	6.5
0.1	6	2.97	2.67	0.3	89.9	7.7	0.4	6
0.1	6	2.31	2.23	0.08	96.54	7	0.36	5.35
0.1	4	1.57	1.57	0	100	7.85	0.25	5.65
0.1	4	2.43	2.16	0.27	88.89	9.5	0.31	7.45
0.1	4	1.98	1.87	0.11	94.44	8.8	0.29	6.65

Table A.5: Interception capacity for L= 10 and n=0.012.

S_L	S_x	Q	Q_i	Q_b	E	T	d	T_0
4	6	2.43	2.43	0	100	3.7	0.24	4.2
4	6	4.04	3.53	0.51	87.38	5	0.31	4.6
4	6	3.56	3.26	0.3	91.57	4.4	0.27	4.5
4	6	2.97	2.88	0.09	96.97	3.9	0.26	4.6
4	4	1.54	1.54	0	100	3.95	0.17	4.2
4	4	3.85	3.36	0.49	87.27	7.9	0.22	5.3
4	4	3.33	3.03	0.3	90.99	7.3	0.21	5.15
4	4	2.48	2.39	0.09	96.37	6.3	0.19	4.65
4	2	0.51	0.51	0	100	6.5	0.06	4.2
4	2	2.06	1.58	0.48	76.7	9.2	0.11	8.2
4	2	1.81	1.5	0.31	82.87	9.15	0.1	7.4
4	2	1.22	1.12	0.1	91.8	7.85	0.09	5.9
2	6	3.31	3.31	0	100	5.4	0.31	5.3
2	6	4.48	3.97	0.51	88.62	5.6	0.35	5.9
2	6	4.17	3.86	0.31	92.57	5.6	0.33	5.8
2	6	3.76	3.66	0.1	97.34	5.2	0.32	5.4
2	4	2.12	2.12	0	100	5.1	0.2	5.3
2	4	3.46	2.96	0.5	85.55	6.8	0.25	6.1
2	4	3.11	2.78	0.33	89.39	6.4	0.23	5.75
2	4	2.68	2.57	0.11	95.9	5.4	0.22	5.7
2	2	0.84	0.84	0	100	5.5	0.09	5.5
2	2	1.57	1.48	0.09	94.27	8.2	0.13	6.8
1	6	2.99	2.99	0	100	6.1	0.27	4.5
1	6	4.91	4.42	0.49	90.02	7.3	0.4	6.5
1	6	4.45	4.13	0.32	92.81	7	0.36	6.1
1	6	3.75	3.64	0.11	97.07	6.7	0.35	5.7
1	4	2.47	2.47	0	100	6.9	0.23	5.7
1	4	3.91	3.41	0.5	87.21	7.8	0.27	7.5
1	4	3.47	3.16	0.31	91.07	7.6	0.26	7.1
1	4	3.01	2.92	0.09	97.01	7.3	0.27	6.6
1	2	1.47	1.47	0	100	8.4	0.14	7.6
0.5	6	3.14	3.14	0	100	6.5	0.35	5
0.5	6	4.98	4.49	0.49	90.16	8	0.39	6.45
0.5	6	4.49	4.18	0.31	93.1	7.8	0.4	6.05
0.5	6	3.83	3.72	0.11	97.13	7.2	0.38	5.7
0.5	4	2.19	2.19	0	100	7.6	0.27	5.5
0.5	4	4.14	3.64	0.5	87.92	9.55	0.3	7.8

Table A.5 – continued from previous page

S_L	S_x	Q	Q_i	Q_b	E	T	d	T_0
0.5	4	3.67	3.37	0.3	91.83	9.1	0.29	7.4
0.5	4	2.97	2.88	0.09	96.97	8.4	0.28	6.4
0.1	6	3.67	3.67	0	100	8.1	0.46	6.3
0.1	6	4.28	4.21	0.07	98.36	9.2	–	6.8

Table A.6: Maximum Q such that flow immediately upstream the inlet is restricted to the depressed gutter section ($T_0 = w$), n=0.012 and L_i is length required to capture incoming flow (ft).

S_L	S_x	$Q_i = Q$	L_i	T	d	d_0
1	6	0.87	4.5	3.3	0.16	0.34
1	2	0.36	3	4.9	0.07	0.23
2	6	0.98	4.7	3.3	0.16	0.34
2	4	0.8	4.55	3.85	0.1	0.31
2	2	0.31	3.5	4	0.05	0.2
4	2	0.21	3.6	3.6	0.04	0.15
4	4	0.58	4.75	3.2	0.08	0.29
4	6	1.05	5.25	3.3	0.12	0.32
0.5	6	0.8	4	3.8	0.18	0.35
0.5	4	0.65	3.5	3.7	0.18	0.34
0.1	4	0.5	3.38	4.4	0.12	0.31
0.1	6	0.65	3.5	3.6	0.18	0.34
0.5	2	0.44	3.3	6	0.08	0.26
0.1	2	0.44	3	7	0.019	0.27
1	4	0.76	3	4	0.14	0.3

Table A.7: Measured water surface profile at the cross-section immediately upstream of the inlet at 100% interception. S_x=2, L=10, and n=0.012.

S_L							
		1		2		4	
X	GL	D	WL	D	WL	D	WL
0	0	0.36	0.36	0.28	0.28	0.24	0.24
0.3	0.062	0.308	0.37	0.22	0.282	0.176	0.238
0.6	0.125	0.242	0.367	0.16	0.285	0.103	0.228
0.9	0.187	0.188	0.375	0.087	0.274	0.018	0.205
1.2	0.249	0.128	0.377	0.023	0.272	0.023	0.272
1.5	0.28	0.06	0.34	0.033	0.313	0.018	0.298
2	0.29	0.054	0.344	0.03	0.32	0.018	0.308
3	0.31	0.047	0.357	0.023	0.333	0.014	0.324
4	0.33	0.041	0.371	0.023	0.353	0.005	0.335
4.2	0.334	–	–	–	–	0	0.334
5	0.35	0.04	0.39	0.012	0.362		
5.5	0.36	–	–	0	0.36		
6	0.37	0.03	0.4				
7	0.39	0.01	0.4				
7.6	0.402	0	0.402				

Table A.8: Measured water surface profile at the cross-section immediately upstream of the inlet at 100% interception. S_x=6, L=10, and n=0.012.

S_L									
		0.5		1		2		4	
X	G_L	D	WL	D	WL	D	WL	D	WL
0	0	0.54	0.54	0.54	0.54	0.51	0.51	0.42	0.42
0.3	0.0743	0.486	0.56	0.474	0.548	0.446	0.52	0.354	0.428
0.6	0.1485	0.413	0.562	0.401	0.55	0.372	0.521	0.257	0.406
0.9	0.2228	0.347	0.57	0.319	0.542	0.292	0.515	0.158	0.381
1.2	0.2971	0.272	0.569	0.243	0.54	0.196	0.493	0.06	0.357
1.5	0.34	0.22	0.56	0.204	0.544	0.12	0.46	0.063	0.403
2	0.37	0.184	0.554	0.169	0.539	0.096	0.466	0.065	0.435
3	0.43	0.123	0.553	0.098	0.528	0.078	0.508	0.044	0.474
4	0.49	0.06	0.55	0.022	0.512	0.05	0.54	0.012	0.502

Table A.8 – continued from previous page

S_L									
		0.5		1		2		4	
X	G_L	D	WL	D	WL	D	WL	D	WL
4.2	0.502	–	–	–	–	–	–	0	0.502
4.4	0.514	–	–	0	0.514	–	–		
5	0.55	0	0.55			0.007	0.557		
5.25	0.565					0	0.565		

Table A.9: Measured water surface profile at the cross-section immediately upstream of the inlet at 100% interception at low S_L. S_x=4, L=10, and n=0.012.

S_L							
		0.1		0.5		1	
X	GL	D	WL	D	WL	D	WL
0	0	0.5	0.5	0.46	0.46	0.43	0.45
0.3	0.06826	0.436	0.504	0.406	0.474	0.3958	0.464
0.6	0.1365	0.368	0.505	0.338	0.475	0.3229	0.459
0.9	0.2048	0.303	0.508	0.27	0.475	0.2604	0.465
1.2	0.273	0.237	0.51	0.203	0.476	0.1771	0.45
1.5	0.31	0.199	0.509	0.16	0.47	0.1354	0.446
2	0.33	0.183	0.513	0.137	0.467	0.1268	0.457
2.5	0.35	–	–	–	–	0.0973	0.447
3	0.37	0.151	0.521	0.097	0.467	0.0783	0.448
4	0.41	0.112	0.522	0.054	0.464	0.0506	0.461
5	0.45	0.082	0.532	0.021	0.471	0.0229	0.473
5.5	0.47	–	–	0	0.47	–	–
5.7	0.478	–	–			0	0.478
6	0.49	0.043	0.533				
7.3	0.542	0	0.542				

Table A.10: Measured water surface profile at the cross-section immediately upstream of the inlet at 100% interception at high S_L. S_x=4, L=10, and n=0.012.

S_L					
		2		4	
X	***GL***	***D***	***WL***	***D***	***WL***
0	0	0.42	0.45	0.36	0.36
0.3	0.06826	0.355	0.423	0.294	0.362
0.6	0.1365	0.283	0.42	0.207	0.344
0.9	0.2048	0.208	0.413	0.114	0.319
1.2	0.273	0.14	0.413	0.031	0.304
1.5	0.31	0.082	0.392	0.034	0.344
2	0.33	0.067	0.397	0.036	0.366
3	0.37	0.056	0.426	0.026	0.396
4	0.41	0.036	0.446	0.01	0.42
4.2	0.418	–	–	0	0.418
5	0.45	0.015	0.465		
5.3	0.462	0	0.462		

Table A.11: Measured water surface profile along inlet length at 100% interception. L=10 and n=0.012.

SL	0.1	0.5	1	1	2	4	4
Sx	4	6	6	2	4	2	6
Y				***D***			
0	0.425	0.477	0.474	0.32	0.377	0.204	0.368
0.25	0.333	0.404	0.397	0.244	0.31	0.167	0.325
0.5	0.25	0.303	0.306	0.185	0.248	0.097	0.276
0.75	0.209	0.252	0.249	0.155	0.197	0.074	0.233
1	0.192	0.219	0.208	0.14	0.174	0.075	0.19
2	0.143	0.197	0.166	0.116	0.144	0.075	0.128
3	0.107	0.125	0.132	0.088	0.137	0.058	0.132
4	0.074	0.103	0.106	0.052	0.108	0.03	0.116
4.25	0.04	–	–	0.019	–	–	–
4.4	–	–	–	–	–	0.005	–
5.4	–	0.065	–	–	–	–	–
5.55	–	–	–	–	0.053	–	–
5.9	–	0.035	0.05	–	–	–	–

Table A.11 – continued from previous page

$\boldsymbol{SL}$	0.1	0.5	1	1	2	4	4
$\boldsymbol{Sx}$	4	6	6	2	4	2	6
$\boldsymbol{Y}$	$\boldsymbol{D}$						
6	0.034	–	–	0.016	0.018	0.004	–
6.5	–	–	0.025	–	–	–	–
6.75	–	–	–	–	–	–	0.052
7	–	0.032	0.03	0.01	0.015	0.003	–
7.25	–	–	–	–	–	–	0.01
8	0.025	–	–	–	–	–	–
9	0.021	0.023	0.019	0.007	0.007	0.001	0.006
10	0.01	0.01	0.01	0.005	0.005	0	0.001

Table A.12: Measured water surface profile along inlet length at 100% interception. L=15 and n=0.0166.

	2 S_L, 2 S_x		**2 S_L, 4 S_x**	
$\boldsymbol{Y}$	**At curb**	**6" from curb**	**At curb**	**6" from curb**
0	0.312	0.23	0.44	0.341
0.5	0.144	0.2	0.24	0.305
1	0.125	0.164	0.174	0.262
1.5	0.115	0.138	0.154	0.233
2	0.102	0.102	0.144	0.203
2.5	0.089	0.075	0.131	0.174
3	0.066	0.016	0.131	0.154
3.5	0.046	0.016	0.125	0.131
4	0.013	0.013	0.115	0.118
4.5	0.013	0.013	0.102	0.102
5	0.013	0.013	0.098	0.079
6	0.013	0.013	0.052	0.043
7	0.013	0.01	0.036	0.036
8	0.007	0.01	0.033	0.033
9	0.01	0.007	0.03	0.03
10	0.01	0.01	0.026	0.026
11	–	0.007	0.023	0.023

Table A.12 – continued from previous page

	2 S_L, 2 S_x		**2 S_L, 4 S_x**	
Y	**At curb**	**6" from curb**	**At curb**	**6" from curb**
12	0.007	0.007	0.02	0.02
13	0.007	0.007	0.013	0.013
14	0.003	0.003	0.01	0.01
15	0	0	0	0.003

Table A.13: Interception of PCO inlet in a sag, L=4.5.

S_L	S_x	d_0	Q_i	S_L	S_x	d_0	Q_i
4	6	1.8	0.19	2	2	3.84	0.91
4	4	2.04	0.22	0.1	4	3.96	0.59
1	2	2.25	0.25	4	4	3.96	1.1
0.1	4	2.375	0.22	0.5	4	4	0.64
0.5	6	2.4	0.22	0.5	2	4.08	0.7
1	4	2.52	0.3	1	2	4.08	0.93
0.1	6	2.64	0.31	4	6	4.08	1.01
4	6	2.64	0.4	0.1	6	4.2	0.65
4	4	2.64	0.43	1	2	4.2	1.12
0.1	4	2.76	0.3	2	2	4.2	1.13
1	2	2.76	0.34	4	4	4.2	1.2
0.5	4	2.875	0.33	0.5	2	4.32	1
0.5	2	2.88	0.36	2	2	4.38	1.23
2	4	2.88	0.5	0.1	4	4.5	0.94
0.5	6	3	0.4	0.1	2	4.56	0.88
2	2	3	0.5	1	2	4.56	1.37
4	6	3	0.52	4	6	4.56	1.32
1	4	3.24	0.54	0.5	2	4.68	1.28
2	2	3.24	0.6	1	4	4.74	1.24
1	2	3.36	0.5	0.1	2	4.8	1.25
2	2	3.36	0.66	4	6	4.8	1.38
4	4	3.36	0.52	0.1	6	4.86	1.09
0.1	6	3.48	0.5	0.5	6	4.875	1.32
0.1	4	3.5	0.48	0.1	4	4.92	1.25
0.5	6	3.6	0.58	1	4	4.92	1.4

Table A.13 – continued from previous page

S_L	S_x	d_0	Q_i	S_L	S_x	d_0	Q_i
4	4	3.6	0.98	2	4	4.92	1.48
1	4	3.78	0.7	0.1	4	5	1.34
0.1	4	3.84	0.7	0.5	4	5	1.31
0.5	2	3.84	0.57	0.5	6	5.04	1.4
0.1	2	5.16	1.45	0.1	6	6.36	1.71
0.1	6	5.16	1.26	0.1	4	6.75	1.68
1	4	5.16	1.5	0.5	4	6.75	1.76
1	6	5.25	1.46	1	2	7	1.71
0.5	4	5.375	1.59	0.5	4	7.375	1.8
1	4	5.4	1.58	0.1	4	7.875	1.76
0.1	6	5.52	1.52	0.5	6	8	1.82
0.5	6	5.52	1.63	0.1	4	8.75	1.84
0.1	4	5.64	1.58	1	2	8.75	1.86
0.1	4	5.75	1.58	0.5	4	9.75	1.91
0.1	6	5.76	1.64	0.1	4	10.75	1.9
0.1	4	5.76	1.59	1	2	10.75	1.96
0.5	6	5.76	1.7	0.5	6	10.875	1.98
0.1	6	6	1.68	1	6	11	1.99

A.3 Reported Data in the Literature for Undepressed Inlets

Li et al. (1951) performed experiments for undepressed and depressed inlets as part of a comprehensive experimental study at the Johns Hopkins University (1956) for testing various types and configurations of storm drain inlets. Curb inlets of varying lengths were tested under 100%/bypass flow conditions. Only data for S_x 8.333% was reported by Li et al. (1951). The data for depressed inlets is reported in §A.4.1. The experiments were conducted for 1:3 scale, and the average roughness n was 0.01.

Table A.14: Experimental data for undepressed inlets by Li et al. (1951), T_c is the normal flow spread calculated as $T_c = d/Sx$.

S_L	S_x	L	Q	Q_i	Q_b	E	d	T_c
4	8.333	2.23	0.0199	0.0199	0	100	0.035	0.42
4	8.333	2.06	0.034	0.0244	0.0096	71.76	0.047	0.564
4	8.333	2.06	0.0565	0.0308	0.0257	54.51	0.05	0.6
4	8.333	2.4	0.0404	0.0314	0.009	77.72	0.048	0.576
4	8.333	3	0.0346	0.0346	0	100	0.046	0.552
4	8.333	3	0.0378	0.0365	0.0013	96.56	0.047	0.564
4	8.333	2.4	0.0642	0.0398	0.0244	61.99	0.058	0.696
4	8.333	3	0.0513	0.0423	0.009	82.46	0.05	0.6
4	8.333	1.63	0.1732	0.0532	0.12	30.72	0.083	0.996
4	8.333	3	0.0802	0.0558	0.0244	69.58	0.062	0.744
3	8.333	1.02	0.0879	0.0257	0.0622	29.24	0.078	0.936
3	8.333	1.02	0.0051	0.0051	0	100	0.024	0.288
3	8.333	1.62	0.0103	0.0103	0	100	0.032	0.384
3	8.333	1.02	0.0302	0.0148	0.0154	49.01	0.048	0.576
3	8.333	1.62	0.0269	0.0205	0.0064	76.21	0.048	0.576
3	8.333	2.06	0.0269	0.025	0.0019	92.94	0.048	0.576
3	8.333	2.21	0.0269	0.0269	0	100	0.048	0.576
3	8.333	2.25	0.0289	0.0289	0	100	0.046	0.552
3	8.333	2.06	0.0532	0.0397	0.0135	74.62	0.06	0.72
3	8.333	1.62	0.0879	0.0398	0.0481	45.28	0.074	0.888
3	8.333	2.41	0.0488	0.0417	0.0071	85.45	0.056	0.672
3	8.333	2.06	0.0661	0.0443	0.0218	67.02	0.066	0.792
3	8.333	2.92	0.0494	0.0494	0	100	0.056	0.672
3	8.333	2.41	0.0898	0.0603	0.0295	67.15	0.072	0.864
3	8.333	3	0.0661	0.0616	0.0045	93.19	0.066	0.792
3	8.333	3.31	0.0661	0.0661	0	100	0.066	0.792
3	8.333	3	0.0898	0.0738	0.016	82.18	0.072	0.864
3	8.333	3	0.1469	0.0994	0.0475	67.67	0.088	1.056
2	8.333	3	0.2823	0.1636	0.1187	57.95	0.115	1.381
2	8.333	3	0.1154	0.0917	0.0237	79.46	0.081	0.972
2	8.333	3	0.075	0.0712	0.0038	94.93	0.07	0.84
2	8.333	3	0.0654	0.0654	0	100	0.067	0.804
2	8.333	2.4	0.2406	0.1187	0.1219	49.33	0.105	1.261
2	8.333	2.4	0.1737	0.0967	0.077	55.67	0.102	1.224
2	8.333	2.4	0.0686	0.0571	0.0115	83.24	0.065	0.78
2	8.333	2.06	0.1918	0.0917	0.1001	47.81	0.095	1.14

Table A.14 – continued from previous page

S_L	S_x	L	Q	Q_i	Q_b	E	d	T_c
2	8.333	2.06	0.0949	0.059	0.0359	62.17	0.075	0.9
2	8.333	2.06	0.0526	0.0436	0.009	82.89	0.058	0.696
2	8.333	1.63	0.1001	0.0469	0.0532	46.85	0.076	0.912
2	8.333	1.63	0.0577	0.0372	0.0205	64.47	0.063	0.756
2	8.333	1.02	0.0828	0.0283	0.0545	34.18	0.072	0.864
2	8.333	1.02	0.0058	0.0058	0	100	0.025	0.3
1	8.333	3	0.1963	0.1482	0.0481	75.5	0.114	1.369
1	8.333	3	0.1161	0.1058	0.0103	91.13	0.09	1.08
1	8.333	3	0.0873	0.086	0.0013	98.51	0.08	0.96
1	8.333	3	0.0744	0.0744	0	100	0.073	0.876
1	8.333	2.4	0.1463	0.102	0.0443	69.72	0.101	1.212
1	8.333	2.4	0.1001	0.0828	0.0173	82.72	0.083	0.996
1	8.333	2.4	0.066	0.0622	0.0038	94.24	0.071	0.852
1	8.333	2.4	0.0552	0.0552	0	100	0.067	0.804
1	8.333	2.08	0.0314	0.0314	0	100	0.051	0.612
1	8.333	2.06	0.0911	0.0635	0.0276	69.7	0.078	0.936
1	8.333	2.06	0.0686	0.0532	0.0154	77.55	0.073	0.876
1	8.333	2.06	0.043	0.0385	0.0045	89.53	0.059	0.708
1	8.333	2.06	0.0334	0.0334	0	100	0.053	0.636
1	8.333	1.63	0.059	0.0398	0.0192	67.46	0.067	0.804
1	8.333	1.63	0.0481	0.0346	0.0135	71.93	0.064	0.768
1	8.333	1.63	0.0308	0.0263	0.0045	85.39	0.051	0.612
1	8.333	1.63	0.0186	0.0186	0	100	0.042	0.504
1	8.333	1.02	0.0699	0.0276	0.0423	39.48	0.075	0.9
0.5	8.333	2.4	0.1373	0.1097	0.0276	79.9	0.112	1.345
0.5	8.333	2.4	0.0956	0.0853	0.0103	89.23	0.075	0.9
0.5	8.333	2.4	0.068	0.0674	0.0006	99.12	0.081	0.972
0.5	8.333	2.4	0.0571	0.0571	0	100	0.068	0.816
0.5	8.333	2.05	0.1219	0.0898	0.0321	73.67	0.106	1.273
0.5	8.333	2.05	0.0802	0.0699	0.0103	87.16	0.089	1.068
0.5	8.333	2.05	0.0584	0.0571	0.0013	97.77	0.078	0.936
0.5	8.333	1.62	0.0949	0.0641	0.0308	67.54	0.098	1.176
0.5	8.333	1.62	0.0641	0.05	0.0141	78	0.083	0.996
0.5	8.333	1.62	0.0385	0.0366	0.0019	95.06	0.067	0.804
0.5	8.333	1.62	0.025	0.025	0	100	0.056	0.672
0.5	8.333	1.02	0.0584	0.0321	0.0263	54.97	0.083	0.996
0.5	8.333	1.02	0.0321	0.0231	0.009	71.96	0.062	0.744

Wasley (1960) conducted experiments for inlets of varied lengths at only 100% interception condition. However, no complete interception was achievable for inlets at 5 S_L and 1.042 S_x as a portion of the flow tended to go past the inlet regardless of the installed inlet length. The measured water surface profile by Wasley is reported herein for two gutter flows at each slope configuration. Wasley noted two interesting observations: 1) Along a significant portion of the inlet length, the flow retained the normal spread from the upstream gutter flow, i.e., the existence of the inlet had a delayed effect on the flow spread. Wasley suggested that the vanishing of the curb wall (start of the inlet opening) sends a negative surge wave in the direction of the spread, and that the spread remains unchanged until the surge wave reaches the edge of the spread after traveling a significant distance in the downstream direction. 2) After some distance along the inlet length, the maximum flow depth at a given cross-section was no longer at the edge of the inlet; instead the maximum depth was observe a short distance away into the direction of the spread. These two observations suggest that flow in the vicinity of undepressed curb inlet is more complex than it is traditionally held to be. The parameters used in this study:

Scale: Full-scale (1:1); $n = 0.01$; Y is the distance along inlet length (ft), Zero being the beginning of the inlet, negative Y is upstream the inlet, and positive Y is in the downstream direction; d_i is measured flow depth at the inlet edge and a given Y (ft); T_i flow spread at a given Y; d_m maximum flow depth along the spread at a given Y (ft); T_{dm} the location of d_m along the spread (ft).

Table A.15: Experimental data for undepressed inlets by Wasley (1960).

S_L	S_x	L	Q	Q_i	d	T
1	1.042	9.7	0.025	0.025	0.023	2.34
1	1.042	10.6	0.035	0.035	0.031	2.75
1	1.042	11.25	0.045	0.045	0.033	2.87
1	1.042	12	0.055	0.055	0.034	3.05
1	1.042	12.9	0.065	0.065	0.036	3.32
1	1.042	13.6	0.08	0.08	0.038	3.45
1	1.042	14.1	0.09	0.09	0.04	3.65
1	1.042	14.6	0.1	0.1	0.041	3.75
1	1.042	15.1	0.115	0.115	0.042	3.95
1	1.042	15.7	0.125	0.125	0.044	4.05
1	1.042	16.1	0.135	0.135	0.045	4.17
0.5	1.042	7.4	0.02	0.02	0.026	2.4
0.5	1.042	8.8	0.04	0.04	0.034	3.25
0.5	1.042	10.05	0.055	0.055	0.037	3.6
0.5	1.042	10.75	0.07	0.07	0.04	3.95
0.5	1.042	11.5	0.09	0.09	0.045	4.35
0.5	1.042	13	0.105	0.105	0.047	4.55
0.5	1.042	13.6	0.12	0.12	0.05	4.75
0.5	1.042	13.8	0.134	0.134	0.052	4.9
0.5	1.042	14	0.15	0.15	0.056	5
0.5	1.042	14.05	0.165	0.165	0.057	5.15
0.5	1.042	14.2	0.18	0.18	0.059	5.25
0.5	1.042	14.3	0.203	0.203	0.06	5.35
3	4.167	9.2	0.13	0.13	0.067	1.55
3	4.167	10.31	0.2	0.2	0.075	1.76
3	4.167	10.75	0.25	0.25	0.079	1.82
3	4.167	11.4	0.28	0.28	0.082	1.93
3	4.167	12.35	0.34	0.34	0.088	2.02
3	4.167	13.28	0.41	0.41	0.093	2.15
3	4.167	13.5	0.44	0.44	0.096	2.18
3	4.167	14.6	0.52	0.52	0.102	2.35
3	4.167	15.2	0.58	0.58	0.107	2.48
3	4.167	15.55	0.63	0.63	0.11	2.6
3	4.167	15.8	0.725	0.725	0.113	2.65
5	8.33	7.45	0.2	0.2	0.081	1.05
5	8.33	8.75	0.3	0.3	0.096	1.21
5	8.33	10	0.394	0.394	0.111	1.35

Table A.15 – continued from previous page

S_L	S_x	L	Q	Q_i	d	T
5	8.33	11.2	0.5	0.5	0.119	1.45
5	8.33	11.95	0.6	0.6	0.127	1.56
5	8.33	12.57	0.7	0.7	0.132	1.64
5	8.33	13.3	0.8	0.8	0.14	1.71
5	8.33	13.86	0.9	0.9	0.152	1.82
5	8.33	14.87	1	1	0.163	1.89
5	8.33	15.45	1.1	1.1	0.171	1.98
5	8.33	15.85	1.2	1.2	0.177	2.05
5	8.33	16.28	1.3	1.3	0.18	2.11
5	8.33	16.66	1.42	1.42	0.184	2.2
1	8.33	4.73	0.2	0.2	0.112	1.36
1	8.33	5.56	0.3	0.3	0.129	1.59
1	8.33	6.86	0.5	0.5	0.157	1.9
1	8.33	7.83	0.695	0.695	0.178	2.2
1	8.33	8.91	0.955	0.955	0.203	2.53
1	8.33	10.12	1.2	1.2	0.228	2.82
1	8.33	10.95	1.45	1.45	0.247	3.01
1	8.33	11.47	1.69	1.69	0.262	3.19
1	8.33	12.02	1.95	1.95	0.274	3.37
1	8.33	12.7	2.2	2.2	0.29	3.57
1	8.33	13.13	2.45	2.45	0.305	3.69
1	8.33	13.79	2.7	2.7	0.32	3.85
1	8.33	14.12	2.98	2.98	0.332	4
0.5	8.33	4.24	0.2	0.2	0.131	1.57
0.5	8.33	4.84	0.3	0.3	0.149	1.8
0.5	8.33	6	0.5	0.5	0.179	2.2
0.5	8.33	6.78	0.695	0.695	0.207	2.5
0.5	8.33	7.6	0.955	0.955	0.233	2.8
0.5	8.33	8.6	1.2	1.2	0.261	3.2
0.5	8.33	9.25	1.45	1.45	0.28	3.41
0.5	8.33	9.87	1.69	1.69	0.295	3.6
0.5	8.33	10.47	1.95	1.95	0.316	3.8
0.5	8.33	10.97	2.2	2.2	0.336	4
0.5	8.33	11.52	2.45	2.45	0.351	4.2
0.5	8.33	11.9	2.7	2.7	0.365	4.35
0.5	8.33	12.37	2.95	2.95	0.38	4.52
5	1.042	10.5	0.0064	0.0032	0.014	0.8
5	1.042	14.5	0.0146	0.0077	0.017	1.1

Table A.15 – continued from previous page

S_L	S_x	L	Q	Q_i	d	T
5	1.042	15.5	0.01597	0.0087	0.018	1.18
5	1.042	17	0.0288	0.0185	0.02	1.49
5	1.042	17	0.0369	0.0255	0.021	1.62
5	1.042	17.5	0.0442	0.0318	0.022	1.72
5	1.042	17.5	0.053	0.04	0.024	1.86
5	1.042	18	0.0632	0.0475	0.026	1.92
5	1.042	18	0.0725	0.055	0.027	2.08
5	1.042	18.5	0.081	0.0625	0.028	2.14
5	1.042	18.5	0.0898	0.07	0.029	2.23

Table A.16: Water surface profile along inlet by Wasley (1960), 0.5 S_L and 8.333 S_x.

	Q		L		Q		L	
	2.95		12.37		0.5		6	
Y	d_i	T_i	d_m	T_{dm}	d_i	T_i	d_m	T_{dm}
-1	0.363	4.55	0.363	0	–	–	–	–
-0.5	0.357	4.55	0.357	0	0.178	2.21	0.178	0
0	0.314	4.55	0.314	0	0.152	2.2	0.152	0
0.25	0.225	4.55	0.289	0.5	0.082	2.19	0.13	0.5
0.5	0.171	4.55	0.271	0.5	0.071	2.17	0.118	0.5
0.75	0.151	4.55	0.258	0.75	0.068	2.15	0.105	0.5
1	0.15	4.48	0.241	1	0.066	2.13	0.094	0.75
1.5	0.139	4.48	0.216	1	0.061	2.1	0.08	0.75
2	0.133	4.47	0.193	1	0.059	1.98	0.065	0.75
3	0.121	4.4	0.159	1.25	0.05	1.73	0.05	0
4	0.113	4.3	0.136	1	0.04	1.32	0.04	0
5	–	–	–	–	0.024	0.77	0.024	0
6	0.098	3.83	0.104	1	0	0	0	0
8	0.077	3	0.081	1				
10	0.057	1.78	0.057	0				
12.37	0	0	0	0				

Table A.17: Water surface profile along inlet by Wasley (1960), 0.5 S_L and 1.042 S_x.

	Q		L		Q		L	
	0.203		14.3		0.07		10.75	
Y	d_i	T_i	d_m	T_{dm}	d_i	T_i	d_m	T_{dm}
-1	0.062	5.55	0.062	0	0.043	3.95	0.043	0
0	0.053	5.55	0.053	0	0.033	3.95	0.033	0.5
0.25	0.023	5.55	0.044	0.5	0.015	3.95	0.027	0.5
0.5	0.023	5.55	0.044	0.75	0.014	3.95	0.026	0.75
0.75	0.023	5.55	0.041	1	0.014	3.95	0.026	0.75
1	0.023	5.55	0.037	1	0.014	3.95	0.025	0.75
1.5	–	–	–	–	0.014	3.95	0.024	0.75
2	0.023	5.55	0.035	1.5	0.014	3.85	0.021	0.75
3	0.023	5.55	0.032	1.5	0.014	3.8	0.02	0.5
4	0.023	5.55	0.031	1.5	0.014	3.63	0.018	0.5
6	0.022	5.45	0.029	1	0.014	2.95	0.016	0.5
8	0.019	4.8	0.021	1	0.011	1.9	0.011	0
10	0.018	4.3	0.018	0.5	–	–	–	–
10.75	–	–	–	–	0	0	0	0
12	0.017	2.5	0.018	0.5				
14.3	0	0	0	0				

Table A.18: Water surface profile along inlet by Wasley (1960), 1 S_L and 8.333 S_x.

	Q		L		Q		L	
	2.98		14.12		0.5		6.86	
Y	d_i	T_i	d_m	T_{dm}	d_i	T_i	d_m	T_{dm}
-0.5	0.327	4	0.327	0	0.158	1.93	0.158	0
0	0.3	4	0.3	0	0.14	1.92	0.14	0
0.25	0.218	4	0.275	0.25	0.075	1.92	0.123	0.25
0.5	0.175	4	0.258	0.5	0.067	1.88	0.111	0.5
0.75	0.15	4	0.245	0.75	0.061	1.88	0.106	0.5
1	0.14	4	0.236	0.75	0.061	1.85	0.097	0.5
1.5	0.129	4	0.216	1	0.059	1.85	0.082	0.5
2	0.124	4	0.194	1	0.057	1.84	0.07	0.5
2.5	0.12	4	0.177	1	0.053	1.84	0.06	0.5
3	0.113	4	0.157	1	0.051	1.79	0.05	0.5
3.5	–	–	–	–	0.048	1.65	0.048	0.5
4	0.106	4	0.134	1	0.044	1.56	0.044	0

Table A.18 – continued from previous page

	Q 2.98		L 14.12		Q 0.5		L 6.86	
Y	d_i	T_i	d_m	T_{dm}	d_i	T_i	d_m	T_{dm}
4.5	–	–	–	–	0.042	1.37	0.042	0
5	0.097	3.91	0.118	1	0.038	1.18	0.038	0
5.5	–	–	–	–	0.031	0.92	0.031	0
6	0.09	3.77	0.104	1.5	0.021	0.61	0.021	0
6.86	–	–	–	–	0	0	0	0
7.25	0.086	3.56	0.088	1				
8	0.084	3.2	0.084	0				
10	0.07	2.61	0.07	0				
11	0.064	2.12	0.064	0				
12	0.051	1.54	0.051	0				
13	0.035	0.85	0.035	0				
14.12	0	0	0	0				

Table A.19: Water surface profile along inlet by Wasley (1960), 1 S_L and 1.042 S_x.

	Q 0.135		L 16.1		Q 0.045		L 11.25	
Y	d_i	T_i	d_m	T_{dm}	d_i	T_i	d_m	T_{dm}
-0.5	0.045	4.18	0.045	0	0.033	2.93	0.033	0
0	0.042	4.15	0.042	0	0.031	2.93	0.031	0
0.25	0.018	4.15	0.037	0.5	0.012	2.93	0.025	0.5
0.5	0.018	4.15	0.037	0.5	0.013	2.93	0.025	0.5
1	0.02	4.13	0.036	0.75	0.013	2.93	0.024	0.5
1.5	0.021	4.13	0.035	1	0.015	2.98	0.022	0.75
2	0.023	4.26	0.029	0.75	0.019	3.05	0.019	0
2.5	0.023	4.4	0.026	1.25	0.019	2..98	0.019	0
3	0.02	4.52	0.024	1.5	0.016	2.86	0.016	0
4	0.02	4.56	0.022	1	0.014	2.88	0.014	0
5	0.018	4.63	0.021	1	0.014	2.84	0.014	0
6	0.016	4.75	0.02	1	0.012	2.65	0.012	0
7.25	0.016	4.32	0.018	1	0.012	2.32	0.012	0

Table A.19 – continued from previous page

	Q 0.135		L 16.1		Q 0.045		L 11.25	
Y	d_i	T_i	d_m	T_{dm}	d_i	T_i	d_m	T_{dm}
9	0.015	4.16	0.015	0	0.011	1.6	0.011	0
11	0.015	3.62	0.015	0	0	0	0	0
11.25	–	–	–	–				
13	0.015	2.59	0.015	0				
16.1	0	0	0	0				

Table A.20: Water surface profile along inlet by Wasley (1960), 5 S_L and 8.333 S_x.

	Q 1.42		L 16.66		Q 0.394		L 10	
Y	d_i	T_i	d_m	T_{dm}	d_i	T_i	d_m	T_{dm}
-0.5	0.186	2.14	0.186	0	0.108	1.37	0.108	0
0	0.186	2.13	0.186	0	0.112	1.36	0.112	0
0.25	0.155	2.13	0.159	0.25	0.065	1.36	0.083	0.25
0.5	0.119	2.13	0.154	0.25	0.05	1.36	0.082	0.25
0.75	0.102	2.13	0.152	0.25	0.048	1.36	0.08	0.25
1	0.091	2.12	0.14	0.25	0.047	1.36	0.079	0.25
1.5	0.086	2.13	0.135	0.5	0.044	1.36	0.07	0.25
2	0.08	2.12	0.131	0.5	0.042	1.35	0.063	0.5
2.5	0.074	2.12	0.129	0.5	0.041	1.35	0.057	0.5
3	0.075	2.11	0.115	0.5	0.04	1.34	0.053	0.5
4	0.07	2.12	0.098	0.5	0.038	1.32	0.041	0.5
5	0.07	2.12	0.09	0.5	0.038	1.27	0.038	0
6	0.07	2.12	0.071	0.5	0.035	1.15	0.035	0
7.5	0.06	2.1	0.068	0.5	0.028	0.89	0.028	0
8.5	–	–	–	–	0.023	0.57	0.023	0
9	0.053	2.05	0.062	0.5	–	–	–	–
10	–	–	–	–	0	0	0	0
11	0.045	1.7	0.053	0.5				
13	0.043	1.25	0.043	0				
15	0.033	0.64	0.033	0				
16.66	0	0	0	0				

Table A.21: Water surface profile along inlet by Wasley (1960), 3 S_L and 4.167 S_x.

	Q		L		Q		L	
	0.725		15.8		0.44		13.5	
Y	d_i	T_i	d_m	T_{dm}	d_i	T_i	d_m	T_{dm}
-1	0.113	2.63	0.113	0	0.097	2.18	0.097	0
0	0.114	2.65	0.114	0	0.095	2.19	0.095	0
0.25	0.055	2.63	0.097	0.25	0.05	2.19	0.082	0.25
0.5	0.052	2.63	0.095	0.25	0.043	2.19	0.078	0.25
0.75	0.047	2.63	0.088	0.25	0.039	2.23	0.073	0.25
1	0.047	2.63	0.085	0.5	0.038	2.24	0.069	0.5
1.5	0.046	2.63	0.081	0.5	0.036	2.24	0.067	0.5
2	0.047	2.63	0.078	0.5	0.038	2.24	0.059	0.75
2.5	0.045	2.63	0.066	1	0.038	2.23	0.058	0.75
3	0.046	2.63	0.064	1	0.036	2.18	0.055	0.75
4	0.045	2.63	0.062	1	0.037	2.18	0.046	0.75
5	0.044	2.63	0.052	1	0.036	2.15	0.04	0.5
6	0.038	2.6	0.05	1	0.033	2.12	0.036	0.5
6.75	0.04	2.46	0.045	1	0.033	2.05	0.033	0
8	0.038	2.36	0.04	0.5	0.029	1.87	0.029	0
9	0.032	2.24	0.037	0.5	0.027	1.65	0.027	0
10	0.033	2.02	0.034	0.5	0.027	1.38	0.027	0
11	0.035	1.74	0.035	0	0.023	1.02	0.023	0
12	0.033	1.45	0.033	0	0.017	0.66	0.017	0
13	0.026	1.15	0.026	0	0.009	0.25	0.009	0
13.5	–	–	–	–	0	0	0	0
14	0.023	0.76	0.023	0				
15	0.012	0.33	0.012	0				
15.8	0	0	0	0				

Spaliviero et al. (2000) conducted experiments on 0.25 and 0.5 meter inlets (0.82025 and 1.6405 ft) as part of testing several types of inlets. Experiments were

conducted mainly for high-bypass condition, at full-scale, and the roughness n was 0.01.

Table A.22: Experimental data for undepressed inlets by Spaliviero et al. (2000), d_c is the normal flow depth calculated as $d_{cal} = S_x\, T$.

S_L	S_x	L	Q	Q_i	Q_b	E	T	d_{cal}
0.2	2	1.6405	0.01624	0.01608	0.00016	100	1.6405	0.03281
0.2	2	1.6405	0.08154	0.03343	0.04811	41	3.281	0.06562
0.2	2	1.6405	0.03777	0.02757	0.0102	73	2.46075	0.04922
0.2	2.5	1.6405	0.01977	0.01621	0.00356	82	1.6405	0.04101
0.2	2.5	1.6405	0.13626	0.05859	0.07767	43	3.281	0.08203
0.2	3.33333	1.6405	0.03424	0.02945	0.00479	86	1.6405	0.05468
0.2	3.33333	1.6405	0.23227	0.09059	0.14169	39	3.281	0.10937
0.2	3.33333	1.6405	0.10978	0.0527	0.05709	48	2.46075	0.08203
0.2	3.33333	0.82025	0.00565	0.00559	5.7E-05	100	0.82025	0.02734
0.333	2	1.6405	0.01412	0.01257	0.00155	89	1.6405	0.03281
0.333	2	0.82025	0.00212	0.00212	0	100	0.82025	0.01641
0.333	2.5	1.6405	0.03212	0.03052	0.00161	95	1.6405	0.04101
0.333	3.33333	1.6405	0.04695	0.04132	0.00563	88	1.6405	0.05468
0.333	3.33333	1.6405	0.03954	0.03242	0.00712	82	1.6405	0.05468
0.5	2	1.6405	0.02295	0.01767	0.00528	77	1.6405	0.03281
0.5	2	1.6405	0.12779	0.04089	0.08689	32	3.281	0.06562
0.5	2	0.82025	0.00459	0.00408	0.00051	89	0.82025	0.01641
0.5	2.5	1.6405	0.03036	0.02338	0.00698	77	1.6405	0.04101
0.5	2.5	1.6405	0.2005	0.06817	0.13233	34	3.281	0.08203
0.5	3.33333	1.6405	0.05083	0.03457	0.01627	68	1.6405	0.05468
0.5	3.33333	1.6405	0.32194	0.0998	0.22214	31	3.281	0.10937
0.5	3.33333	0.82025	0.00741	0.00586	0.00156	79	0.82025	0.02734
1	2	1.6405	0.03777	0.02568	0.01209	68	1.6405	0.03281
1	2	1.6405	0.17721	0.03544	0.14177	20	3.281	0.06562
1	2.5	1.6405	0.04271	0.02819	0.01452	66	1.6405	0.04101
1	2.5	1.6405	0.25875	0.05175	0.207	20	3.281	0.08203
1	3.33333	1.6405	0.08154	0.03262	0.04893	40	1.6405	0.05468
1	3.33333	1.6405	0.38336	0.06134	0.32202	16	3.281	0.10937
1	3.33333	0.82025	0.01624	0.00893	0.00731	55	0.82025	0.02734
2	2	1.6405	0.05083	0.02186	0.02897	43	1.6405	0.03281
2	2.5	1.6405	0.06989	0.01817	0.05172	26	1.6405	0.04101
2	3.33333	1.6405	0.10625	0.02763	0.07863	26	1.6405	0.05468
2	3.33333	1.6405	0.10378	0.02595	0.07784	25	1.6405	0.05468

Hammonds and Holley (1995) performed tests on depressed inlets of two different lengths and gutter depressions. To confirm the proposed inlet capacity equation, experiments were conducted on undepressed inlets with similar lengths to the depressed inlets previously tested. Below we provide the experimental data for the undepressed inlets, while the data for the depressed inlets are reported in §A.4.1. The experiments were full-scale, and the roughness n is 0.017.

Table A.23: Data from tests on undepressed inlets by Hammonds and Holley (1995).

S_L	S_x	L	Q	Q_i	Q_b	E	d	T
0.4	4.17	11.25	1.55	1.55	0	100	0.2756	6.5
0.4	2.08	11.25	0.74	0.74	0	100	0.1673	7.51
0.4	4.17	11.25	4.41	3.49	0.8	79.14	0.4109	9.92
0.4	2.08	11.25	4.26	2.7	1.43	63.38	0.3248	10.51
1	4.17	11.25	1.18	1.18	0	100	0.2141	4.7
1	2.08	11.25	0.48	0.48	0	100	0.1255	5.61
1	2.08	11.25	1.47	1.21	0.33	82.31	0.187	8.59
1	4.17	11.25	3.94	2.93	0.94	74.37	0.342	8.19
2	4.17	11.25	0.92	0.92	0	100	0.1673	4.01
2	2.08	11.25	0.32	0.32	0	100	0.091	4.21
2	4.17	11.25	3.28	2.4	0.87	73.17	0.2584	6.89
2	2.08	11.25	3.38	1.74	1.61	51.48	0.2264	10.11
4	4.17	11.25	0.73	0.73	0	100	0.1353	3.22
4	2.08	11.25	0.29	0.29	0	100	0.0763	4.5
4	4.17	11.25	1.84	1.57	0.36	85.33	0.1846	4.8
4	2.08	11.25	2.28	1.3	1.07	57.02	0.1747	9.82
6	4.17	11.25	0.58	0.58	0	100	0.1157	2.68
6	2.08	11.25	0.17	0.17	0	100	0.0615	5.51
6	2.08	11.25	1.25	0.86	0.43	68.8	0.1255	9.43
6	4.17	11.25	3	1.85	1.18	61.67	0.2338	5.51
0.4	4.2	3.75	0.33	0.33	0	100	0.1476	3.42
0.4	2.08	3.75	0.17	0.17	0	100	0.096	4.21
0.4	4.17	3.75	2.7	1.19	1.53	44.07	0.347	8
0.4	2.08	3.75	2.75	0.88	1.9	32	0.2731	10.51

Table A.23 – continued from previous page

S_L	S_x	L	Q	Q_i	Q_b	E	d	T
1	4.2	3.75	0.27	0.27	0	100	0.128	2.68
1	2.08	3.75	0.16	0.16	0	100	0.0812	3.62
1	4.17	3.75	2.8	1.02	1.8	36.43	0.2978	6.89
1	2.08	3.75	2.96	0.72	2.27	24.32	0.2436	10.51
2	4.2	3.75	0.18	0.18	0	100	0.091	2.19
2	2.08	3.75	0.16	0.16	0	100	0.0714	2.98
2	4.17	3.75	3.01	0.98	2.01	32.56	0.2559	6.6
2	2.08	3.75	2.98	0.68	2.29	22.82	0.2141	10.51
4	4.2	3.75	0.14	0.14	0	100	0.0714	1.8
4	2.08	3.75	0.1	0.1	0	100	0.0468	2.39
4	4.17	3.75	2.12	0.73	1.45	34.43	0.1993	5
4	2.08	3.75	3.12	0.61	2.31	19.55	0.1944	10.51
6	4.17	3.75	0.1	0.1	0	100	0.0591	1.5
6	2.08	3.75	0.08	0.08	0	100	0.0394	2.19
6	2.08	3.75	3.02	0.55	2.46	18.21	0.1747	10.51

Karaki and Haynie (1961) conducted an extensive experimental study on the capacity of locally depressed curb inlets. These experiments and the subsequent analysis by Bauer and Woo (1964) formed the basis of the design equations in the FHWA's Hydraulic Engineering Circular No.22 (HEC-22). One aspect that sets the experimental approach in this study apart from other approaches reported in the literature: In most studies, a fixed inlet length is tested for a range of approach gutter flows. However, in this study, the gutter flow was fixed and the inlet length was increased in increments until the entire gutter flow is intercepted. The experimental data for depressed inlets is reported in §A.4.1. The effect of changing the roadway roughness was also assessed in this study. Karaki and Haynie (1961) conducted few full-scale experiments on undepressed inlets, the data for which are reported herein.

Table A.24: Experimental data on undepressed inlets by Karaki and Haynie (1961).

S_L	S_x	L	Q	Q_i	Q_b	E	d	T	n
4	6	5	6.48	5.295	1.185	0.3	5	18.29	0.011
4	6	10	6.48	4.08	2.4	0.3	5	37.04	0.011
4	6	15	6.48	3.055	3.425	0.3	5	52.85	0.011
4	6	20	6.48	2.07	4.41	0.3	5	68.06	0.011
4	6	25	6.48	0.87	5.61	0.3	5	86.57	0.011
4	6	30	6.48	0.45	6.03	0.3	5	93.06	0.011
4	6	35	6.48	0	6.48	0.3	5	100	0.011
4	6	5	4.66	3.57	1.09	0.3	5	23.39	0.0153
4	6	10	4.66	2.44	2.22	0.3	5	47.64	0.0153
4	6	15	4.66	2.43	2.23	0.3	5	47.85	0.0153
4	6	20	4.66	0.56	4.1	0.3	5	87.98	0.0153
4	6	25	4.66	0	4.66	0.3	5	100	0.0153

A.4 Reported Data in the Literature for Depressed Inlets

A.4.1 Inlets at Locally Depressed Gutter

Experimental data on locally depressed inlets was provided from the University of Texas study in §A.2. Another source for experimental data is provided by the University of South Australia (1995) where several types of locally depressed inlets were tested with and without deflectors, on-grade, and in a sag. Experiments were conducted on full-scale models. The main limitation of this study is that inlets were tested on one fixed cross-slope (3%). Data from this study can be accessed on the web address provided in the citation. Other experimental studies on locally depressed inlets will be provided below.

Conner (1946) conducted experiments on several types of inlets, including locally depressed curb inlets. Inlets were tested for bypass and 100% flow interception conditions, however, only the 100% interception results were reported. The longitudinal slopes was varied from 0.5% to 10% but no information was given regarding the cross-slope. Izzard (1950) used the experimental results of Conner

(1946) and mentioned that a parabolic cross-section was used outside the depressed gutter. No further description of the cross-section was found in the literature. There is a possibility that the cross-section may be inferred using the reported flow measurements, however such an attempt was not attempt herein. The parameters used in this study:

Scale: Full-scale (1:1); E= 100; L= varies; w= 2; a=3; L_u= 10; L_d= 10; n= 0.0176; A is the flow area (ft^2); R is the flow hydraulic radius (ft).

Table A.25: Data from tests on locally depressed inlets by Conner (1946).

S_L	L	Q_i	d	A	R
0.5	1	0.158	0.157	0.148	0.074
0.5	2	0.343	0.209	0.265	0.098
0.5	4	0.9	0.304	0.561	0.143
0.5	5	1.25	0.347	0.73	0.163
1	1	0.115	0.12	0.086	0.056
1	2	0.314	0.18	0.196	0.085
1	4	0.74	0.248	0.371	0.116
1	5	1.005	0.281	0.478	0.132
1	6	1.349	0.311	0.596	0.147
2	1	0.074	0.092	0.05	0.043
2	2	0.224	0.136	0.111	0.064
2	4	0.588	0.2	0.242	0.094
2	5	0.84	0.228	0.313	0.107
2	6	1.127	0.255	0.394	0.102
2	7	1.39	0.268	0.436	0.126
2.5	1	0.06	0.081	0.038	0.037
2.5	2	0.219	0.133	0.107	0.063
2.5	4	0.548	0.187	0.211	0.088
2.5	5	0.772	0.203	0.25	0.095
2.5	6	1.028	0.237	0.339	0.111
2.5	7	1.26	0.256	0.397	0.12
3	1	0.058	0.078	0.035	0.036
3	2	0.181	0.12	0.086	0.056
3	4	0.533	0.18	0.196	0.085
3	5	0.719	0.2	0.242	0.094

Table A.25 – continued from previous page

S_L	L	Q_i	d	A	R
3	6	0.958	0.225	0.307	0.106
3	7	1.206	0.238	0.342	0.111
4	1	0.053	0.071	0.029	0.033
4	2	0.152	0.107	0.068	0.05
4	4	0.46	0.158	0.151	0.074
4	5	0.655	0.183	0.203	0.086
4	6	0.853	0.203	0.248	0.095
4	7	1.093	0.223	0.302	0.105
6	1	0.05	0.065	0.024	0.029
6	2	0.111	0.087	0.044	0.04
6	4	0.376	0.138	0.113	0.064
6	5	0.539	0.158	0.149	0.074
6	6	0.692	0.172	0.178	0.081
6	7	0.885	0.198	0.236	0.093
8	1	0.042	0.058	0.018	0.026
8	2	0.101	0.079	0.037	0.037
8	4	0.321	0.123	0.09	0.057
8	5	0.461	0.14	0.118	0.066
8	6	0.6	0.156	0.146	0.073
8	7	0.769	0.168	0.169	0.079
10	1	0.04	0.053	0.016	0.024
10	2	0.099	0.076	0.033	0.035
10	4	0.285	0.113	0.075	0.052
10	5	0.415	0.129	0.1	0.061
10	6	0.54	0.143	0.122	0.067
10	7	0.69	0.156	0.146	0.073

Experiments conducted by Li et al. (1951) were discussed earlier in §A.3. Although, a value for "calibrated Manning's n" was recorded for each slope combination, only the average n value was reported herein as the roadway roughness is considered a known constant during design. The parameters used in this study for locally depressed inlets:

Scale: scaled (1:3); L= varies; w= 0.9167; a=1.376; L_u= 1.1467; L_d= 0.46; n= 0.01.

Table A.26: Data from tests on locally depressed inlets by Li et al. (1951).

S_L	S_x	L	Q	Q_i	Q_b	E
0.5	8.333	1	0.149	0.143	0.006	95.97
0.5	8.333	1	0.181	0.168	0.013	92.82
0.5	8.333	1	0.207	0.187	0.02	90.34
0.5	8.333	1	0.234	0.2	0.034	85.47
0.5	8.333	1	0.259	0.215	0.044	83.01
1	8.333	1	0.075	0.074	0.001	98.67
1	8.333	1	0.086	0.085	0.001	98.84
1	8.333	1	0.093	0.087	0.006	93.55
1	8.333	1	0.11	0.1	0.01	90.91
1	8.333	1	0.13	0.115	0.015	88.46
1	8.333	1	0.156	0.135	0.021	86.54
1	8.333	1	0.181	0.153	0.028	84.53
1	8.333	1	0.201	0.161	0.04	80.1
2	8.333	1	0.049	0.048	0.001	97.96
2	8.333	1	0.064	0.056	0.008	87.5
2	8.333	1	0.094	0.079	0.015	84.04
2	8.333	1	0.113	0.09	0.023	79.65
2	8.333	1	0.133	0.1	0.033	75.19
2	8.333	1	0.145	0.105	0.04	72.41
2	8.333	1.667	0.12	0.119	0.001	99.17
2	8.333	1.667	0.172	0.168	0.004	97.67
2	8.333	1.667	0.185	0.179	0.006	96.76
2	8.333	1.667	0.211	0.196	0.015	92.89
2	8.333	1.667	0.23	0.212	0.018	92.17
2	8.333	1.667	0.25	0.222	0.028	88.8
2	8.333	1.667	0.274	0.232	0.042	84.67
2	8.333	2.333	0.334	0.332	0.002	99.4
2	8.333	2.333	0.355	0.349	0.006	98.31
3	8.333	1	0.043	0.042	0.001	97.67
3	8.333	1	0.053	0.047	0.006	88.68
3	8.333	1	0.065	0.057	0.008	87.69
3	8.333	1	0.089	0.071	0.018	79.78
3	8.333	1	0.106	0.072	0.034	67.92
3	8.333	1.667	0.122	0.117	0.005	95.9
3	8.333	1.667	0.15	0.139	0.011	92.67

Table A.26 – continued from previous page

S_L	S_x	L	Q	Q_i	Q_b	E
3	8.333	1.667	0.173	0.15	0.023	86.71
3	8.333	1.667	0.189	0.161	0.028	85.19
3	8.333	2.333	0.227	0.227	0	100
3	8.333	2.333	0.254	0.253	0.001	99.61
3	8.333	2.333	0.276	0.27	0.006	97.83
3	8.333	2.333	0.302	0.288	0.014	95.36
3	8.333	2.333	0.309	0.284	0.025	91.91
3	8.333	2.333	0.33	0.291	0.039	88.18
3	8.333	2.333	0.362	0.302	0.06	83.43
4	8.333	1	0.034	0.033	0.001	97.06
4	8.333	1	0.056	0.047	0.009	83.93
4	8.333	1.667	0.09	0.09	0	100
4	8.333	1.667	0.149	0.12	0.029	80.54
4	8.333	1.667	0.17	0.123	0.047	72.35
4	8.333	1.667	0.198	0.134	0.064	67.68
4	8.333	2.333	0.169	0.169	0	100
4	8.333	2.333	0.198	0.19	0.008	95.96
4	8.333	2.333	0.226	0.203	0.023	89.82
4	8.333	2.333	0.273	0.23	0.043	84.25
4	8.333	2.333	0.321	0.251	0.07	78.19
4	8.333	2.333	0.366	0.268	0.098	73.22
4	8.333	3	0.292	0.292	0	100
4	8.333	3	0.311	0.308	0.003	99.04
5	8.333	1	0.024	0.024	0	100
5	8.333	1	0.06	0.052	0.008	86.67
5	8.333	1.667	0.081	0.081	0	100
5	8.333	1.667	0.089	0.081	0.008	91.01
5	8.333	2.333	0.187	0.168	0.019	89.84
5	8.333	2.333	0.237	0.196	0.041	82.7
5	8.333	2.333	0.305	0.23	0.075	75.41
5	8.333	2.333	0.361	0.26	0.101	72.02
5	8.333	3	0.298	0.282	0.016	94.63
5	8.333	3	0.336	0.311	0.025	92.56
5	8.333	3	0.366	0.337	0.029	92.08
6	8.333	1	0.025	0.024	0.001	96
6	8.333	1	0.035	0.032	0.003	91.43
6	8.333	1	0.044	0.037	0.007	84.09
6	8.333	1.667	0.062	0.062	0	100

Table A.26 – continued from previous page

S_L	S_x	L	Q	Q_i	Q_b	E
6	8.333	1.667	0.072	0.065	0.007	90.28
6	8.333	2.333	0.122	0.118	0.004	96.72
6	8.333	2.333	0.14	0.126	0.014	90
6	8.333	2.333	0.155	0.134	0.021	86.45
6	8.333	2.333	0.17	0.145	0.025	85.29
6	8.333	2.333	0.186	0.154	0.032	82.8
6	8.333	3	0.221	0.221	0	100
6	8.333	3	0.26	0.248	0.012	95.38
6	8.333	3	0.275	0.255	0.02	92.73
6	8.333	3	0.302	0.276	0.026	91.39
6	8.333	3	0.327	0.29	0.037	88.69
6	8.333	3	0.35	0.298	0.052	85.14
8	8.333	1	0.025	0.025	0	100
8	8.333	1.667	0.055	0.055	0	100
8	8.333	1.667	0.059	0.052	0.007	88.14
8	8.333	2.333	0.127	0.117	0.01	92.13
8	8.333	3	0.209	0.191	0.018	91.39
8	8.333	3	0.241	0.214	0.027	88.8
8	8.333	3	0.264	0.232	0.032	87.88
8	8.333	3	0.327	0.282	0.045	86.24
8	8.333	3	0.359	0.307	0.052	85.52

Experiments conducted by Karaki and Haynie (1961) was discussed earlier in §A.3. Locally depressed inlets of varied lengths were tested for 100% and bypass flow conditions. Measurements for flow depth and velocity at different locations were recorded but are not reported herein. The parameters used in this study for locally depressed inlets:

Scale: Full-scale (1:1); L= varies; w= 1 or 2; a= 1 or 2; L_u= 2; L_d= 2; n= varies.

Table A.27: Data from tests on locally depressed inlets by Karaki and Haynie (1961).

a	w	S_L	S_x	L	Q	Q_i	Q_b	E	n	T
1	2	4	1.5	10	4.76	1.2	3.56	25.21	0.0096	10
1	2	4	1.5	15	4.77	1.79	2.98	37.53	0.0096	10
1	2	4	1.5	20	4.76	2.4	2.36	50.42	0.0096	10
1	2	4	1.5	25	4.76	2.86	1.9	60.08	0.0096	10
1	2	4	1.5	30	4.73	3.17	1.56	67.02	0.0096	10
1	2	4	1.5	35	4.75	3.46	1.29	72.84	0.0096	10
1	1	4	1.5	5	0.778	0.332	0.446	42.67	0.0093	5
1	1	4	1.5	10	0.775	0.505	0.27	65.16	0.0093	5
1	1	4	1.5	15	0.775	0.635	0.14	81.94	0.0093	5
1	1	4	1.5	20	0.778	0.693	0.085	89.07	0.0093	5
1	1	4	1.5	25	0.775	0.757	0.018	97.68	0.0093	5
1	1	4	1.5	30	0.775	0.775	0	100	0.0093	5
2	2	4	1.5	5	0.775	0.451	0.324	58.19	0.0093	5
2	2	4	1.5	10	0.778	0.722	0.056	92.8	0.0093	5
2	2	4	1.5	15	0.775	0.765	0.01	98.71	0.0093	5
2	2	4	1.5	20	0.775	0.775	0	100	0.0093	5
2	2	4	1.5	5	4.792	0.725	4.067	15.13	0.0096	10
2	2	4	1.5	10	4.792	1.78	3.012	37.15	0.0096	10
2	2	4	1.5	15	4.786	2.501	2.285	52.26	0.0096	10
2	2	4	1.5	20	4.798	2.884	1.914	60.11	0.0096	10
2	2	4	1.5	25	4.786	3.19	1.596	66.65	0.0096	10
2	2	4	1.5	30	4.78	3.435	1.345	71.86	0.0096	10
2	2	4	1.5	35	4.774	3.73	1.044	78.13	0.0096	10
2	2	4	1.5	2.5	0.442	0.204	0.238	46.15	0.016	5
2	2	4	1.5	5	0.442	0.37	0.072	83.71	0.016	5
2	2	4	1.5	7.5	0.447	0.41	0.037	91.72	0.016	5
2	2	4	1.5	10	0.448	0.425	0.023	94.87	0.016	5
2	2	4	1.5	12.5	0.449	0.435	0.014	96.88	0.016	5
2	2	4	1.5	15	0.443	0.443	0	100	0.016	5
2	2	4	1.5	5	3.43	0.92	2.51	26.82	0.013	10
2	2	4	1.5	10	3.44	1.84	1.6	53.49	0.013	10
2	2	4	1.5	15	3.46	2.2	1.26	63.58	0.013	10
2	2	4	1.5	20	3.47	2.5	0.97	72.05	0.013	10
2	2	4	1.5	25	3.47	2.745	0.725	79.11	0.013	10
2	2	4	1.5	30	3.47	2.95	0.52	85.01	0.013	10
2	2	4	1.5	35	3.46	3.14	0.32	90.75	0.013	10
2	2	4	6	5	15.9	2.8	13.1	17.61	0.0177	8.2

Table A.27 – continued from previous page

a	w	S_L	S_x	L	Q	Q_i	Q_b	E	n	T
2	2	4	6	10	15.8	6.21	9.59	39.3	0.0177	8.2
2	2	4	6	15	15.75	6.59	9.16	41.84	0.0177	8.2
2	2	4	6	20	15.7	8.71	6.99	55.48	0.0177	8.2
2	2	4	6	25	15.5	10.06	5.44	64.9	0.0177	8.2
2	2	4	6	30	15.4	11	4.4	71.43	0.0177	8.2
2	2	4	6	5	4.705	1.705	3	36.24	0.0153	5
2	2	4	6	10	4.689	3.46	1.229	73.79	0.0153	5
2	2	4	6	15	4.72	4.5	0.22	95.34	0.0153	5
2	2	4	6	20	4.65	4.65	0	100	0.0153	5
2	2	4	6	5	6.45	1.725	4.725	26.74	0.011	5
2	2	4	6	10	6.49	3.77	2.72	58.09	0.011	5
2	2	4	6	15	6.48	5.03	1.45	77.62	0.011	5
2	2	4	6	20	6.48	5.98	0.5	92.28	0.011	5
2	2	1	6	2.5	15.1	2.335	12.765	15.46	0.0159	10
2	2	1	6	5	14.8	4.86	9.94	32.84	0.0159	10
2	2	1	6	7.5	14.9	8.315	6.585	55.81	0.0159	10
2	2	1	6	10	14.5	7.9	6.6	54.48	0.0159	10
2	2	1	6	15	14.75	12.78	1.97	86.64	0.0159	10
2	2	1	6	20	14.7	14.45	0.25	98.3	0.0159	10
2	2	1	6	2.5	3.305	0.775	2.53	23.45	0.0108	5
2	2	1	6	5	3.32	1.98	1.34	59.64	0.0108	5
2	2	1	6	7.5	3.33	2.8	0.53	84.08	0.0108	5
2	2	1	6	10	3.4	3.14	0.26	92.35	0.0108	5
2	2	1	6	12	3.4	3.4	0	100	0.0108	5
2	2	1	6	2.5	2.35	0.98	1.37	41.7	0.0153	5
2	2	1	6	5	2.35	1.89	0.46	80.43	0.0153	5
2	2	1	6	10	2.35	2.32	0.03	98.72	0.0153	5
2	2	1	6	5	16.3	5.6	10.7	34.36	0.0114	10
2	2	1	6	10	16.2	10.03	6.17	61.91	0.0114	10
2	2	1	6	15	16.2	13.6	2.6	83.95	0.0114	10
2	2	1	6	20	16.1	15.91	0.19	98.82	0.0114	10
2	2	1	1.5	2.5	0.34	0.331	0.009	97.35	0.0106	5
2	2	1	1.5	5	0.343	0.338	0.005	98.54	0.0106	5
2	2	1	1.5	7.5	0.343	0.343	0	100	0.0106	5
2	2	1	1.5	5	2.48	1.105	1.375	44.56	0.0094	10
2	2	1	1.5	10	2.5	1.68	0.82	67.2	0.0094	10
2	2	1	1.5	15	2.49	2.01	0.48	80.72	0.0094	10
2	2	1	1.5	20	2.5	2.31	0.19	92.4	0.0094	10

Table A.27 – continued from previous page

a	w	S_L	S_x	L	Q	Q_i	Q_b	E	n	T
2	2	1	1.5	25	2.5	2.47	0.03	98.8	0.0094	10
2	2	1	1.5	28	2.5	2.5	0	100	0.0094	10

§A.3 contained a discussion of experiments conducted by Hammonds and Holley (1995). Note that no interception could be achieved for 100% interception could be achieved for Longitudinal slope of 7% and 8%, and the reported interception in the original data was zero. Locally depressed inlets tests used the following parameters: Scale: scaled (3:4); L= varies; w= 1.124; a= 2.953 or 2.244; L_u= 3.75; L_d= 3.75; n= 0.017.

Table A.28: Experiments on locally depressed inlets by Hammonds and Holley (1995).

a	S_L	S_x	L	Q	Q_i	Q_b	E	d	T	d_0
2.953	3.75	0.4	2.1	0.71	0.71	0	100	0.1575	7.4069	0.2978
2.953	3.75	0.4	2.1	1.85	1.43	0.52	77.04	0.2362	10.5074	0.3617
2.953	3.75	0.4	2.1	4.13	2.16	1.87	52.33	0.3273	10.5074	0.4306
2.953	3.75	0.4	4.2	1.4	1.4	0	100	0.2928	6.2995	0.4011
2.953	3.75	0.4	4.2	2.48	2.03	0.5	82.14	0.3371	7.899	0.4503
2.953	3.75	0.4	4.2	3.98	2.56	1.34	64.25	0.4036	9.5231	0.5192
2.953	3.75	1	2.1	0.63	0.63	0	100	0.1403	6.1027	0.2781
2.953	3.75	1	2.1	3.11	1.69	1.44	54.43	0.2559	10.5074	0.4109
2.953	3.75	1	2.1	4.06	1.89	2.1	46.51	0.2879	10.5074	0.4109
2.953	3.75	1	4.2	1.14	1.14	0	100	0.2092	4.9953	0.3617
2.953	3.75	1	4.2	2.47	1.95	0.57	79.06	0.2928	6.9885	0.4208
2.953	3.75	1	4.2	3.99	2.36	1.59	59.01	0.342	8.2927	0.4995
2.953	3.75	2	2.1	0.39	0.39	0	100	0.1009	4.6016	0.2485
2.953	3.75	2	2.1	2.14	1.27	0.95	59.47	0.1944	8.4896	0.342
2.953	3.75	2	2.1	4.17	1.68	2.36	40.39	0.2485	10.5074	0.4011
2.953	3.75	2	4.2	1	1	0	100	0.1772	4.2079	0.342
2.953	3.75	2	4.2	1.77	1.5	0.33	84.38	0.219	5.6105	0.3913

Table A.28 – continued from previous page

a	S_L	S_x	L	Q	Q_i	Q_b	E	d	T	d_0
2.953	3.75	2	4.2	4.19	2.09	1.99	49.94	0.2756	7.3084	0.4897
2.953	3.75	4	2.1	0.32	0.32	0	100	0.0861	6.2011	0.2387
2.953	3.75	4	2.1	0.3	0.3	0	100	0.0812	6.7917	0.2288
2.953	3.75	4	2.1	2.2	1.2	1.08	54.49	0.187	10.0153	0.3322
2.953	3.75	4	2.1	2.73	1.31	1.47	47.95	0.1846	10.0153	0.3322
2.953	3.75	4	4.2	0.8	0.8	0	100	0.1353	3.4204	0.3076
2.953	3.75	5	4.2	2.97	1.5	1.49	50.7	0.2362	5.3152	0.3519
2.953	3.75	5	4.2	4.1	1.62	2.41	39.48	0.2682	7.6037	0.4011
2.953	3.75	6	2.1	0.25	0.25	0	100	0.0664	8.1943	0.2288
2.953	3.75	6	2.1	2.01	1.12	0.96	56	0.1599	10.0153	0.3224
2.953	3.75	6	2.1	4.22	1.44	2.61	34.07	0.2042	10.5074	0.3617
2.953	3.75	6	4.2	0.61	0.61	0	100	0.1083	2.7806	0.2781
2.953	3.75	7	4.2	2.64	1.38	1.35	52.31	0.2141	7.5053	0.3519
2.953	3.75	7	2.1	2.65	1.2	1.5	45.4	0.1575	10.0153	0.3322
2.953	11.25	0.4	2.1	1.64	1.64	0	100	0.2239	10.0153	0.3716
2.953	11.25	0.4	2.1	4.14	3.29	0.78	79.36	0.3174	10.5074	0.4306
2.953	11.25	0.4	4.2	3.49	3.49	0	100	0.3716	8.588	0.4897
2.953	11.25	0.4	4.2	4.29	4.06	0.13	94.67	0.3962	9.5231	0.5094
2.953	11.25	1	2.1	1.21	1.21	0	100	0.1698	7.6037	0.3076
2.953	11.25	1	2.1	4.14	2.98	1.08	71.95	0.2731	10.5074	0.4208
2.953	11.25	1	4.2	3.03	3.03	0	100	0.3076	7.3084	0.4503
2.953	11.25	1	4.2	4.28	3.92	0.29	91.52	0.3519	8.3912	0.4897
2.953	11.25	2	2.1	0.92	0.92	0	100	0.128	6.2011	0.2879
2.953	11.25	2	2.1	4.14	2.63	1.4	63.6	0.2338	10.5074	0.4011
2.953	11.25	2	4.2	2.4	2.4	0	100	0.2338	6.1027	0.4011
2.953	11.25	2	4.2	4.29	3.73	0.5	86.93	0.2928	7.4069	0.47
2.953	11.25	4	4.2	1.78	1.78	0	100	0.1846	4.7985	0.3716
2.953	11.25	4	4.2	4.08	3.1	0.88	76	0.2756	6.0042	0.4011
2.953	11.25	4	2.1	4.13	2.52	1.54	60.92	0.2165	10.5074	0.3617
2.953	11.25	5	2.1	0.46	0.46	0	100	0.0886	6.1027	0.2485
2.953	11.25	6	4.2	1.28	1.28	0	100	0.1476	3.8142	0.3322
2.953	11.25	6	4.2	4.08	3	1.02	73.51	0.2633	6.6932	0.3814
2.953	11.25	6	2.1	4.13	2.4	1.66	58.08	0.2042	10.5074	0.3519
2.244	3.75	0.4	2.08	0.73	0.73	0	100	0.1649	7.5053	—
2.244	3.75	0.4	2.08	1.91	1.32	0.67	69	0.2239	10.5074	0.3519
2.244	3.75	0.4	4.17	1.2	1.2	0	100	0.2436	5.9058	0.3716
2.244	3.75	0.4	4.17	2.88	2.06	0.89	71.38	0.3445	8.1943	0.4306
2.244	3.75	1	2.08	0.56	0.56	0	100	0.1353	5.7089	0.2584

Table A.28 – continued from previous page

a	S_L	S_x	L	Q	Q_i	Q_b	E	d	T	d_0
2.244	3.75	1	2.08	4.17	1.73	2.37	41.42	0.2781	10.5074	0.4011
2.244	3.75	1	4.17	1.07	1.07	0	100	0.2042	4.8969	0.3322
2.244	3.75	1	4.17	2.85	1.88	1.02	65.82	0.3027	7.087	0.4503
2.244	3.75	2	2.08	0.42	0.42	0	100	0.1009	4.6016	0.2288
2.244	3.75	2	2.08	4.16	1.5	2.59	35.98	0.2387	10.5074	0.4011
2.244	3.75	2	4.17	0.89	0.89	0	100	0.1649	4.011	0.2978
2.244	3.75	2	4.17	2.85	1.66	1.22	58.29	0.2461	6.4964	0.4109
2.244	3.75	4	2.08	0.27	0.27	0	100	0.0714	4.011	0.1993
2.244	3.75	4	2.08	2.34	1.1	1.33	47.02	0.1698	10.0153	0.3322
2.244	3.75	4	4.17	0.62	0.62	0	100	0.128	3.0759	0.2879
2.244	3.75	4	4.17	4.42	1.61	2.72	36.45	0.2879	6.1027	0.4011
2.244	3.75	6	2.08	0.16	0.16	0	100	0.0566	4.9953	0.1501
2.244	3.75	6	2.08	3.92	1.26	2.57	32.25	0.1796	10.5074	0.342
2.244	3.75	6	4.17	0.49	0.49	0	100	0.1083	2.5838	0.2584
2.244	3.75	6	4.17	3.9	1.45	2.41	37.25	0.2682	—	0.3716
2.244	11.25	0.4	4.17	3.24	3.24	0	100	0.3642	8.6864	0.4602
2.244	11.25	0.4	4.17	4.47	4.04	0.25	90.2	0.406	9.5231	0.4897
2.244	11.25	0.4	2.08	4.27	3.23	0.94	75.68	0.315	10.5074	0.4208
2.244	11.25	1	4.17	2.88	2.88	0	100	0.2978	7.1854	0.4306
2.244	11.25	1	4.17	4.47	3.91	0.32	87.41	0.3543	8.3912	0.4798
2.244	11.25	1	2.08	2.84	2.34	0.53	82.71	0.2387	10.5074	0.3617
2.244	11.25	2	4.17	2.32	2.32	0	100	0.2288	6.0042	0.4011
2.244	11.25	2	4.17	3.97	3.48	0.41	87.66	0.283	7.1854	0.4503
2.244	11.25	2	2.08	4.41	2.74	1.54	62.21	0.2461	10.5074	0.4011
2.244	11.25	4	2.08	0.64	0.64	0	100	0.1009	—	0.2485
2.244	11.25	4	2.08	2.75	1.96	0.87	71.11	0.1895	9.9168	0.3322
2.244	11.25	4	4.17	4.32	3.17	1.03	73.46	0.2879	6.1027	0.4011
2.244	11.25	6	2.08	0.36	0.36	0	100	0.0763	7.087	0.2092
2.244	11.25	6	2.08	3.1	1.99	1.11	64.15	0.1649	10.5074	0.3322
2.244	11.25	6	4.17	2.5	2.23	0.35	89.25	0.2042	4.7	0.342

Experiments by MacCallan and Hotchkiss (1996) covered several types of storm drain inlets, including 6-ft locally depressed inlets. These inlets used a parabolic

depressed gutter-section, the dimensions for an equivalent conventional gutter is reported here. The parameters used in this study:

Scale: Full-scale (1:1); L= 6; w= 5; a= 3.25; L_u= 5; L_d= 5; n= 0.0125.

Table A.29: Experimental data on locally depressed inlets by MacCallan and Hotchkiss (1996).

S_L	S_x	Q	Q_i	Q_b	E	d
1	4	2.73	2.71	0.02	99.27	0.253
1	4	3.05	3	0.05	98.36	0.272
1	4	3.21	3.13	0.08	97.51	0.279
1	4	3.32	3.2	0.12	96.39	0.282
1	4	3.43	3.29	0.14	95.92	0.282
1	4	3.45	3.3	0.15	95.65	0.282
1	4	3.63	3.4	0.23	93.66	0.295
1	4	3.79	3.51	0.28	92.61	0.299
3	2	1.4	1.4	0	100	0.118
3	2	1.63	1.54	0.09	94.48	0.125
3	2	1.85	1.67	0.18	90.27	0.131
3	2	2.09	1.83	0.26	87.56	0.135
3	2	2.27	1.89	0.38	83.26	0.138
3	2	2.44	1.96	0.48	80.33	0.144
3	2	2.62	2.02	0.6	77.1	0.151
3	2	2.81	2.13	0.68	75.8	0.157
3	2	2.96	2.15	0.81	72.64	0.164
3	2	3.11	2.19	0.92	70.42	0.164
3	2	3.23	2.23	1	69.04	0.171
3	2	3.29	2.2	1.09	66.87	0.171
3	2	3.35	2.2	1.15	65.67	0.174
3	2	3.49	2.27	1.22	65.04	0.177
3	2	3.59	2.23	1.36	62.12	0.177
3	2	3.66	2.22	1.44	60.66	0.184
3	4	2.71	2.71	0	100	0.207
3	4	2.88	2.82	0.06	97.92	0.21
3	4	2.97	2.86	0.11	96.3	0.21
3	4	3.14	2.97	0.17	94.59	0.213
3	4	3.26	3.02	0.24	92.64	0.217
3	4	3.38	3.08	0.3	91.12	0.217

Table A.29 – continued from previous page

S_L	S_x	Q	Q_i	Q_b	E	d
3	4	3.46	3.14	0.32	90.75	0.22
3	4	3.51	3.17	0.34	90.31	0.221
5	4	2.32	2.32	0	100	0.177
5	4	2.42	2.41	0.01	99.59	0.177
5	4	2.54	2.49	0.05	98.03	0.18
5	4	2.6	2.52	0.08	96.92	0.184
5	4	2.68	2.59	0.09	96.64	0.187
5	4	2.83	2.7	0.13	95.41	0.19
5	4	2.92	2.75	0.17	94.18	0.194
5	4	2.97	2.78	0.19	93.6	0.194
5	4	3.07	2.83	0.24	92.18	0.197

Hahn (1972) performed experiment on locally depressed curb inlets and combination inlets (curb inlet with a grate) on-grade and in a sag. Hahn reported n= 0.011 as the roughness of the roadway, this value is the typical roughness for the roadway material (planed wood). However, applying Manning's equation for gutter flow (Izzard and Hicks, 1947) to the measurements reported by Hahn yields an n= 0.014. Care should be exercised on choosing the roughness coefficient for this dataset. The parameters for the locally depressed inlets on-grade for this study:

Scale: scaled (1:3); L= 3.9167 and 2.583 (specified in the table caption); w= 0.5; a= 1.333; L_u= 1; L_d= 1.

Table A.30: Experimental data on locally depressed inlets for L=3.9167 ft, by Hahn (1972).

S_L	S_x	Q	Q_i	Q_b	E	d
0.2	2.08	0.1658	0.1658	0	100	–
0.2	2.08	0.2114	0.2061	0.0053	97.49	–

Table A.30 – continued from previous page

S_L	S_x	Q	Q_i	Q_b	E	d
0.2	2.08	0.3	0.2679	0.0321	89.3	–
0.2	2.08	0.3604	0.3024	0.058	83.91	–
0.2	2.08	0.3801	0.3114	0.0687	81.93	–
0.2	2.08	0.4145	0.3299	0.0846	79.59	–
0.2	3.12	0.2207	0.2207	0	100	–
0.2	3.12	0.2658	0.2597	0.0061	97.71	–
0.2	3.12	0.3096	0.2935	0.0161	94.8	–
0.2	3.12	0.3257	0.3024	0.0233	92.85	–
0.2	3.12	0.3412	0.3114	0.0298	91.27	–
0.2	3.12	0.3753	0.3299	0.0454	87.9	–
0.2	3.12	0.4505	0.389	0.0615	86.35	–
0.2	4.16	0.2679	0.2679	0	100	–
0.2	4.16	0.298	0.2935	0.0045	98.49	–
0.2	4.16	0.3445	0.3299	0.0146	95.76	–
0.2	5.21	0.2516	0.2516	0	100	–
0.2	6.25	0.1722	0.1722	0	100	–
0.5	2.08	0.1251	0.1251	0	100	–
0.5	2.08	0.2082	0.1921	0.0161	92.27	–
0.5	2.08	0.2842	0.2358	0.0484	82.97	–
0.5	2.08	0.3695	0.2763	0.0932	74.78	–
0.5	2.08	0.4408	0.3024	0.1384	68.6	–
0.5	2.08	0.5016	0.3206	0.181	63.92	–
0.5	2.08	0.5476	0.3393	0.2083	61.96	–
0.5	2.08	0.586	0.349	0.237	59.56	–
0.5	2.08	0.6284	0.3587	0.2697	57.08	–
0.5	2.08	0.6726	0.3687	0.3039	54.82	–
0.5	3.12	0.0965	0.0965	0	100	–
0.5	3.12	0.1994	0.199	0.0004	99.8	–
0.5	3.12	0.217	0.2133	0.0037	98.29	–
0.5	3.12	0.3108	0.2763	0.0345	88.9	–
0.5	3.12	0.3893	0.3206	0.0687	82.35	–
0.5	3.12	0.4378	0.349	0.0888	79.72	–
0.5	3.12	0.4962	0.3687	0.1275	74.3	–
0.5	3.12	0.5781	0.41	0.1681	70.92	–
0.5	3.12	0.6291	0.4208	0.2083	66.89	–
0.5	3.12	0.6883	0.4427	0.2456	64.32	–
0.5	4.16	0.2436	0.2436	0	100	–
0.5	4.16	0.2481	0.2436	0.0045	98.19	–

Table A.30 – continued from previous page

S_L	S_x	Q	Q_i	Q_b	E	d
0.5	4.16	0.3369	0.3024	0.0345	89.76	–
0.5	4.16	0.4177	0.349	0.0687	83.55	–
0.5	4.16	0.5216	0.3994	0.1222	76.57	–
0.5	4.16	0.6693	0.4539	0.2154	67.82	–
0.5	5.21	0.2436	0.2436	0	100	–
0.5	5.21	0.3439	0.3206	0.0233	93.22	–
0.5	5.21	0.4719	0.3994	0.0725	84.64	–
0.5	5.21	0.5702	0.4427	0.1275	77.64	–
0.5	6.25	0.3299	0.3299	0	100	–
0.5	6.25	0.3779	0.3687	0.0092	97.57	–
0.5	6.25	0.4098	0.3994	0.0104	97.46	–
1	2.08	0.1417	0.1417	0	100	0.0833
1	2.08	0.1965	0.1787	0.0178	90.94	0.09
1	2.08	0.3353	0.2282	0.1071	68.06	0.1
1	2.08	0.4177	0.2516	0.1661	60.23	0.11
1	2.08	0.4991	0.2763	0.2228	55.36	0.1133
1	2.08	0.5464	0.2849	0.2615	52.14	0.12
1	2.08	0.7002	0.3206	0.3796	45.79	0.1267
1	3.12	0.1722	0.1722	0	100	0.1033
1	3.12	0.2861	0.2516	0.0345	87.94	0.11
1	3.12	0.3573	0.2848	0.0725	79.71	0.1133
1	3.12	0.4144	0.3024	0.112	72.97	0.12
1	3.12	0.498	0.3299	0.1681	66.24	0.1267
1	3.12	0.5382	0.3299	0.2083	61.3	0.13
1	3.12	0.5771	0.3393	0.2378	58.79	0.1367
1	3.12	0.627	0.349	0.278	55.66	0.14
1	3.12	0.6716	0.3587	0.3129	53.41	0.14
1	3.12	0.7007	0.3788	0.3219	54.06	0.1467
1	4.16	0.2207	0.2207	0	100	0.1033
1	4.16	0.2825	0.2679	0.0146	94.83	0.1133
1	4.16	0.3786	0.3206	0.058	84.68	0.1267
1	4.16	0.4422	0.349	0.0932	78.92	0.1367
1	4.16	0.5172	0.3788	0.1384	73.24	0.1467
1	4.16	0.5739	0.3994	0.1745	69.59	0.15
1	4.16	0.6254	0.41	0.2154	65.56	0.15
1	4.16	0.6743	0.4208	0.2535	62.41	0.15
1	5.21	0.2516	0.2516	0	100	0.1267
1	5.21	0.3185	0.3024	0.0161	94.95	0.13

Table A.30 – continued from previous page

S_L	S_x	Q	Q_i	Q_b	E	d
1	5.21	0.4475	0.3788	0.0687	84.65	0.1467
1	5.21	0.5171	0.41	0.1071	79.29	0.1567
1	5.21	0.5646	0.4317	0.1329	76.46	0.16
1	5.21	0.5926	0.4427	0.1499	74.7	0.1667
1	5.21	0.6781	0.4769	0.2012	70.33	0.1733
1	6.25	0.2763	0.2763	0	100	0.1367
1	6.25	0.331	0.3206	0.0104	96.86	0.14
1	6.25	0.3908	0.3587	0.0321	91.79	0.15
1	6.25	0.4787	0.41	0.0687	85.65	0.16
1	6.25	0.5249	0.4317	0.0932	82.24	0.1667
1	6.25	0.5547	0.4427	0.112	79.81	0.1733
1	6.25	0.645	0.4769	0.1681	73.94	0.1767
2	2.08	0.0703	0.0703	0	100	0.0467
2	2.08	0.1491	0.1198	0.0293	80.35	0.0567
2	2.08	0.281	0.1535	0.1275	54.63	0.0733
2	2.08	0.298	0.1596	0.1384	53.56	0.0767
2	2.08	0.4149	0.1921	0.2228	46.3	0.0833
2	2.08	0.5472	0.2133	0.3339	38.98	0.09
2	2.08	0.5978	0.2282	0.3696	38.17	0.0933
2	2.08	0.6976	0.2436	0.454	34.92	0.1033
2	3.12	0.1	0.1	0	100	0.0567
2	4.16	0.1361	0.1361	0	100	0.0667
2	4.16	0.2031	0.1853	0.0178	91.24	0.0833
2	4.16	0.3401	0.2597	0.0804	76.36	0.0933
2	4.16	0.4376	0.2935	0.1441	67.07	0.1
2	4.16	0.5087	0.3024	0.2063	59.45	0.1033
2	4.16	0.6066	0.3114	0.2952	51.34	0.1133
2	4.16	0.6705	0.3299	0.3406	49.2	0.1267
2	4.16	0.7186	0.349	0.3696	48.57	0.13
2	5.21	0.1596	0.1596	0	100	0.0833
2	5.21	0.2396	0.2292	0.0104	95.66	0.0933
2	5.21	0.3226	0.2679	0.0547	83.04	0.1033
2	5.21	0.4138	0.3114	0.1024	75.25	0.11
2	5.21	0.4916	0.3587	0.1329	72.97	0.1133
2	5.21	0.5469	0.3788	0.1681	69.26	0.1133
2	5.21	0.5973	0.389	0.2083	65.13	0.1133
2	6.25	0.1921	0.1921	0	100	0.09
2	6.25	0.2811	0.2597	0.0214	92.39	0.1

Table A.30 – continued from previous page

S_L	S_x	Q	Q_i	Q_b	E	d
2	6.25	0.3639	0.3024	0.0615	83.1	0.11
2	6.25	0.4561	0.349	0.1071	76.52	0.12
2	6.25	0.5378	0.3994	0.1384	74.27	0.1267
2	6.25	0.5875	0.4317	0.1558	73.48	0.1267
2	6.25	0.6415	0.4539	0.1876	70.76	0.1267
2	6.25	0.6767	0.4539	0.2228	67.08	0.13
2	6.25	0.7074	0.4539	0.2535	64.16	0.13
3	2.08	0.0594	0.0594	0	100	0.0433
3	2.08	0.1778	0.1198	0.058	67.38	0.0533
3	2.08	0.2639	0.1417	0.1222	53.69	0.0633
3	2.08	0.395	0.1722	0.2228	43.59	0.0767
3	2.08	0.4786	0.1921	0.2865	40.14	0.0833
3	2.08	0.5209	0.199	0.3219	38.2	0.09
3	2.08	0.5659	0.2061	0.3598	36.42	0.0933
3	2.08	0.7089	0.2436	0.4653	34.36	0.1
3	3.12	0.0867	0.0865	0.0002	99.77	0.0467
3	3.12	0.1906	0.1535	0.0371	80.54	0.0633
3	3.12	0.2746	0.1722	0.1024	62.71	0.0733
3	3.12	0.4009	0.2133	0.1876	53.21	0.0833
3	3.12	0.4892	0.2436	0.2456	49.8	0.0933
3	3.12	0.5381	0.2516	0.2865	46.76	0.0933
3	3.12	0.5898	0.2679	0.3219	45.42	0.0933
3	3.12	0.6947	0.2841	0.4106	40.9	0.1033
3	4.16	0.1148	0.1147	0.0001	99.91	0.0633
3	4.16	0.2444	0.199	0.0454	81.42	0.0833
3	4.16	0.3581	0.2359	0.1222	65.88	0.0833
3	4.16	0.4459	0.2516	0.1943	56.43	0.0933
3	4.16	0.5219	0.2763	0.2456	52.94	0.1
3	4.16	0.5715	0.2935	0.278	51.36	0.11
3	4.16	0.6999	0.3687	0.3312	52.68	0.1267
3	5.21	0.1417	0.1417	0	100	0.0633
3	6.25	0.5382	0.2061	0.3321	38.29	0.0833
3	6.25	0.3264	0.2597	0.0667	79.56	0.09
3	6.25	0.4144	0.3024	0.112	72.97	0.0933
3	6.25	0.5326	0.3024	0.2302	56.78	0.1
3	6.25	0.5639	0.3024	0.2615	53.63	0.1033
3	6.25	0.6245	0.3206	0.3039	51.34	0.12
3	6.25	0.6518	0.3299	0.3219	50.61	0.1267

Table A.30 – continued from previous page

S_L	S_x	Q	Q_i	Q_b	E	d
3	6.25	0.6896	0.349	0.3406	50.61	0.1367
4	2.08	0.0464	0.0464	0	100	0.0433
4	2.08	0.1233	0.1	0.0233	81.1	0.0533
4	2.08	0.2527	0.1305	0.1222	51.64	0.0667
4	2.08	0.3216	0.1535	0.1681	47.73	0.0767
4	2.08	0.3941	0.1787	0.2154	45.34	0.0833
4	2.08	0.4758	0.2061	0.2697	43.32	0.1
4	2.08	0.5748	0.2436	0.3312	42.38	0.0933
4	2.08	0.6891	0.2679	0.4212	38.88	0.1033
4	3.12	0.0703	0.0703	0	100	0.0533
4	3.12	0.1738	0.1417	0.0321	81.53	0.0633
4	3.12	0.2442	0.1596	0.0846	65.36	0.0633
4	3.12	0.3294	0.1853	0.1441	56.25	0.0733
4	3.12	0.4073	0.199	0.2083	48.86	0.09
4	3.12	0.4987	0.2207	0.278	44.26	0.09
4	3.12	0.5501	0.2282	0.3219	41.48	0.0933
4	3.12	0.5937	0.2436	0.3501	41.03	0.1
4	3.12	0.6809	0.2597	0.4212	38.14	0.1033
4	4.16	0.0958	0.0954	0.0004	99.58	0.0567
4	4.16	0.1079	0.1048	0.0031	97.13	0.0633
4	4.16	0.2468	0.1853	0.0615	75.08	0.0733
4	4.16	0.384	0.2282	0.1558	59.43	0.0833
4	4.16	0.4326	0.2516	0.181	58.16	0.09
4	4.16	0.4981	0.2679	0.2302	53.78	0.1033
4	4.16	0.5545	0.2848	0.2697	51.36	0.1033
4	4.16	0.5976	0.3024	0.2952	50.6	0.1033
4	4.16	0.6243	0.3114	0.3129	49.88	0.1033
4	4.16	0.6902	0.3206	0.3696	46.45	0.1033
4	5.21	0.1153	0.1147	0.0006	99.48	0.0667
4	5.21	0.19	0.1722	0.0178	90.63	0.0733
4	5.21	0.2897	0.2282	0.0615	78.77	0.0833
4	5.21	0.39	0.2516	0.1384	64.51	0.09
4	5.21	0.4833	0.2679	0.2154	55.43	0.1033
4	5.21	0.5404	0.2948	0.2456	54.55	0.1133
4	5.21	0.5903	0.3206	0.2697	54.31	0.1267
4	5.21	0.7033	0.3994	0.3039	56.79	0.1367
4	6.25	0.1363	0.1361	0.0002	99.85	0.0667
4	6.25	0.2038	0.1921	0.0117	94.26	0.0833

Table A.30 – continued from previous page

S_L	S_x	Q	Q_i	Q_b	E	d
4	6.25	0.3096	0.2516	0.058	81.27	0.0933
4	6.25	0.3912	0.3024	0.0888	77.3	0.0933
4	6.25	0.4613	0.3114	0.1499	67.5	0.1
4	6.25	0.6709	0.349	0.3219	52.02	0.1467
4	6.25	0.6999	0.3687	0.3312	52.68	0.15
5	2.08	0.0865	0.0865	0.0000	100	0.06
5	2.08	0.158	0.1305	0.0275	82.59	0.07
5	2.08	0.2091	0.1476	0.0615	70.59	0.08
5	2.08	0.3009	0.1787	0.1222	59.39	0.08
5	2.08	0.3671	0.2061	0.1610	56.14	0.09
5	2.08	0.451	0.2282	0.2228	50.6	0.10
5	2.08	0.6731	0.2935	0.3796	43.6	0.10
5	3.12	0.1198	0.1198	0.0000	100	0.07
5	3.12	0.1883	0.1722	0.0161	91.45	0.07
5	3.12	0.2836	0.1990	0.0846	70.17	0.08
5	3.12	0.3611	0.2282	0.1329	63.2	0.09
5	3.12	0.4392	0.2516	0.1876	57.29	0.09
5	3.12	0.5057	0.2679	0.2378	52.98	0.10
5	3.12	0.5713	0.2848	0.2865	49.85	0.10
5	3.12	0.691	0.3114	0.3796	45.07	0.11
5	4.16	0.1476	0.1476	0.0000	100	0.07
5	4.16	0.2043	0.1990	0.0053	97.41	0.08
5	4.16	0.2661	0.2207	0.0454	82.94	0.09
5	4.16	0.3368	0.2436	0.0932	72.33	0.10
5	4.16	0.4092	0.2763	0.1329	67.52	0.10
5	4.16	0.4582	0.3024	0.1558	66	0.11
5	4.16	0.5336	0.3393	0.1943	63.59	0.11
5	4.16	0.5713	0.3490	0.2223	61.09	0.12
5	4.16	0.7007	0.3788	0.3219	54.06	0.13
5	5.21	0.1853	0.1853	0	100	0.08
5	5.21	0.2067	0.2061	0.0006	99.71	0.09
5	5.21	0.2912	0.2679	0.0233	92	0.09
5	5.21	0.3694	0.2848	0.0846	77.1	0.10
5	5.21	0.4465	0.3024	0.1441	67.73	0.13
5	5.21	0.5109	0.3299	0.181	64.57	0.14
5	5.21	0.563	0.3687	0.1943	65.49	0.14
5	5.21	0.7147	0.4769	0.2378	66.73	0.15
5	6.25	0.1722	0.1722	0.0000	100	0.08

Table A.30 – continued from previous page

S_L	S_x	Q	Q_i	Q_b	E	d
5	6.25	0.2587	0.2516	0.0071	97.26	0.09
5	6.25	0.3527	0.3206	0.0321	90.9	0.10
5	6.25	0.408	0.3393	0.0687	83.16	0.10
5	6.25	0.4615	0.3393	0.1222	73.52	0.11
5	6.25	0.53	0.3490	0.1810	65.85	0.12
5	6.25	0.5915	0.3687	0.2228	62.33	0.14
5	6.25	0.6372	0.3994	0.2378	62.68	0.15
5	6.25	0.7074	0.4539	0.2535	64.16	0.17
6	2.08	0.0407	0.0407	0.0000	100	0.03
6	2.08	0.0591	0.0560	0.0031	94.75	0.04
6	2.08	0.1352	0.0954	0.0398	70.56	0.04
6	2.08	0.2746	0.1417	0.1329	51.6	0.06
6	2.08	0.3665	0.1722	0.1943	46.98	0.07
6	2.08	0.4446	0.1990	0.2456	44.76	0.08
6	2.08	0.5072	0.2207	0.2865	43.51	0.08
6	2.08	0.5594	0.2282	0.3312	40.79	0.08
6	2.08	0.6232	0.2436	0.3796	39.09	0.08
6	2.08	0.6917	0.2597	0.4320	37.55	0.09
6	3.12	0.0495	0.0495	0.0000	100	0.03
6	3.12	0.1081	0.1000	0.0081	92.51	0.04
6	3.12	0.192	0.1305	0.0615	67.97	0.05
6	3.12	0.2745	0.1361	0.1384	49.58	0.06
6	3.12	0.373	0.1787	0.1943	47.91	0.08
6	3.12	0.4377	0.1921	0.2456	43.89	0.08
6	3.12	0.4998	0.2133	0.2865	42.68	0.09
6	3.12	0.5645	0.2516	0.3129	44.57	0.09
6	3.12	0.6003	0.2597	0.3406	43.26	0.10
6	3.12	0.6293	0.2597	0.3696	41.27	0.10
6	3.12	0.6891	0.2679	0.4212	38.88	0.10
6	4.16	0.0629	0.0629	0.0000	100	0.04
6	4.16	0.1492	0.1361	0.0131	91.22	0.05
6	4.16	0.2321	0.1596	0.0725	68.76	0.06
6	4.16	0.3671	0.1990	0.1681	54.21	0.08
6	4.16	0.4365	0.2282	0.2083	52.28	0.09
6	4.16	0.4971	0.2436	0.2535	49	0.09
6	4.16	0.5381	0.2516	0.2865	46.76	0.09
6	4.16	0.5735	0.2516	0.3219	43.87	0.09
6	4.16	0.6277	0.2679	0.3598	42.68	0.10

Table A.30 – continued from previous page

S_L	S_x	Q	Q_i	Q_b	E	d
6	5.21	0.0782	0.0782	0.0000	100	0.04
6	5.21	0.1871	0.1596	0.0275	85.3	0.06
6	5.21	0.3019	0.1797	0.1222	59.52	0.08
6	5.21	0.4168	0.2358	0.1810	56.57	0.09
6	5.21	0.4907	0.2679	0.2228	54.6	0.10
6	5.21	0.547	0.2935	0.2535	53.66	0.10
6	5.21	0.5721	0.3024	0.2697	52.86	0.11
6	5.21	0.6428	0.3299	0.3129	51.32	0.11
6	6.25	0.0954	0.0954	0.0000	100	0.05
6	6.25	0.2292	0.1921	0.0371	83.81	0.07
6	6.25	0.2938	0.2358	0.0580	80.26	0.08
6	6.25	0.3738	0.2516	0.1222	67.31	0.08
6	6.25	0.454	0.2597	0.1943	57.2	0.09
6	6.25	0.4907	0.2679	0.2228	54.6	0.10
6	6.25	0.5304	0.2848	0.2456	53.7	0.11
6	6.25	0.6066	0.3114	0.2952	51.34	0.13

Table A.31: Experimental data on locally depressed inlets for L=2.583 ft, by Hahn (1972).

S_L	S_x	Q	Q_i	Q_b	E	d
0.2	2.08	0.0703	0.0703	0	100	0.0733
0.2	2.08	0.0885	0.0865	0.002	97.74	0.0833
0.2	2.08	0.1061	0.1	0.0061	94.25	0.0833
0.2	2.08	0.1311	0.1097	0.0214	83.68	0.09
0.2	2.08	0.196	0.1535	0.0425	78.32	0.1033
0.2	2.08	0.2486	0.1722	0.0764	69.27	0.11
0.2	2.08	0.2853	0.1921	0.0932	67.33	0.12
0.2	2.08	0.3283	0.2061	0.1222	62.78	0.1267
0.2	3.12	0.1048	0.1048	0	100	0.0933
0.2	3.12	0.1204	0.1198	0.0006	99.5	0.0933
0.2	3.12	0.1537	0.1476	0.0061	96.03	0.1033
0.2	3.12	0.1836	0.1658	0.0178	90.31	0.1133
0.2	3.12	0.2174	0.1853	0.0321	85.23	0.12

Table A.31 – continued from previous page

S_L	S_x	Q	Q_i	Q_b	E	d
0.2	3.12	0.2474	0.199	0.0484	80.44	0.12
0.2	3.12	0.2957	0.2232	0.0725	75.48	0.1367
0.2	3.12	0.3413	0.2436	0.0977	71.37	0.14
0.2	3.12	0.3872	0.2597	0.1275	67.07	0.1467
0.2	3.12	0.4406	0.2848	0.1558	64.64	0.15
0.2	3.12	0.4745	0.2935	0.181	61.85	0.1567
0.2	4.16	0.1251	0.1251	0	100	0.1033
0.2	4.16	0.1627	0.1596	0.0031	98.09	0.1367
0.2	4.16	0.1891	0.1787	0.0104	94.5	0.1267
0.2	4.16	0.2204	0.199	0.0214	90.29	0.13
0.2	4.16	0.268	0.2282	0.0398	85.15	0.1367
0.2	4.16	0.2951	0.2436	0.0515	82.55	0.1467
0.2	4.16	0.3284	0.2597	0.0687	79.08	0.1467
0.2	4.16	0.3651	0.2763	0.0888	75.68	0.1567
0.2	4.16	0.3959	0.2935	0.1024	74.13	0.16
0.2	4.16	0.4336	0.3114	0.1222	71.82	0.1667
0.2	4.16	0.474	0.3299	0.1441	69.6	0.1733
0.2	4.16	0.5012	0.3393	0.1619	67.7	0.1767
0.2	4.16	0.53	0.349	0.181	65.85	0.1767
0.2	5.21	0.1596	0.1596	0	100	0.1267
0.2	5.21	0.1958	0.1921	0.0037	98.11	0.1367
0.2	5.21	0.2338	0.2207	0.0131	94.4	0.14
0.2	5.21	0.269	0.2436	0.0254	90.56	0.1467
0.2	5.21	0.3104	0.2679	0.0425	86.31	0.16
0.2	5.21	0.355	0.2935	0.0615	82.68	0.1667
0.2	5.21	0.396	0.3114	0.0846	78.64	0.1767
0.2	5.21	0.4323	0.3299	0.1024	76.31	0.1833
0.2	6.25	0.1853	0.1853	0	100	0.14
0.2	6.25	0.2067	0.2061	0.0006	99.71	0.1467
0.2	6.25	0.2553	0.2436	0.0117	95.42	0.1467
0.2	6.25	0.2792	0.2597	0.0195	93.02	0.16
0.2	6.25	0.3169	0.2848	0.0321	89.87	0.1667
0.2	6.25	0.3568	0.3114	0.0454	87.28	0.1833
0.5	2.08	0.0594	0.0594	0	100	0.0633
0.5	2.08	0.1146	0.1	0.0146	87.26	0.0767
0.5	2.08	0.1422	0.1147	0.0275	80.66	0.0767
0.5	2.08	0.173	0.1305	0.0425	75.43	0.0833
0.5	2.08	0.2299	0.1535	0.0764	66.77	0.09

Table A.31 – continued from previous page

S_L	S_x	Q	Q_i	Q_b	E	d
0.5	2.08	0.259	0.1658	0.0932	64.02	0.09
0.5	2.08	0.3196	0.1921	0.1275	60.11	0.1
0.5	2.08	0.3619	0.2061	0.1558	56.95	0.1
0.5	2.08	0.415	0.2207	0.1943	53.18	0.1
0.5	3.12	0.0823	0.0823	0	100	0.0833
0.5	3.12	0.1192	0.1147	0.0045	96.22	0.09
0.5	3.12	0.1409	0.1305	0.0104	92.62	0.09
0.5	3.12	0.1856	0.1535	0.0321	82.7	0.0933
0.5	3.12	0.2237	0.1722	0.0515	76.98	0.1033
0.5	3.12	0.2685	0.1921	0.0764	71.55	0.1133
0.5	3.12	0.3157	0.2133	0.1024	67.56	0.12
0.5	3.12	0.3611	0.2282	0.1329	63.2	0.12
0.5	3.12	0.4074	0.2516	0.1558	61.76	0.1267
0.5	3.12	0.4407	0.2597	0.181	58.93	0.1267
0.5	3.12	0.4706	0.2763	0.1943	58.71	0.1267
0.5	3.12	0.5226	0.2848	0.2378	54.5	0.13
0.5	3.12	0.5721	0.3024	0.2697	52.86	0.1367
0.5	4.16	0.1198	0.1198	0	100	0.1
0.5	4.16	0.133	0.1305	0.0025	98.12	0.1033
0.5	4.16	0.1836	0.1658	0.0178	90.31	0.1133
0.5	4.16	0.2174	0.1853	0.0321	85.23	0.12
0.5	4.16	0.2444	0.199	0.0454	81.42	0.1267
0.5	4.16	0.2713	0.2133	0.058	78.62	0.11
0.5	4.16	0.3046	0.2282	0.0764	74.92	0.13
0.5	4.16	0.3413	0.2436	0.0977	71.37	0.13
0.5	4.16	0.3717	0.2597	0.112	69.87	0.1367
0.5	4.16	0.4204	0.2763	0.1441	65.72	0.1367
0.5	4.16	0.4616	0.2935	0.1681	63.58	0.14
0.5	4.16	0.536	0.3206	0.2154	59.81	0.1467
0.5	4.16	0.5928	0.3393	0.2535	57.24	0.1467
0.5	4.16	0.7194	0.3788	0.3406	52.65	0.1567
0.5	5.21	0.1198	0.1198	0	100	0.09
0.5	5.21	0.1547	0.1535	0.0012	99.22	0.1033
0.5	5.21	0.1793	0.1722	0.0071	96.04	0.1133
0.5	5.21	0.2185	0.199	0.0195	91.08	0.1267
0.5	5.21	0.2454	0.2133	0.0321	86.92	0.1267
0.5	5.21	0.2707	0.2282	0.0425	84.3	0.1267
0.5	5.21	0.3016	0.2436	0.058	80.77	0.13

Table A.31 – continued from previous page

S_L	S_x	Q	Q_i	Q_b	E	d
0.5	5.21	0.3361	0.2597	0.0764	77.27	0.1367
0.5	5.21	0.3695	0.2763	0.0932	74.78	0.14
0.5	5.21	0.4157	0.2935	0.1222	70.6	0.14
0.5	5.21	0.4555	0.3114	0.1441	68.36	0.1467
0.5	5.21	0.5044	0.3299	0.1745	65.4	0.1567
0.5	5.21	0.5815	0.3587	0.2228	61.69	0.1667
0.5	5.21	0.7229	0.41	0.3129	56.72	0.1667
0.5	6.25	0.1658	0.1658	0	100	0.12
0.5	6.25	0.1803	0.1787	0.0016	99.11	0.12
0.5	6.25	0.2002	0.1921	0.0081	95.95	0.12
0.5	6.25	0.2385	0.2207	0.0178	92.54	0.1267
0.5	6.25	0.2633	0.2358	0.0275	89.56	0.1267
0.5	6.25	0.3022	0.2597	0.0425	85.94	0.13
0.5	6.25	0.3535	0.2848	0.0687	80.57	0.1367
0.5	6.25	0.387	0.3024	0.0846	78.14	0.1467
0.5	6.25	0.4046	0.3114	0.0932	76.96	0.1567
0.5	6.25	0.4419	0.3299	0.112	74.65	0.1567
0.5	6.25	0.4777	0.3393	0.1384	71.03	0.1567
0.5	6.25	0.6118	0.389	0.2228	63.58	0.1733
1	2.08	0.037	0.037	0	100	0.0467
1	2.08	0.0566	0.056	0.0006	98.94	0.0533
1	2.08	0.0984	0.0823	0.0161	83.64	0.0667
1	2.08	0.1502	0.1048	0.0454	69.77	0.0833
1	2.08	0.203	0.1305	0.0725	64.29	0.0833
1	2.08	0.2441	0.1417	0.1024	58.05	0.09
1	2.08	0.2976	0.1535	0.1441	51.58	0.0933
1	2.08	0.3534	0.1658	0.1876	46.92	0.1
1	3.12	0.056	0.056	0	100	0.0533
1	3.12	0.0707	0.0703	0.0004	99.43	0.0633
1	3.12	0.0902	0.0865	0.0037	95.9	0.0667
1	3.12	0.1117	0.1	0.0117	89.53	0.0833
1	3.12	0.138	0.1147	0.0233	83.12	0.0833
1	3.12	0.1901	0.1417	0.0484	74.54	0.09
1	3.12	0.259	0.1658	0.0932	64.02	0.0933
1	3.12	0.3265	0.199	0.1275	60.95	0.1033
1	3.12	0.3445	0.2061	0.1384	59.83	0.1033
1	3.12	0.4083	0.2207	0.1876	54.05	0.1133
1	3.12	0.4586	0.2358	0.2228	51.42	0.12

Table A.31 – continued from previous page

S_L	S_x	Q	Q_i	Q_b	E	d
1	3.12	0.5555	0.2516	0.3039	45.29	0.1267
1	4.16	0.0703	0.0703	0	100	0.0767
1	4.16	0.0918	0.0909	0.0009	99.02	0.0767
1	4.16	0.1412	0.1251	0.0161	88.6	0.09
1	4.16	0.1797	0.1476	0.0321	82.14	0.0933
1	4.16	0.2269	0.1722	0.0547	75.89	0.1033
1	4.16	0.2878	0.199	0.0888	69.15	0.1033
1	4.16	0.3253	0.2133	0.112	65.57	0.1133
1	4.16	0.3793	0.2352	0.1441	62.01	0.12
1	4.16	0.4326	0.2516	0.181	58.16	0.1267
1	4.16	0.4907	0.2679	0.2228	54.6	0.13
1	4.16	0.5219	0.2763	0.2456	52.94	0.1367
1	4.16	0.5632	0.2935	0.2697	52.11	0.1367
1	4.16	0.6243	0.3024	0.3219	48.44	0.1467
1	5.21	0.1048	0.1048	0	100	0.0833
1	5.21	0.181	0.1596	0.0214	88.18	0.0933
1	5.21	0.2067	0.1722	0.0345	83.31	0.1033
1	5.21	0.2505	0.199	0.0515	79.44	0.1133
1	5.21	0.282	0.2133	0.0687	75.64	0.12
1	5.21	0.3335	0.2358	0.0977	70.7	0.1267
1	5.21	0.3926	0.2597	0.1329	66.15	0.1267
1	5.21	0.4178	0.2679	0.1499	64.12	0.13
1	5.21	0.4658	0.2848	0.181	61.14	0.1367
1	5.21	0.5326	0.3024	0.2302	56.78	0.1467
1	5.21	0.6164	0.3299	0.2865	53.52	0.1567
1	5.21	0.6802	0.349	0.3312	51.31	0.1567
1	5.21	0.7185	0.3587	0.3598	49.92	0.1567
1	6.25	0.1251	0.1251	0	100	0.0933
1	6.25	0.1373	0.1361	0.0012	99.13	0.0933
1	6.25	0.1713	0.1596	0.0117	93.17	0.1
1	6.25	0.2001	0.1787	0.0214	89.31	0.1033
1	6.25	0.2242	0.1921	0.0321	85.68	0.11
1	6.25	0.2754	0.2207	0.0547	80.14	0.12
1	6.25	0.32	0.2436	0.0764	76.13	0.1267
1	6.25	0.3621	0.2597	0.1024	71.72	0.13
1	6.25	0.4177	0.2848	0.1329	68.18	0.14
1	6.25	0.4769	0.3024	0.1745	63.41	0.1467
1	6.25	0.5453	0.3299	0.2154	60.5	0.1467

Table A.31 – continued from previous page

S_L	S_x	Q	Q_i	Q_b	E	d
1	6.25	0.6025	0.349	0.2535	57.93	0.15
1	6.25	0.6626	0.3587	0.3039	54.14	0.16
1	6.25	0.7194	0.3788	0.3406	52.65	0.1667
1	6.25	0.7289	0.3788	0.3501	51.97	0.1733
2	2.08	0.0328	0.0328	0	100	0.0467
2	2.08	0.0473	0.0464	0.0009	98.1	0.0533
2	2.08	0.0873	0.0742	0.0131	84.99	0.0633
2	2.08	0.1325	0.0954	0.0371	72	0.0733
2	2.08	0.1814	0.1199	0.0615	66.1	0.0733
2	2.08	0.2228	0.1251	0.0977	56.15	0.0767
2	2.08	0.2802	0.1361	0.1441	48.57	0.0833
2	3.12	0.0527	0.0527	0	100	0.0633
2	3.12	0.0936	0.0865	0.0071	92.41	0.0733
2	3.12	0.133	0.1097	0.0233	82.48	0.0733
2	3.12	0.2091	0.1476	0.0615	70.59	0.0833
2	3.12	0.2462	0.1658	0.0804	67.34	0.09
2	3.12	0.2764	0.1787	0.0977	64.65	0.09
2	3.12	0.342	0.1921	0.1499	56.17	0.09
2	3.12	0.3864	0.1921	0.1943	49.72	0.0933
2	4.16	0.0742	0.0742	0	100	0.0633
2	4.16	0.1071	0.1	0.0071	93.37	0.0767
2	4.16	0.1308	0.1147	0.0161	87.69	0.0833
2	4.16	0.165	0.1305	0.0345	79.09	0.0833
2	4.16	0.1815	0.1417	0.0398	78.07	0.09
2	4.16	0.2082	0.1535	0.0547	73.73	0.0933
2	4.16	0.2447	0.1722	0.0725	70.37	0.0933
2	4.16	0.2898	0.1921	0.0977	66.29	0.1
2	4.16	0.3181	0.2061	0.112	64.79	0.1
2	4.16	0.3355	0.2133	0.1222	63.58	0.1033
2	4.16	0.3723	0.2282	0.1441	61.29	0.1033
2	4.16	0.4459	0.2516	0.1943	56.43	0.11
2	4.16	0.4972	0.2516	0.2456	50.6	0.11
2	4.16	0.5549	0.2597	0.2952	46.8	0.12
2	4.16	0.7108	0.2679	0.4429	37.69	0.1467
2	5.21	0.0823	0.0823	0	100	0.0667
2	5.21	0.1052	0.1048	0.0004	99.62	0.0767
2	5.21	0.1322	0.1251	0.0071	94.63	0.0833
2	5.21	0.1522	0.1361	0.0161	89.42	0.09

Table A.31 – continued from previous page

S_L	S_x	Q	Q_i	Q_b	E	d
2	5.21	0.181	0.1535	0.0275	84.81	0.0933
2	5.21	0.2112	0.1658	0.0454	78.5	0.0933
2	5.21	0.2302	0.1722	0.058	74.8	0.1
2	5.21	0.2646	0.1921	0.0725	72.6	0.1033
2	5.21	0.3132	0.2061	0.1071	65.8	0.1133
2	5.21	0.3557	0.2282	0.1275	64.16	0.1133
2	5.21	0.4135	0.2516	0.1619	60.85	0.11
2	5.21	0.4158	0.2348	0.181	56.47	0.1267
2	5.21	0.5207	0.3114	0.2093	59.8	0.1267
2	5.21	0.5741	0.3206	0.2535	55.84	0.1267
2	5.21	0.6425	0.3206	0.3219	49.9	0.1267
2	5.21	0.7207	0.3206	0.4001	44.48	0.1467
2	6.25	0.1048	0.1048	0	100	0.0767
2	6.25	0.1149	0.1147	0.0002	99.83	0.0767
2	6.25	0.1257	0.1251	0.0006	99.52	0.0833
2	6.25	0.1325	0.1305	0.002	98.49	0.0833
2	6.25	0.1568	0.1476	0.0092	94.13	0.0933
2	6.25	0.1933	0.1658	0.0275	85.77	0.1
2	6.25	0.2185	0.1787	0.0398	81.78	0.1033
2	6.25	0.2501	0.1921	0.058	76.81	0.1033
2	6.25	0.3079	0.2133	0.0946	69.28	0.1133
2	6.25	0.3231	0.2207	0.1024	68.31	0.12
2	6.25	0.3765	0.2436	0.1329	64.7	0.1267
2	6.25	0.4155	0.2597	0.1558	62.5	0.1267
2	6.25	0.3773	0.2763	0.101	73.23	0.13
2	6.25	0.4783	0.284	0.1943	59.38	0.1367
2	6.25	0.5268	0.3114	0.2154	59.11	0.1367
2	6.25	0.5868	0.349	0.2378	59.48	0.14
2	6.25	0.6384	0.3687	0.2697	57.75	0.14
2	6.25	0.7194	0.3788	0.3406	52.65	0.1467
3	2.08	0.02	0.02	0	100	0.0367
3	2.08	0.029	0.0281	0.0009	96.9	0.0433
3	2.08	0.0576	0.0495	0.0081	85.94	0.0533
3	2.08	0.0936	0.0703	0.0233	75.11	0.0633
3	2.08	0.108	0.0782	0.0298	72.41	0.0633
3	2.08	0.129	0.0865	0.0425	67.05	0.0667
3	2.08	0.1424	0.0909	0.0515	63.83	0.0667
3	2.08	0.1569	0.0954	0.0615	60.8	0.0667

Table A.31 – continued from previous page

S_L	S_x	Q	Q_i	Q_b	E	d
3	2.08	0.1764	0.1	0.0764	56.69	0.0667
3	2.08	0.2369	0.1147	0.1222	48.42	0.07
3	3.12	0.0379	0.0379	0	100	0.0433
3	3.12	0.0507	0.0495	0.0012	97.63	0.0533
3	3.12	0.0746	0.0665	0.0081	89.14	0.0533
3	3.12	0.1037	0.0823	0.0214	79.36	0.0633
3	3.12	0.1419	0.1048	0.0371	73.85	0.0733
3	3.12	0.1758	0.1198	0.056	68.15	0.0733
3	3.12	0.2338	0.1361	0.0977	58.21	0.0733
3	3.12	0.2917	0.1476	0.1441	50.6	0.0767
3	4.16	0.056	0.056	0	100	0.0533
3	4.16	0.0715	0.0703	0.0012	98.32	0.0633
3	4.16	0.104	0.0909	0.0131	87.4	0.0667
3	4.16	0.1518	0.1147	0.0371	75.56	0.0733
3	4.16	0.1908	0.1361	0.0547	71.33	0.0767
3	4.16	0.24	0.1596	0.0804	66.5	0.0767
3	4.16	0.2811	0.1787	0.1024	63.57	0.0833
3	4.16	0.3196	0.1921	0.1275	60.11	0.0833
3	4.16	0.3609	0.199	0.1619	55.14	0.09
3	4.16	0.4218	0.199	0.2228	47.18	0.0933
3	5.21	0.0742	0.0742	0	100	0.0567
3	5.21	0.0791	0.0782	0.0009	98.86	0.0633
3	5.21	0.1258	0.1097	0.0161	87.2	0.0833
3	5.21	0.1596	0.1251	0.0345	78.38	0.0833
3	5.21	0.215	0.1535	0.0615	71.4	0.09
3	5.21	0.283	0.1853	0.0977	65.48	0.0933
3	5.21	0.3161	0.199	0.1171	62.95	0.0933
3	5.21	0.3935	0.2436	0.1499	61.91	0.0933
3	5.21	0.4326	0.2516	0.181	58.16	0.1
3	5.21	0.4744	0.2516	0.2228	53.04	0.1033
3	5.21	0.5381	0.2516	0.2865	46.76	0.1133
3	6.25	0.0954	0.0954	0	100	0.0667
3	6.25	0.1068	0.1048	0.002	98.13	0.0733
3	6.25	0.1484	0.1251	0.0233	84.3	0.0833
3	6.25	0.2082	0.1535	0.0547	73.73	0.09
3	6.25	0.2591	0.1787	0.0804	68.97	0.0933
3	6.25	0.3014	0.199	0.1024	66.03	0.1
3	6.25	0.3355	0.2133	0.1222	63.58	0.1033

Table A.31 – continued from previous page

S_L	S_x	Q	Q_i	Q_b	E	d
3	6.25	0.3723	0.2282	0.1441	61.29	0.11
3	6.25	0.436	0.2679	0.1681	61.44	0.11
3	6.25	0.4947	0.2935	0.2012	59.33	0.11
3	6.25	0.5326	0.3024	0.2302	56.78	0.11
4	2.08	0.0182	0.0182	0	100	0.03
4	2.08	0.0231	0.0219	0.0012	94.81	0.03
4	2.08	0.0774	0.056	0.0214	72.35	0.0533
4	2.08	0.1196	0.0742	0.0454	62.04	0.0533
4	2.08	0.1713	0.0867	0.0846	50.61	0.0567
4	3.12	0.0259	0.0259	0	100	0.0367
4	3.12	0.0496	0.0435	0.0061	87.7	0.0467
4	3.12	0.0898	0.0665	0.0233	74.05	0.0467
4	3.12	0.1168	0.0823	0.0345	70.46	0.0533
4	3.12	0.1595	0.1048	0.0547	65.71	0.0633
4	3.12	0.213	0.1198	0.0932	56.24	0.0633
4	3.12	0.2526	0.1251	0.1275	49.52	0.0667
4	4.16	0.037	0.037	0	100	0.0433
4	4.16	0.0665	0.0594	0.0071	89.32	0.0533
4	4.16	0.1186	0.0865	0.0321	72.93	0.0533
4	4.16	0.1694	0.1147	0.0547	67.71	0.0633
4	4.16	0.2221	0.1417	0.0804	63.8	0.0667
4	4.16	0.2706	0.1535	0.1171	56.73	0.0733
4	4.16	0.3215	0.1596	0.1619	49.64	0.0767
4	5.21	0.0495	0.0495	0	100	0.0433
4	5.21	0.071	0.0665	0.0045	93.66	0.0533
4	5.21	0.0955	0.0782	0.0173	81.88	0.0633
4	5.21	0.1275	0.0954	0.0321	74.82	0.0633
4	5.21	0.1662	0.1147	0.0515	69.01	0.0733
4	5.21	0.2048	0.1361	0.0687	66.46	0.0733
4	5.21	0.2381	0.1535	0.0846	64.47	0.0833
4	5.21	0.2877	0.1853	0.1024	64.41	0.0833
4	5.21	0.3265	0.199	0.1275	60.95	0.0833
4	5.21	0.3871	0.2061	0.181	53.24	0.09
4	6.25	0.0665	0.0665	0	100	0.0533
4	6.25	0.0884	0.0823	0.0061	93.1	0.0633
4	6.25	0.1275	0.1	0.0275	78.43	0.0733
4	6.25	0.1652	0.1198	0.0454	72.52	0.0767
4	6.25	0.2104	0.1417	0.0687	67.35	0.0833

Table A.31 – continued from previous page

S_L	S_x	Q	Q_i	Q_b	E	d
4	6.25	0.2528	0.1596	0.0932	63.13	0.0833
4	6.25	0.3024	0.1853	0.1171	61.28	0.09
4	6.25	0.3462	0.2133	0.1329	61.61	0.09
4	6.25	0.3723	0.2282	0.1441	61.29	0.0933
4	6.25	0.4664	0.2436	0.2228	52.23	0.0933
5	2.08	0.0182	0.0182	0	100	0.03
5	2.08	0.0255	0.0239	0.0016	93.73	0.03
5	2.08	0.0772	0.0594	0.0178	76.94	0.0433
5	2.08	0.1397	0.0782	0.0615	55.98	0.0533
5	2.08	0.1842	0.0865	0.0977	46.96	0.0567
5	3.12	0.0259	0.0259	0	100	0.03
5	3.12	0.0283	0.0281	0.0002	99.29	0.03
5	3.12	0.0644	0.0527	0.0117	81.83	0.0467
5	3.12	0.1098	0.0823	0.0275	74.95	0.0533
5	3.12	0.1484	0.1	0.0484	67.39	0.0633
5	3.12	0.1861	0.1097	0.0764	58.95	0.0633
5	3.12	0.2171	0.1147	0.1024	52.83	0.0633
5	3.12	0.2527	0.1198	0.1329	47.41	0.0633
5	4.16	0.0353	0.0353	0	100	0.03
5	4.16	0.0526	0.0495	0.0031	94.11	0.0433
5	4.16	0.0721	0.0629	0.0092	87.24	0.0533
5	4.16	0.0943	0.0782	0.0161	82.93	0.0533
5	4.16	0.1369	0.1048	0.0321	76.55	0.0633
5	4.16	0.182	0.1305	0.0515	71.7	0.0667
5	4.16	0.228	0.1476	0.0804	64.74	0.0733
5	4.16	0.2706	0.1535	0.1171	56.73	0.0733
5	5.21	0.0495	0.0495	0	100	0.0433
5	5.21	0.0562	0.056	0.0002	99.64	0.0433
5	5.21	0.0863	0.0782	0.0081	90.61	0.0633
5	5.21	0.1233	0.1	0.0233	81.1	0.0633
5	5.21	0.1735	0.1251	0.0484	72.1	0.0733
5	5.21	0.2185	0.1535	0.065	70.25	0.0833
5	5.21	0.2568	0.1722	0.0846	67.06	0.0833
5	5.21	0.3196	0.1921	0.1275	60.11	0.09
5	5.21	0.3666	0.1921	0.1745	52.4	0.0933
5	5.21	0.4075	0.1921	0.2154	47.14	0.1
5	6.25	0.0629	0.0629	0	100	0.0433
5	6.25	0.0705	0.0703	0.0002	99.72	0.0433

Table A.31 – continued from previous page

S_L	S_x	Q	Q_i	Q_b	E	d
5	6.25	0.0946	0.0865	0.0081	91.44	0.0633
5	6.25	0.1302	0.1048	0.0254	80.49	0.0733
5	6.25	0.1352	0.0954	0.0398	70.56	0.0733
5	6.25	0.2023	0.1476	0.0547	72.96	0.0833
5	6.25	0.2422	0.1658	0.0764	68.46	0.0833
5	6.25	0.2853	0.1921	0.0932	67.33	0.0933
5	6.25	0.3181	0.2061	0.112	64.79	0.1033
5	6.25	0.3536	0.2207	0.1329	62.42	0.1033
5	6.25	0.4158	0.2282	0.1876	54.88	0.1033
5	6.25	0.451	0.2282	0.2228	50.6	0.1033
6	2.08	0.02	0.02	0	100	0.03
6	2.08	0.041	0.0379	0.0031	92.44	0.0367
6	2.08	0.0626	0.0495	0.0131	79.07	0.0433
6	2.08	0.0957	0.0703	0.0254	73.46	0.0433
6	2.08	0.0907	0.0423	0.0484	46.64	0.0467
6	2.08	0.1634	0.0909	0.0725	55.63	0.0533
6	2.08	0.2024	0.1	0.1024	49.41	0.0633
6	2.08	0.2422	0.1147	0.1275	47.36	0.0667
6	3.12	0.0328	0.0328	0	100	0.0367
6	3.12	0.0725	0.0594	0.0131	81.93	0.0433
6	3.12	0.0677	0.056	0.0117	82.72	0.0433
6	3.12	0.1325	0.0954	0.0371	72	0.0467
6	3.12	0.2096	0.1198	0.0898	57.16	0.0633
6	4.16	0.0353	0.0353	0	100	0.03
6	4.16	0.0746	0.0629	0.0117	84.32	0.0433
6	4.16	0.0579	0.0365	0.0214	63.04	0.0533
6	4.16	0.1518	0.1147	0.0371	75.56	0.0633
6	4.16	0.2305	0.1417	0.0888	61.48	0.0733
6	4.16	0.278	0.1476	0.1304	53.09	0.0833
6	4.16	0.3539	0.1596	0.1943	45.1	0.09
6	5.21	0.0495	0.0495	0	100	0.0433
6	5.21	0.0833	0.0742	0.0091	89.08	0.0633
6	5.21	0.1369	0.1048	0.0321	76.55	0.0633
6	5.21	0.1932	0.1417	0.0515	73.34	0.0733
6	5.21	0.2611	0.1722	0.0889	65.95	0.0733
6	5.21	0.3231	0.179	0.1441	55.4	0.0833
6	5.21	0.3799	0.1787	0.2012	47.04	0.0933
6	6.25	0.0629	0.0629	0	100	0.0467

Table A.31 – continued from previous page

S_L	S_x	Q	Q_i	Q_b	E	d
6	6.25	0.0704	0.0703	0.0001	99.86	0.0533
6	6.25	0.086	0.0823	0.0037	95.7	0.0533
6	6.25	0.1195	0.1	0.0195	83.68	0.0567
6	6.25	0.1387	0.1097	0.029	79.09	0.0733
6	6.25	0.1676	0.1251	0.0425	74.64	0.0767
6	6.25	0.1964	0.1417	0.0547	72.15	0.0833
6	6.25	0.2185	0.1535	0.065	70.25	0.0833
6	6.25	0.2462	0.1658	0.0804	67.34	0.09
6	6.25	0.283	0.1853	0.0977	65.48	0.0933
6	6.25	0.311	0.199	0.112	63.99	0.0933
6	6.25	0.3274	0.2133	0.1141	65.15	0.0933
6	6.25	0.5131	0.2516	0.2615	49.04	0.14

A.4.2 Inlets at Continuously Depressed Gutter

Experimental data on inlets at continuously depressed gutter are less available compared to locally depressed inlets. Guo et al. (2012) conducted an extensive experimental study on various grates and curb inlets. In model dimensions, the gutter was depressed 0.667 inch and a local depression was applied at the inlet. The local depression was either 0.667 inch or one inch. The experimental data are readily accessible so they were not reported herein.

A modeling facility at the Clemson University was used for extensive testing of inlets at continuously depressed gutter (Bowman, 1988; Soares, 1991). The capacity of inlets of varying lengths was determined for a wide combination of longitudinal and cross-sectional slopes. Then, Soares (1991) evaluated the effect of increasing the upstream transition from 1.5 ft to 2 ft. No significant effect was observed due to the increase in the transition length by 1 ft, therefore data reported herein will only be

for the 1.5 ft transition. The parameters used in these studies were:

Scale: scaled (1:2); L= 2,4,6,8; w= 0.75; a= 1; a_g= 0.5; L_u= 1.5; L_d= 1.5; n= 0.011.

Table A.32: Experimental data on locally depressed inlets by MacCallan and Hotchkiss (1996).

S_L	S_x	L	Q	Q_i	Q_b	E	T
0.5	2.083	2	1.414	0.707	0.707	50	6.75
0.5	2.083	4	1.414	0.832	0.583	58.8	6.75
0.5	2.083	6	1.414	0.973	0.441	68.8	6.75
0.5	2.083	8	1.414	1.079	0.335	76.3	6.75
0.5	2.083	2	1.061	0.636	0.424	60	6.15
0.5	2.083	4	1.061	0.76	0.3	71.7	6.15
0.5	2.083	6	1.061	0.83	0.23	78.3	6.15
0.5	2.083	8	1.061	0.92	0.141	86.7	6.15
0.5	2.083	2	0.707	0.548	0.159	77.5	5.5
0.5	2.083	4	0.707	0.601	0.106	85	5.5
0.5	2.083	6	0.707	0.654	0.053	92.5	5.5
0.5	2.083	8	0.707	0.672	0.035	95	5.5
0.5	2.083	2	0.354	0.352	0.001	99.7	4
0.5	2.083	4	0.354	0.354	0	100	4
0.5	2.083	6	0.354	0.354	0	100	4
0.5	2.083	8	0.354	0.354	0	100	4
1	2.083	2	1.414	0.707	0.707	50	6.75
1	2.083	4	1.414	0.813	0.601	57.5	6.75
1	2.083	6	1.414	0.884	0.53	62.5	6.75
1	2.083	8	1.414	0.938	0.477	66.3	6.75
1	2.083	2	1.061	0.618	0.442	58.3	5.7
1	2.083	4	1.061	0.671	0.389	63.3	5.7
1	2.083	6	1.061	0.76	0.3	71.7	5.7
1	2.083	8	1.061	0.795	0.265	75	5.7
1	2.083	2	0.707	0.53	0.177	75	5
1	2.083	4	0.707	0.566	0.141	80	5
1	2.083	6	0.707	0.619	0.088	87.5	5
1	2.083	8	0.707	0.636	0.071	90	5
1	2.083	2	0.354	0.354	0	100	3.4
1	2.083	4	0.354	0.354	0	100	3.4
1	2.083	6	0.354	0.354	0	100	3.4
1	2.083	8	0.354	0.354	0	100	3.4

Table A.32 – continued from previous page

S_L	S_x	L	Q	Q_i	Q_b	E	T
3	2.083	2	1.414	0.53	0.884	37.5	5.95
3	2.083	4	1.414	0.655	0.759	46.3	5.95
3	2.083	6	1.414	0.769	0.645	54.4	5.95
3	2.083	8	1.414	0.849	0.566	60	5.95
3	2.083	2	1.061	0.459	0.601	43.3	5.25
3	2.083	4	1.061	0.618	0.442	58.3	5.25
3	2.083	6	1.061	0.654	0.406	61.7	5.25
3	2.083	8	1.061	0.76	0.3	71.7	5.25
3	2.083	2	0.707	0.407	0.301	57.5	4.3
3	2.083	4	0.707	0.495	0.212	70	4.3
3	2.083	6	0.707	0.53	0.177	75	4.3
3	2.083	8	0.707	0.548	0.159	77.5	4.3
3	2.083	2	0.354	0.318	0.035	90	2.9
3	2.083	4	0.354	0.336	0.018	95	2.9
3	2.083	6	0.354	0.354	0	100	2.9
3	2.083	8	0.354	0.354	0	100	2.9
5	2.083	2	1.414	0.46	0.955	32.5	5.35
5	2.083	4	1.414	0.636	0.778	45	5.35
5	2.083	6	1.414	0.636	0.778	45	5.35
5	2.083	8	1.414	0.725	0.689	51.3	5.35
5	2.083	2	1.061	0.442	0.618	41.7	4.85
5	2.083	4	1.061	0.601	0.459	56.7	4.85
5	2.083	6	1.061	0.565	0.495	53.3	4.85
5	2.083	8	1.061	0.628	0.433	59.2	4.85
5	2.083	2	0.707	0.407	0.301	57.5	4.15
5	2.083	4	0.707	0.486	0.221	68.8	4.15
5	2.083	6	0.707	0.451	0.256	63.8	4.15
5	2.083	8	0.707	0.486	0.221	68.8	4.15
5	2.083	2	0.354	0.292	0.062	82.5	3
5	2.083	4	0.354	0.309	0.044	87.5	3
5	2.083	6	0.354	0.309	0.044	87.5	3
5	2.083	8	0.354	0.318	0.035	90	3
7	2.083	2	1.414	0.389	1.025	27.5	5.7
7	2.083	4	1.414	0.522	0.892	36.9	5.7
7	2.083	6	1.414	0.53	0.884	37.5	5.7
7	2.083	8	1.414	0.619	0.795	43.8	5.7
7	2.083	2	1.061	0.389	0.671	36.7	5.05
7	2.083	4	1.061	0.495	0.565	46.7	5.05

Table A.32 – continued from previous page

S_L	S_x	L	Q	Q_i	Q_b	E	T
7	2.083	6	1.061	0.512	0.548	48.3	5.05
7	2.083	8	1.061	0.592	0.469	55.8	5.05
7	2.083	2	0.707	0.371	0.336	52.5	4.15
7	2.083	4	0.707	0.451	0.256	63.8	4.15
7	2.083	6	0.707	0.451	0.256	63.8	4.15
7	2.083	8	0.707	0.486	0.221	68.8	4.15
7	2.083	2	0.354	0.292	0.062	82.5	2.55
7	2.083	4	0.354	0.309	0.044	87.5	2.55
7	2.083	6	0.354	0.309	0.044	87.5	2.55
7	2.083	8	0.354	0.318	0.035	90	2.55
0.5	2.778	2	1.414	0.707	0.707	50	6.75
0.5	2.778	4	1.414	1.107	0.307	78.3	6.75
0.5	2.778	6	1.414	0.902	0.512	63.8	6.75
0.5	2.778	8	1.414	1.008	0.406	71.3	6.75
0.5	2.778	2	1.061	0.654	0.406	61.7	6.4
0.5	2.778	4	1.061	0.724	0.336	68.3	6.4
0.5	2.778	6	1.061	0.814	0.247	76.7	6.4
0.5	2.778	8	1.061	0.867	0.194	81.7	6.4
0.5	2.778	2	0.707	0.566	0.141	80	5.55
0.5	2.778	4	0.707	0.601	0.106	85	5.55
0.5	2.778	6	0.707	0.654	0.053	92.5	5.55
0.5	2.778	8	0.707	0.672	0.035	95	5.55
0.5	2.778	2	0.354	0.354	0	100	4
0.5	2.778	4	0.354	0.354	0	100	4
0.5	2.778	6	0.354	0.354	0	100	4
0.5	2.778	8	0.354	0.354	0	100	4
1	2.778	2	1.414	0.655	0.759	46.3	5.45
1	2.778	4	1.414	0.884	0.53	62.5	5.45
1	2.778	6	1.414	1.008	0.406	71.3	5.45
1	2.778	8	1.414	1.061	0.354	75	5.45
1	2.778	2	1.061	0.601	0.459	56.7	5.05
1	2.778	4	1.061	0.742	0.318	70	5.05
1	2.778	6	1.061	0.849	0.212	80	5.05
1	2.778	8	1.061	0.902	0.159	85	5.05
1	2.778	2	0.707	0.548	0.159	77.5	4
1	2.778	4	0.707	0.619	0.088	87.5	4
1	2.778	6	0.707	0.654	0.053	92.5	4
1	2.778	8	0.707	0.689	0.018	97.5	4

Table A.32 – continued from previous page

S_L	S_x	L	Q	Q_i	Q_b	E	T
1	2.778	2	0.354	0.354	0	100	2.9
1	2.778	4	0.354	0.354	0	100	2.9
1	2.778	6	0.354	0.354	0	100	2.9
1	2.778	8	0.354	0.354	0	100	2.9
3	2.778	2	1.414	0.549	0.865	38.8	5.4
3	2.778	4	1.414	0.751	0.663	53.1	5.4
3	2.778	6	1.414	0.849	0.566	60	5.4
3	2.778	8	1.414	0.875	0.539	61.9	5.4
3	2.778	2	1.061	0.53	0.53	50	4.6
3	2.778	4	1.061	0.671	0.389	63.3	4.6
3	2.778	6	1.061	0.751	0.31	70.8	4.6
3	2.778	8	1.061	0.795	0.265	75	4.6
3	2.778	2	0.707	0.451	0.256	63.8	3.7
3	2.778	4	0.707	0.575	0.132	81.3	3.7
3	2.778	6	0.707	0.619	0.088	87.5	3.7
3	2.778	8	0.707	0.628	0.079	88.8	3.7
3	2.778	2	0.354	0.336	0.018	95	2
3	2.778	4	0.354	0.354	0	100	2
3	2.778	6	0.354	0.354	0	100	2
3	2.778	8	0.354	0.354	0	100	2
5	2.778	2	1.414	0.486	0.928	34.4	4.6
5	2.778	4	1.414	0.725	0.689	51.3	4.6
5	2.778	6	1.414	0.796	0.618	56.3	4.6
5	2.778	8	1.414	0.832	0.583	58.8	4.6
5	2.778	2	1.061	0.459	0.601	43.3	4.15
5	2.778	4	1.061	0.663	0.398	62.5	4.15
5	2.778	6	1.061	0.671	0.389	63.3	4.15
5	2.778	8	1.061	0.707	0.353	66.7	4.15
5	2.778	2	0.707	0.424	0.283	60	3.5
5	2.778	4	0.707	0.557	0.15	78.8	3.5
5	2.778	6	0.707	0.566	0.141	80	3.5
5	2.778	8	0.707	0.593	0.115	83.8	3.5
5	2.778	2	0.354	0.309	0.044	87.5	1.8
5	2.778	4	0.354	0.354	0	100	1.8
5	2.778	6	0.354	0.354	0	100	1.8
5	2.778	8	0.354	0.354	0	100	1.8
7	2.778	2	1.414	0.443	0.972	31.3	5.1
7	2.778	4	1.414	0.636	0.778	45	5.1

Table A.32 – continued from previous page

S_L	S_x	L	Q	Q_i	Q_b	E	T
7	2.778	6	1.414	0.707	0.707	50	5.1
7	2.778	8	1.414	0.707	0.707	50	5.1
7	2.778	2	1.061	0.442	0.618	41.7	4.25
7	2.778	4	1.061	0.628	0.433	59.2	4.25
7	2.778	6	1.061	0.654	0.406	61.7	4.25
7	2.778	8	1.061	0.663	0.398	62.5	4.25
7	2.778	2	0.707	0.424	0.283	60	3.4
7	2.778	4	0.707	0.575	0.132	81.3	3.4
7	2.778	6	0.707	0.566	0.141	80	3.4
7	2.778	8	0.707	0.566	0.141	80	3.4
7	2.778	2	0.354	0.309	0.044	87.5	1.7
7	2.778	4	0.354	0.354	0	100	1.7
7	2.778	6	0.354	0.354	0	100	1.7
7	2.778	8	0.354	0.354	0	100	1.7
0.5	4.167	2	1.414	0.849	0.566	60	5.25
0.5	4.167	4	1.414	1.044	0.371	73.8	5.25
0.5	4.167	6	1.414	1.22	0.194	86.3	5.25
0.5	4.167	8	1.414	1.327	0.088	93.8	5.25
0.5	4.167	2	1.061	0.76	0.3	71.7	4.6
0.5	4.167	4	1.061	0.902	0.159	85	4.6
0.5	4.167	6	1.061	1.026	0.035	96.7	4.6
0.5	4.167	8	1.061	1.061	0	100	4.6
0.5	4.167	2	0.707	0.619	0.088	87.5	3.75
0.5	4.167	4	0.707	0.689	0.018	97.5	3.75
0.5	4.167	6	0.707	0.707	0	100	3.75
0.5	4.167	8	0.707	0.707	0	100	3.75
0.5	4.167	2	0.354	0.354	0	100	2.55
0.5	4.167	4	0.354	0.354	0	100	2.55
0.5	4.167	6	0.354	0.354	0	100	2.55
0.5	4.167	8	0.354	0.354	0	100	2.55
1	4.167	2	1.414	0.655	0.759	46.3	5
1	4.167	4	1.414	0.938	0.477	66.3	5
1	4.167	6	1.414	1.079	0.335	76.3	5
1	4.167	8	1.414	1.15	0.264	81.3	5
1	4.167	2	1.061	0.618	0.442	58.3	4.15
1	4.167	4	1.061	0.814	0.247	76.7	4.15
1	4.167	6	1.061	0.937	0.124	88.3	4.15
1	4.167	8	1.061	0.973	0.088	91.7	4.15

Table A.32 – continued from previous page

S_L	S_x	L	Q	Q_i	Q_b	E	T
1	4.167	2	0.707	0.548	0.159	77.5	3.5
1	4.167	4	0.707	0.636	0.071	90	3.5
1	4.167	6	0.707	0.689	0.018	97.5	3.5
1	4.167	8	0.707	0.707	0	100	3.5
1	4.167	2	0.354	0.354	0	100	2.7
1	4.167	4	0.354	0.354	0	100	2.7
1	4.167	6	0.354	0.354	0	100	2.7
1	4.167	8	0.354	0.354	0	100	2.7
3	4.167	2	1.414	0.636	0.778	45	4
3	4.167	4	1.414	0.955	0.46	67.5	4
3	4.167	6	1.414	1.061	0.354	75	4
3	4.167	8	1.414	1.158	0.256	81.9	4
3	4.167	2	1.061	0.628	0.433	59.2	3.5
3	4.167	4	1.061	0.83	0.23	78.3	3.5
3	4.167	6	1.061	0.92	0.141	86.7	3.5
3	4.167	8	1.061	0.955	0.106	90	3.5
3	4.167	2	0.707	0.548	0.159	77.5	2.75
3	4.167	4	0.707	0.628	0.079	88.8	2.75
3	4.167	6	0.707	0.681	0.026	96.3	2.75
3	4.167	8	0.707	0.707	0	100	2.75
3	4.167	2	0.354	0.354	0	100	1.8
3	4.167	4	0.354	0.354	0	100	1.8
3	4.167	6	0.354	0.354	0	100	1.8
3	4.167	8	0.354	0.354	0	100	1.8
5	4.167	2	1.414	0.549	0.865	38.8	3.85
5	4.167	4	1.414	0.805	0.61	56.9	3.85
5	4.167	6	1.414	0.919	0.495	65	3.85
5	4.167	8	1.414	0.973	0.441	68.8	3.85
5	4.167	2	1.061	0.539	0.522	50.8	3.5
5	4.167	4	1.061	0.795	0.265	75	3.5
5	4.167	6	1.061	0.849	0.212	80	3.5
5	4.167	8	1.061	0.875	0.186	82.5	3.5
5	4.167	2	0.707	0.53	0.177	75	2.75
5	4.167	4	0.707	0.636	0.071	90	2.75
5	4.167	6	0.707	0.663	0.044	93.8	2.75
5	4.167	8	0.707	0.672	0.035	95	2.75
5	4.167	2	0.354	0.336	0.018	95	1.75
5	4.167	4	0.354	0.354	0	100	1.75

Table A.32 – continued from previous page

S_L	S_x	L	Q	Q_i	Q_b	E	T
5	4.167	6	0.354	0.354	0	100	1.75
5	4.167	8	0.354	0.354	0	100	1.75
7	4.167	2	1.414	0.53	0.884	37.5	4.25
7	4.167	4	1.414	0.734	0.68	51.9	4.25
7	4.167	6	1.414	0.938	0.477	66.3	4.25
7	4.167	8	1.414	0.938	0.477	66.3	4.25
7	4.167	2	1.061	0.522	0.539	49.2	3.5
7	4.167	4	1.061	0.734	0.327	69.2	3.5
7	4.167	6	1.061	0.849	0.212	80	3.5
7	4.167	8	1.061	0.849	0.212	80	3.5
7	4.167	2	0.707	0.442	0.265	62.5	2.6
7	4.167	4	0.707	0.628	0.079	88.8	2.6
7	4.167	6	0.707	0.663	0.044	93.8	2.6
7	4.167	8	0.707	0.672	0.035	95	2.6
7	4.167	2	0.354	0.309	0.044	87.5	1.65
7	4.167	4	0.354	0.354	0	100	1.65
7	4.167	6	0.354	0.354	0	100	1.65
7	4.167	8	0.354	0.354	0	100	1.65
0.5	6.25	2	1.414	0.796	0.618	56.3	3.9
0.5	6.25	4	1.414	1.131	0.283	80	3.9
0.5	6.25	6	1.414	1.291	0.123	91.3	3.9
0.5	6.25	8	1.414	1.414	0	100	3.9
0.5	6.25	2	1.061	0.707	0.353	66.7	3.25
0.5	6.25	4	1.061	0.955	0.106	90	3.25
0.5	6.25	6	1.061	1.061	0	100	3.25
0.5	6.25	8	1.061	1.061	0	100	3.25
0.5	6.25	2	0.707	0.601	0.106	85	2.75
0.5	6.25	4	0.707	0.707	0	100	2.75
0.5	6.25	6	0.707	0.707	0	100	2.75
0.5	6.25	8	0.707	0.707	0	100	2.75
0.5	6.25	2	0.354	0.354	0	100	2
0.5	6.25	4	0.354	0.354	0	100	2
0.5	6.25	6	0.354	0.354	0	100	2
0.5	6.25	8	0.354	0.354	0	100	2
1	6.25	2	1.414	0.707	0.707	50	3.5
1	6.25	4	1.414	1.008	0.406	71.3	3.5
1	6.25	6	1.414	1.22	0.194	86.3	3.5
1	6.25	8	1.414	1.327	0.088	93.8	3.5

Table A.32 – continued from previous page

S_L	S_x	L	Q	Q_i	Q_b	E	T
1	6.25	2	1.061	0.654	0.406	61.7	3.05
1	6.25	4	1.061	0.884	0.177	83.3	3.05
1	6.25	6	1.061	1.008	0.053	95	3.05
1	6.25	8	1.061	1.061	0	100	3.05
1	6.25	2	0.707	0.548	0.159	77.5	2.5
1	6.25	4	0.707	0.689	0.018	97.5	2.5
1	6.25	6	0.707	0.707	0	100	2.5
1	6.25	8	0.707	0.707	0	100	2.5
1	6.25	2	0.354	0.354	0	100	1.8
1	6.25	4	0.354	0.354	0	100	1.8
1	6.25	6	0.354	0.354	0	100	1.8
1	6.25	8	0.354	0.354	0	100	1.8
3	6.25	2	1.414	0.707	0.707	50	3
3	6.25	4	1.414	0.981	0.433	69.4	3
3	6.25	6	1.414	1.202	0.212	85	3
3	6.25	8	1.414	1.291	0.123	91.3	3
3	6.25	2	1.061	0.601	0.459	56.7	2.5
3	6.25	4	1.061	0.795	0.265	75	2.5
3	6.25	6	1.061	0.963	0.098	90.8	2.5
3	6.25	8	1.061	1.016	0.045	95.8	2.5
3	6.25	2	0.707	0.53	0.177	75	2.1
3	6.25	4	0.707	0.636	0.071	90	2.1
3	6.25	6	0.707	0.689	0.018	97.5	2.1
3	6.25	8	0.707	0.707	0	100	2.1
3	6.25	2	0.354	0.354	0	100	1.45
3	6.25	4	0.354	0.354	0	100	1.45
3	6.25	6	0.354	0.354	0	100	1.45
3	6.25	8	0.354	0.354	0	100	1.45
5	6.25	2	1.414	0.663	0.751	46.9	3
5	6.25	4	1.414	0.99	0.424	70	3
5	6.25	6	1.414	1.167	0.247	82.5	3
5	6.25	8	1.414	1.281	0.133	90.6	3
5	6.25	2	1.061	0.548	0.512	51.7	2.05
5	6.25	4	1.061	0.814	0.247	76.7	2.05
5	6.25	6	1.061	0.973	0.088	91.7	2.05
5	6.25	8	1.061	1.016	0.045	95.8	2.05
5	6.25	2	0.707	0.451	0.256	63.8	1.85
5	6.25	4	0.707	0.619	0.088	87.5	1.85

Table A.32 – continued from previous page

S_L	S_x	L	Q	Q_i	Q_b	E	T
5	6.25	6	0.707	0.672	0.035	95	1.85
5	6.25	8	0.707	0.707	0	100	1.85
5	6.25	2	0.354	0.309	0.044	87.5	1.55
5	6.25	4	0.354	0.354	0	100	1.55
5	6.25	6	0.354	0.354	0	100	1.55
5	6.25	8	0.354	0.354	0	100	1.55
7	6.25	2	1.414	0.584	0.83	41.3	3
7	6.25	4	1.414	0.902	0.512	63.8	3
7	6.25	6	1.414	1.246	0.168	88.1	3
7	6.25	8	1.414	1.273	0.141	90	3
7	6.25	2	1.061	0.495	0.565	46.7	2.5
7	6.25	4	1.061	0.742	0.318	70	2.5
7	6.25	6	1.061	0.981	0.08	92.5	2.5
7	6.25	8	1.061	0.999	0.062	94.2	2.5
7	6.25	2	0.707	0.433	0.274	61.3	1.75
7	6.25	4	0.707	0.601	0.106	85	1.75
7	6.25	6	0.707	0.672	0.035	95	1.75
7	6.25	8	0.707	0.689	0.018	97.5	1.75
7	6.25	2	0.354	0.354	0	100	1.4
7	6.25	4	0.354	0.354	0	100	1.4
7	6.25	6	0.354	0.354	0	100	1.4
7	6.25	8	0.354	0.354	0	100	1.4

Yong (1965) conducted experiments on the effects of various modifications on the interception capacity of inlets on a continuously depressed gutter. No significant effect on the interception capacity was observed when the length of the upstream transition was increased from 1-ft to 2-ft or when the inlet was recessed 0.5-inches into the curb; therefore only one set of experiments was reported herein. Significant increase in the inlet interception was achieved by using deflecting vanes in the gutter, especially at steep longitudinal slopes. The parameters used in this study are:

Scale: scaled (1:4); S_x=3.125; L= 1.375; w= 0.375; a= 0.5; a_g= 0.2344; L_u= 1 or 2; L_d= 1 or 2; n= 0.0115.

Table A.33: Experimental data for inlet on a continuously depressed gutter at 100% interception by Yong (1965).

S_L	15	12.3	9.6	8	5.4	3.5	2	1	0.5
Q_i	0.014	0.016	0.018	0.02	0.022	0.024	0.045	0.052	0.06
d	0.0283	0.03	0.0317	0.035	0.0383	0.0425	0.0458	0.0642	0.0708

Table A.34: E of the inlet at d= 0.0833 inches by Yong (1965).

S_L	15.7	13.8	9.4	6.6	5.4	4	2.4	1	0.5
E	11.4	11.46	14.01	19.62	21.29	33.32	48.63	73.12	89.7

A.5 Conclusions

Many experimental studies addressed the problem of flow into curb inlets. However, many of these studies are decades old and the experimental data are not readily accessible for re-analysis in light of new findings. Herein, we provided experimental data for undepressed inlets, locally depressed inlets, and inlets on a continuously depressed gutter. Other than the comprehensive studies at Clemson University, experimental data for inlets on a continuously depressed gutter is scarce compared to locally depressed inlets. The reported experimental data for all inlet based on scaled experiments was scaled-down to actual model dimensions to evade potential sources of errors from ignoring Reynolds number effects through Froude number scaling. The provided data presents researcher with a valuable resource for future research into the hydraulic design of curb inlets.

Appendix B

Derivation of HEC-22 Formula for Conveyance in Compound Gutters

To derive an expression for E_o for a compound gutter, we apply the Izzard (1947) approach of integrating Manning's equation. The flow in the uniform section of compound gutter Q_s (Figure 2.1-b) can be given by:

$$Q_s = \frac{k_u}{n} {S_L}^{1/2} {S_x}^{5/3} (T - w)^{8/3} \tag{B.1}$$

Deriving an expression for the flow in the depressed section (Q_w) requires defining an expression for the depth of flow along the width of the depressed section. This depth (D) can be given as:

$$D = (T - x)S_x + a\left(1 - \frac{x}{w}\right) \tag{B.2}$$

Accordingly, the depth at the curb ($x = 0$) is $TS_x + a$, and the depth at the edge of the depressed section ($x = w$) is $(T - w)S_x$ as expected. It follows that Q_w is obtained by integrating over the depressed section as

$$Q_w = \frac{k}{n} {S_L}^{1/2} \int_0^w \left[(T - x)S_x + a\left(1 - \frac{x}{w}\right)\right]^{5/3} dx \tag{B.3}$$

resulting in

$$Q_w = \frac{k_u {S_L}^{1/2} {S_x}^{8/3}}{n S_w} \left\{ \left(T + \frac{a}{S_x} \right)^{8/3} - (T-w)^{8/3} \right\} \tag{B.4}$$

The fraction of the flow carried in the depressed gutter section, from Equation (2.12) is found with Eqs., (B.1) and (B.4), where $Q_g = Q_w + Q_s$:

$$E_o = \frac{\left(T + \frac{a}{S_x} \right)^{8/3} - (T-w)^{8/3}}{\left(T + \frac{a}{S_x} \right)^{8/3} - (T-w)^{8/3} + \frac{S_w}{S_x}(T-w)^{8/3}} \tag{B.5}$$

Equation (2.1), for S_w, can be manipulated as:

$$\frac{a}{S_x} = \frac{w S_w}{S_x} - w \tag{B.6}$$

Substituting Equation (B.6) into Equation (B.5) yields:

$$E_o = \frac{\left(T - w + \frac{w S_w}{S_x} \right)^{8/3} - (T-w)^{8/3}}{\left(T - w + \frac{w S_w}{S_x} \right)^{8/3} - (T-w)^{8/3} + \frac{S_w}{S_x}(T-w)^{8/3}} \tag{B.7}$$

by dividing the numerator and denominator of Equation (B.7) by the numerator and then factoring out $w^{8/3}$ from the numerator and denominator we obtain:

$$E_o = \frac{1}{1 + \frac{S_w S_x^{-1}}{\left(1 + \frac{S_w S_x^{-1}}{T w^{-1} - 1} \right)^{8/3} - 1}} \tag{B.8}$$

Thus Equation (2.13) as proposed by HEC-22 is the above equation with the 8/3 exponent rounded to three significant digits.

Appendix C

Interception Capacity of Recessed Inlets

Depressing the gutter at curb inlets significantly increases the inlet interception capacity (Karaki and Haynie, 1961). However, a large depression is hazardous to cyclists and can interfere with traffic flow (HEC-22). Consequently, drainage design manuals either limit the size of the depression or recommend that depressed inlets are recessed into the curb (TxDOT, 2016). Herein, depressed inlets that are flush with the curb line are called flush depressed inlets and inlets recessed inside the curb line are called recessed inlets. The use of recessed inlets is common around the USA such as in Kansas (McEnroe et al., 1998), Louisiana (Wintz and Kuo, 1970), Texas (Holley et al., 1992), and also in South Africa (Grobler, 1994). Despite the widespread use of these inlets, the effect of recessing the inlet on the interception capacity is rarely discussed in the literature. Yong (1965) experimentally studied recessed and flush depressed inlets, where no difference in interception capacity was observed between the two cases. However, Yong used a 1:4 scaled model so the actual tested dimension of the recession into the curb was only half of an inch, which is a minor modification that is not expected to significantly alter the hydraulics at the inlet.

Generally, design manuals do not provide special design criteria for the sizing of recessed inlets, e.g., HEC-22 provides a design procedure for depressed inlets in general without providing any additional criteria or modifications for recessed inlets. However, the City of Austin (2018) Drainage Criteria Manual (and manuals of other cities in Texas, USA) stipulates that the interception capacity of a recessed inlet is

75% of that of an equivalent flush depressed inlet, yet the drainage manual does not provide any reference for this stipulation. Herein, we compare experimental results for recessed and flush depressed inlets to identify cases where a distinction between the performance of the two configurations is justified, and we provide a method for applying such distinction into commercial design software.

Holley et al. (1992) conducted experiments at the University of Texas at Austin on recessed inlets used in Texas. Few years later, Hammonds and Holley (1995) conducted experiments in the same modeling facility on flush depressed inlets with similar dimensions to the recessed inlets tested by Holley et al. (1992). The experimental data by Hammonds and Holley (1995) was provided in Appendix A and data by Holley et al. (1992) is provided at the end of this appendix. The tested inlets (in both studies) were 3.75 and 11.25 ft, and the gutter width was 1.125 ft. However, the gutter slope S_w for recessed inlets ranged from 30% to 20%, which is equivalent to 4 to 2.7 inches depression height, while the depression height for standard inlets was 2.95 and 2 inches. Herein, we compare between recessed experimental results for 20% S_w and 2.95 inches depression for flush inlets. Recessed experiments for 30% S_w are used where experiments for 20% were unavailable.

Figure C.1 shows the comparison between intercepted flow at 100% interception condition for recessed and flush inlets. No observable difference can be identified in the experiments for 3.75 ft inlets (Figure C.1-a), however, the interception of recessed inlets is 75% of interception by flush inlets for several experiments (Figure C.1-b). The intercepted flow for recessed and flush inlets at partial interception condition is compared in Figure C.2. As with the case of 100% interception, most results are similar for both cases, however, flush inlets show higher interception at significant number of experiments (15% higher on average).

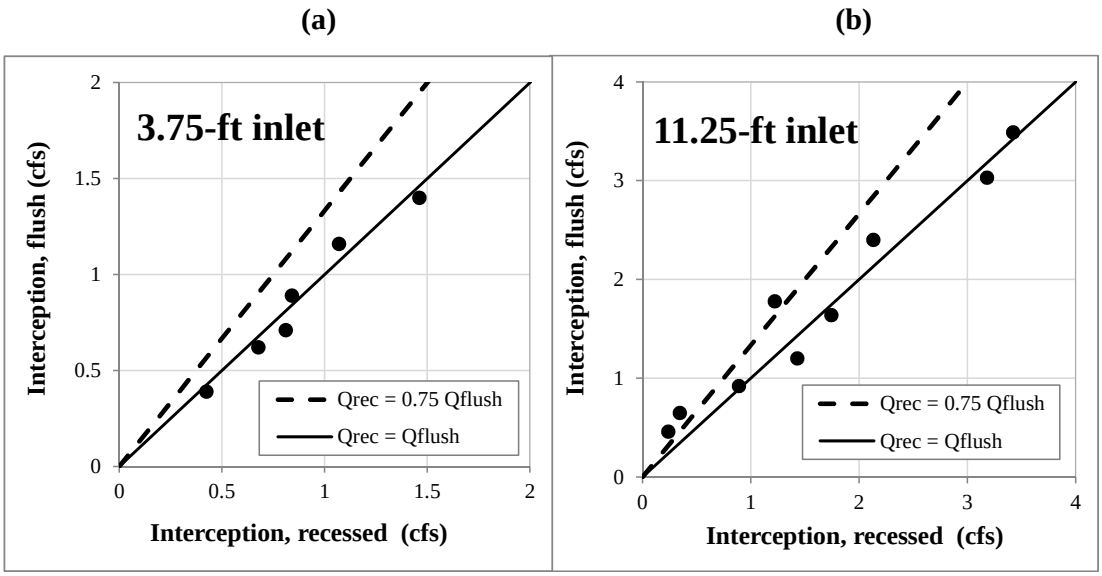

Figure C.1: Comparison between intercepted flow for recessed and flush depressed inlets at 100% interception.

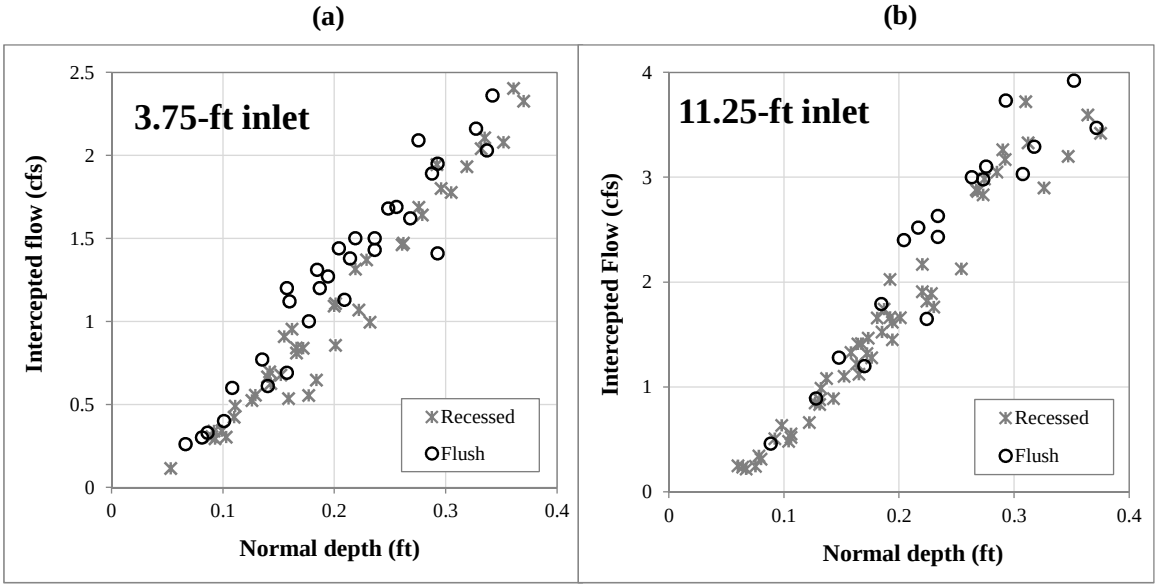

Figure C.2: Comparison between intercepted flow for recessed and flush depressed inlets at partial interception condition.

The comparison between interception by flush and recessed inlets shows that although both inlets generally provide similar interception, flush inlets out-perform recessed inlets under some conditions. Consequently, the 25% reduction in recessed inlet capacity is a conservative yet justified additional criteria for analyzing interception of recessed inlets.

The HEC-22 design Equations are recommended by the FHWA, therefore they are widely used in the design of curb inlets (Hammonds and Holley, 1995). These equations are implemented within commercial design software, such as Bentley StormCAD. HEC-22 equations do not account for potential reduction in interception capacity associated with using recessed inlets. Consequently, the current available software does not provide an option to implement a reduction for modeling recessed inlets. Herein, we provide a method for indirectly applying a reduction factor without modifying the underlying computational code of the software. The design software only models flush inlets (based on HEC-22), therefore the purpose of the following analysis is to estimate the flush inlet length L_f that intercepts the same flow as intercepted by a recessed inlet of length L_r. That is to say, given a recessed inlet of length L_r that is to be modeled in the software, what is the equivalent (shorter) flush inlet length L_f that is to be inputed into the model to indirectly apply the stipulated 25% reduction factor in interception capacity.

HEC-22 defines the inlet efficiency E as:

$$E = \frac{Q_i}{Q_g} \tag{C.1}$$

where Q_i is the intercepted flow and Q_g is the total gutter flow. HEC-22 computes E from the ratio of the installed inlet Length L_c to the total length L_T required to

capture 100% of Q_g as:

$$E = 1 - \left(1 - \frac{L_c}{L_T}\right)^{1.8} \tag{C.2}$$

First we apply Equations (C.1) and (C.2) to the recessed inlet to be modeled:

$$\frac{Q_r}{Q_g} = 1 - \left(1 - \frac{L_r}{L_T}\right)^{1.8} \tag{C.3}$$

where Q_r is the flow intercepted by the recessed inlet of length L_r. Similarly the two equations are applied to a flush inlet:

$$\frac{Q_f}{Q_g} = 1 - \left(1 - \frac{L_f}{L_T}\right)^{1.8} \tag{C.4}$$

where Q_f is the flow intercepted by a flush inlet of length L_f. Dividing Equation (C.3) by Equation (C.4) yields:

$$\frac{Q_r/Q_g}{Q_f/Q_g} = \frac{1 - \left(1 - \frac{L_r}{L_T}\right)^{1.8}}{1 - \left(1 - \frac{L_f}{L_T}\right)^{1.8}} \tag{C.5}$$

We apply the reduction in interception $Q_r = 0.75\ Q_f$ into Equation (C.5):

$$\begin{aligned} \frac{0.75\, Q_f/Q_g}{Q_f/Q_g} &= \frac{1 - \left(1 - \frac{L_r}{L_T}\right)^{1.8}}{1 - \left(1 - \frac{L_f}{L_T}\right)^{1.8}} \\ 0.75 &= \frac{1 - \left(1 - \frac{L_r}{L_T}\right)^{1.8}}{1 - \left(1 - \frac{L_f}{L_T}\right)^{1.8}} \end{aligned} \tag{C.6}$$

After some manipulations:

$$L_f = L_T \left(1 - \left[1 - \left(0.75 \left(1 - \left[1 - \frac{L_r}{L_T}\right]^{1.8}\right)\right)\right]^{1/1.8}\right) \tag{C.7}$$

An example calculation is provided to illustrate the use of Equation (C.7), given an inlet at the following configuration:

S_L=1%; S_x=2%; n=0.014; a=2 inches; w=2 ft; and L_r=10 ft.

If the incoming gutter flow Q_g is 5 cfs, then Q_i (per HEC-22) is 3.22 cfs and L_T is 22.6 ft. The goal is to estimate the inlet length (at this configuration) that would lead to a 25% reduction in Q_i. Applying Equation (C.7) for L_r= 10 ft and L_T=22.6 ft yields L_f= 7.02 ft. The computed Q_i for a 7.02 ft long inlet (per HEC-22) is 2.413 cfs. As a check: 2.413/3.22 =0.74938 $\approx$ 0.75, which results in the required reduction factor. The previous example shows: A recessed inlet of length 10 ft should be inputed into the design software as a 7.02 ft inlet so the recessed inlet would have 75% of the interception capacity of a flush inlet (given the slopes and gutter configurations above).

Applying Equation (C.7) requires knowing L_T, unfortunately determining L_T for each inlet in a connected system can be a cumbersome iterative process. Accordingly, providing a good estimate for the ratio L_f/L_r without prior knowledge of L_T can help simplify the design procedure. Figure C.3 shows L_f as a function of L_T for several values of L_r. For the three values of L_r, L_f rapidly increases at first then the increase plateaued for large values of L_T.

The plots in Figure C.3 were nondimensionalized by plotting L_f/L_r on the y-axis and L_r/L_T on the x-axis, as shown in Figure C.4. The three plots in Figure C.3 collapsed into one line, where: For L_r/L_T=1, L_f/L_r=0.537; and for $L_r/L_T \approx zero$, $L_f/L_r \approx 0.75$. This analysis shows that the upper bound on the ratio L_f/L_r is 0.75 for low inlet efficiencies ($L_r/L_T << 1$), and the lower bound is 0.537 for 100% interception.

To illustrate the effect of selecting a certain ratio: For the inlet configuration used in the example calculation earlier, the gutter flow is varied from 1.1 cfs (100% interception) to 16 cfs. The inlet efficiency that fulfills the reduction in interception

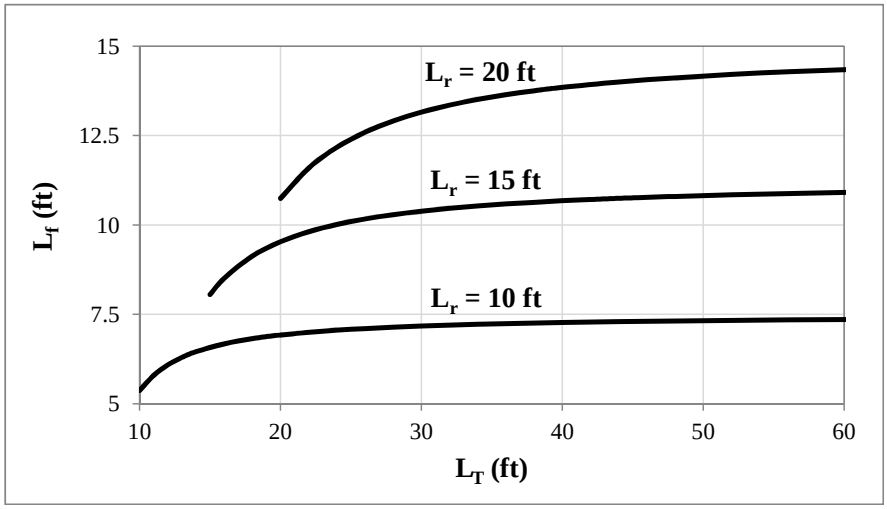

Figure C.3: L_f vs L_T for several values of L_r.

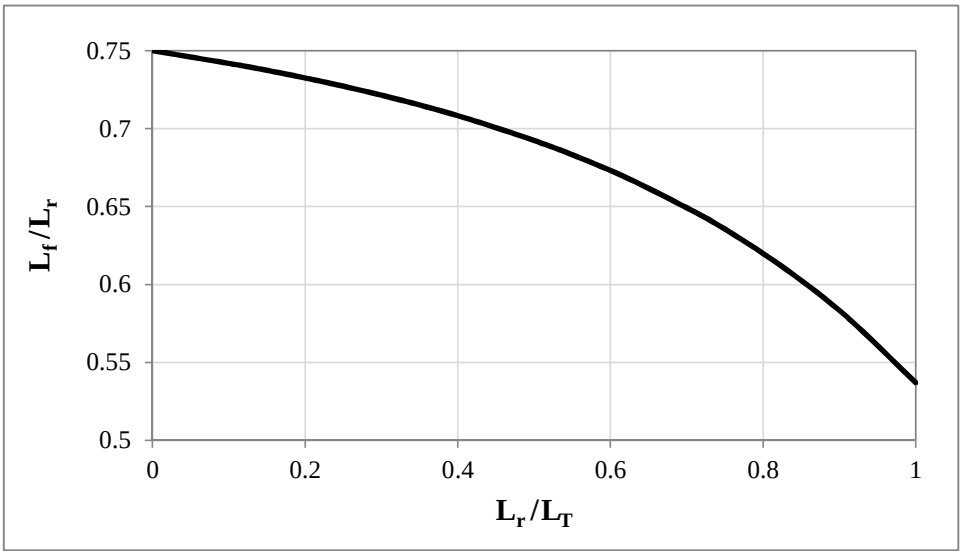

Figure C.4: L_f/L_r as a function of L_r/L_T.

capacity is computed as $E = 0.75Q_i/Q_g$. This *target* efficiency was compared to inlet efficiency computed using L_f/L_r of 0.75, 0.64 (average), and 0.537, as shown in Figure C.5. Using 0.75 significantly overestimate interception at high E but provides good estimate at very low E. Conversely, 0.537 provides good estimate at high E but provides conservative estimates for the rest of flow conditions. Ultimately, 0.64 provides an overall good match with the required E. The selection of the ratio L_f/L_r requires exercise of judgment based on the expected performance of the modeled inlets, i.e., the efficiency range the inlets are likely to be operating in given the incoming gutter flows, or a an average value of 0.64 may be selected for preliminary assessment.

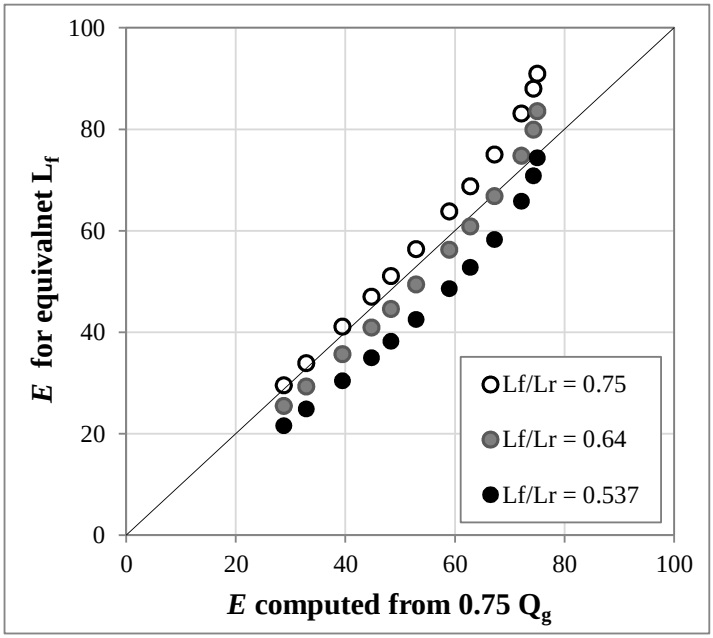

Figure C.5: Comparison between E fulfilling reduction criteria and E computed using different values of L_f/L_r.

Herein, the experimental data for the study by Holley et al. (1992) is provided in original model dimensions. The parameters used in this study are:

Scale: scaled (3:4); L= 3.75 and 11.25; w= 1.125; S_w= 30% and 20%; L_u= 7.5; L_d= 7.5; n=0.019; w=1.125.

Table C.1: Experimental data on recessed inlets for S_w= 30% and L= 11.25 ft, by Holley et al. (1992).

S_L	S_x	Q	Q_i	Q_b	T	d
0.5	1	0.635	0.635	0	10.5	0.098
0.5	2	1.743	1.743	0	10.5	0.187
0.5	4	3.421	3.421	0	8.8	0.375
1	1	0.484	0.484	0	10.5	0.104
1	2	1.411	1.411	0	9	0.164
1	2	2.363	2.025	0.338	10.5	0.192
1	4	3.169	3.169	0	7.8	0.292
1	4	4.517	4.143	0.374	9	0.356
2	2	0.663	0.663	0	6	0.122
2	2	1.57	1.331	0.239	8	0.158
2	4	4.036	3.329	0.707	8	0.312
2	6	3.595	3.595	0	6	0.364
2	6	5.246	4.843	0.403	7	0.375
5	1	0.525	0.25	0.275	10.5	0.06
5	2	0.238	0.238	0	4	0.064
5	2	0.648	0.508	0.14	4.5	0.092
5	2	1.667	0.988	0.679	7.5	0.132
5	4	0.881	0.881	0	3.5	0.131
5	4	2.063	1.66	0.403	5.3	0.181
5	6	1.818	1.818	0	3.5	0.224
5	6	3.442	2.882	0.56	5	0.267
7.5	1	0.754	0.245	0.509	10.5	0.075
7.5	2	0.307	0.221	0.086	6.5	0.067
7.5	2	0.927	0.555	0.372	8	0.106
7.5	4	0.521	0.521	0	2.5	0.106
7.5	4	1.871	1.281	0.59	4.5	0.176
7.5	4	3.245	1.764	1.481	5	0.23
7.5	6	1.123	1.123	0	2.5	0.165
7.5	6	1.943	1.663	0.28	3.3	0.201
7.5	6	2.413	1.911	0.502	4	0.22

Table C.2: Experimental data on recessed inlets for S_w= 30% and L= 7.5 ft, by Holley et al. (1992).

S_L	S_x	Q	Q_i	Q_b	T	d
0.1	4	2.838	2.838	0	9.6	0.36
0.5	1	0.321	0.321	0	9	0.086
0.5	2	1.326	1.326	0	9.5	0.181
0.5	4	2.557	2.557	0	8	0.313
0.5	4	3.639	3.349	0.29	9.4	0.36
1	1	0.273	0.273	0	8.5	0.086
1	1	0.59	0.545	0.045	10.5	0.101
1	2	1.307	1.307	0	7.5	0.156
1	2	2.005	1.632	0.373	10	0.197
1	4	2.006	2.006	0	6.5	0.273
1	4	2.87	2.65	0.22	7.5	0.31
2	1	0.21	0.21	0	6	0.08
2	1	0.846	0.53	0.316	10.5	0.122
2	2	0.624	0.624	0	5.5	0.111
2	2	1.242	0.991	0.251	8	0.141
2	2	2.812	1.486	1.326	10.5	0.182
2	4	1.504	1.504	0	5	0.193
2	4	2.624	2.15	0.474	6.5	0.244
2	4	5.218	3.094	2.124	8.5	0.317
2	6	2.357	2.357	0	5	0.283
2	6	3.661	3.159	0.502	5.5	0.338
5	1	0.676	0.298	0.378	10.5	0.074
5	2	0.316	0.316	0	3.5	0.069
5	2	1.339	0.701	0.638	6.5	0.129
5	4	0.699	0.699	0	3.5	0.12
5	4	1.902	1.288	0.614	5	0.176
5	4	3.881	1.882	1.999	6	0.262
5	6	1.268	1.268	0	3	0.179
5	6	2.749	2.078	0.671	4.5	0.239
7.5	1	0.346	0.126	0.22	10.5	0.059
7.5	2	2.647	0.778	1.869	8.3	0.168
7.5	4	0.412	0.412	0	2.4	0.103
7.5	4	2.047	1.177	0.87	4.5	0.175
7.5	4	2.799	1.169	1.63	5	0.22

Table C.2 – continued from previous page

S_L	S_x	Q	Q_i	Q_b	T	d
7.5	4	5.118	1.683	3.435	6	0.288
7.5	6	0.873	0.873	0	2.5	0.146
7.5	6	1.99	1.368	0.622	3.5	0.207
7.5	6	3.536	1.875	1.661	4.5	0.251

Table C.3: Experimental data on recessed inlets for S_w= 30% and L= 3.75 ft, by Holley et al. (1992).

S_L	S_x	Q	Q_i	Q_b	T	d
0.1	2	0.856	0.856	0	10	0.201
0.1	4	1.932	1.932	0	8.2	0.319
0.5	2	0.81	0.81	0	8.5	0.166
0.5	2	1.295	1.108	0.187	10.5	0.201
0.5	4	1.462	1.462	0	6.5	0.261
0.5	4	1.958	1.801	0.157	7.5	0.296
0.5	4	3.343	2.493	0.85	9.3	0.36
0.5	6	2.079	2.079	0	6	0.352
1	1	0.763	0.525	0.238	10.5	0.126
1	2	0.677	0.677	0	6.5	0.152
1	2	0.951	0.839	0.112	8	0.172
1	2	1.455	1.094	0.361	9.3	0.2
1	4	1.069	1.069	0	5	0.222
1	4	1.958	1.642	0.316	6.5	0.279
1	4	3.691	2.404	1.287	8.5	0.361
1	6	1.777	1.777	0	4.7	0.305
1	6	2.711	2.327	0.384	5.7	0.37
2	1	0.559	0.303	0.256	9	0.103
2	1	1.036	0.491	0.545	10.5	0.111
2	2	0.424	0.424	0	4.5	0.11
2	2	0.982	0.697	0.285	6.6	0.142
2	2	1.676	0.954	0.722	8.5	0.162
2	4	0.84	0.84	0	4	0.166
2	4	1.762	1.315	0.447	5.4	0.219
2	4	2.618	1.472	1.146	6.5	0.262

Table C.3 – continued from previous page

S_L	S_x	Q	Q_i	Q_b	T	d
2	4	4.036	1.945	2.091	8	0.292
2	6	1.372	1.372	0	3.8	0.229
2	6	2.122	1.688	0.434	4.5	0.276
2	6	3.054	2.041	1.013	5.2	0.332
2	6	3.321	2.106	1.215	5.6	0.335
5	1	0.265	0.115	0.15	5.5	0.053
5	1	1.236	0.307	0.929	10.5	0.09
5	2	0.635	0.34	0.295	4.5	0.092
5	2	1.524	0.556	0.968	6.4	0.129
5	2	3.155	0.647	2.508	10	0.184
5	4	0.294	0.294	0	2.2	0.093
5	4	1.343	0.909	0.434	4	0.155
5	6	0.667	0.667	0	2.4	0.14
5	6	2.074	0.996	1.078	3.6	0.232
5	6	3.714	1.019	2.695	5.3	0.277
7.5	2	0.917	0.342	0.575	5	0.099
7.5	2	2.761	0.536	2.225	8	0.159
7.5	2	3.485	0.555	2.93	10.5	0.177
7.5	4	1.248	0.626	0.622	3.5	0.143

Table C.4: Experimental data on recessed inlets for S_w= 20% and L= 7.5 ft, by Holley et al. (1992).

S_L	S_x	Q	Q_i	Q_b	T	d
1	4	2.9	2.9	0	8	0.326
1	4	4.149	1.892	2.257	9	0.376
2	2	0.834	0.834	0	6	0.131
2	2	1.814	1.413	0.401	9.5	0.167
2	4	4.117	3.262	0.855	8	0.29
2	4	1.949	1.892	0.057	5.5	0.228
2	4	3.632	2.984	0.648	7.5	0.274
4	2	0.344	0.344	0	3.5	0.078
4	2	1.377	0.851	0.526	6.5	0.127
4	2	2.785	1.32	1.465	8.5	0.172

Table C.4 – continued from previous page

S_L	S_x	Q	Q_i	Q_b	T	d
4	4	1.143	1.104	0.039	3.5	0.152
4	4	3.127	2.17	0.957	6	0.22
4	4	4.734	2.865	1.869	6.5	0.268

Table C.5: Field tests on recessed inlets for S_w= 30%, L_u= 10 ft, and L_d=10 ft by Holley et al. (1992).

S_L	S_x	L	Q	T	d	n
2.3	2.3	10.1	1.66	7.739	0.178	0.022
4	4.1	15.1	2.54	5.073	0.208	0.016
0.4	3.2	10.2	3.03	10.75	0.344	0.021
2.3	4.4	10.1	2.21	4.727	0.208	0.013
2.7	3.3	10	0.87	4.424	0.146	0.019
12.9	4	9.8	2.01	3.9	0.156	0.018
4	4.3	10	3.15	5.814	0.25	0.021
2.7	3.3	10	0.87	4.424	0.146	0.019
12.1	2	10.1	0.87	4.9	0.098	0.023
2.6	2.8	10	0.87	5.143	0.144	0.021
4.7	2	14.9	1.02	5.95	0.119	0.02
2.1	4.5	9.8	1.33	4.756	0.214	0.022
3.04	6.9	15.2	2.99	3.899	0.269	0.014

Bibliography

Argue, J. R. and Pezzaniti, D. (1996). How reliable are inlet (hydraulic) models at representing stormwater flow? *Science of the total environment*, 189:355–359.

Bagheri, S. and Heidarpour, M. (2011). Characteristics of flow over rectangular sharp-crested side weirs. *Journal of Irrigation and Drainage Engineering*, 138(6):541–547.

Bauer, W. J. and Woo, D.-C. (1964). Hydraulic design of depressed curb opening inlets. *Highway Research Record*, 58.

Bowman, N. K. (1988). *Hydraulic analysis of alternative South Carolina curb inlet structures*. PhD thesis, Clemson University.

Brandson, N. B. (1971). The hydraulic behaviour of the city of winnipeg: standard, storm water, sump inlets.

Brown, S., Schall, J., Morris, J., Doherty, C., Stein, S., and Warner, J. (2009). Urban Drainage Design Manual–Hydraulic Engineering Circular 22 (HEC-22). Technical report, FHWA-NHI-10-009, US Dept. of Transportation, Federal Highway Administration, Washington, DC, National Highway Institute, Virginia.

Chaudhry, M. H. (2007). *Open-channel flow*. Springer Science & Business Media.

City of Austin (2018). Drainage Criteria Manual. `https://library.municode.com/TX/Austin/codes/Drainage_Criteria_Manual`. [Online; accessed 14-October-2018].

Comport, B. C. and Thornton, C. I. (2012). Hydraulic efficiency of grate and curb inlets for urban storm drainage. *Journal of Hydraulic Engineering*, 138(10):878–884.

Conner, N. W. (1946). Design and capacity of gutter inlets. In *Highway Research Board Proceedings*, volume 25.

FHWA (2018). Hydraulic Toolbox, Federal Highway Administration. `https://oldcastleprecast.com/c/drainage/catch-basins-inlets/`. [Online; accessed 8-March-2018].

FHWA and FTA (2017). *2015 Status of the Nation's Highways, Bridges, and Transit Conditions & Performance Report to Congress*. Government Printing Office.

Fiuzat, A., Soares, C., and Sill, B. (2000). Design of curb opening inlet structure.

Grobler, P. (1994). Verification of the inlet capacities of modified stormwater kerb inlets and the development of new design curves. Master's thesis, Stellenbosch University.

Grubert, J. P. (1988). Correlation between full size and half size inlets. ASCE.

Guo, J. C.-Y., MacKenzie, K., et al. (2012). Hydraulic efficiency of grate and curb-opening inlets under clogging effect. Technical report, Colorado Department of Transportation, DTD Applied Research and Innovation Branch.

Hager, W. H. (1987). Lateral outflow over side weirs. *Journal of Hydraulic Engineering*, 113(4):491–504.

Hahn, P. M. (1972). A study of storm-water inlet capacities. Master's thesis, University of South Florida, Florida, USA.

Hammonds, M. A. and Holley, E. (1995). Hydraulic characteristics of flush depressed curb inlets and bridge deck drains. *Rep. No. 1409*, 1.

Holley, E. R., Woodward, C., Brigneti, A., and Ott, C. (1992). Hydraulic characteristics of recessed curb inlets and bridge drains. *Texas Department of Transportation (TxDOT), Austin, Texas*.

Izzard, C. F. (1950). Tentative results on capacity of curb opening inlets. In *Highway Research Board*, pages 11–13.

Izzard, C. F. (1977). Simplified method for design of curb-opening inlets. *Transportation Research Record*, (631).

Izzard, C. F. and Hicks, W. (1947). Hydraulics of runoff from developed surfaces. In *Highway Research Board Proceedings*, volume 26.

Jens, S. (1979). Design of urban highway drainage. *FHWA Pub. No. TS-79*, 225:11.

Johns Hopkins University (1956). *The Design of Storm-water Inlets*. Storm Drainage Research Committee and Johns Hopkins University. Dept. of Sanitary Engineering and Water Resources.

Karaki, S. and Haynie, R. M. (1961). *Depressed Curb Opening Inlets: Supercritical Flow, Experimental Data*. Colorado State University Research Foundation, Civil Engineering Section.

Kranc, S., Romano, F., Ethier, S., Wilmot, J., Deavers, R., Kromolicki, J., Rabens, G., and Cowell, C. (1998). Hydraulic performance of drainage structures, phase i and ii. Technical report.

Krolak, J. (2018). Public discussion at the National Hydraulic Engineers Conference, Columbus, Ohio, USA, August 29, 2018.

Li, W. H., Sorteberg, K. K., and Geyer, J. C. (1951). Hydraulic behavior of storm-water inlets: Ii. flow into curb-opening inlets. *Sewage and Industrial Wastes*, pages 722–738.

MacCallan, R. and Hotchkiss, R. (1996). Hydraulic efficiency of highway stormwater inlets: Final report. Technical report, Research Report NE-DOT.

McEnroe, B. M., Wade, R. P., McEnroe, B. M., Wade, R. P., et al. (1998). Hydraulic performance of set-back curb inlets. Technical report, Kansas. Dept. of Transportation.

McEnroe, B. M., Wade, R. P., and Smith, A. K. (1999). Hydraulic performance of curb and gutter inlets. Technical report, Citeseer.

OldCastle (2018). Catch Basin Products, Oldcastle Precast. `https://www.fhwa.dot.gov/engineering/hydraulics/software/toolbox404.cfm`. [Online; accessed 10-October-2018].

Pisano, P. A., Goodwin, L. C., and Rossetti, M. A. (2008). Us highway crashes in adverse road weather conditions. In *24th Conference on International Interactive Information and Processing Systems for Meteorology, Oceanography and Hydrology, New Orleans, LA*.

Qian, Q., Liu, X., Charbeneau, R., and Barrett, M. (2013). Hydraulic performance of small scale bridge deck drains. Technical report.

Rossman, L. (2017). Storm water management model. reference manual. volume ii–hydraulics.

Russo, B. and Gómez, M. (2013). Discussion of "hydraulic efficiency of grate and curb inlets for urban storm drainage" by brendan c. comport and christopher i. thornton. *Journal of Hydraulic Engineering*, 140(1):121–122.

Schalla, F. E. (2016). Effects of flush slab supports on the hydraulic performance of curb inlets and an analysis of design equations. Master's thesis, Dept. of Civil Eng., University of Texas at Austin, USA.

Schalla, F. E., Ashraf, M., Barrett, M. E., and Hodges, B. R. (2017). Limitations of traditional capacity equations for long curb inlets. *Transportation Research Record: Journal of the Transportation Research Board*, (2638):97–103.

Sill, B., Rich, G., and Nnaji, S. (1986). A study to provide more efficient alternative designs of storm water inlet capacities. final report. Technical report.

Soares, C. E. (1991). *Analysis of the efficiency of an alternative South Carolina storm water drainage structure*. PhD thesis, Clemson University.

Spaliviero, F., May, R., and Escarameia, M. (2000). Spacing of road gullies hydraulic performance of bs en 124 gully gratings and kerb inlets.

TxDOT (2016). *Hydraulic design manual*. TxDOT Austin, Texas.

University of South Australia (1995). South Australian Road Stormwater Drainage Inlets: Hydraulic Study. `http://www.unisa.edu.au/IT-Engineering-and-the-Environment/Natural-and-Built-Environments/Our-research/AFMG/South-Australian-Road-Stormwater-Drainage-Inlets-Hydraulic-Study/`. [Online; accessed 12-October-2018].

Uyumaz, A. (1992). Discharge capacity for curb-opening inlets. *Journal of Hydraulic Engineering*, 118(7):1048–1051.

Wasley, R. (1960). *Hydrodynamics of Flow into Curb-opening Inlets*. PhD thesis, Department of Civil Engineering, Stanford University.

White, M. and Pezzaniti, D. (2002). Evaluation of gully pit inlet litter control systems-final report. *Urban Water Resources Centre, University of South Australia, Australia*.

Wintz, W. A. and Kuo, Y. H. (1970). A study of storm-water inlet capacities.

Yong, K. (1965). *Hydraulic Model Investigation of Kerb-opening Inlets*. University of New South Wales. Water Research Laboratory.

Zwamborn, J. A. (1966). *Stormwater inlet design code*. National Mechanical Engineering Research Institute, Council for Scientific and Industrial Research.